

Healthy and energy efficient buildings

Edited by

Sunil K. Sansaniwal and Roberto Alonso González-Lezcano

Published in

Frontiers in Built Environment



FRONTIERS EBOOK COPYRIGHT STATEMENT

The copyright in the text of individual articles in this ebook is the property of their respective authors or their respective institutions or funders. The copyright in graphics and images within each article may be subject to copyright of other parties. In both cases this is subject to a license granted to Frontiers.

The compilation of articles constituting this ebook is the property of Frontiers.

Each article within this ebook, and the ebook itself, are published under the most recent version of the Creative Commons CC-BY licence. The version current at the date of publication of this ebook is CC-BY 4.0. If the CC-BY licence is updated, the licence granted by Frontiers is automatically updated to the new version.

When exercising any right under the CC-BY licence, Frontiers must be attributed as the original publisher of the article or ebook, as applicable.

Authors have the responsibility of ensuring that any graphics or other materials which are the property of others may be included in the CC-BY licence, but this should be checked before relying on the CC-BY licence to reproduce those materials. Any copyright notices relating to those materials must be complied with.

Copyright and source acknowledgement notices may not be removed and must be displayed in any copy, derivative work or partial copy which includes the elements in question.

All copyright, and all rights therein, are protected by national and international copyright laws. The above represents a summary only. For further information please read Frontiers' Conditions for Website Use and Copyright Statement, and the applicable CC-BY licence.

ISSN 1664-8714
ISBN 978-2-8325-4111-1
DOI 10.3389/978-2-8325-4111-1

About Frontiers

Frontiers is more than just an open access publisher of scholarly articles: it is a pioneering approach to the world of academia, radically improving the way scholarly research is managed. The grand vision of Frontiers is a world where all people have an equal opportunity to seek, share and generate knowledge. Frontiers provides immediate and permanent online open access to all its publications, but this alone is not enough to realize our grand goals.

Frontiers journal series

The Frontiers journal series is a multi-tier and interdisciplinary set of open-access, online journals, promising a paradigm shift from the current review, selection and dissemination processes in academic publishing. All Frontiers journals are driven by researchers for researchers; therefore, they constitute a service to the scholarly community. At the same time, the *Frontiers journal series* operates on a revolutionary invention, the tiered publishing system, initially addressing specific communities of scholars, and gradually climbing up to broader public understanding, thus serving the interests of the lay society, too.

Dedication to quality

Each Frontiers article is a landmark of the highest quality, thanks to genuinely collaborative interactions between authors and review editors, who include some of the world's best academicians. Research must be certified by peers before entering a stream of knowledge that may eventually reach the public - and shape society; therefore, Frontiers only applies the most rigorous and unbiased reviews. Frontiers revolutionizes research publishing by freely delivering the most outstanding research, evaluated with no bias from both the academic and social point of view. By applying the most advanced information technologies, Frontiers is catapulting scholarly publishing into a new generation.

What are Frontiers Research Topics?

Frontiers Research Topics are very popular trademarks of the *Frontiers journals series*: they are collections of at least ten articles, all centered on a particular subject. With their unique mix of varied contributions from Original Research to Review Articles, Frontiers Research Topics unify the most influential researchers, the latest key findings and historical advances in a hot research area.

Find out more on how to host your own Frontiers Research Topic or contribute to one as an author by contacting the Frontiers editorial office: frontiersin.org/about/contact

Healthy and energy efficient buildings

Topic editors

Sunil K. Sansaniwal — The Energy and Resources Institute (TERI), India
Roberto Alonso González-Lezcano — CEU San Pablo University, Spain

Citation

Sansaniwal, S. K., González-Lezcano, R. A., eds. (2023). *Healthy and energy efficient buildings*. Lausanne: Frontiers Media SA. doi: 10.3389/978-2-8325-4111-1

Table of contents

05	Editorial: Healthy and energy efficient buildings Roberto Alonso González-Lezcano and Sunil Kumar Sansaniwal
09	An Investigation of Indoor Air Quality in a Recently Refurbished Educational Building R. S. McLeod, M. Mathew, D. Salman and C. L. P. Thomas
28	Finite element modeling for predicting sound insulation of fixed windows in a laboratory environment Marie Mimura, Takeshi Okuzono and Kimihiro Sakagami
42	The effects of personal green spaces on human's mental health and anxiety symptoms during COVID-19: The case of apartment residents in Tehran Hanieh Jafari Khaledi, Mohsen Faizi and Mehdi Khakzand
55	Recent developments in evaluation methods and characteristics of comfort environment in underground subway Weichao Yan, Xiangzhao Meng, Haiyun Zhou, Chuanjun Yang, Qian Chen, Seung Jin Oh and Xin Cui
64	Long-term performance of a hybrid indirect evaporative cooling-mechanical vapor compression cycle: A case study in Saudi Arabia Qian Chen, Kum Ja M, Muhammad Burhan, Muhammad Wakil Shahzad, Doskhan Ybyraiymkul, Seungjin Oh, Xin Cui and Kim Choon Ng
78	High potential of small-room acoustic modeling with 3D time-domain finite element method Takeshi Okuzono and Takumi Yoshida
97	Advancing the use of the repertory grid technique in the built environment: A systematic review Rawan Rahman, Dana Bidoun, Ahmed Agiel and Ala' Albdour
114	Study on an advanced borehole heat exchanger for ground source heat pump operating in volcanic island: Case study of Jeju island, South Korea Jong Woo Kim, Yeong-Min Kim, Yoon Jung Ko, Qian Chen, Cui Xin and Seung Jin Oh
122	Exploring environmental policy adoption enablers for indoor air quality management in higher educational institutions in South Africa Mpho Ndou and Clinton Aigbavboa
132	Assessment of indoor air quality and comfort by comparing an energy simulation and actual data in Native American shelters Paul Fowler, Fernando Del Ama Gonzalo, Sarah Newell, James Poolman, Maria J. Montero Burgos and Roberto Alonso González Lezcano

- 148 **Construction parameters that affect the air leaks of the envelope in dwellings in Madrid**
Roberto Alonso González-Lezcano, Gastón Sanglier Contreras, Carlos Miguel Iglesias Sanz, Rocío Sancho Alambillaga and Eduardo José López Fernández
- 153 **Strategies for integral rehabilitation and improvement of the energy efficiency of Lagos Park building in Madrid**
María Eugenia Maciá-Torregrosa, Javier Camacho-Diez and Roberto Alonso González-Lezcano



OPEN ACCESS

EDITED AND REVIEWED BY

Hazim Bashir Awbi,
University of Reading, United Kingdom

*CORRESPONDENCE

Roberto Alonso González-Lezcano,
✉ rgonzalezcano@ceu.es
Sunil Kumar Sansaniwal,
✉ sunil.sansaniwal@teri.res.in

RECEIVED 19 November 2023

ACCEPTED 22 November 2023

PUBLISHED 29 November 2023

CITATION

González-Lezcano RA and Sansaniwal SK
(2023), Editorial: Healthy and energy
efficient buildings.
Front. Built Environ. 9:1341133.
doi: 10.3389/fbuil.2023.1341133

COPYRIGHT

© 2023 González-Lezcano and
Sansaniwal. This is an open-access article
distributed under the terms of the
[Creative Commons Attribution License](#)
(CC BY). The use, distribution or
reproduction in other forums is
permitted, provided the original author(s)
and the copyright owner(s) are credited
and that the original publication in this
journal is cited, in accordance with
accepted academic practice. No use,
distribution or reproduction is permitted
which does not comply with these terms.

Editorial: Healthy and energy efficient buildings

Roberto Alonso González-Lezcano^{1*} and
Sunil Kumar Sansaniwal^{2*}

¹Escuela Politécnica Superior, Universidad San Pablo-CEU, CEU Universities, Urbanización
Montepríncipe, Madrid, Spain, ²Centre for Climate Change Research, The Energy and Resources Institute,
New Delhi, India

KEYWORDS

indoor air quality, indoor environment quality, building innovation systems, health
outcomes, energy efficiency, sustainable construction

Editorial on the Research Topic Healthy and energy efficient buildings

The built environment has a significant impact on human health. The extent of the impact of buildings on human health and the environment depends on different environmental factors. The extent of the impact of buildings on human health and the environment depends on the design, materials and methods used for construction and operation (Altomonte, 2019; Awada et al., 2022; López et al., 2023). It is increasingly important to design healthy buildings in the pursuit of sustainable development, where not only the occupants play an important role in ensuring indoor air quality through their habits, but also current developments related to interior finishes with low chemical emissions and good fungal resistance (Rupp et al., 2015; Loftness et al., 2007).

Recent research has shown that people contract COVID-19 through airborne transmission indoors, especially in poorly ventilated environments (Domínguez-amarillo et al., 2020). It is therefore necessary to maintain optimal air quality to eradicate the virus spread. This requires innovative changes to existing indoor and outdoor infrastructure to positively influence occupants even in the most densely populated spaces (Karagulian et al., 2015). This is also a challenge to traditional residential and public building construction in the aftermath of the COVID-19 pandemic (López et al., 2023).

Because as previously stated, people spend most of their time inside buildings and, therefore, a healthy and comfortable indoor environment is essential for human beings. Indoor environmental quality encompasses the four environmental conditions (thermal, air quality, visual and acoustic) within the building (Serrano-Jiménez et al., 2020; González-Lezcano, 2023). Humans have strived to control their built environments in which they can feel comfortable. The use of adaptive actions by occupants, such as opening windows or doors, using blinds, and using fans, substantially influences the indoor environment. Naturally ventilated or free-running buildings provide many adaptive opportunities for occupants to improve their built environment by utilizing natural airflows (Kumar et al., 2016). Opening windows helps in comfortable ventilation of air, distribution of fresh air and extracts overheated and polluted air from the interior space (Kaasalainen et al., 2020). Recently developed research (Sansaniwal et al., 2021a) showed that the adaptive actions of the occupant were governed primarily by the search for comfort and were based primarily on the change in the indoor rather than the outdoor environment and that the behavioral patterns of the occupants can be used to simulate the environment built in buildings with natural ventilation.

The healthy building concept focuses primarily on the creation of a desirable environment, which is measured in terms of indoor environmental quality (IEQ) (Jain et al., 2020; Sansaniwal et al., 2022). A healthy IEQ is expected to positively impact the occupants of most densely populated buildings in terms of physical, mental and social wellbeing. The level of indoor environmental quality depends on several parameters, such as thermal, visual, acoustic and chemical variables (Altomonte, 2019). The parameters, which should be assessed individually and/or collectively, include indoor air quality (Agarwal et al., 2021), thermal comfort (Tartarini et al., 2020), ventilation (Dhahri and Aouinet, 2020), acoustic performance (Baeza Moyano and González Lezcano, 2022; Moyano et al., 2022), lighting (Moyano et al., 2020) and spatial layout (Ribeiro et al., 2020).

Particularly in the workplaces, the satisfaction of building occupants with the qualities of their indoor environment has been associated with their health and wellbeing, self-assessed job performance (Veith et al., 2002; Hormigos-Jimenez et al., 2017), and behavior (Bordass and Leaman, 2005). Some of these can also have a significant influence on buildings' energy requirements due to the adaptive actions (e.g., on thermostats, blinds, lights, etc.) that users exercise in response to changes in environmental conditions (Haldi and Robinson, 2011). In this context, an awareness that people spend almost 90% of their time indoors (Delzendeh et al., 2017), and that salary costs in commercial buildings largely exceed investment and operational expenses, has triggered substantial interest in the potential contribution of green rating systems towards improved workplace experience (Fernandez-Antolin et al., 2021; Soharu et al., 2021).

Therefore, it is necessary to set up a building with a high level of IEQ to promote the health and wellbeing of its occupants (Toyinbo, 2019). Air quality is one of the factors that play a major role in providing a healthy IEQ (Hormigos-Jimenez et al., 2019; López et al., 2023). Indoor air quality can be compromised by both outdoor and indoor sources of pollutants related to building materials, equipment, animals and humans (Van Tran et al., 2020). Recent research has demonstrated new implementation methodologies for quantifying IEQ elements (i.e., thermal comfort, indoor air quality, visual comfort, and acoustic comfort) in real buildings (Sansaniwal et al., 2021b). Below is a summary of the main findings of the articles included in this Research Topic.

McLeod et al. propose a novel indoor air quality testing methodology in the context of post-occupancy performance assessment of a newly renovated architectural studio building at Loughborough University, UK. Additional scenario based testing was incorporated to isolate the presence and source of harmful volatile organic compounds, which were measured using diffuse sampling methods involving analysis using thermal desorption, gas chromatography, and mass spectrometry techniques. The results indicate that existing standards, designed to protect the health and wellbeing of students, are likely to mask potentially serious indoor air quality problems.

Mimura et al. presented a discussion on the prediction ability of three numerical models using the finite element method to predict the sound reduction index (SRI) of fixed windows having different dimensions in a laboratory environment. The results highlighted the importance of including a niche in a numerical model used to accurately predict the sound reduction rate below 1 kHz for smaller windows.

Khaledi et al. evaluated the impact of green spaces and their benefits during COVID-19 on mental health and generalized anxiety disorder. The authors demonstrated that the use of personal green spaces has a negative correlation and significant impact on general mental health and generalized anxiety disorder. It also plays a bigger role in reducing depression than reducing anxiety among individuals. Therefore, maximum land use policies should be reviewed. They further conclude that more attention should be paid to green spaces in post-COVID designs from a macro to small scale.

Okuzono and Yoshida describes the significantly higher efficiency of 3D-FEM (finite element method) against a frequency-domain FEM (FD-FEM) via acoustics simulation in a small cubic room and a small meeting room, including two porous-type sound absorbers and a resonant-type sound absorber. The authors modeled with local-reaction frequency-dependent impedance boundary conditions and an extended-reaction model. Results demonstrated the high potential and computational benefit of time-domain FEM as a 3D small room acoustics prediction tool.

Chen et al. presents the evaluation of a hybrid indirect evaporative cooling-mechanical vapor compression (IEC-MVC) cycle for cooling applications in Saudi Arabia. Over the whole year, IEC contributes 50% of the total cooling capacity and reduces energy consumption by 40% in dry cities, while the saving is lower at 15%–25% in humid cities like Mecca and Jeddah. The average water consumption of the IEC is in the range of 4–12 L/hr. The authors explained that the water consumption can be replenished by the condensate collected from the MVC evaporator if the ambient humidity is high. Based on the annual performance, the cost of the IEC-MVC process is calculated, and it is 15%–35% lower than the standalone MVC.

Yan et al. analyzed the characteristics of the subway environment and sort out six environmental elements that affect passengers' comfort, including thermal environment, vibration, noise, lighting, air quality, and air pressure. In addition, the measurement scheme, calculation model, and evaluation method of each element are outlined based on relevant norms and literature. The authors explained Measures to improve comfort, especially the exploitation of energy-saving air conditioning systems, will provide strong support for the sustainable and sound growth of the rail transit industry.

Kim et al. presents an advanced borehole heat exchanger that has been developed in order to apply a ground source heat pump to a volcanic island where the existing borehole heat exchangers are inapplicable by local ordinance. The proposed heat exchanger was also compared with the conventional heat exchanger that was made of high-density polyethylene (HDPE) heat exchanger. The authors revealed that the maximum heat capacity for the developed heat exchanger was measured at 63.9 kW, which is 160% higher than that of the high-density polyethylene heat exchanger (39.9 kW).

Rahman et al. explore the repertory grid technique (RGT) as a research method and advance its use in the built environment field. Following Preferred Reporting Items for Systematic Reviews and Meta-Analyses guidelines, this study conducted a systematic review to identify studies on Scopus that have used RGT before 2021. These studies were investigated according to subject area, location, year of publication, aim, and research design. The authors indicated the validity of RGT to the built environment by exploring different ways it may be employed. This review strongly recommends advancing the use of RGT in the built environment and taking advantage of its potential.

Ndou and Aigbayboa investigate the extent to which the indoor air quality (IAQ) management of higher educational institutions (HEIs) in South Africa could be improved through the appropriate implementation of environmental policy adoption enablers. According to the authors, an alternative to the management of IAQ is possible through environmental behavioral change. The inferential statistical evaluation using exploratory factor analysis revealed three crucial environmental policy adoption metrical approaches (stakeholder dialogue, institutional commitment, and policy composition) to the management of IAQ in HEIs.

Fowler et al. analyzed if a native American shelter (wigwam) can create comfort and if while doing so can provide healthy indoor air quality (IAQ) levels as defined by current standards. Concurrent to this research a technique to digitally model the outcomes of comfort created within the shelter was developed. It was found that comfort can be achieved to modern standards in this native shelter; as temperature, relative humidity, and rainfall exposure can all be controlled to acceptable levels. Indoor air quality is always at an acceptable level when a fire is not active. When an open fire is introduced, the particulates and VOC released into the interior of the wigwam are at dangerous levels.

González-Lezcano et al. focuses on the characterization of the residential building stock in the Madrid area. Despite the fact that no evidence was found to justify that climate is a significant variable in terms of airtightness, it seems clear that there are different aspects associated with the region where the building is located such as differences in construction quality, dwelling design or materials, or due to differences in the building size or age. The authors delved into the main causes of the lack of airtightness in multi-family homes through 151 tests of blower doors in the Community of Madrid.

Maciá-Torregrosa et al. presents a comprehensive refurbishment project undertaken in the Lagos Park residential building in Madrid. The authors offers a detailed analysis of common building Research Topic related to excessive humidity in the surrounding areas and deficiencies in the energy performance of the building envelope, including facades and roofs. Precise measures for achieving compliance with the Spanish Technical Building Code, as well as enhancing energy efficiency and functionality, are explained through the renovation of the building envelopes. The study also encompasses improvements made to the domestic hot water supply systems and the air-conditioning system, which contribute to the building's attainment of an optimal energy rating

This Research Topic aims to address issues concerning Indoor Environmental Quality (IEQ), which are described more simply as the conditions inside the building. It includes air quality, but also access to daylight and views, pleasant acoustic conditions and

occupant control over lighting and thermal comfort. They will also include the functional aspects of the space, such as whether the layout provides easy access to tools and people when needed and whether there is sufficient space for the occupants. Building managers and operators can increase building occupant satisfaction by considering all aspects of IEQ rather than focusing on temperature or air quality alone.

Author contributions

RG-L: Conceptualization, Formal Analysis, Investigation, Methodology, Resources, Validation, Visualization, Writing—original draft, Writing—review and editing. SS: Conceptualization, Data curation, Formal Analysis, Investigation, Methodology, Project administration, Resources, Supervision, Validation, Writing—review and editing.

Funding

The author(s) declare that no financial support was received for the research, authorship, and/or publication of this article.

Acknowledgments

We would like to thank all of the contributing authors and also the Frontiers team, for their constant efforts and support throughout in managing the Research Topic.

Conflict of interest

The authors declare that the research was conducted in the absence of any commercial or financial relationships that could be construed as a potential conflict of interest.

Publisher's note

All claims expressed in this article are solely those of the authors and do not necessarily represent those of their affiliated organizations, or those of the publisher, the editors and the reviewers. Any product that may be evaluated in this article, or claim that may be made by its manufacturer, is not guaranteed or endorsed by the publisher.

References

- Agarwal, N., Meena, C. S., Raj, B. P., Saini, L., Kumar, A., Gopalakrishnan, N., et al. (2021). Indoor air quality improvement in COVID-19 pandemic: review. *Sustain. Cities Soc.* 70, 102942. doi:10.1016/j.scs.2021.102942
- Altomonte, S. (2019). "Defining comfort, satisfaction, health and well-being," in *Regenerative design in digital practice: a handbook for the built environment*. KADK: COST Action RESTORE (REthinking Sustainability TOWards a Regenerative Economy), 300–305.
- Awada, M., Becerik-Gerber, B., White, E., Hoque, S., O'Neill, Z., Pedrielli, G., et al. (2022). Occupant health in buildings: impact of the COVID-19 pandemic on the opinions of building professionals and implications on research. *Build. Environ.* 207, 108440. doi:10.1016/j.buildenv.2021.108440
- Baeza Moyano, D., and González Lezcano, R. A. (2022). Effects of infrasound on health: looking for improvements in housing conditions. *Int. J. Occup. Saf. Ergonomics* 28 (2), 809–823. doi:10.1080/10803548.2020.1831787
- Bordass, B., and Leaman, A. (2005). Making feedback and post-occupancy evaluation routine 1: a portfolio of feedback techniques. *Build. Res. Inf.* 33, 347–352. doi:10.1080/09613210500162016

- Delzendeh, E., Wu, S., Lee, A., and Zhou, Y. (2017). The impact of occupants' behaviours on building energy analysis: a research review. *Renew. Sustain. Energy Rev.* 80, 1061–1071. doi:10.1016/j.rser.2017.05.264
- Dhahri, M., and Aouinet, H. (2020). CFD investigation of temperature distribution, air flow pattern and thermal comfort in natural ventilation of building using solar chimney. *World J. Eng.* 17 (1), 78–86. doi:10.1108/WJE-09-2019-0261
- Domínguez-amarillo, S., Fernández-agüera, J., Cesteros-garcía, S., and González-lezcano, R. A. (2020). Bad air can also kill: residential indoor air quality and pollutant exposure risk during the covid-19 crisis. *Int. J. Environ. Res. Public Health* 17 (19), 7183–7234. doi:10.3390/ijerph17197183
- Fernandez-Antolin, M. M., del Río, J. M., and Gonzalez-Lezcano, R. A. (2021). The use of gamification in higher technical education: perception of university students on innovative teaching materials. *Int. J. Technol. Des. Educ.* 31 (5), 1019–1038. doi:10.1007/s10798-020-09583-0
- González-Lezcano, R. A. (2023). Editorial: design of efficient and healthy buildings. *Front. Built Environ.* 9. doi:10.3389/fbuil.2023.1210956
- Haldi, F., and Robinson, D. (2011). The impact of occupants' behaviour on building energy demand. *J. Build. Perform. Simul.* 4 (4), 323–338. doi:10.1080/19401493.2011.558213
- Hormigos-Jimenez, S., Padilla-Marcos, M. Á., Meiss, A., Gonzalez-Lezcano, R. A., and Feijó-Muñoz, J. (2017). Ventilation rate determination method for residential buildings according to TVOC emissions from building materials. *Build. Environ.* 123, 555–563. doi:10.1016/j.buildenv.2017.07.032
- Hormigos-Jimenez, S., Padilla-Marcos, M. Á., Meiss, A., Gonzalez-Lezcano, R. A., and Feijó-Muñoz, J. (2019). Assessment of the ventilation efficiency in the breathing zone during sleep through computational fluid dynamics techniques. *J. Build. Phys.* 42 (4), 458–483. doi:10.1177/1744259118771314
- Jain, N., Burman, E., Robertson, C., Stamp, S., Shrubsole, C., Aletta, F., et al. (2020). Building performance evaluation: balancing energy and indoor environmental quality in a UK school building. *Build. Serv. Eng. Res. Technol.* 41 (3), 343–360. doi:10.1177/0143624419897397
- Kaasalainen, T., Mäkinen, A., Lehtinen, T., Moisio, M., and Vinha, J. (2020). Architectural window design and energy efficiency: impacts on heating, cooling and lighting needs in Finnish climates. *J. Build. Eng.* 27, 100996. doi:10.1016/j.job.2019.100996
- Karagulian, F., Belis, C. A., Dora, C. F. C., Prüss-Ustün, A. M., Bonjour, S., Adair-Rohani, H., et al. (2015). Contributions to cities' ambient particulate matter (PM): a systematic review of local source contributions at global level. *Atmos. Environ.* 120, 475–483. doi:10.1016/j.atmosenv.2015.08.087
- Kumar, S., Singh, M. K., Loftness, V., Mathur, J., and Mathur, S. (2016). Thermal comfort assessment and characteristics of occupant's behaviour in naturally ventilated buildings in composite climate of India. *Energy Sustain. Dev.* 33, 108–121. doi:10.1016/j.esd.2016.06.002
- Loftness, V., Hakkinen, B., Adan, O., and Nevalainen, A. (2007). Elements that contribute to healthy building design. *Environ. Health Perspect.* 115 (6), 965–970. doi:10.1289/ehp.8988
- López, L. R., Dessi, P., Cabrera-Codony, A., Rocha-Melognio, L., Kraakman, B., Naddeo, V., et al. (2023). CO₂ in indoor environments: from environmental and health risk to potential renewable carbon source. *Sci. Total Environ.* 856, 159088. doi:10.1016/j.scitotenv.2022.159088
- Moyano, D. B., Fernández, M. S. J., and Lezcano, R. A. G. (2020). Towards a sustainable indoor lighting design: effects of artificial light on the emotional state of adolescents in the classroom. *Sustainability* 12, 4263. doi:10.3390/su12104263
- Moyano, D. B., Paraiso, D. A., and González-Lezcano, R. A. (2022). Possible effects on health of ultrasound exposure, risk factors in the work environment and occupational safety review. *Healthcare* 10, 423. doi:10.3390/healthcare10030423
- Ribeiro, C., Ramos, N. M. M., and Flores-Colen, I. (2020). A review of balcony impacts on the indoor environmental quality of dwellings. *Sustainability* 12, 6453. doi:10.3390/su12166453
- Rupp, R. F., Vásquez, N. G., and Lamberts, R. (2015). A review of human thermal comfort in the built environment. *Energy Build.* 105, 178–205. doi:10.1016/j.enbuild.2015.07.047
- Sansaniwal, S. K., Kumar, S., Jain, N., Mathur, J., and Mathur, S. (2021b). Towards implementing an indoor environmental quality standard in buildings: a pilot study. *Build. Serv. Eng. Res. Technol.* 42 (4), 449–483. doi:10.1177/0143624421997989
- Sansaniwal, S. K., Mathur, J., and Mathur, S. (2021a). Quantifying occupant's adaptive actions for controlling indoor environment in naturally ventilated buildings under composite climate of India. *J. Build. Eng.* 41, 102399. doi:10.1016/j.job.2021.102399
- Sansaniwal, S. K., Mathur, J., and Mathur, S. (2022). Review of practices for human thermal comfort in buildings: present and future perspectives. *Int. J. Ambient Energy* 43, 2097–2123. doi:10.1080/01430750.2020.1725629
- Serrano-Jiménez, A., Lizana, J., Molina-Huelva, M., and Barrios-Padura, Á. (2020). Indoor environmental quality in social housing with elderly occupants in Spain: measurement results and retrofit opportunities. *J. Build. Eng.* 30, 101264. doi:10.1016/j.job.2020.101264
- Soharu, A., Naveen, B. P., and Sil, A. (2021). Effectiveness of existing green rating systems towards zero waste construction. *AIP Conf. Proc.* doi:10.1063/5.0066416
- Tartarini, F., Schiavon, S., Cheung, T., and Hoyt, T. (2020). CBE Thermal Comfort Tool: online tool for thermal comfort calculations and visualizations. *SoftwareX* 12, 100563. doi:10.1016/j.softx.2020.100563
- Toyinbo, O. (2019). "Indoor environmental quality," in *Sustainable construction technologies: life-cycle*. Amsterdam, Netherlands: Elsevier.
- Tran, V., Park, D., and Lee, Y. C. (2020). Indoor air pollution, related human diseases, and recent trends in the control and improvement of indoor air quality. *Int. J. Environ. Res. Public Health* 17, 2927. doi:10.3390/ijerph17082927
- Veitch, J. A., Farley, K. M. J., and Newsham, G. R. (2002). Environmental satisfaction in open-plan environments: 1. Scale validation and methods. Available at <http://nparc.cisti-icist.nrc-cnrc.gc.ca/npsi/ctrl?action=rtldoc&an=20386149>.



An Investigation of Indoor Air Quality in a Recently Refurbished Educational Building

R. S. McLeod^{1*}, M. Mathew², D. Salman³ and C. L. P. Thomas³

¹Institute of Building Physics, Services and Construction, Graz University of Technology, Graz, Austria, ²Grune Designs, Mumbai, India, ³Department of Chemistry, Loughborough University, Loughborough, United Kingdom

OPEN ACCESS

Edited by:

Hasim Altan,
Arkin University of Creative Arts and
Design (ARUCAD), Cyprus

Reviewed by:

Lexuan Zhong,
University of Alberta, Canada
Andrea Spinazzè,
University of Insubria, Italy

*Correspondence:

R. S. McLeod
mcleod@tugraz.at

Specialty section:

This article was submitted to
Indoor Environment,
a section of the journal
Frontiers in Built Environment

Received: 02 September 2021

Accepted: 01 November 2021

Published: 07 January 2022

Citation:

McLeod RS, Mathew M, Salman D and
Thomas CLP (2022) An Investigation of
Indoor Air Quality in a Recently
Refurbished Educational Building.
Front. Built Environ. 7:769761.
doi: 10.3389/fbuil.2021.769761

Young people spend extended periods of time in educational buildings, yet relatively little is known about the air quality in such spaces, or the long-term risks which contaminant exposure places on their health and development. Although standards exist in many countries in relation to indoor air quality in educational buildings, they are rarely subject to detailed post-occupancy evaluation. In this study a novel indoor air quality testing methodology is proposed and demonstrated in the context of assessing the post-occupancy performance of a recently refurbished architecture studio building at Loughborough University, United Kingdom. The approach used provides a monitoring process that was designed to evaluate air quality in accordance with United Kingdom national guidelines (Building Bulletin 101) and international (WELL Building) standards. Additional, scenario-based, testing was incorporated to isolate the presence and source of harmful volatile organic compounds, which were measured using diffusive sampling methods involving analysis by thermal desorption - gas chromatography - mass spectrometry techniques. The findings show that whilst the case-study building appears to perform well in respect to existing national and international standards, these guidelines only assess average CO₂ concentrations and total volatile organic compound limits. The results indicate that existing standards, designed to protect the health and wellbeing of students, are likely to be masking potentially serious indoor air quality problems. The presence of numerous harmful VOCs found in this study indicates that an urgent revaluation of educational building procurement and air quality monitoring guidelines is needed.

Keywords: post-occupancy evaluation (POE), indoor air quality (IAQ), Building Bulletin 101 (BB101), volatile organic compounds (VOCs), thermal desorption gas chromatography mass spectrometry (TD-GC-MS), mechanical ventilation, ventilation in educational buildings, air pollution

INTRODUCTION

Air pollution exerts one of the largest single impacts on human health and life expectancy (Kelly and Fussell, 2015; Health Effects Institute, 2019). Current estimates suggest that around 5 million premature deaths occur each year as a result of indoor and outdoor air pollution (Health Effects Institute, 2019). Although global mortality rates have declined over the past decade, largely due to the tightening of air pollution legislation in China, the impacts of air pollution are not confined to developing economies. Recent research has shown that ambient air pollution in Europe is responsible for a much greater mortality factor than previously assumed. Around 800,000 deaths each year are

directly attributed to air pollution in Europe (EU-28) with the mean loss of life expectancy (LLE) estimated at 2.2 years (Lelieveld et al., 2019). Cardiovascular disease (CVD) (including myocardial infarctions, strokes, hypertension, diabetes, and atherosclerosis) comprises the majority of air pollution induced morbidity and mortality (Münzel et al., 2018). In the USA, ambient air pollution emission levels have dropped steadily since the 1970s as a result of the Clean Air Act (US EPA, 2019). Despite this progress, a recent report by the American Lung Association (ALA, 2020) highlighted that nearly 50% of all Americans inhabit counties with unhealthy levels of ozone and/or particulate pollution.

Indoor air quality (IAQ) is a term used to encompass the 'physical, chemical and biological characteristics of air in the indoor environment and its relation to the occupant's physical and psychological health, comfort and productivity' (Klepeis et al., 2001; Riggs, 2014). The importance of investigating the causes of poor IAQ in (Fanger, 2006; Riggs, 2014) diverse contexts cannot be overstated in light of the fact that, in developed countries, humans spend more than 90% of their time (on average) indoors (Riggs, 2014; ALA, 2020).

In many contexts indoor air has been routinely found to be more contaminated than outdoor air, since it contains additional pollutants emitted from building materials, consumer products and human activities (Klepeis et al., 2001; Chan, 2002; Chen and Zhao, 2011; Li et al., 2017).

Indoor Air Quality Within Educational Buildings

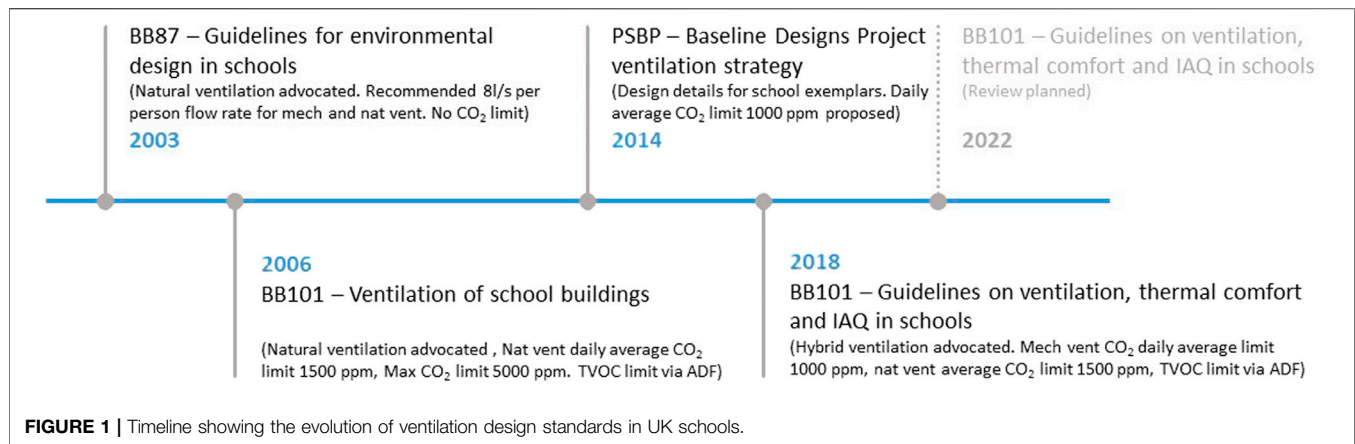
The topic of IAQ in educational buildings is of particular importance because children and young adults spend more time in educational institutions than in any other indoor environment except their home (Bakó-Biró et al., 2012). Furthermore, children and adolescents are known to be particularly susceptible to poor air quality (Yang et al., 2009) since they breathe large volumes of air relative to their body weights, at a stage when their tissues and organs are still developing (RCP, 2016). Documented health impacts associated with educational buildings, include allergies, asthma, airway hyper-reactivity and cardiovascular disease (Carrer et al., 2002; Kim et al., 2007; Cochran Hameen et al., 2020). Moreover, the consequences of poor IAQ in the educational setting are not confined to students, with two US occupational health studies showing that educational employees have the highest prevalence of work related asthma of any single occupation (Fletcher et al., 2006; Mazurek et al., 2008). Beyond these direct health impacts, poor IAQ has been shown to impact student productivity and performance (Bakó-Biró et al., 2012), thereby degrading the learning environment and impacting upon academic attainment and wellbeing (Carrer et al., 2002; Yang et al., 2009; Bakó-Biró et al., 2012; RCP, 2016).

One of the largest studies of indoor air quality (IAQ) and sick building syndrome (SBS) in European schools to date (the SINPHONIE study) (Baloch et al., 2020) collected qualitative data from over 7,000 children and 319 teachers in order to ascertain both the physical and perceived characteristics of

classrooms and the school environment in general. The study was supported by quantitative analysis of key air pollutants and other environmental factors drawn from 115 schools in 54 cities across 23 European countries. The contaminants analysed included: Volatile Organic Compounds (VOCs) ($\mu\text{g}/\text{m}^3$), Particulate Matter (PM) 2.5, Carbon Monoxide (CO) (ppm), Ozone, and Radon (Bq/m^3). The study concluded that European school children are exposed to a wide variety of harmful air pollutants at levels well above those recommended by national and international standards and this was found to be adversely associated with various health outcomes. Despite its breadth, the study was limited by the use of relatively short-term measurements of key indoor air pollutants (IAPs), which might not be representative of long-term exposure levels (Baloch et al., 2020). A similar cross-sectional study carried out in the US Midwest (in 2017) compared the VOC concentrations in high performance elementary schools to conventional school buildings. The study (Zhong et al., 2017) identified 24 different VOC species indoors but found no systematic differences between high performance (EnergyStar and LEED certified buildings) and conventional schools.

Educational buildings, like any other building, must comply with national building regulations; however, the functional requirements of such regulations are often drafted in broad terms. For this reason, government regulatory bodies typically issue guidance documents demonstrating practical ways with which to achieve compliance with the regulations. In England and Wales these are known as Approved Documents (ADs), with ADF (HM Government, 2015) providing guidance on ventilating buildings. Requirement F1 (1), from Part F of Schedule 1 to The Building Regulations 2010, states: "There shall be adequate means of ventilation provided for people in the building" (HM Government, 2000). In relation to schools and educational buildings ADF states that, "Ventilation provisions in schools can be made in accordance with the guidance in Building Bulletin 101" and that "Building Bulletin 101 can also be used as a guide to the ventilation required in other educational buildings such as further education establishments...". (Education and Skills Funding Agency, 2018). Thus, although intended primarily for schools, Building Bulletin 101 (BB101) has been widely adopted in the further education and higher education sectors, in the absence of more specific guidance. Building Bulletins address the whole indoor environment and have evolved over time (Figure 1) in response to emerging evidence regarding issues such as the risk of overheating (McLeod and Swainson, 2017) and poor IAQ in schools, with the most recent guidance being published in BB101 (2018) (Education and Skills Funding Agency, 2018).

CO_2 is a metabolic by-product of cellular respiration and is recognised as a contaminant at elevated room concentrations (Jacobson et al., 2019). Although relatively high levels of CO_2 exposure pose no imminent danger to health, they are known to reduce concentration thereby decreasing the academic performance of students (Mendell et al., 2013; Jacobson et al., 2019) whilst also increasing absenteeism (Shendell et al., 2004). Since CO_2 concentration varies as a function of the occupancy



level and air change rate it has been widely adopted as an indicator of ventilation effectiveness in buildings. According to European Standard EN16798-1:2019 (CEN, 2019) indoor CO₂ levels of 550, 800 and 1,350 ppm above the outdoor concentration, correspond to Categories I; II; III and IV respectively for High; Medium; and Moderate/Low levels of expectation, in terms of IAQ. The recommended United Kingdom Department for Education (DfE) design targets for CO₂ levels set in BB101 correspond to category II (Medium expectation) of EN16789 for mechanically ventilated buildings, with an allowance for category III for part of the time if natural and hybrid ventilation systems are used (Education and Skills Funding Agency, 2018).

Current ventilation standards referred to in the building codes of Europe, North America and elsewhere, have largely been formulated on the basis of establishing minimum ventilation rates to dilute bio effluents (i.e. unpleasant odours) in order to mitigate the risks of occupant discomfort (Carrer et al., 2018). In practice this means that IAQ control in guidance documents such as EN16798 (CEN, 2019), ADF (HM Government, 2015) Building Bulletin (BB)101 (Education and Skills Funding Agency, 2018), ASHRAE 62.1 (ASHRAE, 2019) and the International WELL Building Standard (International WELL Building Institute, 2020a) describe threshold limit values (TLVs) for CO₂ based on achieving the minimum fresh air flow rates needed to dilute gaseous contaminants. As a result, IAQ control strategies in modern mechanically ventilated buildings have relied largely on the use of demand control ventilation (DCV) regulated according to the CO₂ concentration within a space (Awbi, 2003).

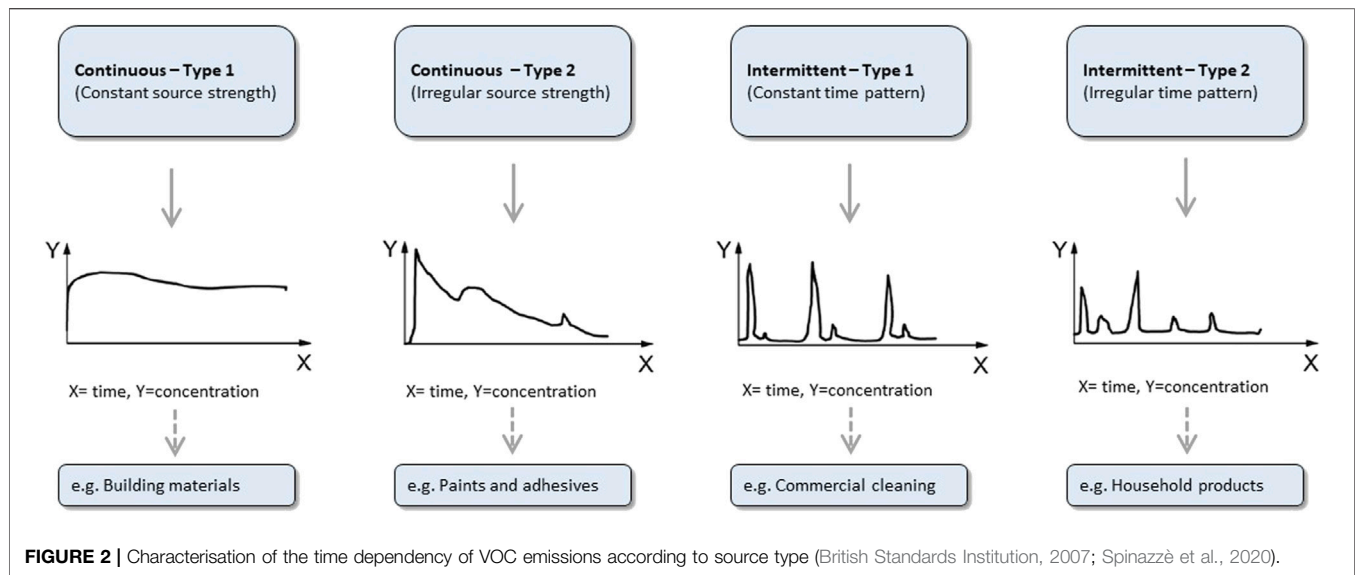
A strong correlation has been demonstrated between the air change rates in schools (which are significantly associated with CO₂ concentrations) and the resultant indoor environmental quality (IEQ) (Zhong et al., 2019). Despite this fact a growing number of studies (Shaughnessy et al., 2006; Haverinen-Shaughnessy et al., 2011; Turunen et al., 2013) have criticised the use of CO₂ as a single proxy indicator of air quality on the basis that it ignores the role of harmful contaminants released from the building fabric, furnishings, appliances and consumer products within the building envelope. Furthermore, it is well established that the indoor environment consists of various

pollutants whose concentration indoors depends upon numerous factors (Jacobson et al., 2019), including:

- Volume of air contained in the indoor space
- Rate of production of each pollutant
- Rate of release of each pollutant
- Rate of removal of the pollutant from the air via reaction or settling
- Rate of air exchange with the outside air
- Quality of the outside air

From this perspective, the precise ventilation rate needed (using a contaminant dilution approach) to maintain acceptable levels of pollutants in a building is difficult to determine and is likely to vary over time. This is further compounded by the fact that the combined effect of two (or more) pollutants (A and B) can be synergistic ($C > A + B$), additive ($C = A + B$), antagonistic ($C < A + B$) or independent (Turunen et al., 2013; Gaihe et al., 2014). Thus, dilution using outside air is not always sufficient in improving IAQ in buildings, and in many contexts it may actually increase indoor air pollutants (Chan, 2002; Chen and Zhao, 2011; Carrer et al., 2018).

In recent decades a number of additional drivers have impacted upon the IAQ in educational buildings. The evolution of teaching pedagogy towards active learning and learner-centred teaching processes (Freeman et al., 2014) coupled with economic constraints led to the 1960s and 70s being characterised by 'open-plan' classrooms. This trend towards fewer but larger classrooms has continued to this day (Wall et al., 2008). Overcrowding has become an ever increasing problem for United Kingdom universities, as many universities have resorted to over-subscribing their courses in order to increase tuition-fee income (Boscott, 2020) with university applications currently at record levels (Weale, 2020). Alongside these transitions, the successive tightening of national building regulations and the introduction of the Energy Performance of Buildings Directive (2010/31/EU) (The European Parliament and The Council of the European Union, 2010) has driven improvements in the energy performance of educational buildings across the EU. It is estimated that these legislative



drivers may have led to a substantial reduction in school ventilation rates, with a corresponding increase in the concentration of some indoor air pollutants (Stranger et al., 2015). The compounding nature of these issues suggests that much clearer guidance is needed when new build and refurbishment measures are undertaken in educational buildings.

Volatile Organic Compounds

According to Yu and Crump (Yu and Crump, 1998) the incorporation of new building materials in energy-efficient building refurbishment can have a significant impact on IAQ for prolonged periods (in some cases beyond 2 years) mainly due to the off-gassing of a wide range of Volatile Organic Compounds (VOCs). VOC concentrations are typically much higher indoors compared to outdoors due to the multitude of potential sources (Brown et al., 1992; Guo et al., 2004; Lee et al., 2005), restricted internal dilution volumes and relatively low air change rates (Brown et al., 1992; The European Parliament and The Council of the European Union, 2010; Weale, 2020). Cross sectional studies, such as the pan-European OFFICAIR study (Campagnolo et al., 2017) have shown (in the context of office buildings) that the most prevalent sources of VOCs, including aldehydes, can be directly linked to building materials (e.g. carpet, flooring, paints etc).

The temporal profile of VOCs in buildings is highly dynamic in nature, this is because building materials can act as emission sinks before subsequently becoming secondary sources as they reemit adsorbed chemicals (ASHRAE, 2017; Lucattini et al., 2018). Indoor climatic characteristics (including temperature and relative humidity) have been shown to be important determinants of VOC and aldehyde concentrations (Spinazzè et al., 2020). Whilst adsorption processes may temporarily lead to lower peak concentrations, the subsequent desorption process prolongs the presence of indoor air pollutants (ASHRAE, 2017;

US EPA, 2020). Thus, the type of materials and compounds and the environmental conditions present in a given space can greatly influence the rate of adsorption and desorption, which can be visualised in time dependency profiles (Figure 2).

Individual VOC concentrations depend upon the presence or absence of an extremely wide range of potential emission sources and sinks (Seifert and Ullrich, 1987; British Standards Institution, 2007; ASHRAE, 2017). Identification and quantification of all of the individual VOCs found in the indoor air is currently limited as the knowledge base is still sparse (Wolkoff and Nielsen, 2001). BB101 acknowledges that “VOCs can present a risk to the health and comfort of occupants...and can adversely affect children particularly those in vulnerable groups (for example, those that suffer asthma and allergies)” (Education and Skills Funding Agency, 2018). However, it goes on to state that, “At the levels found in school buildings their most likely health effect is short-term irritation of the eyes, nose, skin and respiratory tract” (Education and Skills Funding Agency, 2018). BB1010 makes a number of recommendations in relation to VOCs suggesting that potentially harmful emissions can be reduced by avoiding or eliminating the sources of pollutants (e.g., by the careful selection of materials) however it stops short of providing specific recommendations for VOC monitoring or sampling. Some air quality guidelines, including AD F of the United Kingdom Building Regulations (HM Government, 2015), advocate using the simplified method of assessing total volatile organic compounds (TVOC) rather than individual values. As a result TVOC concentrations above $300 \mu\text{g}/\text{m}^3$ (averaged over an 8-h occupancy period) have been widely adopted as an indicator of poor IAQ (Berglund et al., 1997; Molhave et al., 1997; Oppl and Neuhaus, 2008; Abdul-Wahab et al., 2015). Using this approach, the TVOC value is determined by summing the concentrations of both identified and unidentified volatile organic compounds (within a specified range) in the measured air sample (Molhave et al., 1997). There are major drawbacks to this

approach however, in that it is of little help in determining the toxicological properties of the specific substances present (Berglund et al., 1997) nor the source or extent of the problem (Woolley, 2016). Moreover, there is inadequate scientific evidence from which to establish limiting values and guidelines for TVOCs. Hence, proposing a defined TVOC exposure limit entails an unquantifiable risk for the health and wellbeing of building occupants, where the actual risk depends upon the precise mixture of VOCs present in any given situation (Oppl and Neuhaus, 2008) as well the vulnerability of the occupants and the duration of exposure. Even in relation to individual VOCs there are significant discrepancies between the acceptable limits specified in various international standards (Molhave et al., 1997; Oppl and Neuhaus, 2008). Furthermore there are numerous indoor VOCs of concern that remain unregulated by national regulatory bodies and standards (European Parliament, 2004; The European Parliament and The Council of the European Union, 2010; Abdul-Wahab et al., 2015).

Despite the popularity of their usage, the basis for using CO₂ and TVOC as proxy indicators of acceptable IAQ in buildings remain poorly established. According to the Royal College of Physicians CO₂ and TVOC are, “not indicators of potential health effects but rather of problems with ventilation that could lead to health effects” (RCP, 2016, p23). This distinction is important in the context of the standards used to benchmark the safety and acceptability of IAQ in educational buildings. Numerous longitudinal studies have shown that TVOC concentrations display a strong temporal dependency following the completion of new and renovated buildings (Holøs et al., 2019; Persson et al., 2019; Suzuki et al., 2019). Mysen et al. (2003) and Wachenfeldt et al. (2007) proposed that for buildings such as schools and offices indoor air pollution could be successfully controlled using demand-controlled mechanical ventilation. A meta-analysis of longitudinal studies carried out by Holøs et al., 2019) confirmed that whilst the rate of ventilation has no significant impact on emission rates it can be fundamental to controlling airborne contaminant concentrations. In line with this observation European Norm EN16798-1 notes that, “the dilution required for reducing the health risk from a specific air pollutant shall be evaluated separately from the ventilation rates required to obtain a desired perceived air quality level. The highest of these ventilation rate values shall be used for the design. If critical sources are identified for health, it shall be checked that they remain below the health threshold values” (Jacobson et al., 2019). However, in the context of non-residential buildings EN16798-1 states that, “For the design of ventilation systems and calculation of design heating and cooling loads, the design ventilation rate shall be specified based on national requirements. . . . Therefore, in the context of United Kingdom educational buildings the national requirements set out in ADF and BB101 take precedence over EN16798-1. Ignoring legislative constraints, in practice the success of such a strategy would require knowledge of the local emission rates of all harmful pollutants. Despite such realisations little has been published in the way of detailed guidance for the detection and control of indoor air contaminants within educational buildings and in particular

protocols to limit elevated rates of harmful off-gassing in newly built and refurbished buildings.

The following research was conducted in order to shed light on the implications of current IAQ guidance in the context of United Kingdom educational buildings. An action research case study involving IAQ monitoring in a United Kingdom university building, which had undergone extensive refurbishment, in accordance with ADF of the United Kingdom Building Regulations (and therein BB101) is used to explore these issues. The aim of this work is to assess the post-completion IAQ of this building under operational conditions (6–12 months post-completion) in order to evaluate whether the design methodology in BB101, with respect to the identification and management of indoor air contaminants, is adequate to mitigate impaired academic performance as well as potential long terms health effects.

METHODS

The primary focus of this paper is on demonstrating a robust and replicable methodology to address the shortfalls of existing IAQ standards in educational buildings and for this reason a single building was chosen as a pilot case-study. Although no single building can ever be considered representative of the entire education stock from an IAQ perspective, most United Kingdom school, college and university new build and refurbishment projects are procured through procurement partnership frameworks (Crowe et al., 2013). This means that there are a limited number of suppliers registered on any given procurement framework which can bid for a contract, with the result that similar construction materials and products are widely used in educational buildings on a regional and national basis. The purpose of this case study is therefore illustrative, in order to highlight the application of the methodology in relation to current IAQ standards, rather than to generalise more widely about the specific findings.

In order to assess the implications of BB101 and current United Kingdom legislative guidance, in the context of a refurbished educational building, a broad IEQ monitoring strategy was developed which involved monitoring of the dry bulb temperature, globe temperature, relative humidity, ventilation flow rates as well as IAQ parameters. Since the focus of this paper is on the IAQ aspects of this campaign, the methods will discuss only these aspects, which consisted of monitoring CO₂ concentrations at multiple locations and conducting discrete diffusive (passive) air sampling in an attempt to identify the VOCs present in the space. This approach provided the potential to investigate CO₂ concentrations at a relatively high spatial and temporal resolution as well as to detect a wide range of VOCs. The presence of other potentially harmful contaminants, such as particulates, were not addressed in this study, as they are predominantly introduced via the outside air (and combustion and particulate generating activities do not occur inside this building) (Riley et al., 2002). Furthermore, the outdoor air brought in via the ventilation system was not

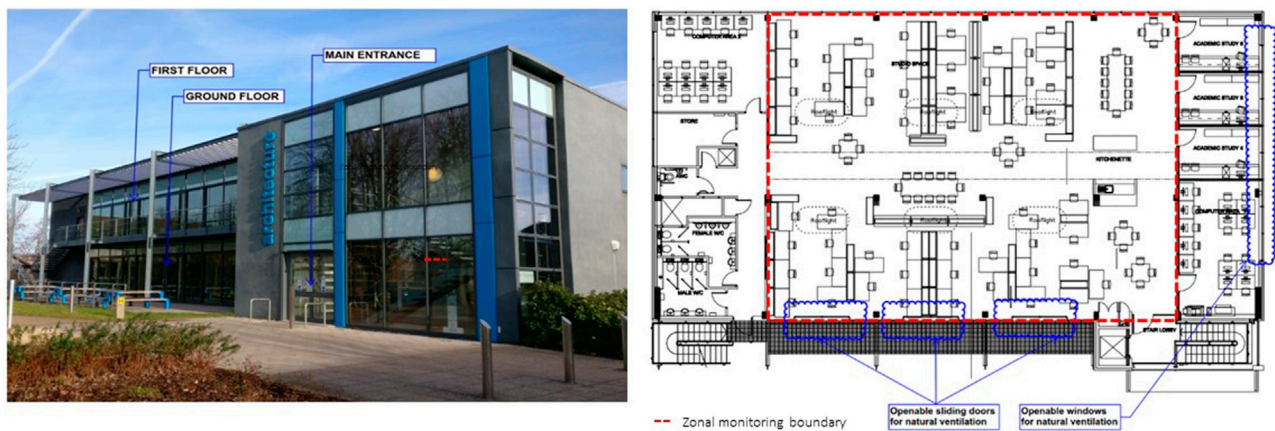


FIGURE 3 | Keith Green Building, School of Architecture, Loughborough University (left) and First Floor Open Studio space used for the IAQ monitoring campaign (right).

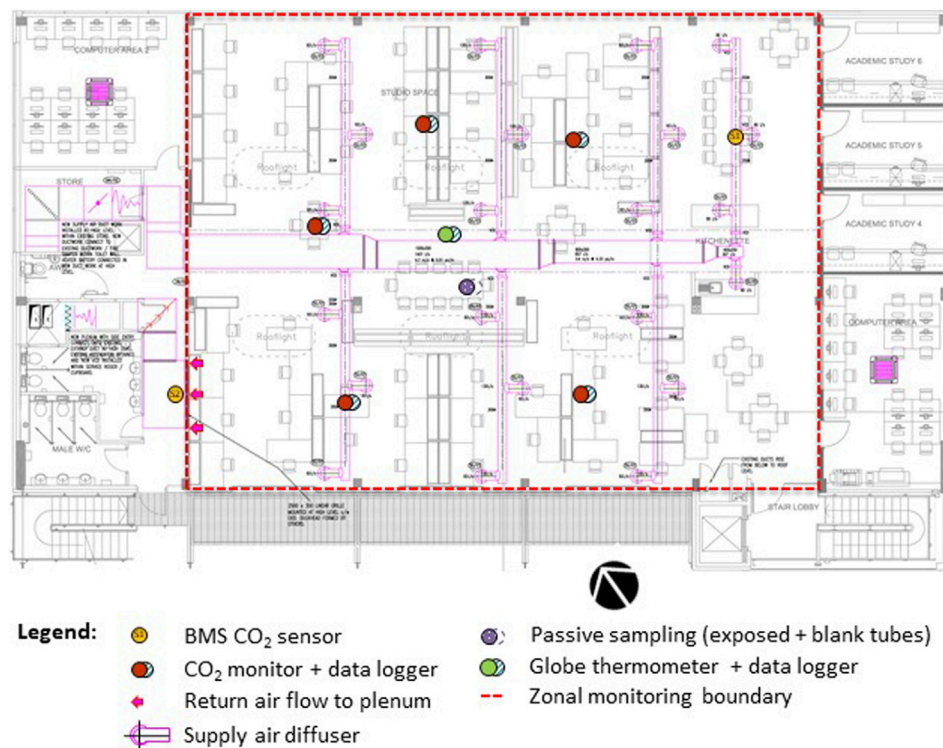


FIGURE 4 | First-floor plan showing ventilation ductwork layout (magenta) and the positions of monitoring and sampling devices.

directly studied as this would have required repeated long-term sampling in the proximity of the building to establish the repeated presence and sources of any external contaminants identified (which would typically be conducted over an extended period, to capture both the cold and warm periods of the year). Thus, the following methodology was adopted in order to evaluate whether the application of BB101 in this context was sufficiently robust to provide good quality

ventilation and avoid VOC exposure which might pose a health risk to the occupants.

Case Study Building

The recently refurbished Keith Green Building (Figure 3, left) serves as one of the main teaching buildings for the School of Architecture at Loughborough University in the United Kingdom Midlands. The open studio space located on the first-floor space is

TABLE 1 | Monitoring and sampling devices - summary of measured variables, location and sampling intervals.

Monitoring/sampling device	Indoor environmental variable(s)	No. of sensors	Position (height)	Monitoring/sampling interval
Telaire CO ₂ monitor connected to HOBO U12 data logger	Carbon Dioxide concentration (ppm)	5	At table height (see Figure 5)	Every 15 min
Passive sampling thermal desorption tube	Volatile Organic Compounds (boiling point range from 50°C-100°C to 240°C-260°C)	2	At table height (see Figure 5)	8-h exposure
Building Management System (BMS)	Dry bulb temperature (°C)	2	At ceiling duct level (see Figure 5)	Every 15 min
	Relative Humidity (%)	2		
	Carbon Dioxide concentration (ppm)	2		

designed to house a maximum of 100 architecture students (**Figure 3**, right) engaged in studio-based (i.e., design and model building) activities. The nature of undergraduate architecture degree programmes means that the space was not occupied at full capacity for a typical 8-h working day, but rather it was intermittently occupied for continuous periods (sometimes up to 24 h per day) in accordance with project submission deadlines. The open studio space was identified for the IAQ monitoring campaign in this study after strong odours (characteristic of VOC off-gassing) were noted to persist several months after completion of refurbishment works, in August 2017. This led to occupants resorting to opening windows for extended periods, in an attempt to purge ventilate, as the mechanical ventilation system was unable to reduce the presence of the odours.

Heating to the first-floor open studio space is provided via a low temperature hot water (LTHW) trench heating system, which is turned off during the summer months. The open studio space is mechanically ventilated using a ducted variable air volume (VAV) supply and extract ventilation system which is controlled by a building energy management system (BEMS) based on the CO₂ concentration in the space (**Figure 4**). The recommended ventilation rate in BB101 is 5–8 L/s per occupant, although it is noted that, “Higher ventilation rates may be required for practical activities, such as science, design and technology and food technology” (Education and Skills Funding Agency, 2018). Based on the maximum design occupancy of 100 people and a zonal volume of approximately 940 m³ (**Figure 4**) the ventilation system would be expected to deliver 2–3 air change per hour (ACH) when the building was fully occupied.

Indoor Air Quality Monitoring Devices - Location Plan

The location of the monitoring and sampling devices in the first-floor open studio space can be seen in **Figure 4**. VOC sampling took place in the centre of the open-plan room at table height, where the air is likely to be well mixed and sufficiently far away from the ventilation supply and extract terminals to avoid local influences. Five stand-alone CO₂ sensors were dispersed in an approximately equidistant constellation to capture local variations in the CO₂



concentration at desk height, whilst the BEMS CO₂ sensors were located at opposite sides of the space (in predetermined locations as specified by the mechanical ventilation system supplier). A detailed description of the indoor environmental variables that were measured with these devices is provided in **Table 1**.

CO₂ Monitoring Scenarios and Objectives

Monitoring of the CO₂ levels within the space was assessed in accordance with current United Kingdom guidelines and the international WELL building standard. In addition to the general ventilation requirements of **Section 6** of AD F, the United Kingdom Department for Education (DfE) has, via BB101, set the following performance standards for teaching and learning spaces which are intended to ensure compliance with Regulation 6 (Ventilation) of the Workplace Regulations (Health, Safety and Welfare) Regulations 1992 (2013 revision) (HSE, 2013). BB101 states that “where mechanical ventilation is used (or when hybrid systems are operating in mechanical mode) in general teaching and learning spaces, sufficient outdoor air should be provided to ensure the daily average CO₂ concentration is less than 1,000 ppm, during the occupied period. Furthermore, the maximum CO₂ concentration cannot exceed 1,500 ppm for more than 20 consecutive minutes each day when the number of room occupants is equal to, or less than the design occupancy (Education and Skills Funding Agency, 2018, p23). The maximum design occupancy of the open studio space is 100 students (**Figure 4**, right) however in practice the occupancy numbers varied greatly throughout the monitoring campaign and rarely exceeded 50% of this capacity.

BB101 assessments are typically carried out at the design stage using dynamic simulation studies, which utilise the modelling assumptions provided in BB101 (Section 8.1 Internal conditions) (Education and Skills Funding Agency, 2018). There is currently no guidance regarding the assumptions which should be used for the post-occupancy evaluation (POE) of CO₂ concentrations. Although CO₂ is denser than air, CO₂ stratification occurs because exhaled breath is warm, and is either immediately entrained into the main body plume or rises as a secondary plume where it typically settles at an intermediate height before being entrained and carried into the upper layer (Bhagat et al., 2020). Pei et al. (2019) showed that temperature and CO₂

TABLE 2 | Measurement scenarios and their objectives.

Measurement scenario	Scenario objectives	Condition of space
<p>Scenario 1. 'Models present - unventilated' (Unoccupied, night-time, ventilation system OFF)</p> <p>In this scenario, the same air sampling procedure was conducted, on 3 separate occasions, during the night time from 22:00–06:00 (i.e. 8 h) on the 25th, 26th and May 27, 2018 when there was no occupancy</p> <p>While conducting the air sampling measurements for this scenario, the open studio space contained numerous small-architecture models prepared by the students</p>	<p>The objective was to sample the building and its typical contents to capture the combined effect of the following</p> <ul style="list-style-type: none"> • Off-gassing from architectural models • Off-gassing from building materials (e.g. floor coverings, furniture, paints etc.) that have gone into the refurbishment • VOCs brought in via the outside air 	<p>Furniture and numerous architectural models and model making equipment were present throughout the space</p> 
<p>Scenario 2. 'Empty building - unventilated' (Unoccupied, daytime, ventilation system off)</p> <p>In this scenario, the same air sampling procedure was conducted on 3 separate occasions during the daytime from 09:00–17:00 (i.e. 8 h) on the 4th, 5th and July 6, 2018 when there was no occupancy</p> <p>While conducting the air sampling measurements for this scenario, the open studio space was cleared of architecture-models and materials to eliminate the off-gassing from them</p>	<p>The objective was to sample the IAQ of the 'empty building' and capture the following</p> <ul style="list-style-type: none"> • Off-gassing from building materials (e.g. floor coverings, furniture, paints etc.) that have gone into the refurbishment • VOCs brought in via outside air 	<p>Only furniture was present in the space</p> 
<p>Scenario 3. 'Empty building -ventilated' (Unoccupied, daytime, ventilation system on)</p> <p>In this scenario, the same air sampling procedure was conducted on 3 separate occasions during the daytime from 09:00–17:00 (i.e. 8 h) on the 17th, 18th and July 19, 2018 when there was no occupancy</p>	<p>The objective was to repeat Scenario 2 but with the ventilation running in order to capture the following</p> <ul style="list-style-type: none"> • Off-gassing from building materials (e.g. floor coverings, furniture, paints etc.) that have gone into the refurbishment • VOCs brought in via outside air • The dilution effect of ventilation (at normal operation levels) on the presence of VOCs 	<p>Only furniture was present in the space</p> 

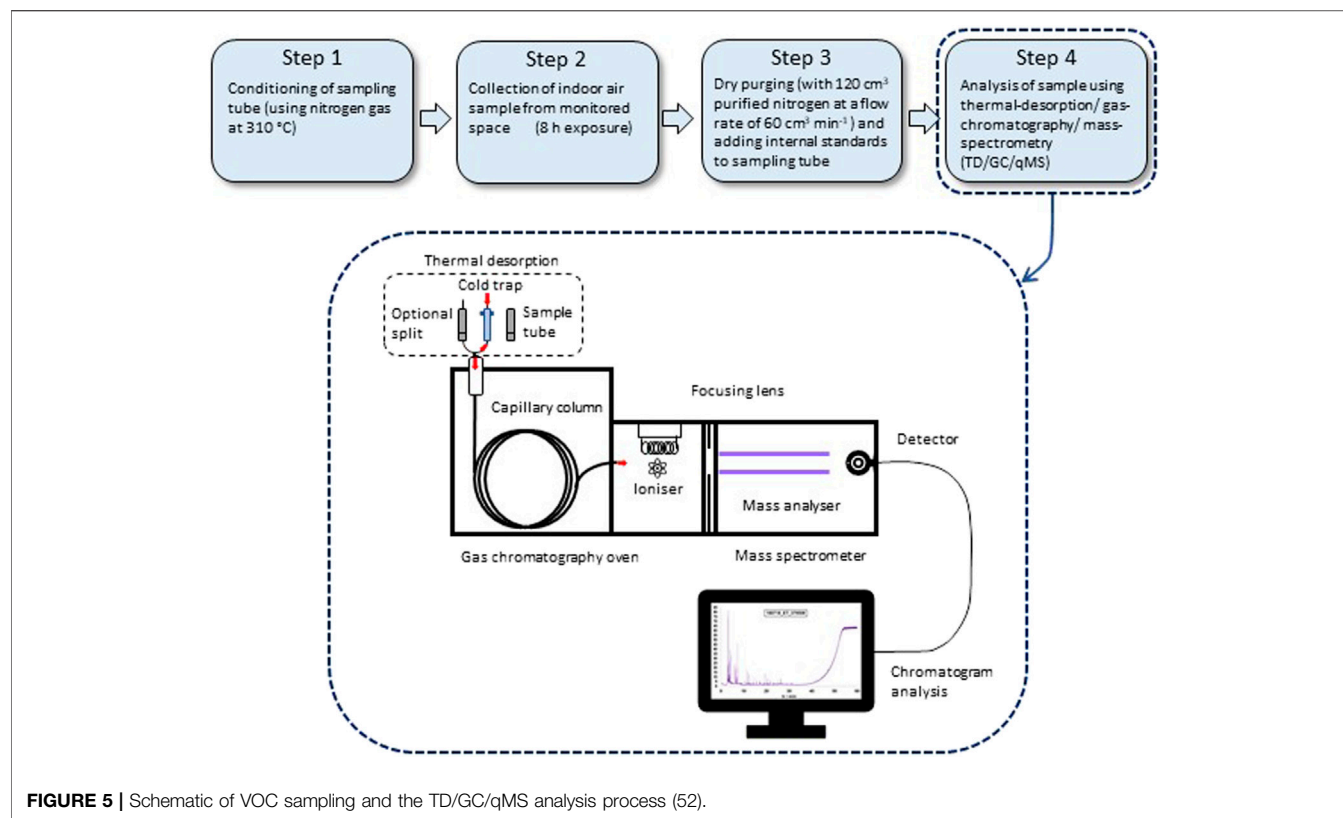


FIGURE 5 | Schematic of VOC sampling and the TD/GC/qMS analysis process (52).

TABLE 3 | GC-MS Instrumentation parameters.

Thermal desorption		Gas chromatography		Mass spectrometer	
Parameters	Setting	Parameters	Setting	Parameters	Setting
t Primary desorption	1 min	F He carrier gas	$2 \text{ cm}^3 \text{ min}^{-1}$	Scan type	Full scan (+ve)
F Primary desorption	$40 \text{ cm}^3 \text{ min}^{-1}$	T Initial	40°C	Mass range	40–550 m/z
T Primary desorption	300°C	t Initial hold	0 min	Ionisation type	EI
T Secondary desorption	5 min	T program	$5^\circ \text{C min to } 300^\circ \text{C}$	ν scan	3 Hz
F Secondary desorption	$50 \text{ cm}^3 \text{ min}^{-1}$	T End	300°C	T line temperature	300°C
T Secondary desorption	300°C	t End hold	0 min	T Quadrupole	150°C
F Cold trap	$20 \text{ cm}^3 \text{ min}^{-1}$	t Total run	60 min	T Manifold	230°C
T Cold trap	-10°C	T Post run	45°C	t Solvent delay	5 min
$(\frac{\delta T}{\delta t})_{\text{trap}}$	$\text{Max}^\circ \text{C min}^{-1}$	t Post run	0 min		
T Trap high	300°C				
t Trap hold	5 min				
T Flow path	200°C				
Mode	Splitless				

Note: t , time; F , flow; T , temperature; and ν , frequency.

stratification is particularly pronounced in mechanically ventilated buildings using displacement ventilation. In this study CO_2 was monitored using two independent systems, in an attempt to establish the most reliable monitoring configuration. The first was situated at the desk-top level using five calibrated Telaire CO_2 sensors (equally distributed in the space) connected to HOBO U12 data loggers logging at 15-min intervals and the second at the ceiling-duct level via two sensors (one at the room outlet plenum and one on the opposite side of

the room, logging at 15-min intervals) connected to the BMS system (Figure 4).

Volatile Organic Compound Monitoring Scenarios and Objectives

Three different VOC sampling scenarios were defined with the intention of identifying the VOCs present under different operational conditions. The VOC sampling objectives

corresponding to the three IAQ scenarios are described in **Table 2**. During the sampling process paired diffusive tubes (i.e., an exposed tube and a blank tube) were deployed side-by-side. VOC samplers used 10 cm Tenax®/Carbotrap 1TD hydrophobic absorbent tube (Markes International Ltd., Llantrisant, United Kingdom) with a 5 mm diffusion gap. Before sampling the tubes were pre-conditioned at 310°C for 30 min with high purity nitrogen gas, before being capped and stored in a closed container ready for sampling. During sampling the exposed tube, with the diffusion cap, was kept open to the indoor environment to capture the VOCs present in the indoor air whilst the blank tube remained closed (thereby acting as a control). Whilst sampling the tubes were placed in an upright position at the centre of the open studio space at table height, as this is considered to be within the height of the breathing zone of seated occupants (Xing et al., 2001; Licina et al., 2015; Lee et al., 2019). For each scenario, three independent sampling measurements were taken in order to establish repeatability between the VOCs detected. All of the air sampling measurements were conducted during unoccupied periods to eliminate the effects of direct off-gassing from the building occupants, as the aim of the study was to identify only the contribution of VOCs originating within the indoor environment due to materials that had gone into the refurbishment as well as any model-making materials stored in the space.

Description of Volatile Organic Compound Analysis Process

The collected samples were analysed using a thermal-desorption/gas-chromatography/mass-spectrometry (TD/GC/qMS) process. A Unity-2 thermal desorption unit (Markes International, Llantrisant, United Kingdom) was interfaced to a GC (Agilent, 7890A) (using an Rtx-5MS, 0.25 µm 0.25 mm ID column) coupled to a quadrupole mass spectrometer (Agilent MS 5977A). The key stages of this process are shown in **Figure 5**, and the GC-MS instrumentation parameters are provided in **Table 3**.

Procedure for Establishing Repeatability for Compounds Detected in the Chromatogram and Elimination of Background Weight of Compounds

The output of the TD/GC/qMS analysis process is given in the form of a chromatogram, which represents the different VOCs present in the indoor environment based on their retention time. The retention time is a measure of the time taken for a particular solute to pass through a chromatography column and is calculated from the time elapsed between injection into the capillary column and its subsequent detection in the mass analyser (**Figure 5**). The analysis of each sample was undertaken with 60 min as the total retention time.

The following procedure was used for the analysis of the data, in order to establish repeatability between compounds and

eliminate any undesirable background effects caused by VOCs present in the conditioned sampling tubes:

- Step 1 – Normalising the peak area value

The peak area values of the compounds detected in the exposed and blank tube were normalised to the internal standard Toluene-d₈. The unit of the peak area value is counts. For the exposed tube, the normalised peak area value is calculated by dividing the peak area of the compounds in the exposed tube by the peak area value of Toluene-d₈ in the exposed tube. Similarly, for the blank tube, the normalised peak area value is calculated by dividing the peak area of the compounds in the blank tube by the peak area value of Toluene-d₈ in the blank tube.

- Step 2 – Elimination of the background effect

The compounds present in the exposed tube for a particular sampling period are cross-referenced against those present in the blank tube for the same sampling period. If a compound is found to be present in both the exposed and the blank tube, then the normalised peak area value calculated in Step 1 for that particular compound in the exposed tube is reduced by the normalised peak area value of the corresponding compound in the blank tube. If the result of this subtraction is positive, it indicates that the background quantity of the compound present in the blank tube has been eliminated thus leaving only the additional contribution arising from the exposed tube during sampling. If the result of this subtraction is negative, it indicates that the compound was present in the blank tube but not in indoor environment and should therefore be discarded from the results. If the compound is not present in the blank tube, then Step 3.

- Step 3 – Accounting for the injection rate of the internal standard Toluene-d₈

The injection rate of the Toluene-d₈ is 69 pg (pg). The normalised peak area values (calculated in Step 1 & 2) are divided by this injection rate to give the quantity of a particular compound in counts/nanograms (ng) equivalent of internal standard Toluene-d₈.

- Step 4 – Establishing repeatability of identified compounds

As a form of quality control three air sampling measurements (as described in **Table 2**) were conducted for each measurement scenario to establish the repeatability of the identified compounds. In this way each compound identified in an air sampling measurement was cross referenced for its availability in the other air sampling measurements of the same measurement scenario. Compounds found to be repeated in all three air sampling measurements of a measurement scenario can be assumed to indicate their undistinguished presence. Once the compounds repeatedly

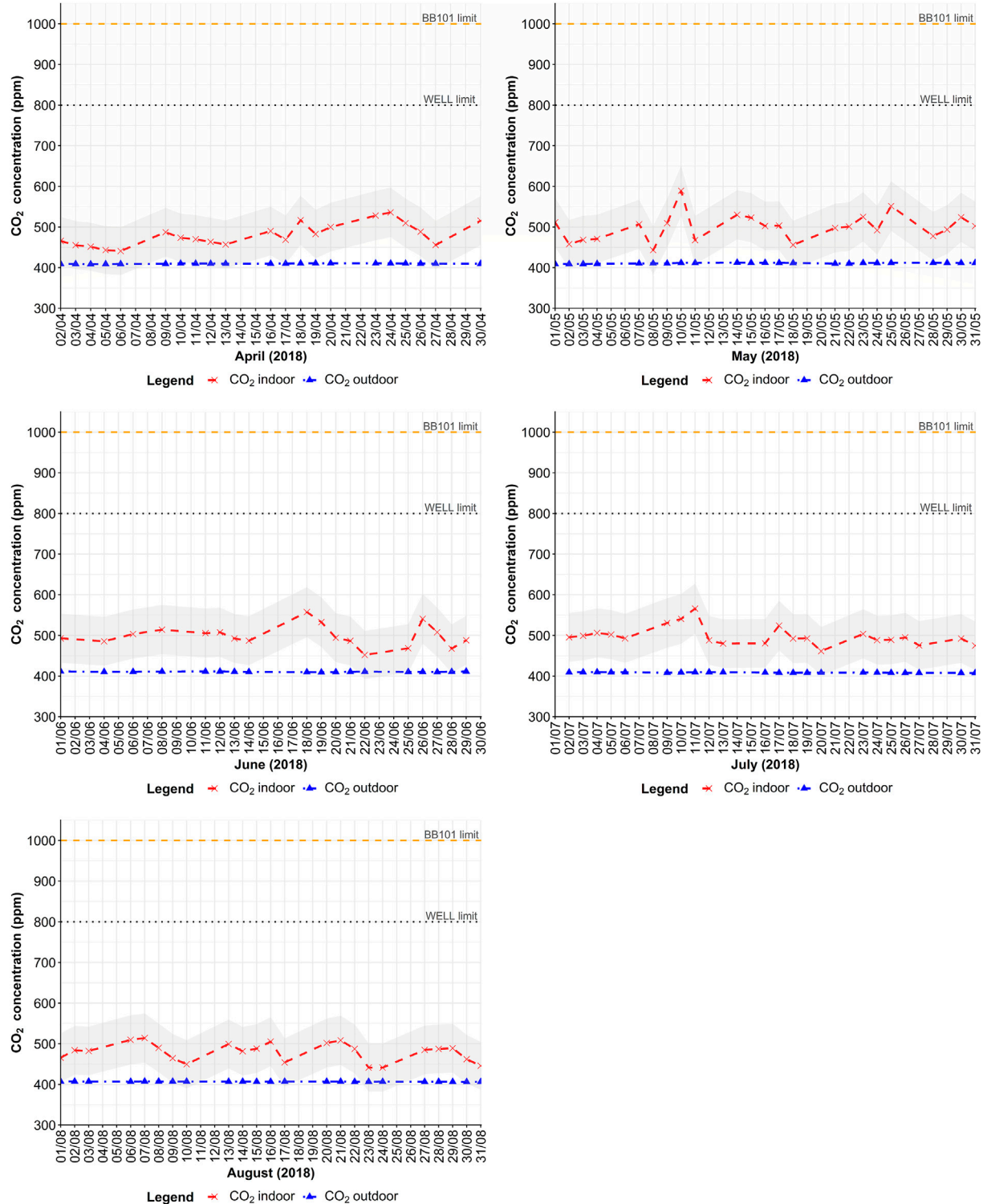


FIGURE 6 | Daily average CO₂ concentrations in the open studio space (Monthly, April–August 2018). Grey ribbon indicates the sensor manufacturer's declared uncertainty interval.

present in all three air sampling measurements for each measurement scenario were identified, these compounds were then checked for their presence across the three

distinct measurement scenarios. Only the compounds which were consistently present in each sample across all of the measurement scenarios are reported.

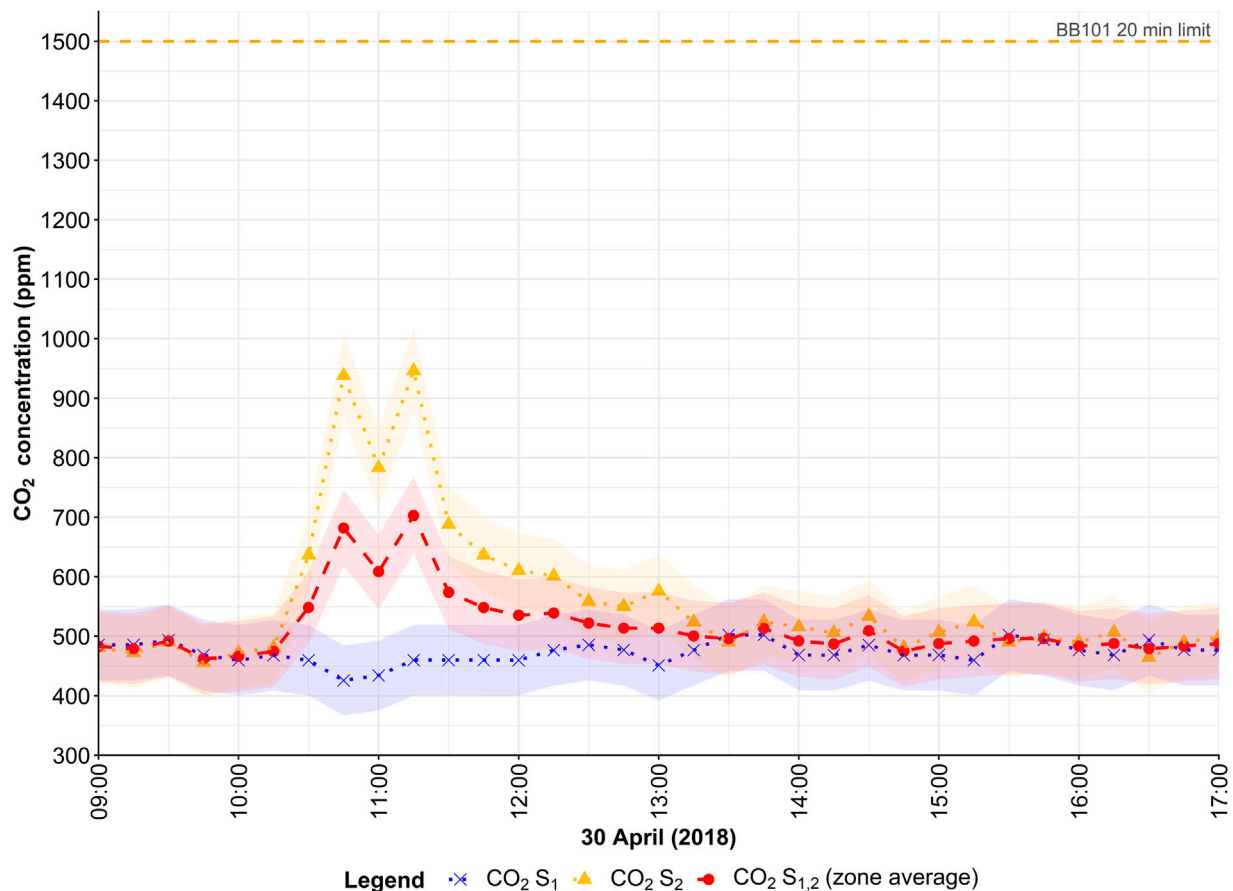


FIGURE 7 | Fifteen-minute CO₂ concentrations in the open studio space (peak day, April 30, 2018) as recorded at S₁, S₂ and the combined zonal average. Coloured ribbons indicate the sensor manufacturer's declared uncertainty interval.

It should be noted that identification of the compounds isolated by this study was limited to those compounds listed by the National Institute for Standards and Technology (NIST) library (NIST, 2019) and specifically to those that possess a chemical compound name and chemical abstract service (CAS) number (putative Level-2 identities following the Metabolomics Standards Initiative (Sumner et al., 2007)). Unknown compounds (i.e., those without a confirmed NIST library match) were not evaluated since their identity could not be established without further investigations.

RESULTS AND ANALYSIS

Assessment of Carbon Dioxide (CO₂) Concentration

Desktop level monitoring of the CO₂ concentration (via the Telaire sensor network) revealed consistently low CO₂ concentrations during the initial monitoring period. This finding was unexpected and is likely to reflect the relatively high ventilation rates set by the BMS system coupled with

CO₂ stratification in the room. The International WELL Building Standard recommends that, for demand-controlled ventilation systems, CO₂ concentration should be measured at 1.2–1.8 m above floor level (International WELL Building Institute, 2020b). Given the possibility that stratification could be influencing the CO₂ levels monitored at desk-top height it was decided that a more representative mean room CO₂ concentration could be obtained from the higher-level sensors linked to the BMS system (Figure 4). The CO₂ concentration was recorded by the BMS system just below the supply ductwork on the NE side of the first-floor open studio (S₁) and at the wall-level exhaust plenum (S₂) at the SW side of the space (Figure 4). The 15-minutely CO₂ readings from S₁ and S₂ were then combined and averaged over the 8-h occupied daytime period (09:00–17:00, Monday to Friday) to obtain the daily average CO₂ values (Figure 6). According to BB101 sufficient ventilation should be provided to achieve a daily average CO₂ concentration of below 1,000 ppm. The monthly plots of the mean daily CO₂ concentration (Figure 6) show that for the entire monitoring period (April–August 2018) the maximum daily average concentration was well within this limit and did not exceed 600 ppm.

TABLE 4 | Ventilation compliance comparison according to national and international ventilation standards, based on the CO₂ concentration in the monitored environment.

Ventilation standards	Criteria for CO ₂ concentration thresholds (ppm)	Meets compliance
BB101 (2018) Guidelines on ventilation, thermal comfort and indoor air quality in schools	'Daily average concentration of CO ₂ during the occupied period of less than 1,000 ppm and so that the maximum concentration does not exceed 1,500 ppm for more than 20 consecutive minutes each day, when the number of room occupants is equal to, or less than the design occupancy' (Education and Skills Funding Agency, 2018)	✓
Chartered Institute of Building Service Engineers (CIBSE) Guide B2 (2016)	800–1,000 ppm recommended range (CIBSE, 2016)	✓
Department for Education, Technical Annex 2F (2020)	Compliance with Section 4 of ADF 2010 with criteria for CO ₂ concentrations as per BB 101 (above). (Department for Education, 2020)	✓
International WELL Building Standard (2020)	CO ₂ levels below 800 ppm need to be maintained in the space (assessed at the 95th percentile) (International WELL Building Institute, 2020a)	✓

BB101 also recommends that the maximum concentration should not exceed 1,500 ppm for more than 20 consecutive minutes each day. To assess this criterion the data was screened to identify the individual days with the highest CO₂ concentrations at a 15 min interval. The peak concentrations were identified as occurring on 30 april (2018). Unsurprisingly, the CO₂ peak was highest at the location of the exhaust sensor (**Figure 4**, S₂) where for a period of approximately 45 min the concentration exceeded 800 ppm (peaking at 950 ppm). The supply side sensor readings (**Figure 4**, S₁) showed a slight drop in CO₂ concentration as the time the exhaust sensor peaked, presumably due to an increase in the flow rate from the BMS in response to the elevated exhaust CO₂ levels. The mean value of the two sensors suggests that the average CO₂ concentration in the space did not exceed 700 ppm at any point (**Figure 6**).

The results of the CO₂ monitoring (**Figures 6, 7**) confirm that the ventilation of the space, during the 5 month long monitoring period, complied with the ventilation performance requirements set out in BB101 (Education and Skills Funding Agency, 2018). Furthermore, the monitored CO₂ concentration compared favourably to other relevant national and international standards as shown in **Table 4**.

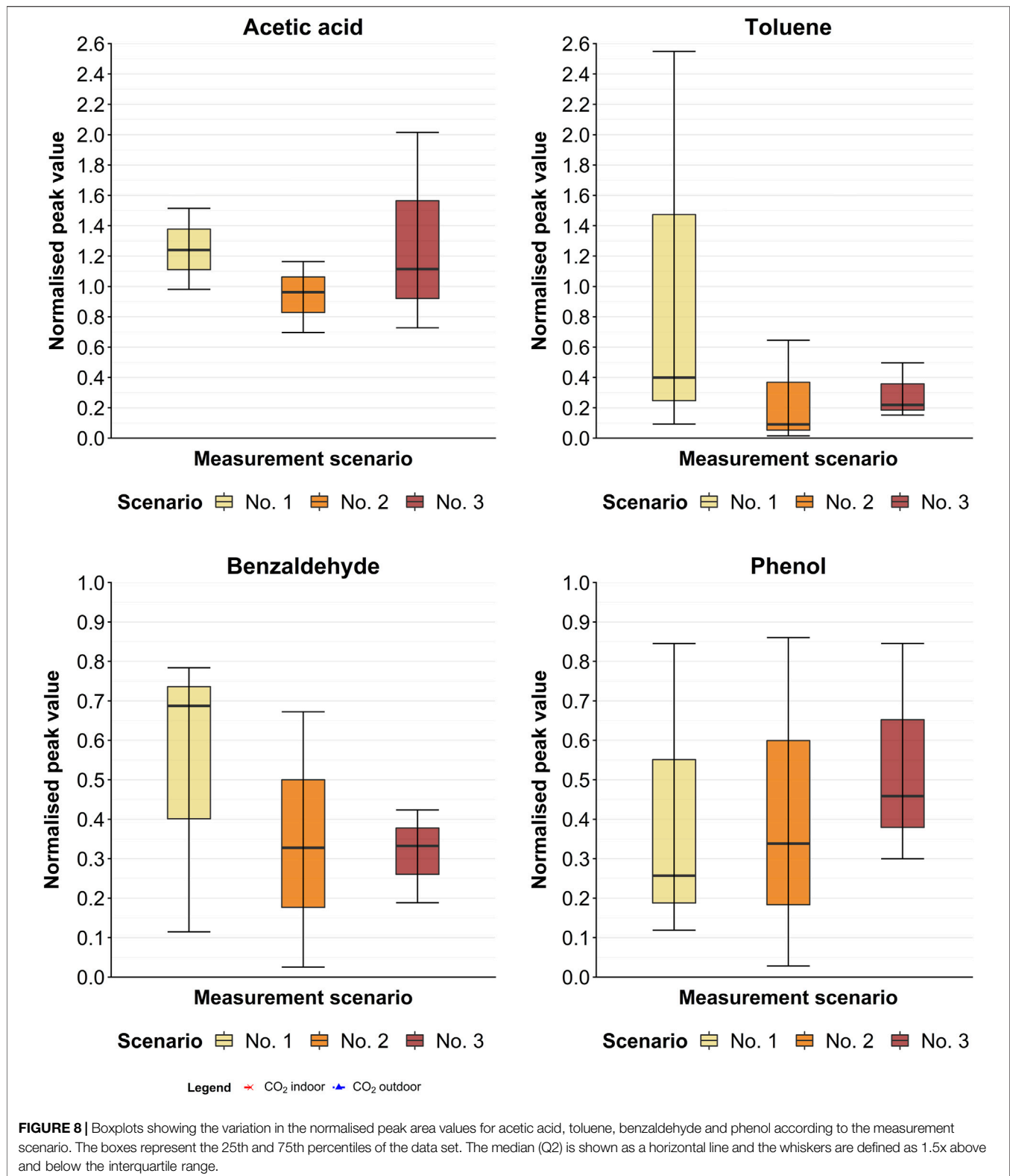
Assessment of Diffusive Sampling for the Detection of Volatile Organic Compounds

The diffusive (passive) samples were analysed by thermal desorption GC-MS (**Figure 5**). This analysis produced a series of graphs known as chromatograms (**Supplementary Appendix**) which represent the spectrum of identified and unidentified compounds obtained for each measurement scenario (**Table 2**). Over two hundred and forty features, including environmental VOCs, ubiquitous artefacts (chemical noise) or siloxane compounds (arising from the analytical components or method) were identified during the sampling scenarios. VOCs such as ethanol, acetic acid, 1-butanol, pentanal, toluene, hexanal, styrene, benzaldehyde and phenol were detected (**Supplementary Appendix**). Of these only four compounds (acetic acid, toluene, benzaldehyde and phenol) were found to be repeatedly present in every measurement scenario, confirming their undistinguished presence in the indoor environment. The variation in the normalised peak values for these compounds, according to the interquartile range for each scenario, is shown in **Figure 8**.

It can be seen (**Figure 8**) that Scenario 1, with the ventilation turned off and architectural models present in the space, provided the highest normalised median peak counts for three of the four isolated compounds (acetic acid, toluene and benzaldehyde). The toluene and benzaldehyde counts were highest in Scenario 1 which suggest some additional contribution of these compounds from the model making process. Notably however, the median value for phenol was higher in Scenario 3 (**Figure 8**) where the ventilation was on and no models were present in the space, which suggests that this VOC was more likely to be associated with the building fabric or even the outside air. Furthermore, it can be seen (**Figure 8**) that although the presence of toluene and benzaldehyde were reduced by the introduction of ventilation in Scenario 3, the presence of acetic acid and phenol were not. This indicates the possibility of an external source for the acetic acid and phenol emissions, or their migration from a source elsewhere in the building, and requires further investigation.

DISCUSSION

The results of the CO₂ monitoring show (**Figure 6**) that the daily average CO₂ concentration remained well within the BB101 1,000 ppm daily average limit throughout the 5-month long monitoring campaign. Similarly, when peak concentrations were assessed (**Figure 7**), according to the BB101 20-min maximum limit of 1,500 ppm, the studio space remained well within the threshold limiting value. Although this study took place prior to the current Covid-19 pandemic it is worth noting that the CO₂ concentrations observed here lie well within the recommended CO₂ limit of 800 ppm published by the United Kingdom Health and Safety Executive (HSE) (HSE, 2021) for the safe operation of ventilation systems during the current SARS-CoV-2 pandemic. It is perhaps unsurprising, in the context of an educational building, that the CO₂ concentration is highly sensitive to the temporal resolution of the monitoring (i.e., daily averaging vs. sub-hourly monitoring). More significantly, in terms of the way guidance and standards are written, this study demonstrates the importance that the spatial positioning of CO₂ sensors exerts on the results. In this study desk-top level monitoring of the CO₂ concentrations was shown to produce relatively low readings (marginally above external



levels) and for this reason higher level sensors, linked to the BMS system, were used to obtain a zonal spatial average (at approximately 2 m above floor level). This finding, regarding

the placement of sensors, is supported by literature which documents the vertical stratification of CO₂ in occupied rooms (Bhagat et al., 2020). In this respect the International Well

Building Standard specifies that CO₂ should be measured at between 1.2 and 1.8 m above the floor level (International WELL Building Institute, 2020b). Whilst BB101 recommends that CO₂ should be measured at seated head height, no information is provided regarding the number of sensors or their recommended location within a space. The paucity of guidance on this issue in BB101 may reflect the fact that there is currently no requirement for *in-situ* monitoring at the post occupancy stage. These findings have significant implications for how future revisions of such standards are written and interpreted, particularly in the context of intermittently occupied open-plan educational spaces.

Across the 5-month monitoring period a broad range of occupancy patterns and densities were observed in monitored space, however the spatially averaged indoor CO₂ concentration remained within a relatively narrow range (433–703 ppm). This finding is in marked contrast with numerous previous studies of educational buildings which have reported CO₂ levels substantially above existing TLVs (CIBSE, 2016; Pei et al., 2019; Baloch et al., 2020); this outcome can be attributed to a number of factors specific to the operation of this building:

- The fresh air supply rate exceeded the 8 L/s per person specified for classrooms according to BB101 (2018).
- CO₂ measurements were spatially averaged using only two locations in the open studio space. This could have led to an underestimation of localised CO₂ concentrations in the context of a single zone space with a relatively large internal floor area (377 m²). Whilst BB101 indicates that the CO₂ levels should be measured at seated head height no information is provided regarding the number of sensors, their accuracy, or their location within a room.
- After June 2018 (during the summer period) low to moderate occupancy was observed.
- The demand control ventilation (DCV) system employed in the building appears to respond rapidly to the changes in the exhaust plenum CO₂ concentration.
- The positioning of the circular supply air diffusers and the exhaust grille (Figure 4) is facilitating good air mixing across the space.

Despite the results of the CO₂ analysis indicating a seemingly well performing ventilation system, it is notable that ventilation specification in United Kingdom educational buildings currently ignores the potential contamination of the indoor air with pollutants stemming from a combination of outdoor and indoor sources (i.e., those introduced via the ventilation system or infiltration or originating from materials within the building). This is in marked contrast to the methodologies set out in the European norm EN 16798-1: 2019 (Awbi, 2003; CEN, 2019) which recommends that the design ventilation rate should be calculated on the basis of two components, 1) ventilation to dilute/remove bio effluents from the occupants and 2) ventilation to remove/dilute pollution from the building and systems. Wherein, the ventilation rate appropriate for a particular occupant category (I-IV) is determined as the corresponding sum for these two

components. In this study a number of VOCs were repeatedly identified through a campaign of diffusive sampling under defined operational scenarios (Figure 8), however the presence of these potentially harmful compounds is unaccounted for in the ventilation system design. Since there are currently no requirements to test for specific VOCs post-construction in any of the standards affecting schools and educational buildings in the United Kingdom, the full magnitude of this problem remains largely undetected.

The diffusive (passive) sampling methodology adopted in this study was designed to provide a non-targeted approach aimed at detecting all of the VOC compounds present in the indoor environment. This was performed by considering three distinct sampling scenarios in order to assess the building in its occupied and unoccupied states, both with and without fresh-air dilution via the mechanical ventilation system (Table 2). By repeating the sampling in this way it was found that four VOC compounds (acetic acid, toluene, benzaldehyde and phenol) were repeatedly present in each scenario (Figure 8). This confirms their undistinguished presence in the indoor environment and suggests that they are originating from the building materials or being introduced via the ventilation system (as opposed to being introduced by occupants or short duration activities). Whilst the toluene and benzaldehyde concentrations were reduced by the provision of ventilation the presence of acetic acid and phenol were not. This is potentially a significant finding as it suggests that ventilation might be ineffective as a control strategy in this context, however this would require further investigation (using paired indoor and outdoor measurements) and a larger sample size to rule out the possibility of transient external sources.

The presence of known, yet unregulated, health endangering VOCs is perhaps the most concerning finding in this study. Toluene, for example, has been associated with nervous system effects including cognitive impairment, vision and hearing loss along with changes in brain structure and chemistry following both chronic and acute exposure (Agency for Toxic Substances and Disease Registry, 2020). At levels above 500 ppm toluene is considered to be an immediate danger to life or health (IDLH) (Toluene, 2014). Toluene levels were found to be highest in scenario 1 which suggest that the source might come from the glues and solvents used in architectural model making. However, its presence was also identified in Scenarios 2 and 3 which suggests the possibility of an additional source from elsewhere in the indoor environment (such as oil-based paints used in the internal finishes) or via exhaust emissions from the adjacent car park (since toluene is a common component of unleaded vehicular emissions (Muttamara et al., 1999)). Acetic acid has a pungent odour and has been linked to sensory irritation of the eyes, nose, and upper respiratory tract; whilst at concentrations above 50 ppm it is considered to be IDLH (Toluene, 2014). Similarly, exposure to phenol is associated with irritation of the skin, eyes, nose, throat, and nervous system and at concentrations above 250 ppm it is considered to be IDLH

(Baron, n. d). Benzaldehyde is a key ingredient in numerous cleaning and household products containing natural fruit flavours and has been shown to cause irritation of respiratory airways in animals and in human occupational exposure studies. There is currently little known about its long term toxicity but some researchers have suggested that inhalation of benzaldehyde poses an emerging health risk (Kosmider et al., 2016).

Further research would be required to isolate the precise indoor and outdoor source(s) responsible for the emission of these VOCs. This would involve testing samples of the indoor materials present under controlled conditions (i.e., emission chamber tests) in order to identify the emission characteristics of the specific compounds. Having identified the source of these compounds a detailed sampling plan would be required in order to capture these compounds in the indoor environment and understand whether their time dependent concentrations pose a serious ongoing health risk to the building occupants. This would involve creating calibration curves comparing a pure form of each identified compound against the one found in the indoor air. This process would quantify the concentration of each compound in ppm or $\mu\text{g}/\text{m}^3$, which could then be compared with recommended guideline values in the literature.

There are a number of additional limitations with respect to extrapolating the results of this study. The VOC sampling commenced 9 months (and was completed 11 months) after the completion of the refurbishment works. Had the study commenced earlier and spanned a longer duration a broader temporal profile of the VOCs arising from the refurbishment works could have been established. Furthermore, the IAQ campaign was carried out during the spring and summer period which could have influenced the actual concentration of CO_2 and VOCs found due to increases in background ventilation rates during the warmer months (through the increased frequency of windows being opened). A further significant problem relates to the fact that many airborne VOCs cannot be routinely captured using the applied technique of diffusive sampling (i.e., using Tenax®/Carbotrap absorbents) followed by TD/GC-qMS (Salthammer, 2016). Finally, the number of VOC samples collected in this study ($n = 18$) would be considered relatively small for reliable quantification or assessing the significance of individual compounds. However, this study was intended to serve as a pilot study to highlight the strengths and limitations of current guidelines used in assessing higher education buildings and not to quantify the IAQ risks associated with this particular building.

Overall, the main findings of this study are in broad agreement with previous studies by Seppänen et al. (1999) and Apte et al. (2000) who demonstrated that concentrations of CO_2 below 1,000 ppm do not always guarantee that the ventilation rate is adequate for the removal of air pollutants from other indoor sources. Indeed, the results of the present study suggest that whilst increased ventilation was capable of diluting some VOCs it was incapable of addressing the IAQ problems associated with every VOC. This suggests that more rigorous source control via environmental protocols designed to restrict the use of toxic materials in the indoor environment and the implementation of strict air quality controls in the vicinity of educational buildings

are likely to play an important role in the solution to this complex problem.

CONCLUSION

The primary aim of this study was to investigate the indoor air quality of a recently refurbished higher education building by assessing the CO_2 concentration and identifying individual volatile organic compounds that could be contributing to the indoor air pollution load as a result of major refurbishment works. CO_2 concentration, which is widely used as a key indicator for ventilation performance for the control of indoor air quality, was found to be well below the threshold limiting values specified by all of the relevant standards, including BB101. This finding may be a result of several factors including the relatively low occupancy of the space, the spring-summer period of the monitoring study and mechanical ventilation flow rates which were intended for a higher designed occupancy level.

The maximum daily average CO_2 concentration threshold for mechanically ventilated educational buildings was reduced from 1500 to 1000ppm in the most recent edition of BB101 (2018), highlighting the importance of low CO_2 levels in achieving a comfortable and effective learning environment. However, the results highlight that CO_2 concentration should not be conflated with providing good indoor air quality. Volatile organic compounds originating from a variety sources, both within and around educational buildings cannot be ignored due to the risk of serious short and long-term health impacts. Currently Approved Document F of the United Kingdom building regulations attempts to address this problem by specifying a total volatile organic compound limit (where TVOC $>300 \mu\text{g}/\text{m}^3$ indicates poor indoor air quality) (HM Government, 2015). Whilst BB101 discusses the risks associated with various common volatile organic compounds (Education and Skills Funding Agency, 2018), the guidance falls short of mandating targeted sampling of known carcinogens or other hazardous compounds.

This study adopted a non-targeted approach to assess the indoor air quality of an open-studio space which led to the detection of numerous harmful volatile organic compounds that could not have been inferred from either the CO_2 concentration or the concept of a total volatile organic compound threshold. The methodology used in this study (involving long-term CO_2 monitoring coupled with scenario based passive VOC sampling) could be readily adopted in future revisions of indoor air quality standards, such as BB101 and WELL, as a post-completion commissioning requirement. Implementing such a strategy in all new and refurbished educational buildings would help to ensure that the provision of 'good indoor air quality' in educational buildings is predicated upon restricting the sources of indoor air contaminants as well as reducing the ingress of unwanted external pollutants. This implies a need for current standards to evolve beyond CO_2 and total volatile organic compound limits, where the quantification of individual volatile organic compounds and their health impacts are factored into the indoor air quality classification. This issue is of paramount importance

in the context of educational buildings in which young people spend a high proportion of their developing lives.

DATA AVAILABILITY STATEMENT

The original contributions presented in the study are included in the article/**Supplementary Material**, further inquiries can be directed to the corresponding author.

AUTHOR CONTRIBUTIONS

RM - Research Design, Ventilation and CO₂ monitoring Methodology, Data Analysis, Original Draft, Final Draft, Project Supervision MM - Research Design, Ventilation and CO₂ and VOC monitoring and sampling, Data Analysis, Original Draft DS - Research Design, VOC Methodology, VOC Data Analysis, Project

REFERENCES

- Abdul-Wahab, S. A., Chin Fah En, S., Elkamel, A., Ahmadi, L., and Yetilmezsoy, K. (2015). A Review of Standards and Guidelines Set by International Bodies for the Parameters of Indoor Air Quality. *Atmos. Pollut. Res.* 6, 751–767. doi:10.5094/APR.2015.084
- Agency for Toxic Substances and Disease Registry (2020). ATSDR - Toxicological Profile: Toluene. Available at: <https://www.atsdr.cdc.gov/ToxProfiles/tp.asp?id=161&tid=29> (Accessed October 7, 2020).
- ALA (2020). State of the Air. Available at: www.stateoftheair.org.
- Apte, M. G., Fisk, W. J., and Daisey, J. M. (2000). Associations between Indoor CO₂ Concentrations and Sick Building Syndrome Symptoms in U.S. Office Buildings: An Analysis of the 1994–1996 BASE Study Data. *Indoor Air* 10, 246–257. doi:10.1034/j.1600-0668.2000.010004246.x
- ASHRAE (2019). ANSI/ASHRAE Standard 62.1. Ventilation for Acceptable Indoor Air Quality. Available at: https://webstore.ansi.org/Standards/ASHRAE/ANSIASHRAE622019?gclid=CjwKCAjwiOv7BRBREiwAXHbv3FRX0GJexdYDlItf4b6VdqURu_c5McT9f4WI63N8oGg_mIVlgk6B0xoCVNcQAvD_BwE (Accessed October 5, 2020).
- ASHRAE (2017). *ASHRAE Handbook*. Atlanta, GA: The American Society of Heating, Refrigerating and Air-Conditioning Engineers (ASHRAE).
- Awbi, H. B. (2003). *Ventilation of Buildings: Second Edition*, Spon Press Taylor & Francis Group. London: Routledge. doi:10.4324/9780203634479
- Bakó-Biró, Z., Clements-Croome, D. J., Kochhar, N., Awbi, H. B., and Williams, M. J. (2012). Ventilation Rates in Schools and Pupils' Performance. *Building Environ.* 48, 215–223. doi:10.1016/j.buildenv.2011.08.018
- Baloch, R. M., Maesano, C. N., Christoffersen, J., Banerjee, S., Gabriel, M., Csobod, É., et al. (2020). Indoor Air Pollution, Physical and comfort Parameters Related to Schoolchildren's Health: Data from the European SINFONIE Study. *Sci. Total Environ.* 739, 139870. doi:10.1016/j.scitotenv.2020.139870
- Baron, P. (n.d). Generation and Behavior of Airborne Particles (Aerosols). Available at: https://www.cdc.gov/niosh/topics/aerosols/pdfs/aerosol_101.pdf (Accessed September 14, 2020).
- Beinfait, D., Fitzner, K., Lindvall, T., Seppanen, O., Woolliscroft, M., Fanger, O., et al. (1992). Guidelines for Ventilation Requirements in Buildings. Report No.11. *Eur. Collaborative Action. (Eca) - Indoor Air Qual. its impact man.* 1, 1.
- Berglund, B., Clausen, G., De, J., and Møllhave, L. (1997). Report 19. *Total Volatile Org. Comp. (Tvoc) Indoor Air Qual. Invest.* 1, 1.
- Bhagat, R. K., Davies Wykes, M. S., Dalziel, S. B., and Linden, P. F. (2020). Effects of Ventilation on the Indoor Spread of COVID-19. *J. Fluid Mech.* 903, F1. doi:10.1017/jfm.2020.720
- Boscott, A. (2020). UK Universities Turning Students Away from Overcrowded Lectures, Redbrick News. Available at: <https://www.redbrick.me/uk-universities-turning-students-away-from-overcrowded-lectures/> (Accessed September 18, 2020).
- British Standards Institution (2007). BS EN ISO 16000–5 : 2007. Indoor Air - Part 5: Sampling Strategy for Volatile Organic Compounds (VOCs), London. Available at: https://infostore.saiglobal.com/en-us/Standards/BS-EN-ISO-16000-5-2007-249382_SAIG_BSI_BSI_579927/ (Accessed September 23, 2020).
- Brown, V. M., Crump, D. R., and Gardiner, D. (1992). Measurement of Volatile Organic Compounds in Indoor Air by a Passive Technique. *Environ. Tech.* 13, 367–375. doi:10.1080/09593339209385164
- Campagnolo, D., Saraga, D. E., Cattaneo, A., Spinazzè, A., Mandin, C., Mabilia, R., et al. (2017). VOCs and Aldehydes Source Identification in European Office Buildings - the OFFICAIR Study. *Building Environ.* 115, 18–24. doi:10.1016/j.buildenv.2017.01.009
- Carrer, P., de Oliveira Fernandes, E., Santos, H., Hänninen, O., Kephelopoulou, S., and Wargocki, P. (2018). On the Development of Health-Based Ventilation Guidelines: Principles and Framework. *Int. J. Environ. Res. Public Health* 15. doi:10.3390/ijerph15071360
- Carrer, P., Bruinen De Bruin, Y., Franchi, M., and Valovirta, E. (2002). The EFA Project: Indoor Air Quality in European Schools. Available at: <https://bit.ly/3y5Y3XR> (Accessed August 31, 2020).
- CEN (2019). EN 16798–1:2019. Energy Performance of Buildings. Ventilation for Buildings. Indoor Environmental Input Parameters for Design and Assessment of Energy Performance of Buildings Addressing Indoor Air Quality, thermal Environment, Lighting and Acoustics. Available at: <https://bit.ly/3eW89D8> (Accessed October 5, 2020).
- Chan, A. T. (2002). Indoor-outdoor Relationships of Particulate Matter and Nitrogen Oxides under Different Outdoor Meteorological Conditions. *Atmos. Environ.* 36, 1543–1551. doi:10.1016/S1352-2310(01)00471-X
- Chen, C., and Zhao, B. (2011). Review of Relationship between Indoor and Outdoor Particles: I/O Ratio, Infiltration Factor and Penetration Factor. *Atmos. Environ.* 45, 275–288. doi:10.1016/j.atmosenv.2010.09.048
- CIBSE Guide A (2015). *Environmental Design*. London: The Chartered Institution of Building Services Engineers (CIBSE).
- CIBSE (2016). Guide B2: Ventilation and Ductwork. Available at: <https://www.cibse.org/knowledge/knowledge-items/detail?id=a0q2000008JuB7AAK> (Accessed September 17, 2020).
- Cochran Hameen, E., Ken-Opurum, B., Priyadarshini, S., Lartigue, B., and Pisipati, S. (2020). “Effects of School Facilities Mechanical and Plumbing Characteristics and Conditions on Student Attendance, Academic Performance and Health,” in *International Conference on Green Building (IEEE)*. Available at: <https://bit.ly/3zzhuZg> (Accessed September 28, 2020).
- Crowe, P. (2013). “The Implementation of UK Procurement Policy in University Refurbishment Projects,” in *IPGRC 2013 Int. Post Grad. Res. Conf.* Editors

ACKNOWLEDGMENTS

The authors would like to gratefully acknowledge the support of Dr Robert Schmidt III, of the School of Architecture, Building and Civil Engineering at Loughborough University, for providing unrestricted access to the Keith Green building in support of this research study.

SUPPLEMENTARY MATERIAL

The Supplementary Material for this article can be found online at: <https://www.frontiersin.org/articles/10.3389/fbuil.2021.769761/full#supplementary-material>

- V. Ahmed, C. Egbu, J. Underwood, A. Lee, and P. Chynoweth Available at: <http://www.ipgrc.com/2013/> (Accessed October 12, 2020).
- Daisey, J. M., Angell, W. J., and Apte, M. G. (2003). Indoor Air Quality, Ventilation and Health Symptoms in Schools: An Analysis of Existing Information. *Indoor Air* 13, 53–64. doi:10.1034/j.1600-0668.2003.00153.x
- Department for Education (2020). Technical Annex 2F: Mechanical Services and Public Health Engineering. Available at: https://assets.publishing.service.gov.uk/government/uploads/system/uploads/attachment_data/file/939408/Annex_2F_Mechanical_Services_Nov_2020.pdf.
- Education and Skills Funding Agency (2018). BB 101: Guidelines on Ventilation, thermal comfort and Indoor Air Quality in Schools. Available at: <https://www.gov.uk/government/publications/building-bulletin-101-ventilation-for-school-buildings#history> (Accessed September 11, 2020).
- European Parliament (2004). Directive 2004/42/CE of the European Parliament and of the Council of 21 April 2004 on the Limitation of Emissions of Volatile Organic Compounds Due to the Use of Organic Solvents in Certain Paints and Varnishes and Vehicle Refinishing Products and Amending Directive 1999/13/EC, off. J. L 143. Available at: <https://eur-lex.europa.eu/legal-content/EN/ALL/?uri=celex:32004L0042> (Accessed September 23, 2020).
- Fletcher, A. M., London, M. A., Gelberg, K. H., and Grey, A. J. (2006). Characteristics of Patients with Work-Related Asthma Seen in the New York State Occupational Health Clinics. *J. Occup. Environ. Med.* 48, 1203–1211. doi:10.1097/01.jom.0000245920.87676.7b
- Freeman, S., Eddy, S. L., McDonough, M., Smith, M. K., Okoroafor, N., Jordt, H., et al. (2014). Active Learning Increases Student Performance in Science, Engineering, and Mathematics. *Proc. Natl. Acad. Sci.* 111, 8410–8415. doi:10.1073/pnas.1319030111
- Gaihre, S., Semple, S., Miller, J., Fielding, S., and Turner, S. (2014). Classroom Carbon Dioxide Concentration, School Attendance, and Educational Attainment. *J. Sch. Health* 84, 569–574. doi:10.1111/josh.12183
- Guo, H., Lee, S. C., Chan, L. Y., and Li, W. M. (2004). Risk Assessment of Exposure to Volatile Organic Compounds in Different Indoor Environments. *Environ. Res.* 94, 57–66. doi:10.1016/S0013-9351(03)00035-5
- Haverinen-Shaughnessy, U., Moschandreas, D. J., and Shaughnessy, R. J. (2011). Association between Substandard Classroom Ventilation Rates and Students' Academic Achievement. *Indoor Air* 21, 121–131. doi:10.1111/j.1600-0668.2010.00686.x
- Health Effects Institute (2019). State of Global Air 2019. *Spec. Rep.* 1, 2578–6873.
- HM Government (2015). Approved Document F. Ventilation, 2010 Edition Incorporating 2013 Amendments. Available at: https://www.gov.uk/government/uploads/system/uploads/attachment_data/file/468871/ADF_LOCKED.pdf (Accessed July 1, 2020).
- HM Government (2000). The Building Regulations, Queen's Printer of Acts of Parliament. Available at: <https://www.legislation.gov.uk/ukxi/2000/2531/schedule/1/made> (Accessed September 22, 2020).
- Holøs, S. B., Yang, A., Lind, M., Thunshelle, K., Schild, P., and Mysen, M. (2019). VOC Emission Rates in Newly Built and Renovated Buildings, and the Influence of Ventilation – a Review and Meta-Analysis. *Int. J. Vent* 18, 153–166. doi:10.1080/14733315.2018.1435026
- HSE (2021). Ventilation and Air Conditioning during the Coronavirus (COVID-19) Pandemic, Heal. Saf. Exec. Guid. Available at: <https://www.hse.gov.uk/coronavirus/equipment-and-machinery/air-conditioning-and-ventilation/identifying-poorly-ventilated-areas.htm> (Accessed October 12, 2020).
- HSE (2013). Workplace Health, Safety and Welfare. Workplace (Health, Safety and Welfare) Regulations 1992. Approved Code of Practice and Guidance L24. Available at: www.nationalarchives.gov.uk/doc/open-government-licence/.
- International WELL Building Institute (2020). The International WELL Building Standard. Section 18: Air Quality Monitoring and Feedback. Available at: <https://standard.wellcertified.com/air/air-quality-monitoring-and-feedback> (Accessed September 11, 2020).
- International WELL Building Institute (2020). Ventilation Effectiveness. Available at: <https://standard.wellcertified.com/air/ventilation-effectiveness> (Accessed October 7, 2020).
- Jacobson, T. A., Kler, J. S., Hernke, M. T., Braun, R. K., Meyer, K. C., and Funk, W. E. (2019). Direct Human Health Risks of Increased Atmospheric Carbon Dioxide. *Nat. Sustain.* 2, 691–701. doi:10.1038/s41893-019-0323-1
- Kelly, F. J., and Fussell, J. C. (2015). Air Pollution and Public Health: Emerging Hazards and Improved Understanding of Risk. *Environ. Geochem. Health* 37, 631–649. doi:10.1007/s10653-015-9720-1
- Kim, J. L., Elfman, L., and Norbäck, D. (2007). Respiratory Symptoms, Asthma and Allergen Levels in Schools ? Comparison between Korea and Sweden. *Indoor Air* 17, 122–129. doi:10.1111/j.1600-0668.2006.00460.x
- Klepeis, N. E., Nelson, W. C., Ott, W. R., Robinson, J. P., Tsang, A. M., Switzer, P., et al. (2001). The National Human Activity Pattern Survey (NHAPS): a Resource for Assessing Exposure to Environmental Pollutants. *J. Expo. Sci. Environ. Epidemiol.* 11, 231–252. doi:10.1038/sj.jea.7500165
- Kosmider, L., Sobczak, A., Prokopowicz, A., Kurek, J., Zacierka, M., Knysak, J., et al. (2016). Cherry-flavoured Electronic Cigarettes Expose Users to the Inhalation Irritant, Benzaldehyde. *Thorax* 71, 376–377. doi:10.1136/thoraxjnl-2015-207895
- Lee, C. S., Haghighat, F., and Ghaly, W. S. (2005). A Study on VOC Source and Sink Behavior in Porous Building Materials - Analytical Model Development and Assessment. *Indoor Air* 15, 183–196. doi:10.1111/j.1600-0668.2005.00335.x
- Lee, J. Y., Wargocki, P., Chan, Y. H., Chen, L., and Tham, K. W. (2019). Indoor Environmental Quality, Occupant Satisfaction, and Acute Building-related Health Symptoms in Green Mark-certified Compared with Non-certified Office Buildings. *Indoor Air* 29, 112–129. doi:10.1111/ina.12515
- Lelieveld, J., Klingmüller, K., Pozzer, A., Pöschl, U., Fnais, M., Daiber, A., et al. (2019). Cardiovascular Disease burden from Ambient Air Pollution in Europe Reassessed Using Novel hazard Ratio Functions. *Eur. Heart J.* 40, 1590–1596. doi:10.1093/eurheartj/ehz135
- Licina, D., Melikov, A., Sekhar, C., and Tham, K. W. (2015). Transport of Gaseous Pollutants by Convective Boundary Layer Around a Human Body. *Sci. Tech. Built Environ.* 21, 1175–1186. doi:10.1080/23744731.2015.1060111
- Lu, C.-Y., Tsai, M.-C., Muo, C.-H., Kuo, Y.-H., Sung, F.-C., and Wu, C.-C. (2017). Personal, Psychosocial and Environmental Factors Related to Sick Building Syndrome in Official Employees of Taiwan. *Ijerph* 15, 7. doi:10.3390/ijerph15010007
- Lucattini, L., Poma, G., Covaci, A., de Boer, J., Lamoree, M. H., and Leonards, P. E. G. (2018). A Review of Semi-volatile Organic Compounds (SVOCs) in the Indoor Environment: Occurrence in Consumer Products, Indoor Air and Dust. *Chemosphere* 201, 466–482. doi:10.1016/j.chemosphere.2018.02.161
- Maroni, M., Seifert, B., and Lindvall, T. (1995). *Indoor Air Quality, Volume 3-1st Edition*. Elsevier Sci. Available at: <https://www.elsevier.com/books/indoor-air-quality/maroni/978-0-444-81642-9> (Accessed September 17, 2020).
- Matson, U. (2005). Indoor and Outdoor Concentrations of Ultrafine Particles in Some Scandinavian Rural and Urban Areas. *Sci. Total Environ.* 343, 169–176. doi:10.1016/j.scitotenv.2004.10.002
- Mazurek, J. M., Filios, M., Willis, R., Rosenman, K. D., Reilly, M. J., McGreevy, K., et al. (2008). Work-related Asthma in the Educational Services Industry: California, Massachusetts, Michigan, and New Jersey, 1993–2000. *Am. J. Ind. Med.* 51, 47–59. doi:10.1002/ajim.20539
- McLeod, R., and Swainson, M. (2017). Chronic Overheating in Low Carbon Urban Developments in a Temperate Climate. *Renew. Sust. Energ. Rev.* 74, 201–220.
- Mendell, M. J., Eliseeva, E. A., Davies, M. M., Spears, M., Lobscheid, A., Fisk, W. J., et al. (2013). Association of Classroom Ventilation with Reduced Illness Absence: a Prospective Study in California Elementary Schools. *Indoor Air* 23, 515–528. doi:10.1111/ina.12042
- Miller, J., Semple, S., and Turner, S. (2010). High Carbon Dioxide Concentrations in the Classroom: the Need for Research on the Effects of Children's Exposure to Poor Indoor Air Quality at School. *Occup. Environ. Med.* 67, 799. doi:10.1136/oem.2010.057471
- Molhave, L., Clausen, G., Berglund, B., Ceaurriz, J., Kettrup, A., Lindvall, T., et al. (1997). Total Volatile Organic Compounds (TVOC) in Indoor Air Quality Investigations*. *Indoor Air* 7, 225–240. doi:10.1111/j.1600-0668.1997.00002.x
- Münzel, T., Gori, T., Al-Kindi, S., Deanfield, J., Lelieveld, J., Daiber, A., et al. (2018). Effects of Gaseous and Solid Constituents of Air Pollution on Endothelial Function. *Eur. Heart J.* 39, 3543–3550. doi:10.1093/eurheartj/ehy481
- Muttamara, S., Leong, S. T., and Lertvisansak, I. (1999). Assessment of Benzene and Toluene Emissions from Automobile Exhaust in Bangkok. *Environ. Res.* 81, 23–31. doi:10.1006/enrs.1998.3941
- Mysen, M., Rydbeck, J. P., and Tjellflaot, P. O. (2003). Demand Controlled Ventilation for Office Cubicles-Can it Be Profitable? *Energy and Buildings* 35, 657–662. doi:10.1016/S0378-7788(02)00212-8

- NIST (2019). NIST/EPA/NIH Mass Spectral Library-PC Version, NIST Standard Reference Database 1A. NIST. Available at: <https://doi.org/10.18434/T4H594>. doi:10.18434/T4H594
- Fanger, P. O. (2006). What Is IAQ? *Indoor Air* 16, 328–334. doi:10.1111/j.1600-0668.2006.00437.x
- Oppl, R., and Neuhaus, T. (2008). *Emission Specifications in Europe and the US-Limit Values (TVOC, LCI, CREL,...) in Critical Discussion*. Copenhagen: Indoor Air Conference.
- Pei, G., Rim, D., Schiavon, S., and Vannucci, M. (2019). Effect of Sensor Position on the Performance of CO₂-based Demand Controlled Ventilation. *Energy Build* 202, 1. doi:10.1016/j.enbuild.2019.109358
- Persson, J., Wang, T., and Hagberg, J. (2019). Indoor Air Quality of Newly Built Low-Energy Preschools - Are Chemical Emissions Reduced in Houses with Eco-Labelled Building Materials? *Indoor Built Environ.* 28, 506–519. doi:10.1177/1420326X18792600
- RCP (2016). Every Breath We Take: the Lifelong Impact of Air Pollution. Available at: <https://www.rcplondon.ac.uk/projects/outputs/every-breath-we-take-lifelong-impact-air-pollution> (Accessed August 31, 2020).
- Riggs, J. J. (2014). An Approach to Increasing Awareness of IAQ, Middlesex. Available at: <https://eprints.mdx.ac.uk/id/eprint/13523> (Accessed August 31, 2020).
- Riley, W. J., McKone, T. E., Lai, A. C. K., and Nazaroff, W. W. (2002). Indoor Particulate Matter of Outdoor Origin: Importance of Size-dependent Removal Mechanisms. *Environ. Sci. Technol.* 36, 200–207. doi:10.1021/es010723y
- Salthammer, T. (2016). Very Volatile Organic Compounds: an Understudied Class of Indoor Air Pollutants. *Indoor Air* 26, 25–38. doi:10.1111/ina.12173
- Seifert, B., and Ullrich, D. (1987). Methodologies for Evaluating Sources of Volatile Organic Chemicals (VOC) in Homes. *Atmos. Environ.* (1967) 21, 395–404. doi:10.1016/0004-6981(87)90018-7
- Seppänen, O. A., Fisk, W. J., and Mendell, M. J. (1999). Association of Ventilation Rates and CO₂ Concentrations with Health and Other Responses in Commercial and Institutional Buildings. *Indoor Air* 9, 226–252. doi:10.1111/j.1600-0668.1999.00003.x
- Shaughnessy, R. J., Haverinen-Shaughnessy, U., Nevalainen, A., and Moschandreas, D. (2006). A Preliminary Study on the Association between Ventilation Rates in Classrooms and Student Performance. *Indoor Air* 16, 465–468. doi:10.1111/j.1600-0668.2006.00440.x
- Shendell, D. G., Prill, R., Fisk, W. J., Apte, M. G., Blake, D., and Faulkner, D. (2004). Associations between Classroom CO₂ Concentrations and Student Attendance in Washington and Idaho. *Indoor Air* 14, 333–341. doi:10.1111/j.1600-0668.2004.00251.x
- Spinazzè, A., Campagnolo, D., Cattaneo, A., Urso, P., Sakellaris, I. A., Saraga, D. E., et al. (2020). Indoor Gaseous Air Pollutants Determinants in Office Buildings-The OFFICAIR Project. *Indoor Air* 30, 76–87. doi:10.1111/ina.12609
- Stranger, M., Aerts, W., Daems, J., Spruy, M., Geyskens, F., Verbeke, L., et al. (2015). *Explorative Study on the Quality of the Indoor Environment in Buildings after (Energy-efficient) Renovations*. Boeretang, Belgium: Vito. https://www.milieuinfo.be/dms/d/d/workspace/SpacesStore/3022641f-ea68-4873-b5ca-f07f964339c1/renovair_eindrapport.pdf.
- Sumner, L. W., Amberg, A., Barrett, D., Beale, M. H., Beger, R., Daykin, C. A., et al. (2007). Proposed Minimum Reporting Standards for Chemical Analysis. *Metabolomics* 3, 211–221. doi:10.1007/s11306-007-0082-2
- Suzuki, N., Nakaoka, H., Hanazato, M., Nakayama, Y., Tsumura, K., Takaya, K., et al. (2019). Indoor Air Quality Analysis of Newly Built Houses. *Int. J. Environ. Res. Public Health* 16, 1. doi:10.3390/ijerph16214142
- The European Parliament and The Council of the European Union (2010). Directive 2010/31/EU of the European Parliament and of the Council of 19 May 2010 on the Energy Performance of Buildings. *Off. J. Eur. Union* 53, 1. doi:10.3000/17252555.L_2010.153.eng
- Toluene (2014). The National Institute for Occupational Safety and Health (NIOSH). Immediately Dangerous to Life or Health Concentrations (IDLH): Toluene - NIOSH Publications and Products. Available at: <https://www.cdc.gov/niosh/idlh/108883.html> (Accessed October 7, 2020).
- Turunen, M., Toyinbo, O., Putus, T., Nevalainen, A., Shaughnessy, R., and Haverinen-Shaughnessy, U. (2013). Indoor Environmental Quality in School Buildings, and the Health and Wellbeing of Students. *Int. J. Hyg. Environ. Health* 217, 733–739. doi:10.1016/j.ijheh.2014.03.002
- US EPA (2019). Air Quality - National Summary. Available at: <https://www.epa.gov/air-trends/air-quality-national-summary> (Accessed August 28, 2020).
- US EPA (2020). Technical Overview of Volatile Organic Compounds. Available at: <https://www.epa.gov/indoor-air-quality-iaq/technical-overview-volatile-organic-compounds> (Accessed September 28, 2020).
- Wachenfeldt, B. J., Mysen, M., and Schild, P. G. (2007). Air Flow Rates and Energy Saving Potential in Schools with Demand-Controlled Displacement Ventilation. *Energy and Buildings* 39, 1073–1079. doi:10.1016/j.enbuild.2006.10.018
- Wall, K., Dockrell, J., and Peacey, N. (2008). Primary Schools: The Built Environment. Available at: www.primaryreview.org.uk.
- Weale, S. (2020). UK Universities Receive Record Number of Applications in Lockdown, Guard. Available at: <https://www.theguardian.com/education/2020/jul/09/uk-universities-record-number-applications-lockdown> (Accessed September 18, 2020).
- Wolkoff, P., and Nielsen, G. D. (2001). Organic Compounds in Indoor Air-Their Relevance for Perceived Indoor Air Quality? *Atmos. Environ.* 35, 4407–4417. doi:10.1016/S1352-2310(01)00244-8
- Woolley, T. (2016). *Building Materials, Health and Indoor Air Quality: No Breathing Space?* London, Routledge: Taylor and Francis Group. Available at: <https://www.routledge.com/Building-Materials-Health-and-Indoor-Air-Quality-No-Breathing-Space/Woolley/p/book/9781138934498> (Accessed September 17, 2020).
- Xing, H., Hatton, A., and Awbi, H. B. (2001). A Study of the Air Quality in the Breathing Zone in a Room with Displacement Ventilation. Available at: www.elsevier.com/locate/buildenv. doi:10.1016/S0360-1323(01)00006-3
- Xu, J., Szyszkowicz, M., Jovic, B., Cakmak, S., Austin, C. C., and Zhu, J. (2016). Estimation of Indoor and Outdoor Ratios of Selected Volatile Organic Compounds in Canada. *Atmos. Environ.* 141, 523–531. doi:10.1016/j.atmosenv.2016.07.031
- Yang, W., Sohn, J., Kim, J., Son, B., and Park, J. (2009). Indoor Air Quality Investigation According to Age of the School Buildings in Korea. *J. Environ. Manage.* 90, 348–354. doi:10.1016/j.jenvman.2007.10.003
- Yu, C., and Crump, D. (1998). A Review of the Emission of VOCs from Polymeric Materials Used in Buildings. *Building Environ.* 33, 357–374. doi:10.1016/S0360-1323(97)00055-3
- Zhong, L., Su, F.-C., and Batterman, S. (2017). Volatile Organic Compounds (VOCs) in Conventional and High Performance School Buildings in the U.S. *Ijerp* 14, 100. doi:10.3390/ijerp14010100
- Zhong, L., Yuan, J., and Fleck, B. (2019). Indoor Environmental Quality Evaluation of Lecture Classrooms in an Institutional Building in a Cold Climate. *Sustainability* 11, 6591. doi:10.3390/su11236591

Conflict of Interest: The authors declare that the research was conducted in the absence of any commercial or financial relationships that could be construed as a potential conflict of interest.

Publisher's Note: All claims expressed in this article are solely those of the authors and do not necessarily represent those of their affiliated organizations, or those of the publisher, the editors and the reviewers. Any product that may be evaluated in this article, or claim that may be made by its manufacturer, is not guaranteed or endorsed by the publisher.

Copyright © 2022 McLeod, Mathew, Salman and Thomas. This is an open-access article distributed under the terms of the Creative Commons Attribution License (CC BY). The use, distribution or reproduction in other forums is permitted, provided the original author(s) and the copyright owner(s) are credited and that the original publication in this journal is cited, in accordance with accepted academic practice. No use, distribution or reproduction is permitted which does not comply with these terms.



OPEN ACCESS

EDITED BY

Gaetano Licita,
Agenzia Regionale per la Protezione
Ambientale della Toscana (ARPAT), Italy

REVIEWED BY

Luca Fredianelli,
Pisa Research Area, Italian National
Research Council, Italy
Giuseppe Ciaburro,
Università della Campania, Italy

*CORRESPONDENCE

Takeshi Okuzono,
okuzono@port.kobe-u.ac.jp

SPECIALTY SECTION

This article was submitted to Indoor
Environment,
a section of the journal
Frontiers in Built Environment

RECEIVED 17 June 2022

ACCEPTED 01 August 2022

PUBLISHED 29 August 2022

CITATION

Mimura M, Okuzono T and Sakagami K
(2022), Finite element modeling for
predicting sound insulation of fixed
windows in a laboratory environment.
Front. Built Environ. 8:971459.
doi: 10.3389/fbuilt.2022.971459

COPYRIGHT

© 2022 Mimura, Okuzono and
Sakagami. This is an open-access article
distributed under the terms of the
[Creative Commons Attribution License](#)
(CC BY). The use, distribution or
reproduction in other forums is
permitted, provided the original
author(s) and the copyright owner(s) are
credited and that the original
publication in this journal is cited, in
accordance with accepted academic
practice. No use, distribution or
reproduction is permitted which does
not comply with these terms.

Finite element modeling for predicting sound insulation of fixed windows in a laboratory environment

Marie Mimura^{1,2}, Takeshi Okuzono^{2*} and Kimihiro Sakagami²

¹Technology and Innovation Center, YKK Corporation, Toyama, Japan, ²Environmental Acoustic Laboratory, Department of Architecture, Graduate School of Engineering, Kobe University, Kobe, Japan

This paper presents discussion of the prediction capability of three numerical models using finite element method for predicting the sound reduction index (SRI) of fixed windows having different dimensions in a laboratory environment. The three numerical models tested here only discretize the window part or windows part and the space around the windows to reduce the necessary computational cost for vibroacoustics simulations. An ideal diffused sound incidence condition is assumed for three models. Their predictability and numerical efficiency were examined over five fixed windows with different dimensions compared to measured SRIs. First, the accuracy of the simplest model in which the window part is only discretized with finite elements was examined. Acoustic radiation to the transmission field is computed using Rayleigh's integral. Calculations were performed under two loss factor setups respectively using internal loss factors of each material and measured total loss factor of each window. The results were then compared with the measured values. Results revealed the effectiveness of using the measured total loss factor at frequencies around and above the coincidence frequencies. Subsequently, we tested the prediction accuracy of a numerical model that includes a niche existing in a laboratory environment. Also, hemispherical free fields around the window are discretized using fluid elements and infinite fluid elements. The results underscored the importance of including a niche in a numerical model used to predict sound reduction index below 1 kHz for smaller windows accurately. Nevertheless, this numerical model, including a niche, entails high computational costs. To enhance the prediction efficiency, we examined the applicability of a weak-coupling model that divides calculation procedures into three steps: (1) incidence field calculation to the window surface, (2) sound transmission calculation in fixed windows, and (3) sound radiation calculation from a window surface to a transmission field. Results revealed that the weak-coupling model produces almost identical results to those of a strong-coupling model, but with higher efficiency.

KEYWORDS

computational cost, finite element method, loss factor, random incidence, sound insulation, sound reduction index, vibroacoustic analysis, window

1 Introduction

Noise is one of the major environmental problems, especially in urbanized areas. It can cause various health problems. For example, exposure to noise is known to be associated with sleep disorders with awakenings (Muzet, 2007). Also, it is reported that transportation and recreational noise affects blood pressure and hypertension (Petri et al., 2021). Among the problems caused by noise, reducing working performance caused by noise is also concerned: for example, learning impairment in schools associated with noise is studied (Minichilli et al., 2018). Considering these situations, noise abatement is of vital importance in built environments. One of the most efficient devices is improving the sound insulation performance of façades, particularly windows, which are often its weak points compared to other building components.

Therefore, developing windows with high sound insulation characteristics is necessary for comfortable and healthy indoor sound environments. The sound insulation performance of windows is generally tested using laboratory measurements such as those stipulated by ISO 10140 (ISO 10140-1, 2016). However, measurement-based evaluation entails high development costs to prepare test samples and to perform tests themselves. Therefore, numerical analyses such as the finite element method (FEM) and the boundary element method can be key technologies to realize efficient development of high sound insulation windows. One can expect to reduce development costs and lead times. Numerical analyses present benefits for modeling the detailed structure of real windows and surrounding laboratory environment. However, computationally expensive vibroacoustics analyses are necessary for simulating sound transmission through windows to incorporate consideration of coupling between vibration fields in structural parts of windows and sound fields in surrounding laboratory environments, as well as in air gaps of multilayer structures. Computationally efficient modeling is an important but challenging objective that must be achieved for the prediction of sound insulation performance of windows and for other building components such as walls. Another means for predicting the sound insulation performance of windows is using theories (Sewell, 1970; Davy, 2009, 2010; Rindel, 2018; Cambridge et al., 2020; Santoni et al., 2020) for single-leaf and double-leaf partitions. A well-reviewed article (Santoni et al., 2020) describing theories for calculating sound transmission through partitions is available. Theoretical predictions, which are faster than numerical analyses, are useful to elucidate the fundamental mechanisms of sound transmission through partitions. However, their modeling capabilities are lower than numerical analyses. Furthermore, recently, a prediction method combined with a linear regression analysis to measure data and Cremer's theory (Davy, 2009) have been explored as a practical prediction method used for single-glazed windows (Tsukamoto et al., 2021). The study described herein specifically examines

vibroacoustics numerical modeling using FEM to predict random-incidence sound reduction indices (SRIs) of fixed windows in a laboratory environment.

Some earlier works have discussed the prediction accuracy of SRIs of actual windows or window-like structures using vibroacoustic FEM with comparison of measurement data. Soussi et al. (Soussi et al., 2021) conducted the prediction of SRIs of double glazing windows with a wooden frame at low frequencies up to 630 Hz using FEM. They tested the prediction accuracy of numerical models, calibrated with an experimental modal analysis, with comparison of measured values. Løvholt et al. (Løvholt et al., 2017) used FEM to simulate the sound transmission between two rectangular rooms via a lightweight wall with a double glazing window at very low frequencies below 100 Hz. A comparison with measured results revealed the importance of detailed modeling in the structural connection to obtain a better agreement of SRIs between the simulations and measurements. Mimura et al. (Mimura et al., 2022a) predicted SRIs of a scale model of a double window using FEM at 100 Hz to 5 kHz. Also, a comparison between FEM results and measured SRIs was made in cases with and without frame absorbers. They showed that superior agreement is obtained for a case with frame absorbers in all perimeters in the air cavity. They also demonstrated the importance of sound transmission modeling in the structurally connected parts in some poor prediction cases. Apart from SRI prediction of windows, some researchers (Papadopoulos, 2003; Arjunan et al., 2013, 2014; Wawezynowicz et al., 2014) have put great effort into predicting SRI of walls or composite panels. Accurate and efficient modeling is a challenging task because of the necessity for structure–acoustic analysis.

Nevertheless, almost all earlier works exploring SRI predictions of windows only examine prediction accuracy by FEM for single-sized windows and for a limited frequency range. Therefore, the applicability of FEM to SRI predictions of real windows having different sizes remains unclear. Because actual dwellings use various-sized windows and because their sound insulation performance is influenced by the window or plate size (Guy et al., 1985; Mimura et al., 2022b), the prediction accuracy of SRIs using FEM should be examined for windows of multiple sizes. Furthermore, as described earlier, SRI predictions of windows using FEM in a wide frequency range require great computational effort when a detailed structure of the window is modeled. For that reason, exploring computationally efficient modeling of real window systems is expected to enhance the applicability of numerical analyses to window system design with a high sound insulation performance.

For the reasons described above, this study was conducted to elucidate the efficient and accurate finite element modeling for predicting SRI of fixed windows at random incidence in a laboratory environment. Therefore, we discuss the predictive accuracy and required computational costs of three FEM models for predicting random incidence SRI of fixed windows by

comparing the measured SRIs of five fixed windows having different sizes of 0.2–2.0 m². We only specifically examine numerical models that discretize the window part or windows part and the space around the windows for computational efficiency reasons. In that model, source and receiving reverberation rooms are not discretized with finite elements. This paper is organized as follows. In [Section 2](#), we evaluate the accuracy of the simplest numerical model that discretizes only a window part with finite elements under two loss factor setups that contribute to energy loss of vibrations in windows. One uses measured frequency-dependent total loss factors, as measured respectively for five windows. Sound incidence conditions to window surfaces are assumed as an ideal diffuse sound incidence. The acoustic radiation to an opposite transmission field is computed using Rayleigh's integral. Then, [Section 3](#) examines effects of including a niche in the numerical model on the resulting accuracy of SRI predictions at frequencies below 1 kHz because the discrepancies from measured SRIs can be found at this frequency range in [Section 2](#), especially for smaller windows. [Section 4](#) explores the applicability of the weak-coupling model to predict SRI for a numerical model with a niche more efficiently. [Section 5](#) concludes the presentation, giving some important perspectives on creating an accurate and efficient numerical model to predict random-incidence SRI of fixed windows in a laboratory environment.

2 Prediction using model with window part only

This section presents a discussion of the prediction accuracy of SRI using a numerical model that discretizes only the window parts with finite elements for five fixed windows having different sizes of 0.2–2.0 m². The considered fixed windows are all used in actual dwellings. In the numerical model, an ideal diffuse field incidence condition is applied to the incident window surface. Also, acoustic radiation from the window surface on the transmitted side is computed using Rayleigh's integral. Two numerical models, each with a different loss factors setup, were tested. The first setup gives an internal loss factor to each material. The second setup gives a measured total loss factor having frequency-dependence to window glazing. We examined the accuracy of the numerical model by comparing it with measured SRIs in laboratory measurements described in the authors' earlier work ([Mimura et al., 2022b](#)). For readers' convenience, we explain the measurement briefly in [Section 2.1](#).

2.1 Measurement outline

Measurements were taken in two irregularly shaped reverberation chambers following JIS A 1416 ([JIS A 1416, 2000](#)), which is comparable to ISO 10140-1 ([ISO 10140-1,](#)

[2016](#)). The source reverberation room has a volume of 492.8 m³ and the receiving room has 264.5 m³ volume. We measured SRIs and the total loss factors of five fixed windows with area of 0.2–2.0 m². [Figure 1A,B](#) portrays a photo of the interior appearance of the reverberation room and a block diagram of the SRI measurement, respectively. [Figure 2](#) presents a tested, fixed window of $W \times H$ size settled in an opening between two reverberation rooms. Those windows comprise glass, window frames of aluminum and PVC, and the gasket. Each window uses a float glass of 5 mm thickness. [Table 1](#) presents detailed dimensions of five fixed windows (A)–(E) appearing in [Figure 2](#) as the window size $W \times H$, the glass size $W_{FL5} \times H_{FL5}$, the exposed glass size $W_g \times H_g$, area and the aspect ratio. The windows were first attached to a sufficiently high-density wooden frame that had been filled with mortar inside. Then the resulting window component was mounted to the test opening. The measurements were taken in airtight conditions. We sealed the air gaps between the wooden frame and the opening with clay and sealed the air gaps between the wooden frame and window frame with tape.

We also took the total loss factor η_{tot} measurements to consider effects of boundary loss simply in the numerical model. [Figures 3A, B](#) portrays a photo of the impulse test and a block diagram of the equipment set-up for the measurement, respectively. The η_{tot} s for five fixed windows (A)–(E) were calculated, respectively, from a structural reverberation time T_s , as measured using an impulse test with a steel ball pendulum. The accelerometers were mounted on the glass surface with small amounts of wax to fix them on the surface. The T_s is a value taken from averaging five times measuring results with three excitation points and three measured positions. [Figures 4A, B](#) respectively depict results of random incidence SRIs, in addition to the total loss factors for five fixed windows.

2.2 Finite element model

We performed FEM simulations using vibroacoustic simulation software: Actran 2020. Simulations were performed at 1/24-octave band center frequencies of 90 Hz to 5.6 kHz in the frequency domain to predict the respective SRIs for the five fixed windows (A)–(E) having different dimensions. The calculation results were evaluated as 1/3-octave band SRIs at 100 Hz–5 kHz. A linear direct frequency response analysis was used. A linear system of equations at each frequency was solved with a sparse direct solver called MUMPS. [Figures 5A, B](#) show the simplest and the baseline model that discretizes the window part with finite elements. The discretized model comprises aluminum and PVC frames, a glass, rubber sheet instead of a gasket, and an air cavity within the frames. Simplified geometries in a rubber sheet and window frame were used because they have complicated geometries. In the vibroacoustic simulation, the structural domains, aluminum and PVC frames, a glass, and a rubber

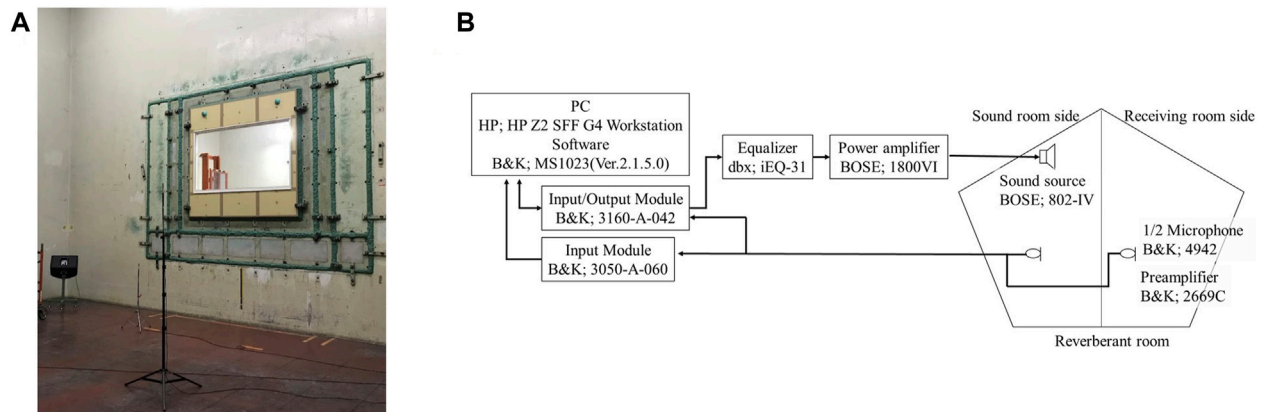


FIGURE 1

SRI measurement of window D: (A) interior appearance of source room and (B) a block diagram of measurement equipment.

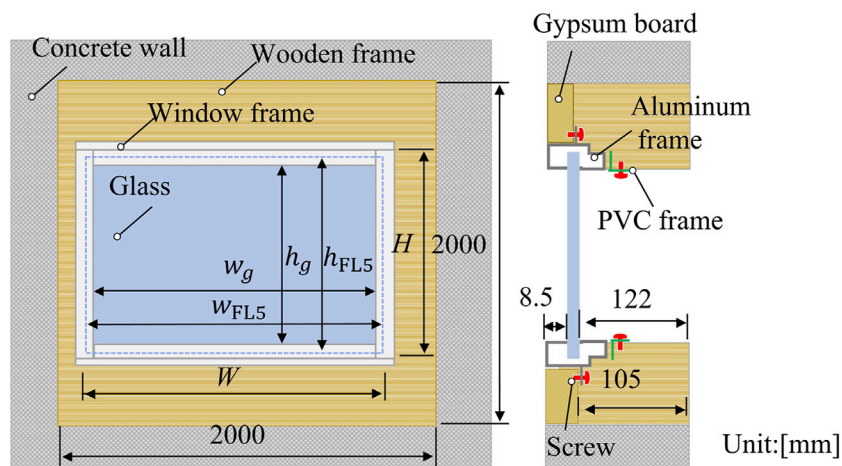


FIGURE 2

Appearance of fixed window using in measurements.

TABLE 1 Dimensions of five fixed windows.

Window	Window size $W \times H$, mm	Glass size $w_{FL5} \times h_{FL5}$, mm	Exposed glass size $w_g \times h_g$, mm	Area, m ²	Aspect ratio
(A)	580 × 350	523 × 299	508 × 284	0.2	1.7
(B)	900 × 550	843 × 499	828 × 484	0.5	1.6
(C)	1250 × 800	1193 × 749	1178 × 734	1.0	1.6
(D)	1800 × 1100	1743 × 1049	1728 × 1034	2.0	1.6
(E)	1800 × 550	1743 × 499	1728 × 484	1.0	3.3

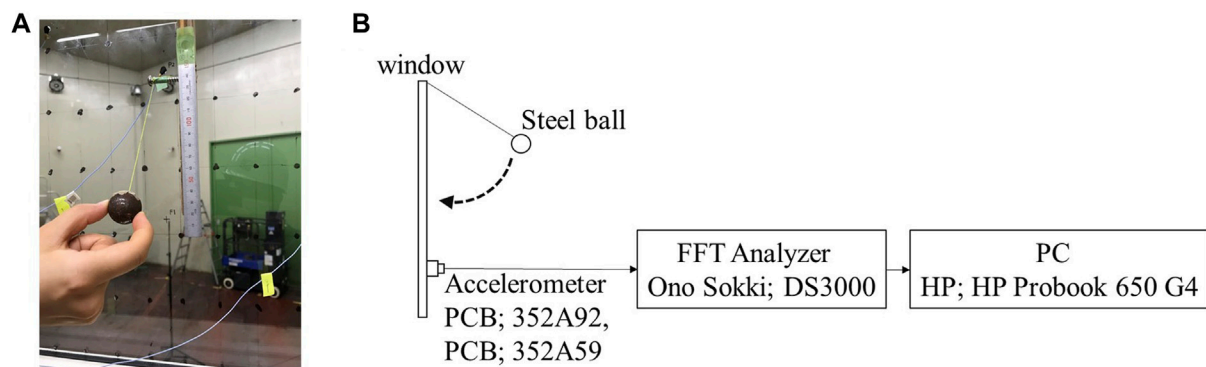


FIGURE 3

Total loss factor measurement: (A) a picture of impulse test and (B) a block diagram of measurement equipment.

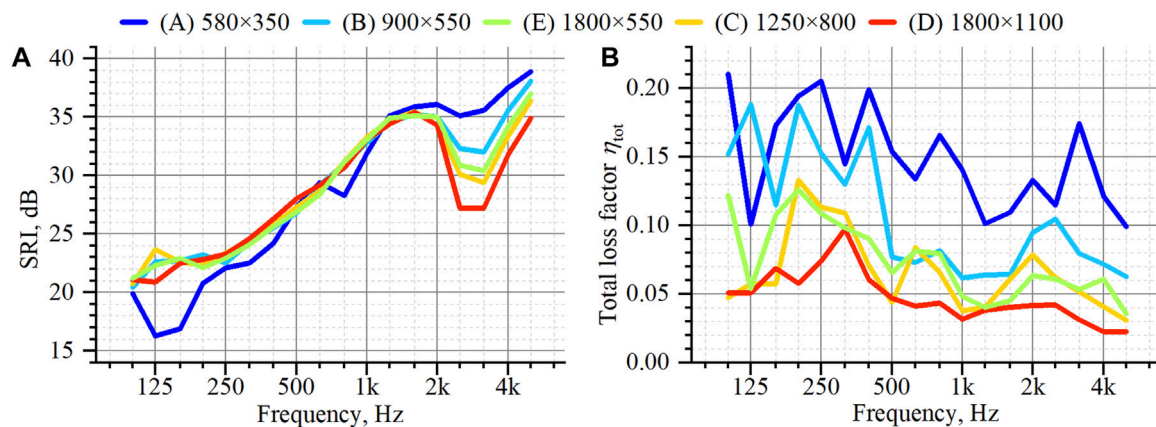


FIGURE 4

Measurement results of five fixed windows, (A) Sound reduction indices, and (B) Total loss factors (Mimura et al., 2022b).

sheet, are described by the differential equation of motion for a continuum body assuming only slight deformation as (Sandberg et al., 2008)

$$\tilde{\nabla}^T \tilde{\sigma}^s + \mathbf{b}^s = \rho^s \frac{\partial^2 \mathbf{u}^s}{\partial t^2}, \quad (1)$$

where ρ^s is the density of material, $\tilde{\sigma}^s$ is the stress vector in Voigt notation, \mathbf{b}^s is the body force vector, \mathbf{u}^s is the displacement vector. With the strain vector $\tilde{\epsilon}^s$ represented by Voigt notation, the strain-displacement relation is written as

$$\tilde{\epsilon}^s = \tilde{\nabla} \mathbf{u}^s. \quad (2)$$

The stress-strain relation is given for an isotropic material as

$$\tilde{\sigma}^s = \mathbf{D} \tilde{\epsilon}^s, \quad (3)$$

where $\tilde{\sigma}^s = [\sigma_{11}^s \ \sigma_{22}^s \ \sigma_{33}^s \ \sigma_{12}^s \ \sigma_{13}^s \ \sigma_{23}^s]^T$, and $\tilde{\epsilon}^s = [\epsilon_{11}^s \ \epsilon_{22}^s \ \epsilon_{33}^s \ \gamma_{12}^s \ \gamma_{13}^s \ \gamma_{23}^s]^T$. The constitutive matrix \mathbf{D} is described as

$$\mathbf{D} = \begin{bmatrix} \lambda + 2\mu & \lambda & \lambda & 0 & 0 & 0 \\ \lambda & \lambda + 2\mu & \lambda & 0 & 0 & 0 \\ \lambda & \lambda & \lambda + 2\mu & 0 & 0 & 0 \\ 0 & 0 & 0 & \mu & 0 & 0 \\ 0 & 0 & 0 & 0 & \mu & 0 \\ 0 & 0 & 0 & 0 & 0 & \mu \end{bmatrix}. \quad (4)$$

The Lamé coefficients λ and μ are defined as

$$\lambda = \frac{\nu E}{(1 + \nu)(1 - 2\nu)}, \quad (5)$$

$$\mu = \frac{E}{2(1 + \nu)}, \quad (6)$$

where E is the Young's modules, and ν is the Poisson's ratio. The acoustic domain, the air in the air cavity, is described with the lossless wave equation as

$$\frac{\partial^2 p}{\partial t^2} - c^2 \nabla^2 p = 0, \quad (7)$$

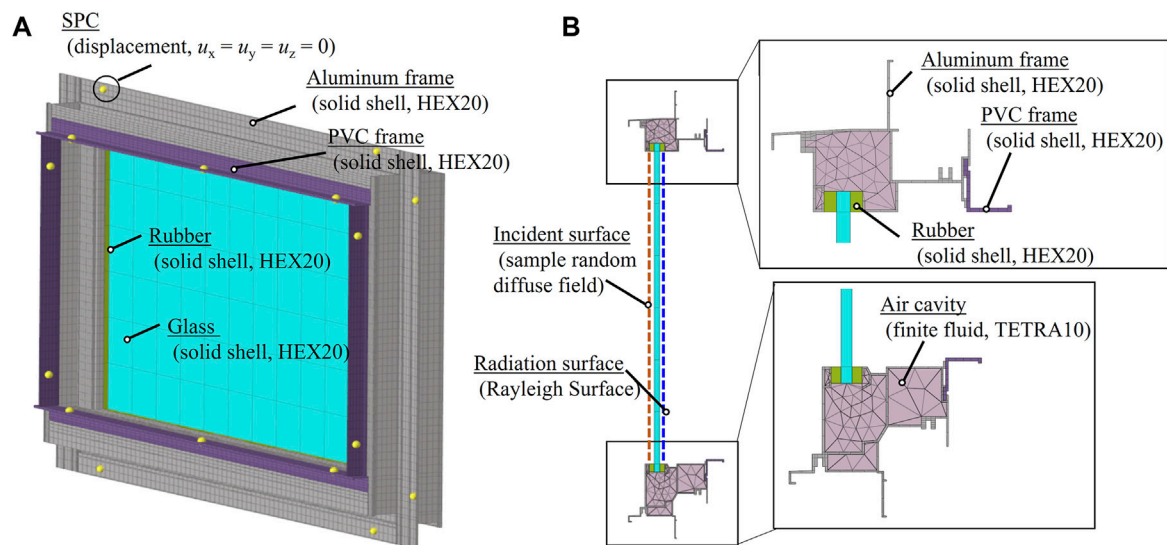


FIGURE 5
Numerical fixed window model discretized with solid shell elements in structural domains and fluid elements in acoustic domain for window: (A) Overall view, and (B) Cross-sectional view.

where p is the sound pressure, and c is the speed of sound in air. The coupling condition at the boundary between structural and acoustic domains is given by the displacement boundary condition and the continuity in pressure as

$$u^s|_n = u^a|_n, \quad (8)$$

$$\sigma^s|_n = -p, \quad (9)$$

where u^a is the fluid displacement at the interface, and n is the normal vector. The computations were performed in frequency domain using a computer (Proliant DL380; HP Inc., Xeon(R) CPU E5-2690 v4 @ 2.60 GHz, 28 cores; Intel Corp.). The calculations were done using four processes with IntelMPI parallel computation. The parallel computations were performed in a frequency direction. For example, four pure tone analyses were performed in parallel when using four processes. Using this strategy, four times the memory must be used compared to that used for serial computations.

We created three FE meshes, each having a different spatial resolution according to the analyzed frequency range for efficient computation. To account for vibration fields in structural domains, the glass, the aluminum and PVC frames, and the rubber sheet were discretized with three-dimensional solid shell HEX20 elements, which are twenty-node second-order hexahedron solid shell element (Petyt, 2010; Free Field Technologies, 2019) with three degrees of freedom at each node for the displacement u_x , u_y and u_z in x -, y - and z -axes. The solid shell elements can avoid thickness-locking and shear-locking effects. The element size for the window frames was set as 10 mm, irrespective of the analyzed frequency, which corresponds to one-fourth of the bending wavelength in the

aluminum frame at 5 kHz. It is noteworthy that we use the same sized elements for the PVC frame, although a smaller element size might be necessary when considering its bending wavelength. For this study, we assumed that this choice has a minor role in affecting the results because the proportion of PVC frames is much smaller than the aluminum frame, as shown in Figure 5. For glass and rubber, their element sizes are one-fifth smaller than the bending wavelength of the glass. Although the rubber needs a smaller element size, we used the same size as in the glass, assuming that rubber deforms along with the glass. For these window frames, and the glass and rubber, the number of elements in their thickness direction was one. We used three-dimensional TETRA10 finite fluid elements, the second-order ten-node tetrahedron elements, for the air cavity inside the window frames. Moreover, we set the element length as less than 20 mm at all frequencies, corresponding to one-third of the acoustic wavelength at 5 kHz. As might be apparent in Figure 5B, we used non-congruent meshes to deal with different element sizes and different element types in each structural domain and acoustic domain efficiently. The aluminum frame is discretized with HEX20 solid shell elements and the air inside the frame is discretized with TETRA10 finite fluid elements having different element size as in the solid shell elements. Therefore, the interface connection (Free Field Technologies, 2019) was used to consider mutual propagation between domains having different element types and sizes at those interfaces. The interface connection formulates coupling constraints by projecting nodes on the coupling surface to another surface. The displacement

TABLE 2 Number of screws attaching the window frame.

Window	Aluminium frame	PVC frame
(A)	8	10
(B)	10	14
(C)	12	16
(D)	10	22
(E)	8	20

continuity is maintained in the structure–structure connection. The total node numbers in the baseline model were approximately 240,000–534,000 for windows (A)–(E).

Regarding the sound-incidence condition to the window surface, we used an Actran component, the sampled random diffuse field (Wittig and Sinha, 1975; Van den Nieuwenhof et al., 2010; Coyette et al., 2014; Free Field Technologies, 2019), to simulate a diffuse-incidence condition. Two sampling methods can be selected for a diffuse field in the component. The first is a method based on a Cholesky decomposition of the cross PSD matrix. The present discussion is an assessment of using this first method. The second is a method based on a superposition of many discrete plane waves. The second approach is used for the explanations presented in Section 3 and Section 4. To calculate SRI at random-incidence, the maximum sound incidence angle is assumed to be 78°. The acoustic radiation from the window was computed with a Rayleigh surface (Kirkup, 1994; Free Field Technologies, 2019). The SRI is calculated as

$$\text{SRI} = 10 \log_{10} (W_{\text{inc}}/W_{\text{rad}}), \quad (10)$$

where W_{inc} represents the incident sound power computed from the spatial correlation on the glass surface. The radiated sound power W_{rad} is calculated using Rayleigh's integral of vibration velocities on the glass surface, including air resistance. For the diffuse field incidence condition, we set the sample number as 40. This sample number choice is based on results obtained from our earlier work (Mimura et al., 2022a), where the deviation in SRI on the use of this sample number from 100 sample number results was only 0.3 dB. In the numerical window model, screws are represented by clamped boundary conditions as a support condition (SPC). For the solid shell elements, this boundary condition is expressed as follows: three displacement components u_x , u_y and u_z were set to be zero at the node positions of the screws, as shown in Figure 5A. Table 2 presents the number of screws for the five fixed windows. They differ among the respective windows.

Table 3 presents the material properties of the glass, aluminum, PVC, rubber, and air. We used the calibrated Young's modulus for rubber with the measured results of window (A) so that the first modal frequency in the analysis matches the measured first modal frequency. Because the actual rubber material used for real windows is a hollow material, the

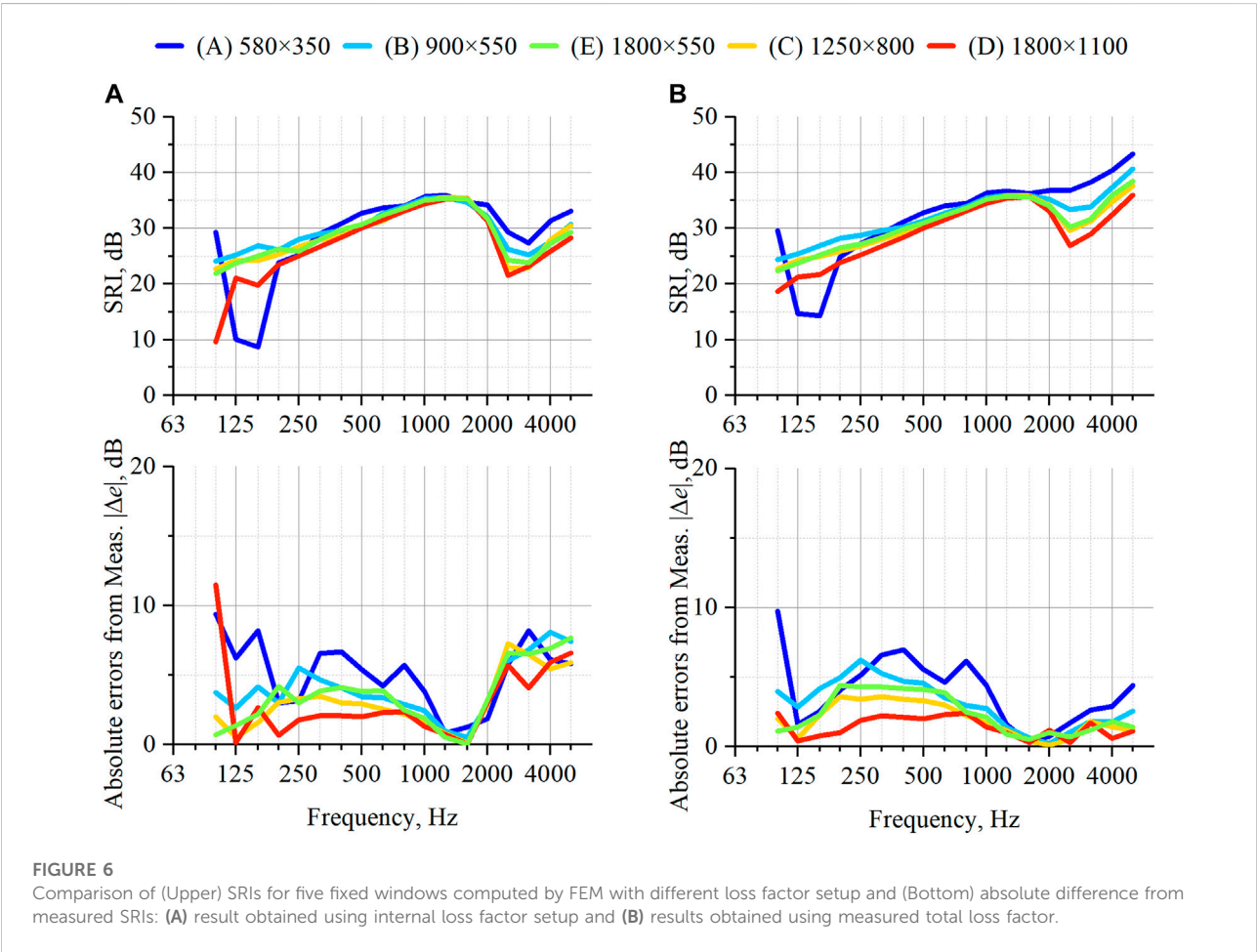
adjusted Young's modulus for the numerical model is smaller than the general values. Table 3 shows that we used two loss factor setups for the numerical model: Type 1 and Type 2. Type 1 uses an internal loss factor η_{int} of each solid material as a complex Young's modulus, in which the η_{int} s of the glass and PVC were obtained using a preliminary experiment with the central excitation method. For the rubber and the aluminum, their η_{int} s were set to values included in Actran's material library. However, Type 2 uses the measured frequency-dependent total loss factor η_{tot} , as shown in Figure 4B to the glass. Here, we considered that the measured total loss factor expresses the vibration energy loss of glass including losses from the connections to the surrounding structure. It was given as an effective loss factor of materials.

2.3 Results

Figures 6A, B respectively portray SRI values computed using the simplest model in the upper panel and absolute errors from measurements in the lower panel for five fixed windows in applied loss factor setups of Type 1 and Type 2. Figures 6A, B, respectively present results for Type 1 and Type 2. We first qualitatively evaluate whether the numerical results reproduced the measured SRIs of fixed windows of different sizes. Two numerical results show consistent behavior with the measured SRIs in Figure 4A for the magnitude relation of SRIs above the coincidence frequencies and show a dip in window (A) because of the first mode. However, both numerical results clearly show size-dependent SRIs below 400 Hz for windows (B)–(E). In those cases, smaller windows show larger SRI. Although the size-dependent SRI for the numerical results is explainable by the difference of radiation efficiency coming from the window dimensions, this size-dependent effect cannot be observed in the measured results. We infer that this difference between numerical results and measured results might derive from the fact that FEM predictions assumes an ideal diffuse incidence conditions and that it does not consider actual incidence conditions in the laboratory environment. However, detailed investigations are left as a subject for future study. Regarding differences in numerical results between the two loss factor setups, results show suggest that the resulting SRI difference occurs mainly at the first normal mode of window (A) and around and above the coincidence frequency for all windows. For the minimum sized window (A), the SRI computed using Type 1 shows a deeper dip at 125–160 Hz, which derives from the first normal mode of the window, than for SRI computed using Type 2. Some fluctuations are apparent below 160 Hz for the largest-sized window (D) when using the setup of Type 1. Additionally, the SRIs computed using Type 2 show higher SRI values than those using Type 1 above the coincidence frequencies. The boundary loss factor can be said to have a strong effect on the resulting SRI values above the coincidence frequencies because

TABLE 3 Material properties.

	Young's modulus [Pa]	Poisson's ratio [-]	Density [kg/m ³]	Loss factor (Type 1) [-]	Loss factor (Type 2) [-]
Glass	7.16×10^{10}	0.23	2500	0.002	η_{tot}
Aluminum	7.00×10^{10}	0.3	2700	0.01	0
PVC	3.50×10^9	0.3	1400	0.05	0
Rubber	0.50×10^6	0.48	890	0.05	0
	sound speed [m/s]	Density [kg/m ³]	—	—	—
Air	340	1.205	—	—	—



the presented windows have low internal loss factors for the respective solid materials.

Furthermore, from a quantitative perspective, the numerical results obtained using Type 2, which uses η_{tot} as an effective loss factor of material, show better agreement to the measured SRIs at the first normal mode for window (A) and around and above the coincidence frequencies for all windows, as might be apparent from the lower panels of Figure 6. The absolute errors of the

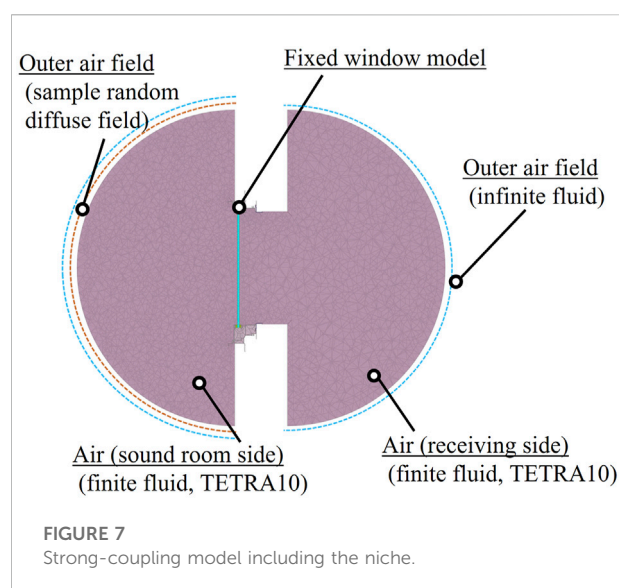
results obtained using Type 2 are 0.1–4.4 dB, whereas those of the results obtained using Type 1 show larger errors of 4.0–8.2 dB. The absolute errors in Type 2 results become smaller for larger windows. We also confirmed for numerical models using Type 1 and Type 2 that there is a difference in vibration attenuation on the glass surface at the first normal mode and at frequencies above the coincidence frequencies. Large vibration amplitude was observed at the coupling interface between the rubber and the aluminum frame for those frequencies, which indicates that boundary losses can contribute an important influence at those frequencies. The numerical model using Type 2 includes this boundary loss effect. Therefore, it was able to show higher accuracy than the numerical model using Type 1. Although the total loss factor remains an unknown value at a design stage, our earlier study (Mimura et al., 2022b) revealed that its frequency-averaged value shows a linear relation with the parameter $\frac{U}{S}$ of windows, where U and S represent the window perimeter and area, which indicates the possibility of predicting the total loss factor of different-sized windows. This possibility will be explored further in our future studies. However, both numerical results obtained using Type 1 and Type 2 show large absolute errors below 1 kHz for smaller-sized windows. At that frequency range, numerical results show overestimation of the measured SRI values. We infer that this discrepancy mainly derives from neglecting the niche in the simplest numerical model used in this section because the numerical results show larger discrepancies from the measured results for smaller windows at frequencies below the coincidence frequency, which indicates that the SRI of the measured results might be reduced by the niche effect (Kim et al., 2004; Vinokur, 2006; Sakuma et al., 2017). The next section will elucidate whether the modeling of niche engenders improved SRI predictions.

Regarding the computational cost of this baseline model which discretizes the window part only, total computational times were 9,491 s and 27,443 s, respectively, for the smallest window (A) and the largest window (D). The maximum memory requirements for the window (A) and (D) models were, respectively, 13.5 and 44.9 GB per process. Those results indicate that the necessary computational costs for the baseline model are acceptable and sufficiently practical in recent computational environments.

This section describes that using a measured total loss factor yields higher prediction accuracy at the first normal mode and around and above coincidence frequency than using internal loss factors.

3 Improvement by including a niche

This section presents discussion of whether or not including a niche into the numerical model produces better agreement with the measured SRI for five fixed windows. The examination



specifically emphasizes SRI below 1 kHz, for which large discrepancies from the measured results were observed. The numerical model used for this examination requires assumption of a diffuse sound incidence condition, but hemispherical free spaces around the window are discretized by finite fluid elements combined with infinite elements. In doing so, the niche in a laboratory environment is included in the numerical model. For the discussion presented herein, Type 2 loss factor setup using measured η_{tot} is used because this setup showed better accuracy in the preceding section.

3.1 Strong-coupling model

Figure 7 portrays the numerical model with a niche in which the fixed window part uses the same discretized model in Figure 5. However, this model further discretizes the sound incidence field and radiating sound field around the fixed window as hemispherical free spaces to model the niche. The structure–acoustics coupling between the sound fields around the windows and vibration fields in windows are considered. A strong-coupling model is used for the explanation presented in this section. Because this model considers free field sound radiations around the window, infinite elements are used on the hemispherical surfaces. The sound fields in the hemispherical spaces are discretized by TETRA10 second-order finite fluid elements. The element sizes were set below 114 mm, thereby satisfying element size of less than one-third of the acoustic wavelength at 1 kHz. The radius of the hemisphere spaces is 1.4 m, corresponding to four times the wavelength at 1 kHz. We use a non-congruent mesh for this model. The hemispherical sound fields and windows are connected by the interface connector. As an infinite element, an Actran component,

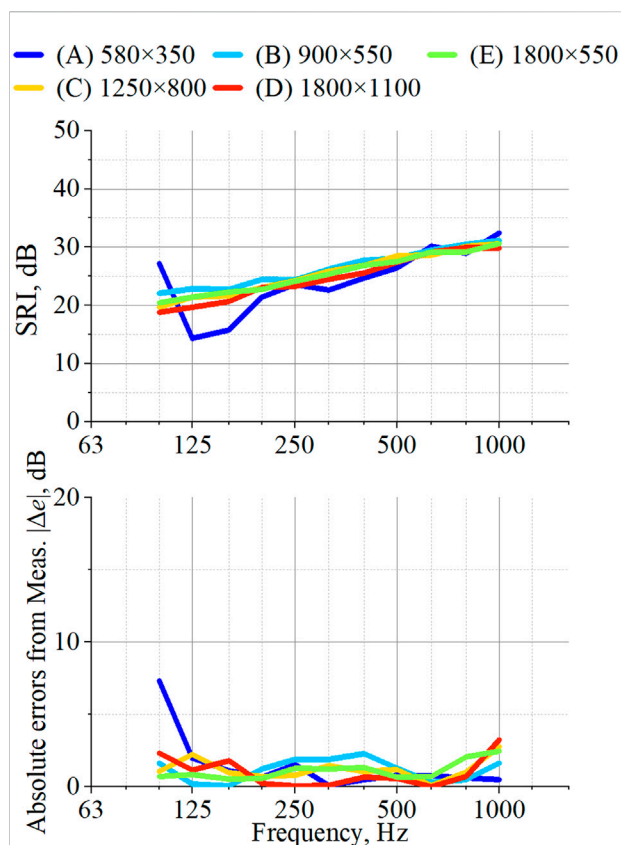


FIGURE 8

Results obtained using the strong-coupling model (Upper) SRI for five fixed windows and (Bottom) absolute difference from measured SRI.

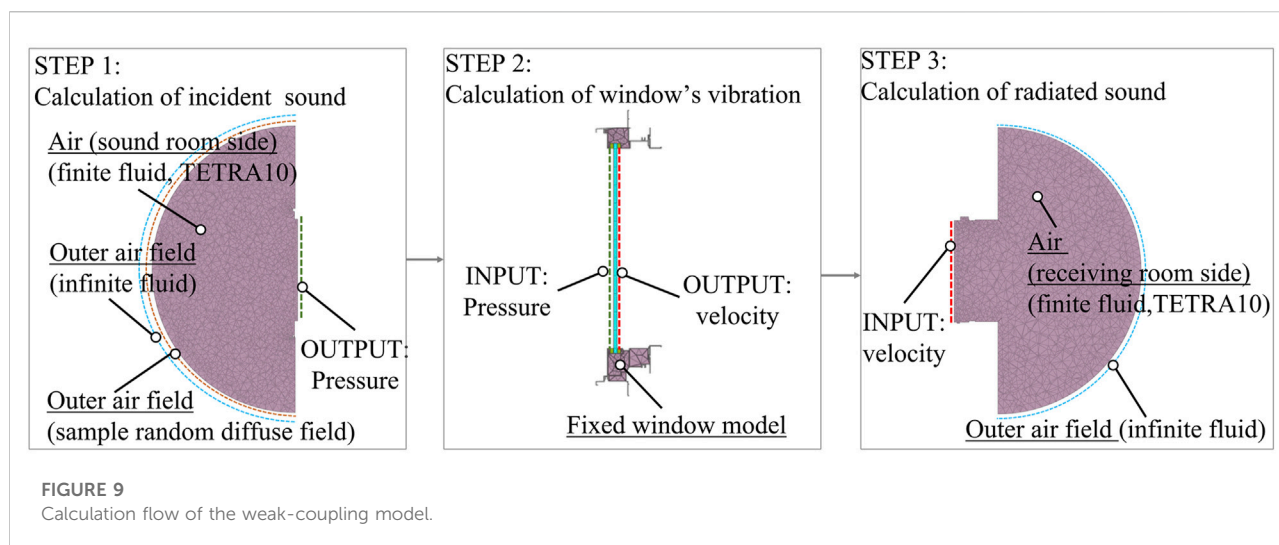
infinite fluid (Free Field Technologies, 2019; Astley and Coyette, 2001a,b), was used on the hemisphere surfaces to reproduce free-field sound radiation. With this component, the sound radiation to infinite distance is calculated based on the sound distance attenuation, using a complement factor in radius direction including the Sommerfeld condition and the coordinate system of the acoustic field. To realize the diffuse sound-incidence condition, the sampled random diffuse field component is again used on the outside surface of the hemisphere on the incident side, but the method based on the superposition of numerous plane waves at random phase is used here. The number of sampled random diffuse fields was set as 40. More than 8,000 plane waves were summed to reproduce a diffuse sound field. The maximum incident angle was set to 90°. The SRI was calculated using Eq. 10. The incident sound power W_{inc} was calculated on the glass surface of the incident side. The radiated sound power W_{rad} was calculated on the infinite fluid surface of radiating side. Actually, this model naturally has many more degrees of freedom than the baseline model used in the preceding section because of the discretization requirement of sound fields around the window. The total node

numbers of the strong-coupling models were 1,080,977–1,963,834, respectively, for windows (A)–(E). Comparison of the node numbers of the baseline model shows that the strong-coupling models require approximately four times more nodes.

3.2 Results

Figure 8 portrays the SRIs computed using the numerical model with the niche for five fixed windows and absolute errors from measurements, respectively, in the upper and lower panels. Compared to the model results that discretize only the window part in Figure 6B, the present model results with the niche produce much better accuracy at 125 Hz–1 kHz for all windows. Considered quantitatively, the absolute errors by the numerical model with the niche are smaller than 3.3 dB, except for the results obtained for window (A) at 100 Hz. One can find that inclusion of the niche improves prediction accuracy in a laboratory environment for smaller windows. For the smallest window (A), the absolute errors from the measured result become less than 1.5 dB at 125 Hz–1 kHz. In addition, the numerical result of window (A) reproduces small dips at 315 and 800 Hz, which are found in the measured results. This result suggests that these small dips in the measurement derive from the niche effect. Based on those results, probably the niche effect is the primary reason for discrepancies using the baseline model from the measurement below 1 kHz, especially for smaller windows. Therefore, we can propose that the niche should be modeled in a numerical model to predict the SRI of fixed windows in a laboratory environment accurately. However, a large discrepancy exceeding 5 dB from the measured SRI can still be found at 100 Hz for the smallest window (A). This discrepancy in the stiffness control region might be derived from the numerical model that still does not include the source and receiving reverberant rooms. This is left as a subject to be addressed in our future work.

Furthermore, using a strong-coupling model with a niche entails remarkably high computational costs. For instance, the computational cost in the minimum window (A) and the maximum window (D) were 60,432 s and 358,201 s in computational times. Moreover, windows (A) and (D) models respectively require 79 and 204 GB per process. It is noteworthy that the computations were made under two process parallel computations and a serial computation for window (A) and window (D) because of limitations of memory of our computational environment. Compared to the computational costs of baseline model, the strong-coupling model required 12–34 times longer computational times and 6–7.5 times more memory. Therefore, from the aspect of memory requirement, the strong-coupling model is difficult for practical use, especially for larger-sized windows and higher frequencies. We can infer the propriety of using the baseline



model around and above the coincidence frequencies and of using the model with the niche below coincidence frequencies for efficient and accurate prediction of the SRI of fixed windows in a laboratory environment.

4 Applicability of weak-coupling calculation

The preceding section revealed that the strong-coupling model, including niches, provides high accuracy for SRI prediction below 1 kHz, with markedly high computational efforts. This section presents an exploration of the applicability of a weak-coupling model at frequencies below 1 kHz to realize more efficient computation. This coupling model does not consider interaction between sound fields around the windows and vibration fields in the windows, but the niche is included in the numerical model. Using this weak-coupling model, faster computation with lower memory than the strong-coupling model can be expected, but it requires two additional acoustics analyses.

4.1 Weak-coupling model

Figure 9 portrays a three-step calculation procedure using the weak-coupling model. Although the considered situation is the same as the strong-coupling model, the calculations are divided into three steps. This division can reduce the magnitude of the problem in the considered situation. Step 1 computes sound pressure distributions and incident sound power on the glass surface under the numerical model that considers only the incident sound field around the window. The sound field is discretized with TETRA10 second-order finite fluid elements.

The infinite fluid are applied to the hemisphere surface. A sampled random diffuse field with a superposition of many plane waves is used to reproduce a diffuse incidence condition. Step 2 computes the vibration velocities on the glass surface on the transmitted side with sound pressure loading on the incident glass surface calculated in Step 1. The discretized model used for these analyses is the same as the baseline model. Then, Step 3 computes sound radiation from the window surface and sound radiation power with the vibration velocity distributions on the glass surface calculated in Step 2. The numerical model used for this step considers only radiated sound fields around the windows. It is discretized with TETRA10 second-order finite fluid elements and infinite fluid elements as in Step 1.

Regarding the problem size of each step, the total nodes in the numerical model of Step 1 are 377,896 and 750,873, respectively, for window (A) and window (D). For Step 2, the window (A) and (D) models have 240,446 nodes and 497,591 nodes, respectively, which is the same as the baseline model. In Step 3, the total numbers of nodes are 402,635 and 715,370, respectively, for windows (A) and (D). Compared to the strong-coupling model, the maximum problem size is reduced to less than half. This problem size reduction markedly reduces memory consumption, especially for larger windows. However, the two additional analyses of Step 1 and Step 3 entail larger problem sizes than the baseline model. The computations are performed in parallel using four processes.

The SRI is also computed from the incident sound power W_{inc} computed in Step 1 and sound radiation power W_{rad} computed in Step 3, with Eq. 10. The element sizes are the same as those for the models used in the strong-coupling model described in an earlier section. It is noteworthy that Step 1 and Step 3 can perform as acoustic analysis.

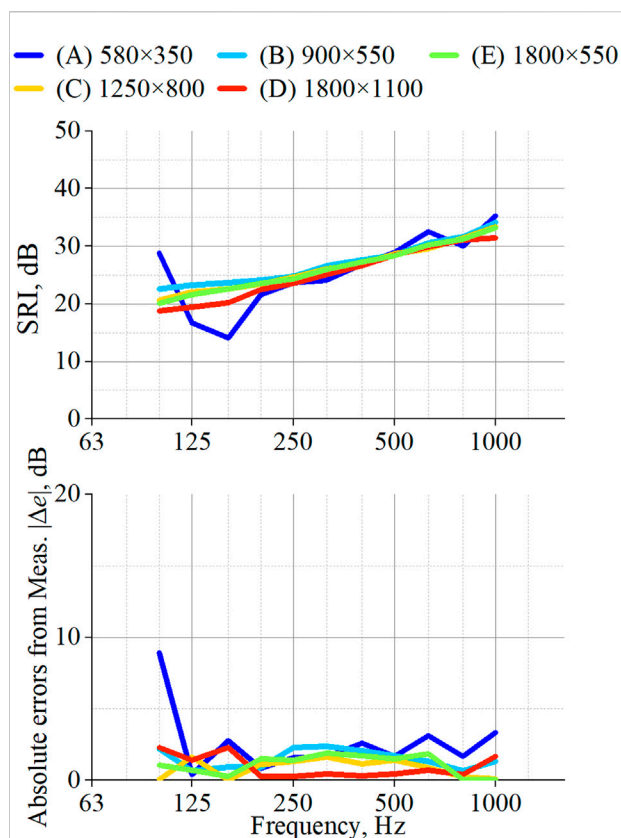


FIGURE 10

Results obtained using the weak-coupling model (Upper) SRIs of five fixed windows and (Bottom) absolute difference from measured SRIs.

4.2 Results

Figure 10 shows the SRIs of fixed windows calculated respectively using the weak-coupling model and absolute errors from measurements in the upper and lower panels. The weak-coupling model produced much better accuracy than the baseline model results as shown in Figure 6B at 125 Hz–1 kHz. Greater improvement can be found for smaller windows. It is noteworthy that the weak-coupling model can also reproduce the small dips in SRI at 315 and 800 Hz appeared in the measured results of window (A). The absolute errors in the weak-coupling model are less than 3.3 dB, except for the result of window (A) at 100 Hz. The resulting accuracy is comparable to strong-coupling model results obtained for windows (B)–(E), but slightly lower accuracy to the smallest window (A) can be observed.

Furthermore, as expected, the weak-coupling model has special benefits for maximum memory requirements. For the minimum-sized window (A) and the maximum-sized window (D), the weak-coupling models respectively require 29 and 51 GB per process, which are 1/2.7 and 1/4 less memory than the strong-

coupling models. Moreover, the computational times for windows (A) and (D) are 36,288 s and 98,921 s. They are 1.7 and 3.6 times faster, respectively, than the strong-coupling model. The results demonstrate the effectiveness of using the weak-coupling model to compute SRIs in a laboratory environment at a low frequency range.

5 Conclusion

This study explored efficient and accurate finite element modeling to predict SRI of different-sized fixed windows at random incidence in a laboratory environment. To this end, we examined the prediction accuracy of three numerical models over five fixed windows with different dimensions of 0.2–2.0 m² by comparison with measured results. All numerical models incorporate the assumption of a diffused sound-incidence condition. Sound radiated from windows is computed using Rayleigh's integral or sound field analysis using acoustic analysis. We also examined necessary computational costs for the three numerical models to infer a practical prediction model according to the analyzed frequency range. The findings obtained from our study are presented below.

- 1) The simplest model that discretizes only window parts with finite elements shows higher accuracy at first normal mode and around and above coincidence frequencies when using measured total loss factors instead of using internal loss factors of the respective materials. The computational costs are practical for computing SRI up to 5 kHz, with the calculation of 1/24 octave band center frequencies. The largest window (D) can be calculated within 8 h using 45 GB per process. However, an important shortcoming of this simplest model is that it can not accurately reproduce SRI in a laboratory environment below coincidence frequencies, especially for smaller windows, because of neglect of the niche in the numerical model.
- 2) The strong-coupling model with a niche that discretizes the window and surrounding hemisphere sound fields with niche has the best prediction of SRI below 1 kHz in a laboratory environment. A niche must be included in the numerical model for the accurate prediction of SRI in smaller-sized windows. However, the strong-coupling model entails high computational burdens. The strong-coupling model requires 6–7.5 times larger computational memory than the simplest model, even for the analysis below 1 kHz. Therefore, the practical use of the strong-coupling model is difficult for SRI prediction at high frequencies.
- 3) The weak-coupling model which divides the strong-coupling model calculation into three steps can still produce a comparable accuracy to the strong-coupling model in SRI predictions below 1 kHz, with higher efficiency. The

computational cost reduced to 1/2.7–1/4 than the strong coupling model. The SRI of the largest window (D) can calculate within 27 h until 1 kHz. Therefore, using the weak-coupling model is a practical selection to predict SRI at low frequencies when considering niche effects in a laboratory environment.

Data availability statement

The raw data supporting the conclusions of this article will be made available by the authors, without undue reservation.

Author contributions

MM contributed to the conception and design of the study, conducted the experiment and numerical simulations, and prepared the draft of the manuscript. TO and KS contributed to give feedback about the research design and numerical simulations, analyzed the results, and supported writing of the

manuscript. All authors contributed to manuscript revision, reading, and approval of the submitted version.

Conflict of interest

Author MM is employed by YKK Corporation.

The remaining authors declare that the research was conducted in the absence of any commercial or financial relationships that could be construed as a potential conflict of interest.

Publisher's note

All claims expressed in this article are solely those of the authors and do not necessarily represent those of their affiliated organizations, or those of the publisher, the editors and the reviewers. Any product that may be evaluated in this article, or claim that may be made by its manufacturer, is not guaranteed or endorsed by the publisher.

References

- Arjunan, A., Wang, C., Yahiaoui, K., Mynors, D., Morgan, T., and English, M. (2013). Finite element acoustic analysis of a steel stud based double-leaf wall. *Build. Environ.* 67, 202–210. doi:10.1016/j.buildenv.2013.05.021
- Arjunan, A., Wang, C., Yahiaoui, K., Mynors, D., Morgan, T., Nguyen, V., et al. (2014). Development of a 3d finite element acoustic model to predict the sound reduction index of stud based double-leaf walls. *J. Sound Vib.* 333, 6140–6155. doi:10.1016/j.jsv.2014.06.032
- Astley, R. J., and Coyette, J.-P. (2001a). Conditioning of infinite element schemes for wave problems. *Commun. Numer. Methods Eng.* 17, 31–41. doi:10.1002/1099-0887(200101)17:1;1::AID-CNM386;3.0.CO;2-A
- Astley, R. J., and Coyette, J.-P. (2001b). The performance of spheroidal infinite elements. *Int. J. Numer. Methods Eng.* 52, 1379–1396. doi:10.1002/nme.260
- Cambridge, J. E., Davy, J. L., and Pearse, J. (2020). The sound insulation and directivity of the sound radiation from double glazed windows. *J. Acoust. Soc. Am.* 148, 2173–2181. doi:10.1121/1.50002167
- Coyette, J.-P., van den Nieuwenhof, B., and Lielsen, G. (2014). “Computational strategies for modeling distributed random excitations (diffuse field and turbulent boundary layer) in a vibro-acoustic context,” in *Congres francais d'Acoustique*.
- Davy, J. L. (2009). Predicting the sound insulation of single leaf walls: Extension of cremer's model. *J. Acoust. Soc. Am.* 126, 1871–1877. doi:10.1121/1.3206582
- Davy, J. L. (2010). The improvement of a simple theoretical model for the prediction of the sound insulation of double leaf walls. *J. Acoust. Soc. Am.* 127, 841–849. doi:10.1121/1.3273889
- Free Field Technologies (2019). *Actran 2020 user's guide—volume 1: Installation, operations, theory and utilities*. Mont-Saint-Guibert, Belgium: Free Field Technologies.
- Guy, R., De Mey, A., and Sauer, P. (1985). The effect of some physical parameters upon the laboratory measurements of sound transmission loss. *Appl. Acoust.* 18, 81–98. doi:10.1016/0003-682X(85)90039-8
- ISO 10140-1 (2016). *Acoustics – laboratory measurement of sound insulation of building elements – Part 1: Application rules for specific products*. Geneva: International Organization for Standardization.
- JIS A 1416 (2000). *Acoustics-method for laboratory measurement of airborne sound insulation of building elements*.
- Kim, B.-K., Kang, H.-J., Kim, J.-S., Kim, H.-S., and Kim, S.-R. (2004). Tunneling effect in sound transmission loss determination: Theoretical approach. *J. Acoust. Soc. Am.* 115, 2100–2109. doi:10.1121/1.1698815
- Kirkup, S. (1994). Computational solution of the acoustic field surrounding a baffled panel by the Rayleigh integral method. *Appl. Math. Model.* 18, 403–407. doi:10.1016/0307-904x(94)90227-5
- Løvholt, F., Norèn-Cosgriff, K., Madshus, C., and Ellingsen, S. E. (2017). Simulating low frequency sound transmission through walls and windows by a two-way coupled fluid structure interaction model. *J. Sound Vib.* 396, 203–216. doi:10.1016/j.jsv.2017.02.026
- Mimura, M., Okuzono, T., and Sakagami, K. (2022a). Pilot study on numerical prediction of sound reduction index of double window system: Comparison of finite element prediction method with measurement. *Acoust. Sci. Technol.* 43, E2131–E2142. doi:10.1250/ast.43.32
- Mimura, M., Tsukamoto, Y., Tomikawa, Y., Okuzono, T., and Sakagami, K. (2022b). Sound insulation characteristics of small fixed windows in a laboratory and prediction with an existing theory. *Acoust. Sci. Technol.* In print.
- Minichilli, F., Gorini, F., Ascari, E., Bianchi, F., Coi, A., Fredianelli, L., et al. (2018). Annoyance judgment and measurements of environmental noise: A focus on Italian secondary schools. *Int. J. Environ. Res. Public Health* 15, 208. doi:10.3390/ijerph15020208
- Muzet, A. (2007). Environmental noise, sleep and health. *Sleep. Med. Rev.* 11, 135–142. doi:10.1016/j.smrv.2006.09.001
- Papadopoulos, C. I. (2003). Development of an optimised, standard-compliant procedure to calculate sound transmission loss: Numerical measurements. *Appl. Acoust.* 64, 1069–1085. doi:10.1016/S0003-682X(03)00066-5
- Petri, D., Licitra, G., Vigotti, M. A., and Fredianelli, L. (2021). Effects of exposure to road, railway, airport and recreational noise on blood pressure and hypertension. *Int. J. Environ. Res. Public Health* 18, 9145. doi:10.3390/ijerph18179145
- Petyt, M. (2010). *Introduction to finite element vibration analysis*. New York: Cambridge University Press.
- Rindel, J. (2018). *Sound insulation in buildings*. Boca Raton: CRC Press.
- Sakuma, T., Inoue, N., and Seike, T. (2017). Numerical examination of niche effect on sound transmission loss of glass panes. *Acoust. Sci. Technol.* 38, 279–286. doi:10.1250/ast.38.279
- Sandberg, G., Wernberg, P.-A., and Davidsson, P. (2008). “Fundamentals of fluid-structure interaction,” in *Computational aspects of structural acoustics and vibration* (Berlin, Germany: Springer), 23–101.

Santoni, A., Davy, J. L., Fausti, P., and Bonfiglio, P. (2020). A review of the different approaches to predict the sound transmission loss of building partitions. *Build. Acoust.* 27, 253–279. doi:10.1177/1351010X20911599

Sewell, E. (1970). Transmission of reverberant sound through a single-leaf partition surrounded by an infinite rigid baffle. *J. Sound Vib.* 12, 21–32. doi:10.1016/0022-460X(70)90046-5

Soussi, C., Aucejo, M., Larbi, W., and Deü, J.-F. (2021). Numerical analyses of the sound transmission at low frequencies of a calibrated domestic wooden window. *Proc. Institution Mech. Eng. Part C J. Mech. Eng. Sci.* 235, 2637–2650. doi:10.1177/09544062211003621

Tsukamoto, Y., Tamai, K., Sakagami, K., Okuzono, T., and Tomikawa, Y. (2021). Basic study of practical prediction of sound insulation performance of single-glazed window. *Acoust. Sci. Technol.* 42, E2143–E2353. doi:10.1250/ast.42.350

Van den Nieuwenhof, B., Lielens, G., and Coyette, J. (2010). “Modeling acoustic diffuse fields: Updated sampling procedure and spatial correlation function eliminating grazing incidences,” in *The Proceedings of ISMA Conference*, 4723–4736.

Vinokur, R. (2006). Mechanism and calculation of the niche effect in airborne sound transmission. *J. Acoust. Soc. Am.* 119, 2211–2219. doi:10.1121/1.2179656

Wawezynowicz, A., Krzaczek, M., and Tejchman, J. (2014). Experiments and *fe* analyses on airborne sound properties of composite structural insulated panels. *Archives Acoust.* 39, 351–364. doi:10.2478/aoa-2014-0040

Wittig, L. E., and Sinha, A. K. (1975). Simulation of multicorrelated random processes using the fft algorithm. *J. Acoust. Soc. Am.* 58, 630–634. doi:10.1121/1.380702



OPEN ACCESS

EDITED BY

Samad Sepasgozar,
University of New South Wales, Australia

REVIEWED BY

Amir Mahdiyar,
University of Science Malaysia, Malaysia
Mahua Mukherjee,
Indian Institute of Technology Roorkee,
India

*CORRESPONDENCE

Mehdi Khakzand,
mkhakzand@iust.ac.ir

SPECIALTY SECTION

This article was submitted to Sustainable
Design and Construction,
a section of the journal
Frontiers in Built Environment

RECEIVED 29 June 2022

ACCEPTED 17 August 2022

PUBLISHED 14 September 2022

CITATION

Khaledi HJ, Faizi M and Khakzand M
(2022), The effects of personal green
spaces on human's mental health and
anxiety symptoms during COVID-19:
The case of apartment residents
in Tehran.
Front. Built Environ. 8:981582.
doi: 10.3389/fbuil.2022.981582

COPYRIGHT

© 2022 Khaledi, Faizi and Khakzand.
This is an open-access article
distributed under the terms of the
[Creative Commons Attribution License](#)
(CC BY). The use, distribution or
reproduction in other forums is
permitted, provided the original
author(s) and the copyright owner(s) are
credited and that the original
publication in this journal is cited, in
accordance with accepted academic
practice. No use, distribution or
reproduction is permitted which does
not comply with these terms.

The effects of personal green spaces on human's mental health and anxiety symptoms during COVID-19: The case of apartment residents in Tehran

Hanieh Jafari Khaledi¹, Mohsen Faizi² and Mehdi Khakzand^{3*}

¹PhD. candidate in Architecture at School of Architecture and Environmental Design, Iran University of Science and Technology (IUST), Tehran, Iran, ²Professor of Landscape Architecture School of Architecture and Environmental Design, Iran University of Science and Technology (IUST), Tehran, Iran, ³Associate Professor of Landscape Architecture School of Architecture and Environmental Design, Iran University of Science and Technology (IUST), Tehran, Iran

The governments implemented social distancing and isolation with the spread of COVID-19. However, these ways efficiently prevent coronavirus transmission, but they caused unprecedented changes in most people's day-to-day lives. One of the concerns is mental health, and many experts are concerned about the tsunami of mental illnesses during and after coronavirus. Being exposed to nature has an efficient role in mental health. Under pandemic conditions, people reduced their outdoor activities, but personal green spaces are still available. This research assessed the impact of these spaces as an alternative to public green spaces and their benefits during COVID-19 on mental health and generalized anxiety disorder. Accordingly, by designing an online self-administered questionnaire, a total of 700 residents of Tehran apartments were evaluated. A structural equation model was created. The results demonstrate that using personal green spaces has a negative correlation and significant impact on general mental health and generalized anxiety disorder. It also plays a more substantial role in reducing depression than its role in reducing anxiety among individuals. Therefore, maximum land use policies should be reviewed. Also, green spaces should be given more attention in post-COVID designs on a macro-scale to a small scale.

KEYWORDS

COVID-19, personal green space, mental health, anxiety symptom, apartment residents

1 Introduction

The coronavirus disease 2019 (COVID-19) outbreak raised a public health emergency on 30 January 2020 and a global pandemic on 11 March 2020 (World Health Organization, 2020). This pandemic has impacted all aspects of human lives (Lu et al., 2021), such as the global market, economy, agriculture, industries, health care,

and human health (Kumar and Nayar, 2021). The WHO is concerned about the pandemic's psychosocial consequences and mental health (World Health Organization, 2020). Also, the global community is worried about COVID-19 and its long-term outcomes (Kumar and Nayar, 2021), and many experts have predicted a "tsunami of psychiatric illnesses" as the aftermath of the COVID pandemic (Tandon, 2020). Most governments worldwide issued stay-at-home orders (Gostin and Wiley, 2020; Petersen et al., 2020) for an unprecedented time (Brooks et al., 2020). Also, they have implemented various social distancing measures as the most effective way to control the spread of this virus (Gu et al., 2020; Tian et al., 2020; Wilder-Smith and Freedman, 2020), forbidding visiting parks, playgrounds, community gardens, and all outdoor activity spaces (Shoari et al., 2020). These strategies are essential to break the transmission, but it has also created lots of problems for humans, even for children, who become restless and, in some cases, violent (Kumar and Nayar, 2021). These social distancing measures may keep people away from nature (Lu et al., 2021). Quarantine, self-isolation, and the concern and uncertainty instilled by the perceived health risk and economic ramifications of the pandemic have increased insomnia, loneliness, drug use, harmful alcohol, depression, anxiety, suicidal behavior, self-harm, and suicide rates (Huang and Zhao, 2020; Rajkumar, 2020; Wang et al., 2020; World Health Organization, 2020; Zhu et al., 2020). Furthermore, it is expected that well-being and mental health effects are likely to be profound and long-lasting (Holmes et al., 2020; Hotopf et al., 2020). There are various available pathways for mitigating the stress of this pandemic, which seems that connecting with nature is one of these ways. Connecting with greenery in public outdoor spaces benefits human physical and mental health (Barton and Pretty, 2010; Hartig et al., 2014; Gascon et al., 2015; Triguero-Mas et al., 2015; WHO, 2016; Douglas et al., 2017; Van den Bosch and Sang, 2017; Callaghan et al., 2021). However, with quarantine, impeding the outdoor interaction with green spaces, and spending almost all of the time at home, most of these ways toward improving mental health are not available (Dzhambov et al., 2021).

Many studies have been concerned with measuring public green spaces in different dimensions and their impact on humans, and fewer studies have examined the different dimensions of the effects of personal green spaces. On the other hand, new conditions were created due to the coronavirus outbreak. It became necessary to create suitable alternatives to improve the mental conditions of humans that were previously available. One of the suitable alternatives is personal green spaces that were created which can affect mental health and anxiety levels. However, this study seeks to assess the impact of personal green spaces on mental health, anxiety levels, and the relationship between demographic characteristics and mental health and anxiety symptoms by eliminating activities that were previously helpful for mental health and anxiety levels. This study was conducted during the fifth wave of coronavirus in Iran, which was more dangerous

than previous waves, and the country was under an emergency. This article aims to target the corona era when quarantine orders were enforced throughout the country, and people were denied access to urban green spaces to examine the relationship between personal green space utilization, mental health, general anxiety symptoms, and demographic characteristics to provide solutions for designing apartments in Tehran for the post-COVID period. Therefore, this research seeks to answer three questions: 1) what is the impact of personal green spaces on mental health? 2) What is the effect of personal green spaces on anxiety symptoms? Also, 3) what is the relationship between demographic characteristics and mental health and anxiety symptoms? Based on the literature, visible greenery, both outdoors and indoors, reduces stress and increases concentration (Duijn et al., 2011; Alker et al., 2014). Also, connecting with greenery in public outdoor spaces benefits human physical and mental health (Barton and Pretty, 2010; Hartig et al., 2014; Gascon et al., 2015; Triguero-Mas et al., 2015; WHO, 2016; Douglas et al., 2017; Van den Bosch and Sang, 2017; Callaghan et al., 2021). The authors hypothesized the following: (H1) personal green space has positive effects on the level of human general mental health; (H2) personal green space has positive effects on reducing symptoms of generalized anxiety disorder; (H3) there is a relationship between demographic characteristics and mental health and the symptoms of generalized anxiety disorder. Overall, the authors expect that these pathways of private green spaces are an efficient alternative for outdoor green spaces; also, through these ways, humans demonstrate lower symptoms of anxiety or depression. The hypotheses are shown in Figure 1. Moreover, it needs to mention that the authors refer to the personal green space, a natural space that is physically accessible. Therefore, there have not been examples such as the existence of a painting of nature that is mounted on the wall.

2 Materials and methods

2.1 Connecting with greenery in quarantine

With the widespread coronavirus and the application of quarantine and stay-at-home orders, humans' connection with nature becomes limited. However, there are still some alternative forms to connect with nature as an element of improving mental health. First, the plant symbolizes nature (Smardon, 1988; Bringslimark et al., 2009). Also, each green environment could improve mood and self-esteem, improve general psychological well-being, reduce anger, and positively affect emotions or behavior. On the other hand, the presence of water generated more significant effects (Barton and Pretty, 2010; Windhager et al., 2011; Keniger et al., 2013; Wolf and

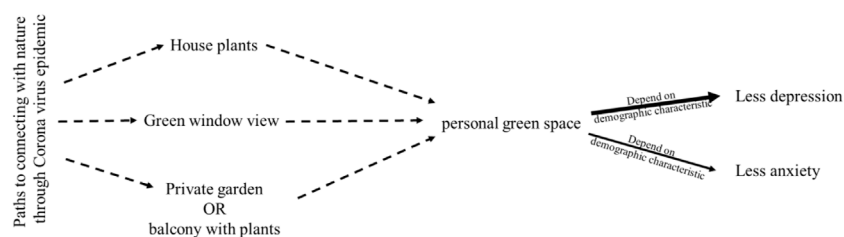


FIGURE 1

Conceptual framework showing the authors' hypotheses. * Line widths represent hypothesized pathway strength and thicker lines denoting stronger associations. Moreover, dashed lines are for introducing selected variables of personal green spaces in this research.

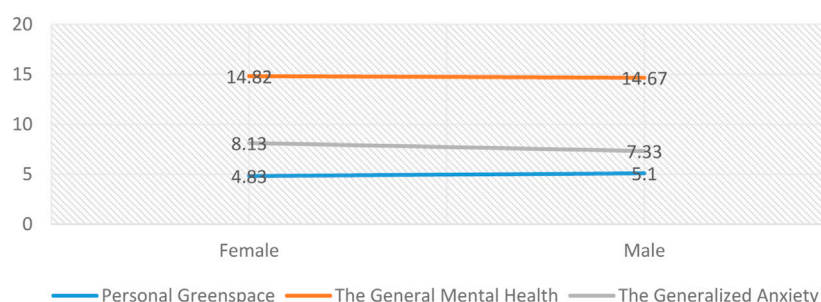


FIGURE 2

Mean personal green spaces, general mental health, and generalized anxiety disorder at gender levels.

Housley, 2014; Mensah et al., 2016). Moreover, visible greenery, both outdoors and indoors, reduces stress and increases concentration (Duijn et al., 2011; Alker et al., 2014). Many people place plants indoors such as in the living area or their workspaces (Dravigne et al., 2008), where research and empirical studies demonstrated that potted plants could reduce physical discomfort, stress, depressive symptoms, anxiety, and mental health (Fjeld, 2000; Chang and Chen, 2005; Doxey et al., 2009; Han, 2018; Hall and Knuth, 2019; Han and Ruan, 2019). In a study, interior plants can lead to healthy and productive workplaces through decreased stress levels, enhanced attention capacity, and higher job satisfaction (Raanaas et al., 2011; Hartig et al., 2014; Gilchrist et al., 2015). Moreover, placing plants in the classroom can increase children's performance, and it was shown they were progressing through the school curriculum 20%–26% faster (Duijn et al., 2011). Therefore, indoor vegetation at home is an effective way to engage with greenery and benefit from its positive effects. Second, based on empirical research, green window views can provide micro-restorative episodes over the days or a few hours, which promote healing (Ulrich, 1984; Kaplan, 2001; Jo et al., 2019). This way recovery from stressful events (Li and Sullivan, 2016) and psychological restoration (Lee et al., 2015) can be achieved. If it extends to

several months, a person's ability to complete complex cognitive tasks such as earning high grades will increase (Benfield et al., 2015). When people observe plants, oxy-Hb (oxyhemoglobin) concentrations in the right prefrontal cortex are significantly lower, indicating a physiological state of relaxation (Park et al., 2017). Biophilic workplaces with views of nature and daylight can lead to greater employee attention and productivity (Elzeyadi, 2011; Windhager et al., 2011); for instance, studies showed that offices in Great Britain and the Netherlands with plants had an increase of 15% in worker's productivity (Nieuwenhuis et al., 2014; Korpela et al., 2017). Employees exposed to views of nature, such as trees or flowers, are less stressed and more satisfied in comparison with those who lack window views entirely or see only buildings outside (Kaplan, 1995). Even the views of artificial nature can help with anxiety and stress relief (Ulrich and Dimberg, 1991). Therefore, greenery views through windows effectively connect relationships with nature and benefit their positive impact. Third, mental fatigue recovery, stress reduction, and improved concentration levels happen when individuals spend time on natural spaces (Entrix, 2010; Kjellgren and Buhrkall, 2010; Keniger et al., 2013; White et al., 2017) live near green environments, or view greenery and vegetation (Abraham et al., 2010; Carrus et al., 2015; Watts, 2017). The

benefits of gardening and gardening to well-being are considered adequate for human mental health. The design of “healing” gardens becomes a topic of study in itself and as a credible ingredient for convalescent patients in health care situations (Marcus and Sachs, 2013). Also, a domestic garden can reduce anxiety and depression (Dennis and James, 2017; Soga et al., 2017; de Bell et al., 2020). A research on participants involved in outside horticultural therapy activities such as landscaping or gardening demonstrated that people have reduced incidents of aggressive behavior, have improved cognitive capacity, and are more actively engaged (Gigliotti and Jarrott, 2005). So, having a private garden or balcony with greenery is one of these ways. These three alternatives for engaging humans with greenery have rarely been compared, even much less directly (Akpınar et al., 2016; Korpela et al., 2017; Dzhambov et al., 2018). Most previous research on indoor greenery was related to workplaces, especially classrooms or office spaces (Raanaas et al., 2011; Han and Ruan, 2019).

2.2 Study design

This research was conducted during the COVID-19 pandemic with the aim of evaluating the effects of personal green spaces on human mental health and the level of anxiety symptoms. Between 20 August and 1 September 2021, the authors conducted an online self-administered survey among 700 apartment residents in Tehran. Severities of anxiety and depression symptoms over the past 2 weeks were measured by the Patient Health Questionnaire 12-item and the Generalized Anxiety Disorder 7-item Scale comparing two indoor measures (number of houseplants and the proportion of visible exterior from inside the home through windows, balcony, or terrace). Sampling was performed using the nonprobability (simple random sampling) method. The questionnaire was developed on a site, and its link was delivered to the respondents through the social media platform. At first, the questionnaire had questions such as the area of residence and the number of apartment floors. Given that these two factors seem to affect the results, the authors only analyzed the responses of middle-class (middle-income) residents living in mid-rise buildings. Table 1 shows the scale range of personal green space components used in the questionnaire.

2.3 Greenery assessment

For assessing all greenery variables, a self-reported analysis was performed. Moreover, questions such as the amount of change in the number and frequency of public green spaces were measured to control the impact of this variable on the research outcome. Accordingly, cases, where quarantine did not affect the use of green spaces, were removed.

2.4 Mental health assessment

In this research, for evaluating the symptom of depression and anxiety over the past 2 weeks, two widely used and valid screening instruments were used. Since 1970, when Goldberg developed the General Health Questionnaire (GHQ), it has been extensively used in different cultures and settings (Goldberg and Blackwell, 1970; Goldberg, 1988; Jacob et al., 1997; Schrnitz et al., 1999; Donath, 2001) for measuring mental health and determining the risk of developing a psychiatric disorder (Goldberg, 1988). The 12-item General Health Questionnaire (GHQ-12) was translated into Iranian language. The Iranian version of GHQ-12 has a valid and reliable instrument and a good factor structure to measure minor psychological distress (Montazeri et al., 2003). It has 12 items in which each question has four response options based on Likert style. The total score could range from 0 to 36, in which a higher score indicates more symptoms of depression and anxiety.

Also, the Generalized Anxiety Disorder 7-item (GAD-7) Scale was used, which was generated by Spitzer et al. (2006) to measure generalized anxiety disorders. A systematic review and diagnostic meta-analysis have demonstrated that this test has acceptable psychometric properties in adults (Plummer et al., 2016). Moreover, this test has become a widely used measure in adults in different cultures and an efficient screening tool for detecting the generalized anxiety disorder in primary care patients (Delgadillo et al., 2012; Parkerson et al., 2015). The response options of each item, based on Likert style, include 0 (not at all), 1 (sometimes), 2 (often), and 3 (nearly every day). The total score could range from 0 to 21; the higher score demonstrates more anxiety symptoms.

3 Results

3.1 Reliability and validity

The estimation of the reliability of the questionnaire using Cronbach's alpha index and the combined reliability performed using SmartPLS software to check the internal consistency were assessed. Cronbach's alpha index (generalized anxiety disorder: 0.92, general mental health: 0.92, personal green space: 0.74, and total questionnaire: 0.82) and combined reliability (generalized anxiety disorder: 0.93, general mental health: 0.93, and personal green space: 0.85) for all questionnaire variables were greater than 0.7, so the questionnaire has suitable reliability. Also, the average variance extracted (AVE) criterion showed that the extracted variance for all structures was more than 0.5 (generalized anxiety disorder: 0.67, general mental health: 0.54, and personal green space: 0.66), so their convergent validity is confirmed. In addition, the divergent validity of the research variables was examined using Fornell and Larker methods. The results of Table 2 demonstrate that except for

TABLE 1 Scale range of personal green space components.

Selected variables of personal green spaces	Scale (a 5-point scale)
The existence of apartment plants	0 Without houseplants 1 Less than 5 plants 2 Between 6 and 15 plants 3 Between 16 and 25 plants 4 26 plants or more
The view of windows	0 100% built-up view 1 A larger share (60%–70%) of built space and a smaller share (40%–30%) of green space 2 Half (50%) is built space and half (50%) is green space 3 A smaller share (30%–40%) of built space and a larger share (60%–70%) of green space 4 100% green view
Private garden or balcony with flowers or green cover	0 No private garden or balcony with plants 1 At least one of these two spaces with a total of less than 5 square meters 2 At least one of these two spaces with a total area of more than 5 square meters and less than 10 square meters 3 At least one of these two spaces with a total area of more than 10 square meters and less than 20 square meters 4 At least one of these two spaces with a total area of more than 20 square meters

TABLE 2 Divergent validity matrix using Fornell and Larker methods for research variables.

Variable	Generalized anxiety disorder	General mental health	Personal green space
Generalized anxiety disorder	0.81		
General mental health	0.79	0.73	
Personal green space	−0.31	−0.38	0.81

the variable of general mental health, the correlation of other variables with their items is more than the correlation of that variable with other variables. Therefore, it has a relatively suitable divergent narrative model.

3.2 Descriptive statistics of research

The authors recruited a nonprobability sample from apartment residents in Tehran, and their mental health related to the amount of connection with greenery was evaluated. Demographic characteristics of the participants ($n = 700$) are presented in Table 3.

Table 4 shows the descriptive statistics indicators including mean, median, standard deviation, skewness, kurtosis, and minimum and maximum scores related to research variables.

According to the questionnaire, the average score for private green spaces, general mental health, and generalized anxiety disorder equals 6, 18, and 10.5, respectively. According to the results obtained from Table 5, the personal green space use is less than desirable. In

addition, the level of anxiety and depression among the participants in this study is less than average, so they are at an acceptable level in terms of mental health and anxiety disorder.

3.3 Inferential statistics of research

To test the hypotheses of this research, first, the normality of the research variables is measured, and then the correlation between them is calculated. Finally, the research hypotheses are tested based on the partial least squares method.

The results of Table 6 show that the significance level of the test for all variables is less than the test error level (0.000). Therefore, the hypothesis of normality of variables is rejected using the Kolmogorov–Smirnov test. Nevertheless, the values of skewness and kurtosis of variables are in the range between 2 and −2. Therefore, the normality of the research variables is accepted. In this way, parametric tests can be used to analyze the data.

The results of the correlation table show that the significance level of the test between all variables in the model is less than 0.01.

TABLE 3 Demographic variables.

Category	Subcategory	Frequency	Frequency percentage
Gender	Female	558	79.7
	Male	142	20.3
	Total	700	100
Marital status	Married	461	65.9
	Single	239	34.1
	Total	700	100
Age	Under 18 years old	7	1
	Between 18 and 28	123	17.6
	Between 29 and 39	162	23.1
	Between 40 and 50	157	22.4
	Between 51 and 60	192	27.4
	Between 61 and 71	49	7
	Over 72 years old	10	1.4
	Total	700	100
Monthly income (in Iranian rial)	Without income	129	18.4
	20.000.000 and less	67	9.6
	20.000.001–30.500.000	52	7.4
	30.500.001–50.000.000	124	17.7
	50.000.001–10.000.000	255	36.4
	10.000.001 or above	73	10.4
	Total	700	100
Education	Diploma or less	98	14.0
	Bachelor degree	327	46.7
	Master degree	249	35.6
	Ph.D. or above	26	3.7
	Total	700	100

TABLE 4 Indicators of descriptive statistics of research variables.

Variable	Number	Mean	Median	Standard deviation	Skewness	Kurtosis	Lowest score	Highest score
Personal green space	700	4.88	4.00	3.22	0.52	−0.71	0	12
The General Health Questionnaire (GHQ)	700	14.79	14.00	7.07	0.44	−0.37	0	36
The Generalized Anxiety Disorder 7-item (GAD-7)	700	7.97	7.00	5.52	0.47	−0.77	0	21

So there is a correlation between the variables. Among these, the highest correlation is observed between generalized anxiety disorder and general mental health (0.800), and the lowest correlation is observed between generalized anxiety disorder and personal green spaces (−0.309).

The amount of personal green spaces, general mental health, and generalized anxiety in the levels of demographic variables were examined using parametric tests. To investigate this issue at different levels of demographic characteristics, a *t*-test of two independent communities with an error level of 0.05 was used.

TABLE 5 Correlation of model variables.

Variable	Personal green space	The General Health Questionnaire (GHQ)	The Generalized Anxiety Disorder 7-item (GAD-7)
Personal green space	1.00		
The General Health Questionnaire (GHQ)	−0.374**	1.00	
The Generalized Anxiety Disorder 7-item (GAD-7)	−0.309**	0.800**	1.00

p-value < 0.01.

TABLE 6 Evaluation of normality of research variables using the Kolmogorov–Smirnov test.

Variable	Significance level of the test	Skewness	Kurtosis
Personal green space	0.000	0.52	−0.71
The General Health Questionnaire (GHQ)	0.000	0.44	−0.37
The Generalized Anxiety Disorder 7-item (GAD-7)	0.000	0.47	−0.77

TABLE 7 *t*-test at the gender level.

Variable	Gender	Mean	Equality of variance test		Mean comparison test	
			F-statistic	Significance level	t-statistic	Significance level
Personal green space	Female	4.83	8.77	0.00	−0.90	0.37
	Male	5.10				
The General Health Questionnaire (GHQ)	Female	14.82	17.32	0.00	0.23	0.81
	Male	14.67				
The Generalized Anxiety Disorder 7-item (GAD-7)	Female	8.13	2.92	0.09	1.55	0.12
	Male	7.33				

3.3.1 Gender

The results of Table 7 show that the significance level of the test for the variables of personal green spaces, general mental health, and generalized anxiety disorder is more than 0.05, so the use of green spaces and the rate of depression and anxiety are the same among males and females. The graph of the relationship between personal green space, mental health, and generalized anxiety disorder at gender levels is shown in Figure 2.

3.3.2 Marital status

The results demonstrate that the significance level of the test for the personal green space variable is more than 0.05, so the amount of green spaces used is the same among single and married people. Also, the significance level of the test for general mental health variables and generalized anxiety disorder is less than 0.05, so the assumption of the equality of means is rejected with 95% confidence. In other words, the rate of general mental health and generalized anxiety disorder varies between married and single people, and

based on the average values of each group, single people are more anxious and depressed than married people.

3.3.3 Age

This factor was used based on the ANOVA test at an error level of 0.05. According to the results, the significance level of the test for the personal green space variable is more than 0.05, so the amount of green space used is the same among different age groups. Also, the significance level of the test for general mental health variables and generalized anxiety disorder is less than 0.05, so the assumption of the equality of means is rejected with 95% confidence. In other words, the rate of general mental health and generalized anxiety disorder varies between different age groups. Based on the mean values of each group, people between 18 and 28 years have the highest rate of depression, and people under 18 years have the highest level of anxiety. The rate of depression and anxiety decreases and the rate of green space use increases with age.

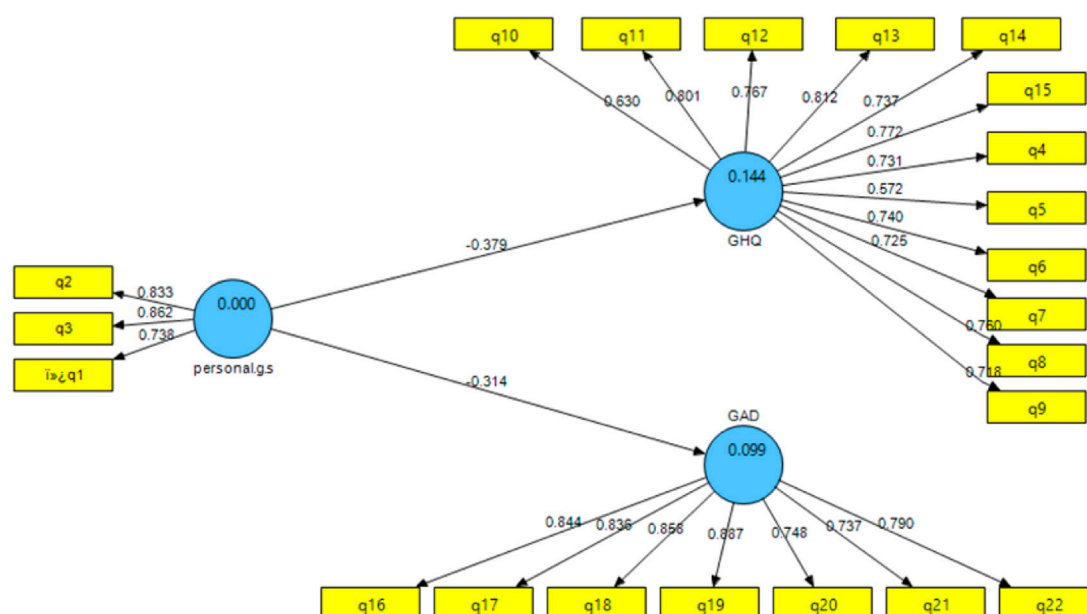


FIGURE 3
Standard path coefficient of the structural model.

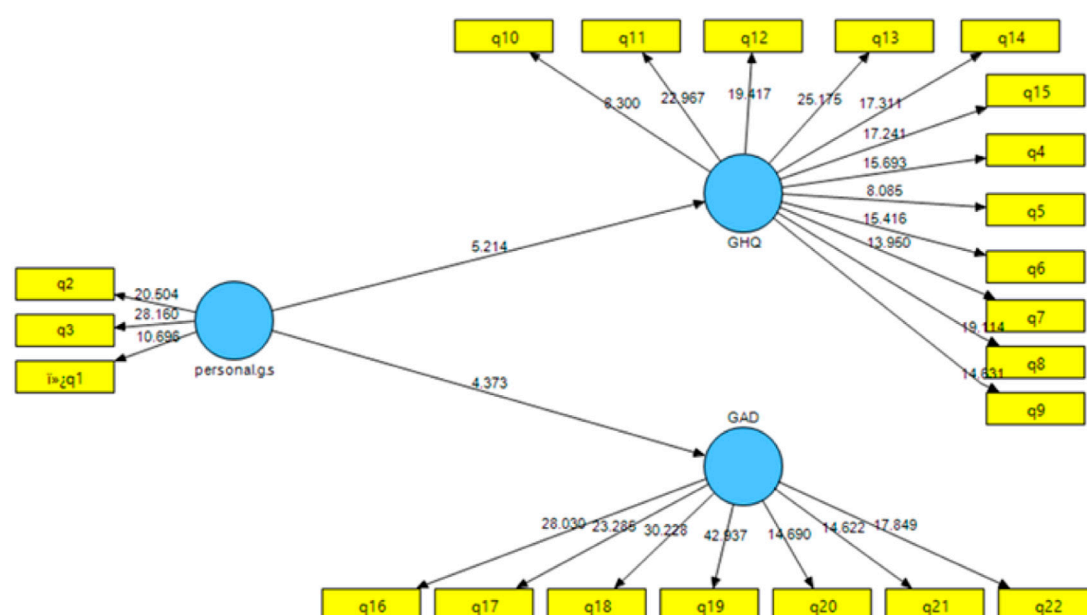


FIGURE 4
Significance level of the path in the structural model.

3.3.4 Monthly income

According to the results, the significance level of the test for the variables of general mental health, personal green space, and generalized anxiety disorder is less than 0.05, so the assumption

of mean equivalence is rejected with 95% confidence. In other words, the level of general mental health, personal green space, and generalized anxiety disorder varies between people with different income levels and based on the average values of

each group. People with incomes over 100,000,001 million rial have the most use of personal green spaces. People with a revenue of 20,000,000 million rial or less have the highest rate of depression and anxiety. Also, with increasing income, the rate of anxiety and depression has a decreasing trend. The average use of personal green space is not much different among people who earn less than 100,000,000 million rial.

3.3.5 Education

According to the results, the significance level of the test for the variable of personal green space and generalized anxiety disorder is more than 0.05, so the use of green space and the level of anxiety are the same among people with different levels of education. Also, the significance level of the test for general mental health variables is less than 0.05, so the assumption of the equality of means is rejected with 95% confidence. In other words, the rate of general mental health and generalized anxiety disorder varies among people with different education levels. Based on the average values of each group, people with a master's degree have the highest rate of depression. The results show that as the level of education increases, the rate of depression increases.

3.3.6 Structural equation modeling

Figure 3 demonstrates the Standard path coefficient of the structural model. The structural model is a part of the model that shows the relationships between the latent variables of the research. After the quality of the measurement model was confirmed, the authors evaluated the structural fit of the model. For this purpose, the *t*-statistic and R^2 index were used. The value of *t*-statistic between the variable of personal green space and general mental health and personal green space on generalized anxiety disorder is more than 1.96. Therefore, the personal green space affects general mental health and generalized anxiety disorder. The significance level of the path in the structural model is shown in Figure 4.

3.3.7 Determination coefficient (R square)

The overall fit using the GOF criterion for the comprehensive research model is 0.272, which indicates the average fit of the general research model. After reviewing the fit criteria of the model and ensuring the suitability of the model, the authors analyzed the research hypotheses.

3.3.8 Evaluation of hypothesis (1): The personal green space has positive effects on the level of human general mental health

The *t*-test (statistics *T*: 5.21) and the standard coefficient of the path (standard path coefficient: -0.38) between personal green space and general mental health were assessed. Based on this evaluation, it was evaluated that the personal green space has a negative correlation and significant effect on general mental health. In other words, increasing the use of personal green spaces in residence reduces depression.

3.3.9 Evaluation of hypothesis (2): The personal green space has positive effects on reducing symptoms of generalized anxiety disorder

The *t*-test (statistics *T*: 4.37) and the standard coefficient of the path (standard path coefficient: -0.31) between personal green space and generalized anxiety disorder were assessed. This assessment indicates a negative correlation and significant impact of personal green space on generalized anxiety disorder. In other words, increasing the use of personal green spaces reduces anxiety.

3.3.10 Evaluation of hypothesis (3): There is a relationship between demographic characteristics and the level of human general mental health and symptoms of generalized anxiety disorder.

According to the analysis, there is a relationship between demographic characteristics of people with their level of mental health and the degree of symptoms of general anxiety. Therefore, personal green spaces are not the same for all age groups, gender, education, marital status, and income levels.

Moreover, by comparing the results of the first and second hypotheses, it can be concluded that the personal green space in reducing the rate of depression is more significant than its role in reducing anxiety among individuals.

4 Discussion

With the outbreak of the corona pandemic and government orders for social isolation, reduced outdoor activities, and people spending more time at home, more symptoms of depression and anxiety among people in the community were seen. One way to reduce the symptoms of depression and anxiety is to be exposed to green spaces, which has decreased during the corona epidemic. This research considers three methods of personal green spaces, including having houseplants, a view of the green space through windows, and having a private garden or balcony with flowers and plants, as alternatives to the green space outside the house, through a questionnaire. Among 700 residents of apartments in Tehran, this study assessed the incidence of symptoms of depression and anxiety. Also, a structural equation model was developed.

This study examined the effects of demographic characteristics concerning personal green space on mental health, depression, and anxiety separately. Gender differences in the effects of environmental factors on different dimensions of health are beginning to emerge (Roe et al., 2013). The results of research on students in India during COVID-19 to evaluate built environment attributes with anxiety and depression risk demonstrated that gender has no significant associations with anxiety and depression risk (Asim et al., 2021). Another study showed a significant interaction effect between gender and

percentage green space on mean cortisol concentrations, demonstrating a positive effect of higher green space concerning cortisol measures in women but not in men (Roe et al., 2013). In the current research, there was no significant difference, and the rate of green space use and the rate of depression and anxiety were the same between men and women. Moreover, the marital status is another demographic variable, which was evaluated in this study. The result showed that personal green space used by married people is slightly higher than that used by single people. Moreover, single people are more anxious and depressed than married people. Also, there are many research studies conducted on the positive effects of nature on the elderly. For instance, research on older adults demonstrated that green space characteristics are linked to their mental health status (Zhifeng and Yin, 2021) although some studies have not found significant differences between different age groups. For example, a study in the COVID-19 era for assessing garden use and mental well-being in the elderly showed no significant differences between gardeners and non-gardeners in some demographic variables such as gender (Corley et al., 2021). In this study, there was a difference between the uses of personal green spaces. According to this, the rate of green space use increases while depression and anxiety decrease with age. Also, people between 18 and 28 years have the highest rate of depression, and people under 18 years have the highest level of anxiety. Moreover, income is another demographic variable in this study. The results showed that people with incomes over 100,000,001 million rial have the most use of personal green space. With increasing income, the rate of anxiety and depression has a decreasing trend. This factor may be due to housing policies in Tehran, where people with higher income levels have larger apartments, generally with a more favorable and spacious view, and in most cases people have green balconies, courtyards, or roof gardens. In comparison, people with low-income levels have fewer of these facilities. The education level is another variable. However, a study conducted in the COVID-19 era assessing garden use and mental well-being in the elderly showed no significant differences between gardeners and non-gardeners at the education level (Corley et al., 2021). Also, the results of a study on students in India during the corona pandemic for assessing built environment attributes with anxiety and depression risk demonstrated that gender has no significant associations with anxiety and depression risk, and the effect on productivity showed that. Although the educational level was linked to anxiety level and productivity, the educational level has no associations with depression risk (Asim et al., 2021). In this research, as the level of education increases, the rate of depression increases, and people with a master's degree have the highest rate of depression.

This study showed that personal green spaces affected depression and anxiety of apartment residents in Tehran during the COVID-19 pandemic and that green spaces can be introduced as an appropriate alternative solution during

quarantine at home. The findings are in line with earlier studies. The research was carried out on the general mental health of Plovdiv students and demonstrated that spending more time on the greenery and having a green view were associated with a higher level of general mental health (Dzhambov et al., 2018). Moreover, the research on prisoners visually exposed to natural sceneries through watching videos of natural settings reported higher restoration and affective state (Nadkarni et al., 2017; Moran, 2019). Numerous studies in various situations have shown that the presence of plants indoors can be effective. For instance, placing plants in the classroom can increase children's performance (Duijn et al., 2011). In addition, the studies on hospitalized patients demonstrated that patients staying in a room with a view of green landscapes or having plants in the room reported less fatigue and anxiety, and they ultimately had faster recovery after their surgical interventions (Ulrich, 1984; Park and Mattson, 2009; Aslam et al., 2016). The research showed that interior plants could lead to productive workplaces and health by decreasing stress levels, enhancing attention capacity, and achieving higher job satisfaction (Raanaas et al., 2011; Hartig et al., 2014; Gilchrist et al., 2015). A greenery view through windows can help recover from stressful events (Li and Sullivan, 2016) and psychological restoration (Lee et al., 2015). Also, there is increasing evidence that gardening provides substantial health benefits for humans (Soga et al., 2017). Moreover, many researchers reported that gardening during COVID-19 positively affects human mood (Carvalho and Gois, 2020; Lades et al., 2020). Overall, the findings of this research support the hypotheses that personal green spaces have a significant and negative correlation impact on mental health and anxiety. These findings support the hypothesis that the personal green space can be a suitable alternative for the public green space during COVID-19 for apartment residents in Tehran. However, no causal interpretation of these associations is possible.

5 Conclusion

This study investigated the effects of personal green spaces as an alternative to public green spaces unavailable during the COVID-19 pandemic. For this purpose, information was collected from 700 apartment residents in Tehran through surveys and questionnaires. The results demonstrated that personal green spaces affected depression and anxiety levels of apartment residents in Tehran during the COVID-19 pandemic, and that green spaces can be introduced as an appropriate alternative solution during quarantine at home.

Based on the results, in future designs, the connection between the house and green spaces should be maintained as much as possible, and green space should be drawn into the house as much as possible so that individuals' connection with

nature remains at its maximum. As a result, architects in their future designs need to have a patio where there are conditions for keeping houseplants, designing semi-open spaces, and space hierarchy. Also, urban planners, in comprehensive plans, should consider the relationship between buildings and construction permits in terms of height (a building should not obstruct the view of the occupants of another building in green and blue). Also, the distance between the blocks in front of each other should be calculated accurately. In the design of buildings, it should be considered that in addition to the balcony, windows are the primary communication with the view and landscape outside the building. In terms of number and quantity, logical calculations should be applied to maintain sufficient visibility of green and blue spaces. Finally, it should not be forgotten that according to what the literature has shown, nature is the source of human peace. Also, this study showed that the current approaches to the apartment building in Tehran, which are based on the maximum use of land without considering the visual space, could severely threaten residents' mental health. Urban designs consider the presence of green spaces among building blocks, the creation of pocket parks, and green spaces in general at different scales. In order, it is recommended in future residential plans to create a suitable space to maintain the view of the green space, allocate a part of the land area for a private garden, or create suitable conditions for creating a roof garden for residents to communicate with nature.

The current research has some limitations. First, this study only analyzed the responses of middle-class (middle-income) residents who live in medium-sized buildings. Because these two factors can affect the results, future researchers can investigate these factors at other levels. On the other hand, each personal green space can have different effects that can be analyzed in future research. Also, mental health consists of different dimensions, and the effects of personal green spaces on each of these dimensions can be investigated.

On the other hand, the findings showed that personal green spaces have a significant and negative correlation impact on mental health and anxiety. However, no causal interpretation of these associations is possible. Therefore, future studies can examine the reasons for this. Also, the research on the effect of different dimensions of green spaces on other psychological and physical dimensions of human beings can be among future

studies. Moreover, examining the effects of these spaces on spatial functions and individuals' satisfaction with the space is one of the concerns that should be studied.

Data availability statement

The original contributions presented in the study are included in the article/Supplementary Materials; further inquiries can be directed to the corresponding authors.

Author contributions

The authors confirm contribution to the manuscript as follows: study conception and design: MK and MF; data collection: HK; analysis and interpretation of results: HK and MK; and draft manuscript preparation: HK, MF, and MK. All authors reviewed the results and approved the final version of the manuscript.

Acknowledgments

The authors consider it necessary to express their gratitude to the people who took time to answer the questionnaire.

Conflict of interest

The authors declare that the research was conducted in the absence of any commercial or financial relationships that could be construed as a potential conflict of interest.

Publisher's note

All claims expressed in this article are solely those of the authors and do not necessarily represent those of their affiliated organizations, or those of the publisher, the editors, and the reviewers. Any product that may be evaluated in this article, or claim that may be made by its manufacturer, is not guaranteed or endorsed by the publisher.

References

- Abraham, A., Sommerhalder, K., and Abel, T. (2010). Landscape and well-being: A scoping study on the health-promoting impact of outdoor environments. *Int. J. Public Health* 55, 59–69. doi:10.1007/s00038-009-0069-z
- Akpınar, A., Barbosa-Leiker, C., and Brooks, K. R. (2016). Does green space matter? Exploring relationships between green space type and health indicators. *Urban For. Urban Green*. 20, 407–418. doi:10.1016/j.ufug.2016.10.013
- Alker, J., Malanca, M., Pottage, C., and O'Brien, R. (2014). *Health, wellbeing & productivity in offices: The next chapter for green building*. United States: World Green Build. Council.
- Asim, F., Chani, P., and Shree, V. (2021). Impact of COVID-19 containment zone built-environments on students' mental health and their coping mechanisms. *Build. Environ.* 203, 108107. doi:10.1016/j.buildenv.2021.108107

- Aslam, A., Shaheen, I., Afzal, N., Ain, Q., Qasim, M., Zaman, F., et al. (2016). Effect of hospital landscaping on the health and recovery of patients. *Adv. Agric. Biol.* 5, 86–88.
- Barton, J., and Pretty, J. (2010). What is the best dose of nature and green exercise for improving mental health? A multi-study analysis. *Environ. Sci. Technol.* 44, 3947–3955. doi:10.1021/es903183r
- Benfield, J. A., Rainbolt, G. N., Bell, P. A., and Donovan, G. H. (2015). Classrooms with nature views: Evidence of differing student perceptions and behaviors. *Environ. Behav.* 47, 140–157. doi:10.1177/0013916513499583
- Bringslimark, T., Hartig, T., and Patil, G. G. (2009). The psychological benefits of indoor plants: A critical review of the experimental literature. *J. Environ. Psychol.* 29, 422–433. doi:10.1016/j.jenvp.2009.05.001
- Brooks, S. K., Webster, R. K., Smith, L. E., Woodland, L., Wessely, S., Greenberg, N., et al. (2020). The psychological impact of quarantine and how to reduce it: Rapid review of the evidence. *Lancet* 395, 912–920. doi:10.1016/s0140-6736(20)30460-8
- Callaghan, A., McCombe, G., Harrold, A., McMeel, C., Mills, G., Moore-Cherry, N., et al. (2021). The impact of green spaces on mental health in urban settings: A scoping review. *J. Ment. Health* 30, 179–193. doi:10.1080/09638237.2020.1755027
- Carrus, G., Scopelliti, M., Laforteza, R., Colangelo, G., Ferrini, F., Salbitano, F., et al. (2015). Go greener, feel better? The positive effects of biodiversity on the well-being of individuals visiting urban and peri-urban green areas. *Landsc. Urban Plan.* 134, 221–228. doi:10.1016/j.landurbplan.2014.10.022
- Carvalho, V. O., and Gois, C. O. (2020). COVID-19 pandemic and home-based physical activity. *J. Allergy Clin. Immunol. Pract.* 8, 2833–2834. doi:10.1016/j.jaip.2020.05.018
- Chang, C.-Y., and Chen, P.-K. (2005). Human response to window views and indoor plants in the workplace. *HortScience* 40, 1354–1359. doi:10.21273/hortsci.40.5.1354
- Corley, J., Okely, J. A., Taylor, A. M., Page, D., Welstead, M., Skarabela, B., et al. (2021). Home garden use during COVID-19: Associations with physical and mental wellbeing in older adults. *J. Environ. Psychol.* 73, 101545. doi:10.1016/j.jenvp.2020.101545
- de Bell, S., White, M., Griffiths, A., Darlow, A., Taylor, T., Wheeler, B., et al. (2020). Spending time in the garden is positively associated with health and wellbeing: Results from a national survey in England. *Landsc. Urban Plan.* 200, 103836. doi:10.1016/j.landurbplan.2020.103836
- Delgadillo, J., Payne, S., Gilbody, S., Godfrey, C., Gore, S., Jessop, D., et al. (2012). Brief case finding tools for anxiety disorders: Validation of GAD-7 and GAD-2 in addictions treatment. *Drug Alcohol Depend.* 125, 37–42. doi:10.1016/j.drugalcdep.2012.03.011
- Dennis, M., and James, P. (2017). Evaluating the relative influence on population health of domestic gardens and green space along a rural-urban gradient. *Landsc. Urban Plan.* 157, 343–351. doi:10.1016/j.landurbplan.2016.08.009
- Donath, S. (2001). The validity of the 12-item General Health Questionnaire in Australia: a comparison between three scoring methods. *Aust. N. Z. J. Psychiatry* 35, 231–235.
- Douglas, O., Lennon, M., and Scott, M. (2017). Green space benefits for health and well-being: A life-course approach for urban planning, design and management. *Cities* 66, 53–62. doi:10.1016/j.cities.2017.03.011
- Doxey, J. S., Waliczek, T. M., and Zajicek, J. M. (2009). The impact of interior plants in University classrooms on student course performance and on student perceptions of the course and instructor. *HortScience* 44, 384–391. doi:10.21273/hortsci.44.2.384
- Dravigne, A., Waliczek, T. M., Lineberger, R., and Zajicek, J. (2008). The effect of live plants and window views of green spaces on employee perceptions of job satisfaction. *HortScience* 43, 183–187. doi:10.21273/hortsci.43.1.183
- Duijn, B., Bergen, S., Klein Hesselink, J., Kuijt-Evers, L., Jansen, J., Spitters, H., et al. (2011). *Plant in de klas*. Den Haag, Netherlands: TNO.
- Dzhambov, A., Hartig, T., Markevych, I., Tilov, B., and Dimitrova, D. (2018). Urban residential greenspace and mental health in youth: Different approaches to testing multiple pathways yield different conclusions. *Environ. Res.* 160, 47–59. doi:10.1016/j.envres.2017.09.015
- Dzhambov, A. M., Lercher, P., Browning, M. H., Stoyanov, D., Petrova, N., Novakov, S., et al. (2021). Does greenery experienced indoors and outdoors provide an escape and support mental health during the COVID-19 quarantine? *Environ. Res.* 196, 110420. doi:10.1016/j.envres.2020.110420
- Elzeyadi, I. (2011). *Daylighting-bias and biophilia: Quantifying the impact of daylighting on occupants health*. Washington, DC: US Green Build. Council. http://www.usgbc.org/sites/default/files/OR10Daylighting_20Bias_20and_20Biophilia.pdf.
- Entrix, I. (2010). *Portland's green infrastructure: Quantifying the health, energy, and community livability benefits*. Portland OR: Environmental Services.
- Fjeld, T. (2000). The effect of interior planting on health and discomfort among workers and school children. *HortTechnology* 10, 46–52. doi:10.21273/horttech.10.1.46
- Gascon, M., Triguero-Mas, M., Martínez, D., Dadvand, P., Fors, J., Plasència, A., et al. (2015). Mental health benefits of long-term exposure to residential green and blue spaces: A systematic review. *Int. J. Environ. Res. Public Health* 12, 4354–4379. doi:10.3390/ijerph120404354
- Gigliotti, C. M., and Jarrott, S. E. (2005). Effects of horticulture therapy on engagement and affect. *Can. J. Aging* 24, 367–377. doi:10.1353/cja.2006.0008
- Gilchrist, K., Brown, C., and Montarzino, A. (2015). Workplace settings and wellbeing: Greenspace use and views contribute to employee wellbeing at peri-urban business sites. *Landsc. Urban Plan.* 138, 32–40. doi:10.1016/j.landurbplan.2015.02.004
- Goldberg, D. P., and Blackwell, B. (1970). Psychiatric illness in general practice: A detailed study using a new method of case identification. *Br. Med. J.* 2, 439–443.
- Goldberg, D. P. (1988). *User's guide to the General Health Questionnaire* Windsor.
- Gostin, L. O., and Wiley, L. F. (2020). Governmental public health powers during the COVID-19 pandemic: Stay-at-home orders, business closures, and travel restrictions. *Jama* 323, 2137–2138. doi:10.1001/jama.2020.5460
- Gu, C., Jiang, W., Zhao, T., and Zheng, B. (2020). Mathematical recommendations to fight against COVID-19. Available at SSRN: <https://ssrn.com/abstract=3551006> (Accessed August 4, 2021).
- Hall, C., and Knuth, M. (2019). An update of the literature supporting the well-being benefits of plants: A review of the emotional and mental health benefits of plants. *J. Environ. Hortic.* 37, 30–38. doi:10.24266/0738-2898-37.1.30
- Han, K.-T. (2018). Influence of passive versus active interaction with indoor plants on the restoration, behaviour and knowledge of students at a junior high school in Taiwan. *Indoor Built Environ.* 27, 818–830. doi:10.1177/1420326x17691328
- Han, K.-T., and Ruan, L.-W. (2019). Effects of indoor plants on self-reported perceptions: A systemic review. *Sustainability* 11, 4506. doi:10.3390/su11164506
- Hartig, T., Mitchell, R., De Vries, S., and Frumkin, H. (2014). Nature and health. *Annu. Rev. Public Health* 35, 207–228. doi:10.1146/annurev-publhealth-032013-182443
- Holmes, E. A., O'Connor, R. C., Perry, V. H., Tracey, I., Wessely, S., Arseneault, L., et al. (2020). Multidisciplinary research priorities for the COVID-19 pandemic: A call for action for mental health science. *Lancet Psychiatry* 7, 547–560. doi:10.1016/s2215-0366(20)30168-1
- Hotopf, M., Bullmore, E., O'Connor, R. C., and Holmes, E. A. (2020). The scope of mental health research during the COVID-19 pandemic and its aftermath. *Br. J. Psychiatry* 217, 540–542. doi:10.1192/bjp.2020.125
- Huang, Y., and Zhao, N. (2020). Generalized anxiety disorder, depressive symptoms and sleep quality during COVID-19 outbreak in China: A web-based cross-sectional survey. *Psychiatry Res.* 288, 112954. doi:10.1016/j.psychres.2020.112954
- Jacob, K., Bhugra, D., and Mann, A. (1997). Brief Communication The Validation of the 12-item General Health Questionnaire among ethnic Indian women living in the United Kingdom. *Psychol. Med.* 27, 1215–1217.
- Jo, H., Song, C., and Miyazaki, Y. (2019). Physiological benefits of viewing nature: A systematic review of indoor experiments. *Int. J. Environ. Res. Public Health* 16, 4739. doi:10.3390/ijerph16234739
- Kaplan, R. (2001). The nature of the view from home: Psychological benefits. *Environ. Behav.* 33, 507–542. doi:10.1177/00139160121973115
- Kaplan, S. (1995). The restorative benefits of nature: Toward an integrative framework. *J. Environ. Psychol.* 15, 169–182. doi:10.1016/0272-4944(95)90001-2
- Keniger, L. E., Gaston, K. J., Irvine, K. N., and Fuller, R. A. (2013). What are the benefits of interacting with nature? *Int. J. Environ. Res. Public Health* 10, 913–935. doi:10.3390/ijerph10030913
- Kjellgren, A., and Buhrkall, H. (2010). A comparison of the restorative effect of a natural environment with that of a simulated natural environment. *J. Environ. Psychol.* 30, 464–472. doi:10.1016/j.jenvp.2010.01.011
- Korpela, K., De Bloom, J., Sianoja, M., Pasanen, T., and Kinnunen, U. (2017). Nature at home and at work: Naturally good? Links between window views, indoor plants, outdoor activities and employee well-being over one year. *Landsc. Urban Plan.* 160, 38–47. doi:10.1016/j.landurbplan.2016.12.005
- Kumar, A., and Nayar, K. R. (2021). COVID 19 and its mental health consequences. *J. Ment. Health* 30 (1), 1–2. doi:10.1080/09638237.2020.1757052
- Lades, L. K., Laffan, K., Daly, M., and Delaney, L. (2020). Daily emotional well-being during the COVID-19 pandemic. *Br. J. Health Psychol.* 25, 902–911. doi:10.1111/bjhp.12450

- Lee, K. E., Williams, K. J., Sargent, L. D., Williams, N. S., and Johnson, K. A. (2015). 40-second green roof views sustain attention: The role of micro-breaks in attention restoration. *J. Environ. Psychol.* 42, 182–189. doi:10.1016/j.jenvp.2015.04.003
- Li, D., and Sullivan, W. C. (2016). Impact of views to school landscapes on recovery from stress and mental fatigue. *Landsc. Urban Plan.* 148, 149–158. doi:10.1016/j.landurbplan.2015.12.015
- Lu, Y., Zhao, J., Wu, X., and Lo, S. M. (2021). Escaping to nature during a pandemic: A natural experiment in asian cities during the COVID-19 pandemic with big social media data. *Sci. Total Environ.* 777, 146092. doi:10.1016/j.scitotenv.2021.146092
- Marcus, C. C., and Sachs, N. A. (2013). *Therapeutic landscapes: An evidence-based approach to designing healing gardens and restorative outdoor spaces*. United States: John Wiley & Sons.
- Mensah, C. A., Andres, L., Perera, U., and Roji, A. (2016). Enhancing quality of life through the lens of green spaces: A systematic review approach. *Intnl. J. Wellbeing* 6, 142–163. doi:10.5502/ijw.v6i1.445
- Montazeri, A., Harirchi, A. M., Shariati, M., Garmaroudi, G., Ebadi, M., and Fateh, A. (2003). The 12-item general health questionnaire (GHQ-12): Translation and validation study of the Iranian version. *Health Qual. Life Outcomes* 1, 66. doi:10.1186/1477-7525-1-66
- Moran, D. (2019). Back to nature? Attention restoration theory and the restorative effects of nature contact in prison. *Health Place* 57, 35–43. doi:10.1016/j.healthplace.2019.03.005
- Nadkarni, N. M., Hasbach, P. H., Thys, T., Crockett, E. G., and Schnacker, L. (2017). Impacts of nature imagery on people in severely nature-deprived environments. *Front. Ecol. Environ.* 15, 395–403. doi:10.1002/fee.1518
- Nieuwenhuis, M., Knight, C., Postmes, T., and Haslam, S. A. (2014). The relative benefits of green versus lean office space: Three field experiments. *J. Exp. Psychol. Appl.* 20, 199–214. doi:10.1037/xap0000024
- Park, S.-H., and Mattson, R. H. (2009). Therapeutic influences of plants in hospital rooms on surgical recovery. *HortScience* 44, 102–105. doi:10.21273/hortsci.44.1.102
- Park, S., Song, C., Oh, Y.-A., Miyazaki, Y., and Son, K.-C. (2017). Comparison of physiological and psychological relaxation using measurements of heart rate variability, prefrontal cortex activity, and subjective indexes after completing tasks with and without foliage plants. *Int. J. Environ. Res. Public Health* 14, 1087. doi:10.3390/ijerph14091087
- Parkerson, H. A., Thibodeau, M. A., Brandt, C. P., Zvolensky, M. J., and Asmundson, G. J. (2015). Cultural-based biases of the GAD-7. *J. Anxiety Disord.* 31, 38–42. doi:10.1016/j.janxdis.2015.01.005
- Petersen, E., McCloskey, B., Hui, D. S., Kock, R., Ntoumi, F., Memish, Z. A., et al. (2020). COVID-19 travel restrictions and the International Health Regulations—Call for an open debate on easing of travel restrictions. *Int. J. Infect. Dis.* 94, 88–90. doi:10.1016/j.ijid.2020.04.029
- Plummer, F., Manea, L., Trepel, D., and McMillan, D. (2016). Screening for anxiety disorders with the GAD-7 and GAD-2: A systematic review and diagnostic metaanalysis. *Gen. Hosp. Psychiatry* 39, 24–31. doi:10.1016/j.genhosppsych.2015.11.005
- Raanaas, R. K., Evensen, K. H., Rich, D., Sjøstrøm, G., and Patil, G. (2011). Benefits of indoor plants on attention capacity in an office setting. *J. Environ. Psychol.* 31, 99–105. doi:10.1016/j.jenvp.2010.11.005
- Rajkumar, R. P. (2020). COVID-19 and mental health: A review of the existing literature. *Asian J. Psychiatr.* 52, 102066. doi:10.1016/j.ajp.2020.102066
- Roe, J. J., Thompson, C. W., Aspinall, P. A., Brewer, M. J., Duff, E. I., Miller, D., et al. (2013). Green space and stress: Evidence from cortisol measures in deprived urban communities. *Int. J. Environ. Res. Public Health* 10, 4086–4103. doi:10.3390/ijerph10094086
- Schnitz, N., Kruse, J., and Tress, W. (1999). Psychometric properties of the General Health Questionnaire (GHQ-12) in a German primary care sample. *Acta Psychiatr. Scand.* 100, 462–468.
- Shoari, N., Ezzati, M., Baumgartner, J., and Fecht, D. (2020). Accessibility and allocation of public parks and gardens during COVID-19 social distancing in England and Wales. Available SSRN 3590503.
- Spitzer, R., Kroenke, K., and Williams, J. (2006). Generalized anxiety disorder 7-item (GAD-7) scale. *Arch Intern Med* 166, 1092–7.
- Smardon, R. C. (1988). Perception and aesthetics of the urban environment: Review of the role of vegetation. *Landsc. Urban Plan.* 15, 85–106. doi:10.1016/0169-2046(88)90018-7
- Soga, M., Gaston, K. J., and Yamaura, Y. (2017). Gardening is beneficial for health: A meta-analysis. *Prev. Med. Rep.* 5, 92–99. doi:10.1016/j.pmedr.2016.11.007
- Tandon, R. (2020). COVID-19 and mental health: Preserving humanity, maintaining sanity, and promoting health. *Asian J. Psychiatr.* 51, 102256. doi:10.1016/j.ajp.2020.102256
- Tian, H., Liu, Y., Li, Y., Wu, C.-H., Chen, B., Kraemer, M. U., et al. (2020). An investigation of transmission control measures during the first 50 days of the COVID-19 epidemic in China. *Science* 368, 638–642. doi:10.1126/science.abb6105
- Triguero-Mas, M., Davdand, P., Cirach, M., Martínez, D., Medina, A., Mompart, A., et al. (2015). Natural outdoor environments and mental and physical health: Relationships and mechanisms. *Environ. Int.* 77, 35–41. doi:10.1016/j.envint.2015.01.012
- Ulrich, R., and Dimberg, U. (1991). “Psychophysiological indicators of leisure benefits,” in *Benefits of leisure*. Editors B. Driver, P. Brown, and G. Peterson, 73–89.
- Ulrich, R. S. (1984). View through a window may influence recovery from surgery. *Science* 224, 420–421. doi:10.1126/science.6143402
- Van den Bosch, M., and Sang, Å. O. (2017). Urban natural environments as nature-based solutions for improved public health—A systematic review of reviews. *Environ. Res.* 158, 373–384. doi:10.1016/j.envres.2017.05.040
- Wang, C., Pan, R., Wan, X., Tan, Y., Xu, L., McIntyre, R. S., et al. (2020). A longitudinal study on the mental health of general population during the COVID-19 epidemic in China. *Brain Behav. Immun.* 87, 40–48. doi:10.1016/j.bbi.2020.04.028
- Watts, G. (2017). The effects of “greening” urban areas on the perceptions of tranquillity. *Urban For. Urban Green.* 26, 11–17. doi:10.1016/j.ufug.2017.05.010
- White, M. P., Pahl, S., Wheeler, B. W., Depledge, M. H., and Fleming, L. E. (2017). Natural environments and subjective wellbeing: Different types of exposure are associated with different aspects of wellbeing. *Health Place* 45, 77–84. doi:10.1016/j.healthplace.2017.03.008
- WHO (2016). *Urban green spaces and Health*. Copenhagen: World Health Organization.
- Wilder-Smith, A., and Freedman, D. O. (2020). Isolation, quarantine, social distancing and community containment: Pivotal role for old-style public health measures in the novel coronavirus (2019-nCoV) outbreak. *J. Travel Med.* 27, taaa020. doi:10.1093/jtm/taaa020
- Windhager, S., Atzwanger, K., Bookstein, F. L., and Schaefer, K. (2011). Fish in a mall aquarium—an ethological investigation of biophilia. *Landsc. Urban Plan.* 99, 23–30. doi:10.1016/j.landurbplan.2010.08.008
- Wolf, K., and Housley, E. (2014). *Reflect and restore: Urban green space for mental wellness*. Annapolis, MD: The TKF Foundation.
- World Health Organization, 2020. WHO.
- Zhifeng, W., and Yin, R. (2021). The influence of greenspace characteristics and building configuration on depression in the elderly. *Build. Environ.* 188, 107477. doi:10.1016/j.buildenv.2020.107477
- Zhu, S., Wu, Y., Zhu, C., Hong, W., Yu, Z., Chen, Z., et al. (2020). The immediate mental health impacts of the COVID-19 pandemic among people with or without quarantine managements. *Brain Behav. Immun.* 87, 56–58. doi:10.1016/j.bbi.2020.04.045



OPEN ACCESS

EDITED BY
Xiaolin Wang,
University of Tasmania, Australia

REVIEWED BY
Francesco Leccese,
University of Pisa, Italy

*CORRESPONDENCE
Xin Cui,
cuixin@xjtu.edu.cn

SPECIALTY SECTION
This article was submitted to Indoor
Environment,
a section of the journal
Frontiers in Built Environment

RECEIVED 31 August 2022
ACCEPTED 03 October 2022
PUBLISHED 17 October 2022

CITATION
Yan W, Meng X, Zhou H, Yang C,
Chen Q, Oh SJ and Cui X (2022), Recent
developments in evaluation methods
and characteristics of comfort
environment in underground subway.
Front. Built Environ. 8:1033046.
doi: 10.3389/fbuil.2022.1033046

COPYRIGHT
© 2022 Yan, Meng, Zhou, Yang, Chen,
Oh and Cui. This is an open-access
article distributed under the terms of the
[Creative Commons Attribution License
\(CC BY\)](https://creativecommons.org/licenses/by/4.0/). The use, distribution or
reproduction in other forums is
permitted, provided the original
author(s) and the copyright owner(s) are
credited and that the original
publication in this journal is cited, in
accordance with accepted academic
practice. No use, distribution or
reproduction is permitted which does
not comply with these terms.

Recent developments in evaluation methods and characteristics of comfort environment in underground subway

Weichao Yan¹, Xiangzhao Meng¹, Haiyun Zhou²,
Chuanjun Yang¹, Qian Chen³, Seung Jin Oh⁴ and Xin Cui^{1*}

¹Institute of Building Environment and Sustainable Technology, School of Human Settlements and Civil Engineering, Xi'an Jiaotong University, Xi'an, Shaanxi, China, ²China State Construction Silkroad Construction Investment Group Co., Ltd., Xi'an, Shaanxi, China, ³Institute for Ocean Engineering, Shenzhen International Graduate School, Tsinghua University, Shenzhen, China, ⁴Sustainable Technology and Wellness R&D Group, Korea Institute of Industrial Technology, Cheonan, South Korea

In recent years, due to the rapid progress of urbanization, the subway system with the advantages of large transport capacity, punctuality, efficiency, convenience and safety has become one of the main transportation modes in metropolitan areas. With the increase in passenger flow, the comfort of subway passengers has attracted extensive attention from the academic community. In this paper, we begin by analyzing the characteristics of the subway environment and sort out six environmental elements that affect passengers' comfort, including thermal environment, vibration, noise, lighting, air quality, and air pressure. In addition, the measurement scheme, calculation model, and evaluation method of each element are outlined based on relevant norms and literature. Through reviewing the studies in the past 2 decades, it is found that the in-depth research is still in demand for a comprehensive comfort evaluation model with multi-element coupling. A deep understanding of the subway passengers' comfort is the basis for the design, development, and operation regulation of the subway environmental control system. Measures to improve comfort, especially the exploitation of energy-saving air conditioning systems, will provide strong support for the sustainable and sound growth of the rail transit industry.

KEYWORDS

subway, passenger comfort, thermal environment, air quality, vibration

Introduction

Recently, along with the global economic development and urbanization construction, urban population and buildings have increased dramatically, resulting in increased pressure on urban traffic. In addition, problems such as traffic congestion and environmental pollution have gradually emerged. Therefore, in order to alleviate the

contradiction of land use, expand land resources and improve the population capacity of the city, practitioners turn their attention to the development of underground space, thus the subway came into being (Nezhnikova, 2016; Yu et al., 2020). As a novel transportation mode, compared with traditional transportation modes, the subway has the advantages of large passenger volume, high speed, punctuality, and small occupation of urban land area. With the rapid popularization of subways in metropolitan areas, the ridership is increasing steadily. People's requirements for taking the subway are no longer only safety and convenience. The comfortable environment has also become a major factor motivating passengers to choose subway travel (Mohammadi et al., 2020).

As a classification of the underground space, the guarantee of the comfort of subway environment is not the same as that of the aboveground buildings. Because the internal space form, environmental elements, and internal personnel activities in underground spaces are significantly different from those in conventional buildings, personnel requirements for environmental comfort vary greatly (Li et al., 2017). In general, the physical environment elements closely related to human comfort mainly include the vibration level, noise intensity, thermal and humid environment, air pressure variation, and air quality conditions. Moreover, there may be mutual synergistic or antagonistic effects among them, which jointly affect the physiological response and subjective evaluation of the human body to the artificial environment. Currently, a considerable amount of research has been devoted to analyzing the subway environment and evaluating passengers' comfort. This paper aims to make a systematic review of the relevant studies in the past 2 decades and critically point out the future research direction, expecting that the follow-up targeted work can facilitate the sustainable and sound growth of the rail transit industry.

The remaining sections of this paper are structured as follows: *Characteristics of the subway environment* Section illustrates the characteristics of subway environment by comparing the aboveground buildings. *Elements affecting passengers' comfort* Section outlines the environmental elements affecting passengers' comfort and lists the research work in the last 2 decades. *Evaluation of environmental elements* Section elaborates on the evaluation approaches of the six key elements respectively based on relevant standards or literature. *Limitations and future directions* Section proposes the limitations of the existing research and the priorities for future work. The major conclusions of this review are presented in *Conclusion* Section.

Characteristics of the subway environment

In order to maintain a comfortable subway environment, it is necessary to have an accurate and comprehensive grasp of the

characteristics of subway environment. Undoubtedly, the design and evaluation criteria of aboveground buildings cannot be automatically applied to the interior environment of the subway because of their different characteristics.

For the subway environment, the characteristics are explained as follows. 1) Subway belongs to underground space, which is less affected by solar radiation, and the surrounding rock and soil have strong heat storage capacity (Kajtar et al., 2015; Li et al., 2017). Hence, the air temperature fluctuation in the subway environment is small and usually behaves as cool in summer and warm in winter. However, the air humidity in underground space is generally higher than that in buildings above ground, especially in summer. The humid environment not only seriously degrades people's comfort, but also endangers human health. 2) High levels of noise and vibration can result in discomfort to the human body. Since the subway environment is relatively closed, severe noise pollution and long reverberation time become a trigger for neurasthenia syndrome (Dong et al., 2021). 3) Due to the lack of natural lighting in the subway environment, people are unable to connect to the external environment through windows as in the aboveground buildings, which easily leads to the loss of sense of time and direction. People in this environment for a long time are also prone to depression and loneliness (Martinez-Nicolas et al., 2014). 4) The air pollution problem in the subway environment is also quite tricky. Due to the difficulty of direct access to sunlight and natural outdoor breeze, fresh air is often in short supply. As a result, various pollutants are not easy to be diluted, and bacteria and molds tend to breed. The overall air quality is thus an essential concern. (Xu and Hao, 2017). 5) High-speed trains passing through tunnels and stations produce a piston effect, namely, the air in the tunnel is driven by the train and flows at high speed in the direction of the train, thereby generating positive pressure at the front of the train and negative pressure at the rear. The resulting drastic air pressure changes will also have a significant impact on passengers' comfort (Xue et al., 2014).

Elements affecting passengers' comfort

Like aboveground buildings (Leccese et al., 2021), the subway space is also an artificial environment, which is an overall environmental state formed by physical elements such as thermal environment, light level, noise, air quality, mechanical vibration, and atmospheric pressure. These elements are inherently closely related to the comfort of subway passengers. Furthermore, each element can be subdivided in detail: the thermal environment can be represented by air temperature, relative humidity, air velocity near the human body, temperature of the envelope structure' inner surface and other objects (Ampofo et al., 2004); the light environment can be

TABLE 1 Previous work on the comfort of subway passengers in recent years.

Research	Scenarios		Environmental elements					
	Subway station	Subway cabin	Thermal environment	Vibration	Noise	Lighting	Air quality	Air pressure
Ampofo et al. (2004)	✓	✓	✓	—	—	—	—	—
Abbaspour et al. (2008)								
Katavoutas et al. (2016)								
Pan et al. (2020)								
Passi et al. (2022)								
Burnett and Pang, (2004)	✓	—	—	—	—	✓	—	—
Casals et al. (2016)								
Lai et al. (2020)								
Zhou et al. (2022a)								
Gershon et al. (2006)	✓	✓	—	—	✓	—	—	—
Iachini et al. (2012)								
Ghotbi et al. (2012)	✓	—	—	—	✓	—	—	—
Vogiatzis, (2012)	✓	—	—	✓	✓	—	—	—
Zou et al. (2015)								
Vogiatzis et al. (2018)								
Sun et al. (2014)	—	✓	—	—	✓	—	—	✓
Han et al. (2016)	✓	—	✓	—	✓	✓	✓	—
Liu et al. (2017)	✓	—	✓	—	—	—	—	—
Assimakopoulos and Katavoutas, (2017)								
Li et al. (2021)								
Yang et al. (2022)								
Niu et al. (2017)	✓	✓	—	—	—	—	—	✓
Amador-Jimenez et al. (2017)	—	✓	✓	✓	✓	✓	✓	—
Pan et al. (2019)	✓	—	—	—	—	—	✓	—
Izadi et al. (2019)	✓	—	—	—	—	—	—	✓
Li et al. (2020)	✓	—	✓	—	—	—	✓	—
Wu et al. (2020)								
Yu et al. (2021)								
Lin et al. (2022)								
Mohammadi et al. (2020)	—	✓	✓	✓	✓	✓	✓	—
Xu et al. (2020)	—	✓	—	—	—	✓	—	—
Xu et al. (2022)								
Xiong et al. (2020)	—	✓	—	—	—	—	—	✓
Li et al. (2022)								
Ren et al. (2022)	✓	✓	—	—	—	—	✓	—
Zhou et al. (2022b)	—	✓	✓	✓	✓	—	—	—

characterized by luminous flux, illuminance, color temperature, etc. (Kruisselbrink et al., 2018); the sound environment can be reflected by sound power, sound intensity, sound pressure, etc. (Teodorović and Janić, 2017); the air quality is implicated in the concentration levels of particulate matter (PM), total volatile organic compounds (TVOC), carbon dioxide (CO₂), carbon monoxide (CO), nitrogen oxide (NO_x), sulfur oxide (SO_x),

ozone (O₃), bacteria, fungi, etc. (Passi et al., 2021); the mechanical vibration can be characterized by vibration frequency, vibration intensity, etc. (Barone et al., 2016); the air pressure can be quantified by background pressure, pressure change rate, pressure transient intensity, etc. (Schwanitz et al., 2013). In recent years, a considerable amount of work has been dedicated to studying the impact of

these six elements on the comfort of subway passengers, with some researchers only examining the association between a single element and comfort, and others exploring the coupling effects of several elements on comfort. Table 1 lists the representative relevant studies in the last 2 decades.

Evaluation of environmental elements

Thermal environment

Thermal environment is generally the most important factor in an artificial environment. Maintaining an almost constant body temperature is a basic physiological requirement of the human body. The thermal environment acts on the heat transfer process between the human body and the outside, thus directly affecting the thermal balance of the human body. As shown in Eq. 1, when the body heat storage (S) is greater than zero, in other words, heat production is greater than heat dissipation, the body temperature rises. As a result, the human body will have a warm feeling, and *vice versa*.

$$M - W - C - R - E - S = 0 \quad (1)$$

where M represents the metabolism rate and can be obtained based on the size of the body's activity, W/m^2 ; W means the human mechanical work, W/m^2 ; C denotes the amount of heat that a person transferred into the surrounding environment by convection, W/m^2 ; R represents the amount of heat that a person transferred into the surrounding environment by radiation, W/m^2 ; E means the heat lost by evaporation of sweat and the water vapor exhaled by the body, W/m^2 ; and S represents the heat storage, W/m^2 .

Among the large number of thermal comfort indicators proposed in the literature (Rocca, 2017), the most widely used indicators are the Predicted Mean Vote (PMV) and the Predicted Percentage of Dissatisfied (PPD). PMV proposed by Professor Fanger represents the hot and cold sensation of the vast majority of people in the same environment (Fanger, 1970). PMV adopts the seven-point scale (ASHRAE-55, 2013), namely from +3 (hot) to 0 (neutral) and then to -3 (cold). PMV is defined as:

$$PMV = (0.303e^{-0.036M} + 0.028) \left\{ (M - W) - 3.05 \times 10^{-3} \times [5733 - 6.99(M - W) - p_a] - 0.42 \times [(M - W) - 58.15] - 1.7 \times 10^{-5} M (5867 - p_a) - 0.0014M (34 - t_a) - 3.96 \times 10^{-8} f_{cl} \times \left[(t_{cl} + 273)^4 - (\bar{t}_r + 273)^4 \right] - f_{cl} h_c (t_{cl} - t_a) \right\} \quad (2)$$

where f_{cl} denotes the ratio of a person's surface area while clothed to the surface area while naked; t_a means the air temperature, °C; \bar{t}_r represents the mean radiant temperature, °C; p_a means the partial vapor pressure, Pa; h_c is the convective heat transfer coefficient, $W/(m^2 \cdot ^\circ C)$; t_{cl} is the surface temperature of clothing, °C.

PPD provides the relationship between PPD and PMV through the method of probability analysis. It is adopted to predict the percentage of dissatisfied people under the current PMV value. ISO7730 standard uses PMV - PPD index to evaluate and describe the thermal environment (ISO, 2005). The standard's recommended value for the PMV index is between -0.5 and +0.5, representing no more than 10% of the population allowed to feel unsatisfied. The quantitative relationship between PMV and PPD is as follows:

$$PPD = 100 - 95 \exp[-(0.03353PMV^4 + 0.2179PMV^2)] \quad (3)$$

In addition, there is often a transition interval where people stay briefly in buildings, which may connect two spaces with different thermal environment parameters. When a person passes through or stays in the area for a short time and his/her activity state changes, the thermal sensation in this space will differ from that when he/she stays in the same space for a long time. Therefore, it is necessary to put forward the thermal comfort index for this kind of transition space to guide the determination of air conditioning design parameters. Thus, the U.S. Department of Transportation proposed the Relative Warmth Index (RWI) and Heat Deficit Rate (HDR) to decide the design parameters of the subway stations' platform, hall, and carriage, respectively for warm and cold environments (United States Department of Transportation, 1976). RWI and HDR can be calculated as follows (Yang et al., 2022):

$$RWI = \frac{(M(I_{cw} + I_a) + 6.42(t_a - 35) + R_0 I_a)}{((65.2 \times (5858.44 - p))/1000)} \quad (p > 2269Pa) \quad (4)$$

$$RWI = \frac{(M(I_{cw} + I_a) + 6.42(t_a - 35) + R_0 I_a)}{234} \quad (p \leq 2269Pa) \quad (5)$$

$$HDR = \frac{D}{\Delta\tau} = 28.89 - M - \frac{(6.42(t_a - 30.56) + R_0 I_a)}{(I_{cw} + I_a)} \quad (6)$$

where I_{cw} denotes the insulation of clothing based on wet cloth assumption, clo; I_a denotes the insulation effect of air boundary layer, clo; R_0 represents the average incident radiant heat from sources other than walls at room temperature, W/m^2 ; p is the vapor pressure at dry bulb temperatures, Pa; $\Delta\tau$ means the exposure time, s; D means the thermal debt, J/m^2 .

$$M = M_1 - \frac{T}{360} (M_1 - M_2) \quad (T < 360 s) \quad (7)$$

$$M = M_2 \quad (T \geq 360 s) \quad (8)$$

$$I_{cw} = I_{cw1} - \frac{T}{360} (I_{cw1} - I_{cw2}) \quad (T < 360 s) \quad (9)$$

$$I_{cw} = I_{cw2} (T \geq 360 \text{ s}) \quad (10)$$

where M_1 and M_2 are the initial and terminal metabolic rate, respectively, W/m^2 ; I_{cw1} and I_{cw2} are the initial and terminal insulation of clothing based on wet cloth assumption, respectively, clo ; T is the time required to go from the previous environment to the next, s .

$$I_a = 0.3923 v_a^{-0.4294} \quad (11)$$

where v_a is the inducing speed of human body movement, m/s .

The parameters in the calculation formula of the above evaluation indexes are usually obtained through field tests and questionnaires, in other words, a combination of objective and subjective means (Abbaspour et al., 2008; Pan et al., 2020). On the one hand, the field measurement is carried out by selecting representative locations in the subway environment, so as to arrange corresponding sensors to monitor and record thermal environmental parameters. It is worth emphasizing that the layout density and height of measuring points in a certain space need to be carefully determined (Katavoutas et al., 2016). On the other hand, thermal comfort is a subjective feeling of passengers. Even in the same thermal environment, passengers will make different judgments. A large number of questionnaires are needed to derive statistical rules. The content of the questionnaire generally includes some basic information, such as the age, gender, activity status and clothing of passengers. In addition, thermal sensation vote (TSV), humidity sensation vote (HSV), draft sensation vote (DSV), and thermal comfort vote (TCV) should also be collected and analyzed (Yang et al., 2022).

Vibration

Subway vibration will not only make passengers stand unstable, but also easy to make passengers feel tired. Moreover, it may even cause resonance in the internal organs of the human body, endangering the physical and mental health of passengers. The types of train vibration can be divided into transverse vibration, longitudinal vibration, vertical vibration and yaw vibration, longitudinal pendulum vibration, torsional pendulum vibration around each axis. Among them, vertical vibration, transverse vibration and yaw vibration have great influence on passengers' comfort. The main effect of vibration on the human body is the frequency of vibration. The range of vibration frequencies that humans can perceive is 1–1,000 Hz. Generally, ground vibration in the frequency range of 1–80 Hz is considered as perceptible whole-body vibration, to which the human body is particularly sensitive and in which the resonant frequencies of the organs are concentrated.

Vibration comfort is an indicator of how good or bad passengers feel when riding the subway caused by vibration.

Currently, the evaluation of vibration comfort is primarily from two perspectives: operating stability and riding comfort. According to GB/T 5599–1985, operating stability (W_0) is determined by vibration frequency and vibration acceleration, and its expression is:

$$W_0 = 3.57 \sqrt[10]{\frac{A^3}{f}} F(f) \quad (12)$$

where A denotes the vibration acceleration, m/s^2 ; f means the vibration frequency, $1/\text{s}$; $F(f)$ denotes the frequency correction coefficient, $1/\text{s}$.

In accordance with the above standard, when W_0 is less than 2.5, the stability level is I (excellent); when W_0 spans 2.5–2.75, the stability level is II (good); when W_0 spans 2.75–3.0, the stability level will be III (qualified).

Additionally, riding comfort is a measure of the average comfort of passengers and staffs on the subway. The evaluation procedure is based on the measurement of the vibration acceleration on the train floor. It can be obtained by calculating the acceleration in different directions at the position of the human body in line with the UIC 513–1994 standard (Mohammadi et al., 2020). It is worth highlighting that both two standards also elaborate on the measurement methods for the parameters in each indicator, guiding the placement of acceleration sensors and the sampling duration.

Noise

Noise, in the definition of physics, is the sound of a sounding object doing irregular vibrations; in the definition of physiology, it is the discordant sound that interferes with people's normal study, work and rest. In a noisy environment, it is easy to make people bored and agitated. Prolonged and high-decibel noise can also cause damage to the auditory system (Basner et al., 2014). The subway itself will produce some noise when operating, coupled with the noise of numerous passengers, thus the disturbing sound affects the comfort of subway passengers to a great extent.

The effect of noise on human body is not only related to the noise value, but also related to the exposure time (Rocca et al., 2022). To this end, the concept of "equivalent continuous A-weighted sound pressure level (L_{eq})" is defined, with the following expression (Ordoñez and Hammershoi, 2014):

$$L_{eq} = 10 \times \lg \left(\frac{1}{T_0} \int_0^{T_0} \frac{p^2(t)}{p_0^2} dt \right) \quad (13)$$

where T_0 denotes the duration of time signal; $p(t)$ denotes the instantaneous sound pressure; p_0 denotes the reference effective sound pressure (20 μPa).

As a reference for noise thresholds, the U.S. Environmental Protection Agency (EPA) and the World Health Organization

(WHO) suggested a maximum daily L_{eq} of 70 dBA over 24 h and a limit of 75 dBA over 8 h with the same energy (Mohammadi et al., 2020). Furthermore, for shorter exposure durations, the health threshold can be set to 80 dBA for 3 h and 90 dBA for 30 min (Neitzel et al., 2009). In addition, the maximum permissible limits for train noise can also be identified from the Chinese standard GB 14892-2006.

Lighting

The influence of subway lighting environment on passengers is reflected on both physiological and psychological levels. The subway lighting system mainly relies on artificial light sources. Poor lighting environment will have a physiological impact on passenger comfort, primarily caused by inappropriate illumination, low illumination uniformity, glare, and maladaptive light-dark transitions. In addition, the psychological influence mainly includes color temperature, light color and atmosphere sense, light source height and relaxation degree, space shadow and tension sense.

To examine the visual comfort of passengers in the subway environment, it is necessary to combine objective field tests with subjective questionnaires (Bian and Luo, 2017). The objective approach is proposed to use relevant equipment to measure indicators that can characterize the light environment. A convincing test protocol can be adopted in accordance with the standards (e.g., Method for Determination of Illumination in Public Places GB/T 18204.21-2000). The physical quantities to be recorded cover illuminance, irradiation uniformity, color temperature of light source, glare, color rendering, etc. (Carlucci et al., 2015; Leccese et al., 2020; Shafavi et al., 2020). In turn, the design limits of the indicators specified by the relevant standards (e.g., General Technical Specification for Metro Vehicles GB/T 7928-2003, Railway Applications - Electrical Lighting for Rolling Stock in Public Transport System EN 13272-1:2019) can be used to compare with the measured data (Xu et al., 2022). The subjective approach aims to obtain passengers' visual responses to the subway environment through questionnaire surveys. In addition to collecting basic data and behaviors of passengers, designers also need to ask passengers to rate their visual comfort through non-professional language and ask for information such as their preferences (Allan et al., 2019).

Air quality

Poor air quality not only brings people discomfort, but also seriously threatens human health. In such a relatively closed environment as subway space, air pollution deserves more and more attention. The poor air quality in the subway environment can be caused by the following reasons. Firstly, the subway station is a long and narrow underground space with good air tightness. Only a few station entrances and ventilation shafts are

connected to the outside, and the internal air environment of the station is regulated only by the air conditioning system. Hence, too little fresh air and insufficient exhaust air will lead to an increase in the concentration of pollutants (Klepczyńska Nyström et al., 2010; Martins et al., 2015). Secondly, people will carry particulate matter and breathe out certain organic matters, such as inhalable particulate matter, carbon dioxide, volatile organic compounds, etc. Thirdly, formaldehyde and volatile organic compounds released by construction and decoration materials in the station also deteriorate indoor air quality (Passi et al., 2021). Fourthly, most of the subway stations are buried deep underground, lacking sunlight, and it is easy to breed bacteria, mold and other microorganisms.

The existing literature has comprehensively expounded the air pollutants' types, concentration levels, sources, influencing factors and impacts on human health in the subway environment (Cepeda et al., 2017; Xu and Hao, 2017; Luo et al., 2018; Chang et al., 2021). This section focuses on the evaluation scheme of subway air quality. The evaluation of subway air quality is subjective in nature because different people have different levels of perception of air conditions. Consequently, in addition to the data obtained from field measurement, it is also essential to acquire a certain number of passengers and staffs' satisfaction with subway air quality, environmental comfort, and air odor sense. Therefore, on the one hand, testing instruments should be reasonably set up in the subway environment according to relevant standards or norms (refer to Indoor Air Quality Standard GB/T 18883-2002) to monitor the concentration of air pollutants. Mathematical models can be used to synthesize the measured data and assess the subway air quality against the standard limits. For example, some Chinese standards set concentration limits for major pollutants (Ambient Air Quality Standard GB 3095-2012, Code for Design of Metro GB 50157-2013, Standard for Design of Ventilation Air Conditioning and Heating of Urban Rail Transit GB/T 51357-2019, etc.) (Leng and Wen, 2021). On the other hand, the subjective evaluation of the subway air quality can be collected by questionnaire survey. This method directly takes into account the human factor and is a perfect complement to the objective field test method. Passengers' background information (gender, age, etc.), exposure to the subway environment (duration of each ride, number of rides per week, etc.), and subjective perceptions about air quality in different periods and locations should be included in the questionnaire setting. In short, a favorable air quality in the subway environment can be characterized as: no known pollutants in the air reach the concentration index limits determined by the recognized authority, and the vast majority of people (>80%) do not express dissatisfaction.

Air pressure

During the high speed of a subway train, the air inside the tunnel fluctuates violently, forming complex pressure waves (pressure transients). The sharp pressure fluctuations outside

the train will be transmitted into the cabins through the gaps in the train body, air ducts and air conditioning system, causing pressure fluctuations inside the train. The pressure waves act on the eardrum, producing pressure difference between the inner and outer sides of the tympanic membrane, thereby resulting in symptoms such as tinnitus and earache (Raghunathan et al., 2002). In extreme cases, pressure fluctuations may rupture the eardrum. Therefore, the issue of subway passengers' comfort caused by aerodynamic characteristics is gaining attention.

The criteria used to ensure the eardrum comfort of the crews and passengers comprise the pressure change magnitude Δp , the pressure change rate (pressure gradient) dp/dt , and the pressure monotonic change value in a certain period $\Delta p/\Delta t$. Among them, $\Delta p/\Delta t$ overcomes the limitations of the former two. It provides the threshold of pressure fluctuation associated with comfort level from the physiological perspective. The standard UIC 799–11 states that the maximum pressure change within 3 s should not exceed 800 Pa (Liu et al., 2020). In addition, it is worth mentioning that the investigation of pressure fluctuation patterns can rely on both data acquisition from field pressure sensors and numerical simulation (Kim and Kim, 2007; Niu et al., 2017; Li et al., 2022).

Limitations and future directions

The current research on subway passengers' comfort still has limitations and is expected to be improved by the forthcoming work. As can be seen from Table 1, most of the work has focused on exploring the correlation between a single environmental element and comfort level. However, comfort is a synthesis of physical, physiological and psychological reflections, and is jointly affected by various factors in the passengers' environment. Therefore, it is essential to consider the integrated effect of multiple elements when evaluating passengers' comfort. At this stage, it is already possible to monitor environmental parameters through gauges, record physiological indicators through wearable sensors, and access subjective evaluations through questionnaire surveys. The next challenge is how to judiciously incorporate the collected data sets to develop a comprehensive comfort evaluation model with multi-element coupling. There have been several active attempts to assign subjective and objective weight coefficients for each environmental element by fuzzy analytic hierarchy process and rough set theory, so as to establish a comprehensive comfort evaluation index (Huang and Shuai, 2018; Ebrahimi and Bridgelall, 2021).

Improving the service level of the rail transit industry to enhance subway passengers' comfort is still a critical issue to be addressed. Based on the above-mentioned comprehensive comfort theory, the significance of each environmental element can be ranked, so that corresponding mitigation measures can be targeted. The progressive improvement of the subway environmental control system can start from the following aspects: heating, ventilation and air conditioning (HVAC) systems, train shock absorption modules, air tightness

regulation, lighting equipment, air purification devices, building materials, etc.

The HVAC system is a key link to control the thermal environment and air quality of the subway space, while it is the major energy consumer of the subway system (Guan et al., 2018). More efforts are needed to achieve reduced energy consumption in HVAC systems while maintaining inherent functionality and passenger comfort. A recent study has reviewed ten energy-saving strategies for HVAC systems and suggested highlights for future work (Yu et al., 2021). The proper use of passive ventilation strategies as well as variable frequency devices is expected to contribute to the construction of a sustainable metro network.

Conclusion

The subway has emerged as an indispensable means of transportation for inhabitants in metropolitan areas. With the improvement of living standards, passengers' requirements for subway transportation are not limited to safety and convenience. A comfortable environment has gradually become a focus of people's attention. This paper systematically reviews the achievements of the past 2 decades on the topic of subway passengers' comfort. Six environmental elements that have significant impacts on comfort level are identified, covering thermal environment, vibration, noise, lighting, air quality, and air pressure. Moreover, measurement schemes, calculation models, and evaluation methods for each element are summarized according to the relevant standards and references. At present, considerable research has been devoted to elucidating the relationship between a single element and passengers' comfort, while the establishment of a comprehensive comfort evaluation model coupled with multiple elements still needs further effort. In addition, the HVAC system plays an important role in the subway environmental control system and consumes a large amount of energy. The rational employment of passive ventilation strategies and variable frequency devices will help to build a comfortable, healthy and sustainable subway network.

Author contributions

WY: Conceptualization, Writing-Original draft preparation; XM: Conceptualization, Methodology; HZ: Methodology; CY: Investigation; QC: Investigation; SO: Writing-Review and editing; XC: Supervision, Writing-Review and editing.

Funding

This work was supported by National Natural Science Foundation of China (52106025), Natural Science Basic Research Program of Shaanxi (2021JQ-048), and Postdoctoral Science Foundation of Shaanxi Province (2018BSHYDZZ31).

Conflict of interest

HZ was employed by the Company China State Construction Silkroad Construction Investment Group Co., Ltd.

The remaining authors declare that the research was conducted in the absence of any commercial or financial relationships that could be construed as a potential conflict of interest.

References

- Abbaspour, M., Jafari, M. J., Mansouri, N., Moattar, F., Nouri, N., and Allahyari, M. (2008). Thermal comfort evaluation in tehran metro using relative Warmth index. *Int. J. Environ. Sci. Technol.* 5, 297–304. doi:10.1007/BF03326024
- Allan, A. C., Garcia-Hansen, V., Isoardi, G., and Smith, S. S. (2019). Subjective assessments of lighting quality: A measurement review. *LEUKOS* 15, 115–126. doi:10.1080/15502724.2018.1531017
- Amador-Jimenez, L., Mohammadi, A., and Nasiri, F. (2017). “Level of comfort and safety in railway transit,” in 4th Int. Conf. Transp. Inf. Saf., 1060–1066. doi:10.1109/ICTIS.2017.8047901
- Ampofo, F., Maidment, G., and Missenden, J. (2004). Underground railway environment in the UK Part 1: Review of thermal comfort. *Appl. Therm. Eng.* 24, 611–631. doi:10.1016/j.applthermaleng.2003.10.017
- Ashrae-55 (2013). *Thermal environmental conditions for human occupancy*. Atlanta, USA: American Society of Heating, Refrigerating and Air-conditioning Engineers.
- Assimakopoulos, M. N., and Katavoutas, G. (2017). Thermal comfort conditions at the platforms of the athens metro. *Procedia Eng.* 180, 925–931. doi:10.1016/j.proeng.2017.04.252
- Barone, V., Mongelli, D. W. E., and Tassitani, A. (2016). Vibrational comfort on board the vehicle: Influence of speed bumps and comparison between different categories of vehicle. *Adv. Acoust. Vib.* 2016, 1–6. doi:10.1155/2016/2676021
- Basner, M., Babisch, W., Davis, A., Brink, M., Clark, C., Janssen, S., et al. (2014). Auditory and non-auditory effects of noise on health. *Lancet* 383, 1325–1332. doi:10.1016/S0140-6736(13)61613-X
- Bian, Y., and Luo, T. (2017). Investigation of visual comfort metrics from subjective responses in China: A study in offices with daylight. *Build. Environ.* 123, 661–671. doi:10.1016/j.buildenv.2017.07.035
- Burnett, J., and Panghim, A. Y. (2004). Design and performance of pedestrian subway lighting systems. *Tunn. Undergr. Space Technol.* 19, 619–628. doi:10.1016/j.tust.2004.03.001
- Carlucci, S., Causone, F., De Rosa, F., and Pagliano, L. (2015). A review of indices for assessing visual comfort with a view to their use in optimization processes to support building integrated design. *Renew. Sustain. Energy Rev.* 47, 1016–1033. doi:10.1016/j.rser.2015.03.062
- Casals, M., Gangoelle, M., Forcada, N., and Macarulla, M. (2016). Reducing lighting electricity use in underground metro stations. *Energy Convers. Manag.* 119, 130–141. doi:10.1016/j.enconman.2016.04.034
- Cepeda, M., Schoufour, J., Freak-Poli, R., Koolhaas, C. M., Dhana, K., Bramer, W. M., et al. (2017). Levels of ambient air pollution according to mode of transport: A systematic review. *Lancet Public Health* 2, e23–e34. doi:10.1016/S2468-2667(16)30021-4
- Chang, L., Chong, W. T., Wang, X., Pei, F., Zhang, X., Wang, T., et al. (2021). Recent progress in research on PM_{2.5} in subways. *Environ. Sci. Process. Impacts* 23, 642–663. doi:10.1039/d1em00002k
- Dong, X., Wu, Y., Chen, X., Li, H., Cao, B., Zhang, X., et al. (2021). Effect of thermal, acoustic, and lighting environment in underground space on human comfort and work efficiency: A review. *Sci. Total Environ.* 786, 147537. doi:10.1016/j.scitotenv.2021.147537
- Ebrahimi, S., and Bridgelall, R. (2021). A fuzzy delphi analytic hierarchy model to rank factors influencing public transit mode choice: A case study. *Res. Transp. Bus. Manag.* 39, 100496. doi:10.1016/j.rtbm.2020.100496
- Fanger, P. O. (1970). *Thermal comfort: Analysis and applications in environmental engineering*. Copenhagen: Danish Technical Press.
- Gershon, R. R. M., Neitzel, R., Barrera, M. A., and Akram, M. (2006). Pilot survey of subway and bus stop noise levels. *J. Urban Health* 83, 802–812. doi:10.1007/s11524-006-9080-3
- Ghotbi, M. R., Monazzam, M. R., Baneshi, M. R., Asadi, M., and Fard, S. M. B. (2012). Noise pollution survey of a two-storey intersection station in Tehran metropolitan subway system. *Environ. Monit. Assess.* 184, 1097–1106. doi:10.1007/s10661-011-2024-8
- Guan, B., Liu, X., Zhang, T., and Xia, J. (2018). Energy consumption of subway stations in China: Data and influencing factors. *Sustain. Cities Soc.* 43, 451–461. doi:10.1016/j.scs.2018.09.018
- Han, J., Kwon, S. B., and Chun, C. (2016). Indoor environment and passengers’ comfort in subway stations in Seoul. *Build. Environ.* 104, 221–231. doi:10.1016/j.buildenv.2016.05.008
- Huang, W., and Shuai, B. (2018). A methodology for calculating the passenger comfort benefits of railway travel. *J. Mod. Transp.* 26, 107–118. doi:10.1007/s40534-018-0157-y
- Iachini, T., Maffei, L., Ruotolo, F., Senese, V. P., Ruggiero, G., Masullo, M., et al. (2012). Multisensory assessment of acoustic comfort aboard metros: A virtual reality study. *Appl. Cogn. Psychol.* 26, 757–767. doi:10.1002/acp.2856
- ISO (2005). *Ergonomics of the thermal environment - analytical determination and interpretation of thermal comfort using calculation of the PMV and PPD indices and local thermal comfort criteria*. Geneva, Switzerland: International Organization for Standardization, 7730.
- Izadi, T., Mehrabian, M. A., Abouali, O., and Ahmadi, G. (2019). 3-D numerical analysis of train-induced flow inside four ventilated underground subway stations and connecting tunnels. *J. Wind Eng. Industrial Aerodynamics* 193, 103974. doi:10.1016/j.jweia.2019.103974
- Kajtar, L., Nyers, J., and Szabo, J. (2015). Dynamic thermal dimensioning of underground spaces. *Energy* 87, 361–368. doi:10.1016/j.energy.2015.04.112
- Katavoutas, G., Assimakopoulos, M. N., and Asimakopoulos, D. N. (2016). On the determination of the thermal comfort conditions of a metropolitan city underground railway. *Sci. Total Environ.* 566–567, 877–887. doi:10.1016/j.scitotenv.2016.05.047
- Kim, J. Y., and Kim, K. Y. (2007). Experimental and numerical analyses of train-induced unsteady tunnel flow in subway. *Tunn. Undergr. Space Technol.* 22, 166–172. doi:10.1016/j.tust.2006.06.001
- Klepczyńska Nyström, A., Svartengren, M., Grunewald, J., Pousette, C., Rödin, I., Lundin, A., et al. (2010). Health effects of a subway environment in healthy volunteers. *Eur. Respir. J.* 36, 240–248. doi:10.1183/09031936.00099909
- Kruisselbrink, T., Dangol, R., and Rosemann, A. (2018). Photometric measurements of lighting quality: An overview. *Build. Environ.* 138, 42–52. doi:10.1016/j.buildenv.2018.04.028
- Lai, X. D., Dai, M. Y., and Rameezdeen, R. (2020). Energy saving based lighting system optimization and smart control solutions for rail transportation: Evidence from China. *Results Eng.* 5, 100096. doi:10.1016/j.rineng.2020.100096
- Leccese, F., Rocca, M., Salvadori, G., Belloni, E., and Buratti, C. (2021). Towards a holistic approach to indoor environmental quality assessment: Weighting schemes to combine effects of multiple environmental factors. *Energy Build.* 245, 111056. doi:10.1016/j.enbuild.2021.111056
- Leccese, F., Salvadori, G., Rocca, M., Buratti, C., and Belloni, E. (2020). A method to assess lighting quality in educational rooms using analytic hierarchy process. *Build. Environ.* 168, 106501. doi:10.1016/j.buildenv.2019.106501
- Leng, J., and Wen, Y. (2021). Environmental standards for healthy ventilation in metros: Status, problems and prospects. *Energy Build.* 245, 111068. doi:10.1016/j.enbuild.2021.111068
- Li, C., Liu, M., Chang, R., Wang, X., Liu, W., and Zhang, H. (2022). Air pressure and comfort study of the high-speed train passing through the subway station. *Sustain. Cities Soc.* 81, 103881. doi:10.1016/j.scs.2022.103881

Publisher’s note

All claims expressed in this article are solely those of the authors and do not necessarily represent those of their affiliated organizations, or those of the publisher, the editors and the reviewers. Any product that may be evaluated in this article, or claim that may be made by its manufacturer, is not guaranteed or endorsed by the publisher.

- Li, G., Meng, X., Zhang, X., Zhang, L., Du, C., Li, N., et al. (2020). An innovative ventilation system using piston wind for the thermal environment in Shanghai subway station. *J. Build. Eng.* 32, 101276. doi:10.1016/j.jobe.2020.101276
- Li, J., Li, A., Hou, Y., Zhang, C., Yang, C., Zhang, X., et al. (2021). Air distribution and thermal environment optimization on subway platform using an innovative attached ventilation mode. *Build. Environ.* 204, 108226. doi:10.1016/j.buildenv.2021.108226
- Li, Y., Geng, S., Zhang, X., and Zhang, H. (2017). Study of thermal comfort in underground construction based on field measurements and questionnaires in China. *Build. Environ.* 116, 45–54. doi:10.1016/j.buildenv.2017.02.003
- Lin, C., Wu, L., Xia, H., Zhen, M., Shen, C., Zhu, J., et al. (2022). Characteristics of the thermal environment, air quality, and passenger comfort in the underground transfer space of metro stations in Beijing. *J. Build. Eng.* 59, 105093. doi:10.1016/j.jobe.2022.105093
- Liu, C., Li, A., Yang, C., and Zhang, W. (2017). Simulating air distribution and occupants' thermal comfort of three ventilation schemes for subway platform. *Build. Environ.* 125, 15–25. doi:10.1016/j.buildenv.2017.08.036
- Liu, T., Geng, S., Chen, X., and Krajnovic, S. (2020). Numerical analysis on the dynamic airtightness of a railway vehicle passing through tunnels. *Tunn. Undergr. Space Technol.* 97, 103286. doi:10.1016/j.tust.2020.103286
- Luo, J., Wang, H., and Chen, L. (2018). Advances in research of airborne microbes in subway systems. *Chin. J. Appl. Environ. Biol.* 24, 934–940. doi:10.19675/j.cnki.1006-687x.2017.10007
- Martinez-Nicolas, A., Madrid, J. A., and Rol, M. A. (2014). Day-night contrast as source of health for the human circadian system. *Chronobiol. Int.* 31, 382–393. doi:10.3109/07420528.2013.861845
- Martins, V., Moreno, T., Minguillón, M. C., Amato, F., de Miguel, E., Capdevila, M., et al. (2015). Exposure to airborne particulate matter in the subway system. *Sci. Total Environ.* 511, 711–722. doi:10.1016/j.scitotenv.2014.12.013
- Mohammadi, A., Amador-Jimenez, L., and Nasiri, F. (2020). A multi-criteria assessment of the passengers' level of comfort in urban railway rolling stock. *Sustain. Cities Soc.* 53, 101892. doi:10.1016/j.scs.2019.101892
- Neitzel, R., Gershon, R. R. M., Zeltser, M., Canton, A., and Akram, M. (2009). Noise levels associated with New York City's mass transit systems. *Am. J. Public Health* 99, 1393–1399. doi:10.2105/AJPH.2008.138297
- Nezhnikova, E. (2016). The use of underground city space for the construction of civil residential buildings. *Procedia Eng.* 165, 1300–1304. doi:10.1016/j.proeng.2016.11.854
- Niu, J., Zhou, D., Liang, X., Liu, T., and Liu, S. (2017). Numerical study on the aerodynamic pressure of a metro train running between two adjacent platforms. *Tunn. Undergr. Space Technol.* 65, 187–199. doi:10.1016/j.tust.2017.03.006
- Ordoñez, R., and Hammershoi, D. (2014). Temporary threshold shifts from exposures to equal equivalent continuous a-weighted sound pressure level. *Acta Acust. United Acust.* 100, 513–526. doi:10.3813/AAA.918731
- Pan, S., Du, S., Wang, X., Zhang, X., Xia, L., Liu, J., et al. (2019). Analysis and interpretation of the particulate matter (PM10 and PM2.5) concentrations at the subway stations in Beijing, China. *Sustain. Cities Soc.* 45, 366–377. doi:10.1016/j.scs.2018.11.020
- Pan, S., Liu, Y., Xie, L., Wang, X., Yuan, Y., and Jia, X. (2020). A thermal comfort field study on subway passengers during air-conditioning season in Beijing. *Sustain. Cities Soc.* 61, 102218. doi:10.1016/j.scs.2020.102218
- Passi, A., Nagendra, S. M. S., and Maiya, M. P. (2021). Characteristics of indoor air quality in underground metro stations: A critical review. *Build. Environ.* 198, 107907. doi:10.1016/j.buildenv.2021.107907
- Passi, A., Shiva Nagendra, S. M., and Maiya, M. P. (2022). Evaluation of comfort perception of passengers in urban underground metro stations. *Energy sustain. Dev.* 68, 273–288. doi:10.1016/j.esd.2022.04.003
- Ragunathan, R. S., Kim, H. D., and Setoguchi, T. (2002). *Aerodynamics of high-speed railway train*. doi:10.1016/S0376-0421(02)00029-5
- Ren, J., He, J., Kong, X., Xu, W., Kang, Y., Yu, Z., et al. (2022). A field study of CO2 and particulate matter characteristics during the transition season in the subway system in Tianjin, China. *Energy Build.* 254, 111620. doi:10.1016/j.enbuild.2021.111620
- Rocca, M. (2017). Health and well-being in indoor work environments: A review of literature. *Conf. Proc. - 2017 17th IEEE Int. Conf. Environ. Electr. Eng.* 2017 1st IEEE Ind. Commer. Power Syst. Eur. IEEEIC / I CPS Eur. doi:10.1109/IEEEIC.2017.7977516
- Rocca, M., Puccio, F. D., Forte, P., and Leccese, F. (2022). Acoustic comfort requirements and classifications: Buildings vs. yachts. *Ocean. Eng.* 255, 111374. doi:10.1016/j.oceaneng.2022.111374
- Schwanitz, S., Wittkowski, M., Rolny, V., Samel, C., and Basner, M. (2013). Continuous assessments of pressure comfort on a train - a field-laboratory comparison. *Appl. Ergon.* 44, 11–17. doi:10.1016/j.apergo.2012.04.004
- Shafavi, N. S., Zomorodian, Z. S., Tahsildoost, M., and Javadi, M. (2020). Occupants visual comfort assessments: A review of field studies and lab experiments. *Sol. Energy* 208, 249–274. doi:10.1016/j.solener.2020.07.058
- Sun, Z. X., Yang, G. W., and Zhu, L. (2014). Study on the critical diameter of the subway tunnel based on the pressure variation. *Sci. China Technol. Sci.* 57, 2037–2043. doi:10.1007/s11431-014-5664-4
- Teodorović, D., and Janić, M. (2017). in *Transportation engineering*. doi:10.1016/b978-0-12-803818-5.00011-1 *Transportation, environment, and society*
- United States Department of Transportation (1976). Subway environmental design handbook. *Princ. Appl.* 1.
- Vogiatzis, K. (2012). Environmental ground borne noise and vibration protection of sensitive cultural receptors along the Athens Metro Extension to Piraeus. *Sci. Total Environ.* 439, 230–237. doi:10.1016/j.scitotenv.2012.08.097
- Vogiatzis, K., Zafropoulou, V., and Mouzakis, H. (2018). Monitoring and assessing the effects from Metro networks construction on the urban acoustic environment: The Athens Metro Line 3 Extension. *Sci. Total Environ.* 639, 1360–1380. doi:10.1016/j.scitotenv.2018.05.143
- Wu, L., Xia, H., Wang, X., Dong, Q., Lin, C., Liu, X., et al. (2020). Indoor air quality and passenger thermal comfort in Beijing metro transfer stations. *Transp. Res. Part D Transp. Environ.* 78, 102217. doi:10.1016/j.trd.2019.102217
- Xiong, X., Zhu, L., Zhang, J., Li, A., Li, X., and Tang, M. (2020). Field measurements of the interior and exterior aerodynamic pressure induced by a metro train passing through a tunnel. *Sustain. Cities Soc.* 53, 101928. doi:10.1016/j.scs.2019.101928
- Xu, B., and Hao, J. (2017). Air quality inside subway metro indoor environment worldwide: A review. *Environ. Int.* 107, 33–46. doi:10.1016/j.envint.2017.06.016
- Xu, J., Xiang, Z.-r., Zhi, J.-y., Xu, X.-f., He, S.-j., Wang, J., et al. (2020). *Research on virtual simulation evaluation system for passenger compartments lighting of subway trains in China*. Cham: Springer International Publishing. doi:10.1007/978-3-030-20476-1_35
- Xu, J., Xiang, Z. R., Zhi, J. Y., Chen, Y. D., and Xu, X. F. (2022). Assessment of visual comfort in the lighting environments of subway cabins in China. *Int. J. Rail Transp.* 00, 1–22. doi:10.1080/23248378.2022.2082571
- Xue, P., You, S., Chao, J., and Ye, T. (2014). Numerical investigation of unsteady airflow in subway influenced by piston effect based on dynamic mesh. *Tunn. Undergr. Space Technol.* 40, 174–181. doi:10.1016/j.tust.2013.10.004
- Yang, B., Yang, C., Ni, L., Wang, Y., and Yao, Y. (2022). Investigation on thermal environment of subway stations in severe cold region of China: A case study in harbin. *Build. Environ.* 212, 108761. doi:10.1016/j.buildenv.2022.108761
- Yu, J., Kang, Y., Zhai, Z., and John (2020). Advances in research for underground buildings: Energy, thermal comfort and indoor air quality. *Energy Build.* 215, 109916. doi:10.1016/j.enbuild.2020.109916
- Yu, Y., You, S., Zhang, H., Ye, T., Wang, Y., and Wei, S. (2021). A review on available energy saving strategies for heating, ventilation and air conditioning in underground metro stations. *Renew. Sustain. Energy Rev.* 141, 110788. doi:10.1016/j.rser.2021.110788
- Zhou, B., Gui, Y., Xie, X., Li, W., and Li, Q. (2022a). A multi-category intelligent method for the evaluation of visual comfort in underground space. *Tunn. Undergr. Space Technol.* 124, 104488. doi:10.1016/j.tust.2022.104488
- Zhou, X., Liu, Y., Luo, M., Zheng, S., Yang, R., and Zhang, X. (2022b). Overall and thermal comfort under different temperature, noise, and vibration exposures. *Indoor Air* 32, e12915–e12916. doi:10.1111/ina.12915
- Zou, C., Wang, Y., Wang, P., and Guo, J. (2015). Measurement of ground and nearby building vibration and noise induced by trains in a metro depot. *Sci. Total Environ.* 536, 761–773. doi:10.1016/j.scitotenv.2015.07.123



OPEN ACCESS

EDITED BY

Xiaolin Wang,
University of Tasmania, Australia

REVIEWED BY

Hadi Rostamzadeh (Kalkhoran),
Eindhoven University of Technology,
Netherlands
Bidyut Baran Saha,
Kyushu University, Japan

*CORRESPONDENCE

Qian Chen,
chen_qian@u.nus.edu
Kim Choon Ng,
kimchoon.ng@kaust.edu.sa

SPECIALTY SECTION

This article was submitted
to Indoor Environment,
a section of the journal
Frontiers in Built Environment

RECEIVED 31 August 2022

ACCEPTED 25 October 2022

PUBLISHED 08 November 2022

CITATION

Chen Q, M KJ, Burhan M, Shahzad MW,
Ybyraiymkul D, Oh S, Cui X and Ng KC
(2022), Long-term performance of a
hybrid indirect evaporative cooling-
mechanical vapor compression cycle: A
case study in Saudi Arabia.
Front. Built Environ. 8:1032961.
doi: 10.3389/fbuil.2022.1032961

COPYRIGHT

© 2022 Chen, M, Burhan, Shahzad,
Ybyraiymkul, Oh, Cui and Ng. This is an
open-access article distributed under
the terms of the [Creative Commons
Attribution License \(CC BY\)](#). The use,
distribution or reproduction in other
forums is permitted, provided the
original author(s) and the copyright
owner(s) are credited and that the
original publication in this journal is
cited, in accordance with accepted
academic practice. No use, distribution
or reproduction is permitted which does
not comply with these terms.

Long-term performance of a hybrid indirect evaporative cooling-mechanical vapor compression cycle: A case study in Saudi Arabia

Qian Chen^{1*}, Kum Ja M¹, Muhammad Burhan¹,
Muhammad Wakil Shahzad², Doskhan Ybyraiymkul¹,
Seungjin Oh³, Xin Cui⁴ and Kim Choon Ng^{1*}

¹Water Desalination and Reuse Center, Biological and Environmental Science and Engineering Division, King Abdullah University of Science and Technology, Thuwal, Saudi Arabia, ²Department of Mechanical and Construction Engineering, Northumbria University, Newcastle Upon Tyne, United Kingdom, ³Clean Innovation Technology Group (Jeju Regional Division), Korea Institute of Industrial Technology (KITECH), Jeju, South Korea, ⁴Institute of Building Environment and Sustainable Technology, Xi'an Jiaotong University, Xi'an, China

In Saudi Arabia, air conditioning is the main consumer of electricity, and increasing its energy efficiency is of great importance for energy conservation and carbon footprint reduction. This study presents the evaluation of a hybrid indirect evaporative cooling-mechanical vapor compression (IEC-MVC) cycle for cooling applications in Saudi Arabia. Most cities in this country are characterized by a high sensible cooling demand, and a few cities near the coasts of the Red sea and the Persian Gulf also need dehumidification. By employing the hybrid system, IEC can undertake about 60% of the cooling load in the summer of arid cities, and energy consumption can be reduced by up to 50%. The contribution of IEC and energy saving are less significant in humid cities because the latent loads have to be handled by MVC. Over the whole year, IEC contributes 50% of the total cooling capacity and reduces energy consumption by 40% in dry cities, while the saving is lower at 15%–25% in humid cities like Mecca and Jeddah. The average water consumption of the IEC is in the range of 4–12 L/hr. The water consumption can be replenished by the condensate collected from the MVC evaporator if the ambient humidity is high. Based on the annual performance, the cost of the IEC-MVC process is calculated, and it is 15%–35% lower than the standalone MVC. The results demonstrate the great potential of the hybrid IEC-MVC cycle in Saudi Arabia.

KEYWORDS

indirect evaporative cooling, mechanical vapor compression, long-term analysis, energy saving, water consumption, economic analysis

1 Introduction

Buildings represent a major consumer of electricity in the Gulf Cooperation Council (GCC) region. For example, in Saudi Arabia, all building sectors, including residential, commercial, governmental, and industrial sectors, consume almost 80% of electricity (Krarti et al., 2017). A significant portion of the electricity consumption is attributed to air conditioning, which can account for 50% of the peak electricity demand (Eveloy and Ayoub, 2019). Therefore, increasing the energy efficiency of air conditioning systems is crucial for conserving energy and reducing the corresponding CO₂ emission from power plants.

The air conditioning systems in Saudi Arabia are dominated by mechanical vapor compression (MVC) technology. Considering the residential houses alone, more than 24 million MVC units (mainly window units and split units) are installed (Housing GStat, 2018a). The advantages of MVC include high technology maturity and low initial costs. However, the energy efficiency of MVC is low in Saudi Arabia. This is because the ambient temperature is high, leading to a high condensation temperature. Moreover, the air quality in Saudi Arabia is poor, and corrosion of outdoor condensers is very common (Shahzad et al., 2019; Shahzad et al., 2021). The corroded condensers have extra thermal barriers and further increase the condensation temperature.

The indirect evaporative cooler (IEC) is deemed a promising alternative to MVC and has gained substantial research interest in recent years. It utilizes the evaporation of water to create a cooling effect, and the power consumption is very low. Compared to MVC, the energy efficiency of IEC is several times higher (Jradi and Riffat, 2014). Extensive research efforts have been reported to improve the performance of IEC, including parameter optimization by mathematical modelling (Anisimov et al., 2014; Cui et al., 2014; Heidarinejad and Moshari, 2015; Cui et al., 2016; Zhu et al., 2017; Dizaji et al., 2020), proposing novel configurations (Riffat and Zhu, 2004; Duan et al., 2012; Wang et al., 2017; Boukhanouf et al., 2018; Jia et al., 2019; Pandelidis et al., 2020), adding internal structures to enhance heat and mass transfer (Kabeel and Abdelgaied, 2016; Kabeel et al., 2017; Moshari and Heidarinejad, 2017; Park et al., 2019; Ali et al., 2021), and exploring different materials (Zhao et al., 2008; Lee and Lee, 2013; Boukhanouf et al., 2017; Wang et al., 2017; Rashidi et al., 2019).

As Saudi Arabia is characterized by high ambient temperatures, IEC is highly applicable and has huge potential for energy saving. However, IEC is a passive cooler and the outlet temperature is highly dependent on the inlet temperature. When the outdoor temperature is extremely high, the supply air from IEC cannot achieve room thermal comfort. Another limitation of IEC is the lack of dehumidification capability, which restricts its application to dry areas (Chen et al., 2022).

To address the limitations of IEC, several researchers have proposed the hybridization of IEC with MVC. In the hybrid cycle, IEC is used to pre-cool the outdoor air, and then MVC further reduces the temperature and humidity (Chen et al., 2021). Such a hybrid process combines the advantages of the two, i.e. IEC's high efficiency in sensible cooling and MVC's capability of temperature and humidity control. Its energy-saving potential has been evaluated in several areas, including China (Beijing (Duan et al., 2019) and Xi'an (Cui et al., 2019a)), Iran (Delfani et al., 2010), Italy (Zanchini and Naldi, 2019), and Singapore (Vargas Bautista, 2014; Cui et al., 2015). The energy consumption was observed to be reduced by up to 35% (Cui et al., 2019a).

This study evaluates the potential of the hybrid IEC-MVC cycle in Saudi Arabia. The climatic and geographical conditions of the country are firstly analyzed. Then the daily performance of IEC-MVC on typical days in several cities is investigated on an hourly basis. Afterward, such efforts are extended to the major cities over the whole year to get the annual energy saving, IEC contribution, and water consumption. Finally, the annual cost of IEC-MVC is compared with standalone MVC to demonstrate the economic benefits.

2 Regional characteristics of Saudi Arabia

Saudi Arabia is the largest country in the MENA region. It has an estimated land area of 2.15 million square km, spanning 1700 km from north to south and 2000 km from east to west (Mikayilov et al., 2020). The country is divided into 13 provinces, as shown in Figure 1A. Based on the topography and climatic conditions, these provinces are divided into four regions by the Saudi Electricity Company (SEC), namely, the Western region, Eastern region, Central region, and Southern region (Saudi Electricity Company, 2015).

The Central region spans 19–29° north and includes three provinces: Al-Riyadh, Hail, and Al-Qaseem. In the past few decades, it has experienced fast urbanization and economic growth. Currently, it has 32% of the country's population (SAMA, 2019) and the third highest region GDP (GDP per capita = \$21,591 (Lopez-Ruiz et al., 2018)). Figure 2 shows the total floor areas of living houses in each province. Most houses in the central region are located in the Al-Riyadh province, which holds the capital city Riyadh. More than half of the houses are villas, while the share of apartments and traditional houses is small.

The Eastern region covers 19–32° north and consists of three provinces: Eastern Region, Al-Jouf, and Northern Borders. It has the largest land area and second population density (2018 people per km² (SAMA, 2019)). The East region is famous for its industrial activities, as it contains the country's most immense oil reserves. Most of the houses in the Eastern region are villas and apartments, and they are

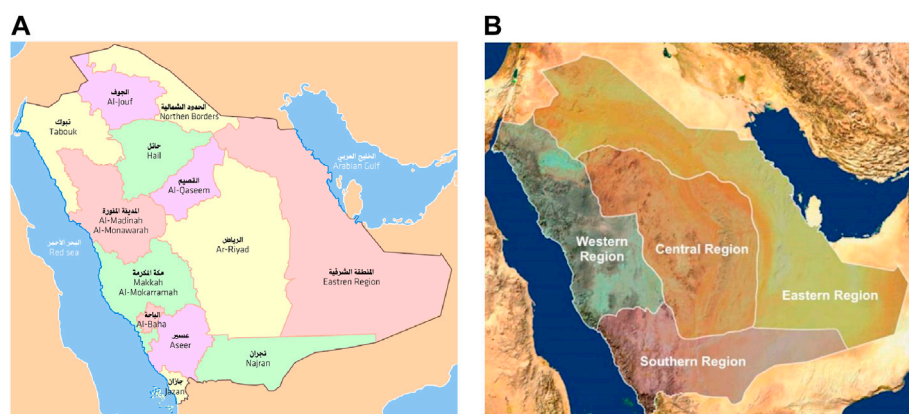


FIGURE 1

(A) Provinces (Provinces of Saudi Arabia, 2015) and (B) operating regions (Saudi Electricity Company, 2015) of Saudi Arabia.

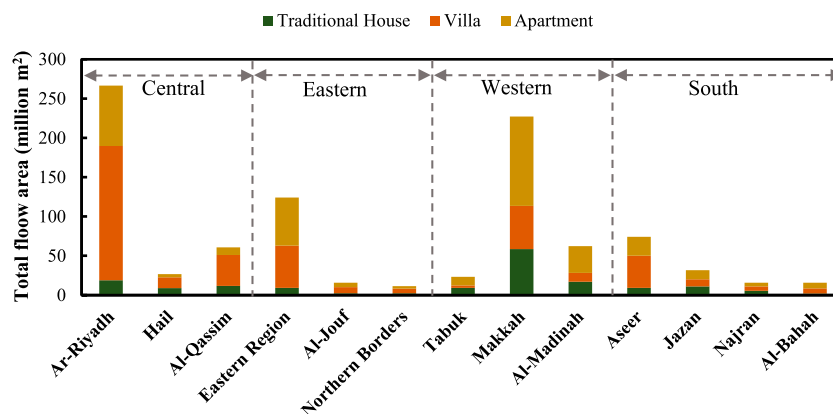


FIGURE 2

Total floor area per housing type in different provinces of Saudi Arabia.

mainly located near the Persian Gulf in the Eastern region province.

The Western region is located on the coast of the Red Sea (19–30° north), and it consists of three provinces: Tabouk, Makkah, and Al-Madinah. This region is home to many important cities, including Jeddah, Mecca, and Medina. The former is the commercial center of Saudi Arabia, and the latter two are the holiest sites for Muslims. The Western region houses 35% of the country's population and the population density is the highest (3423 people per km²) (SAMA, 2019). The total floor area in the Western region is as large as that of the Middle region, but nearly half of them are apartments. As apartments are better conditioned (52% of the livable floor area is cooled, as compared to 45% for villas

(Housing GStat, 2018b)), a higher share of apartments will lead to higher cooling energy consumption.

The South region spans 16–21° north and consists of Aseer, Jazan, Najran, and Al-Bahah. It has fertile land and adequate water reserves and is a place for agriculture and tourism. It houses only 15% of the country's population and the population density is 1871 people per km² (SAMA, 2019). The total house area is only 138 million m², much smaller than other provinces.

Due to its vast territory, Saudi Arabia has a variety of climatic conditions. Figure 3A shows the annual climatic data of Riyadh, the most important city in the Central region. The weather is hot and dry in the summer, as it is in the desert area and has no access to any natural water source. The maximum temperature exceeds 40 °C in the summer, while the RH is below 15%. The winter

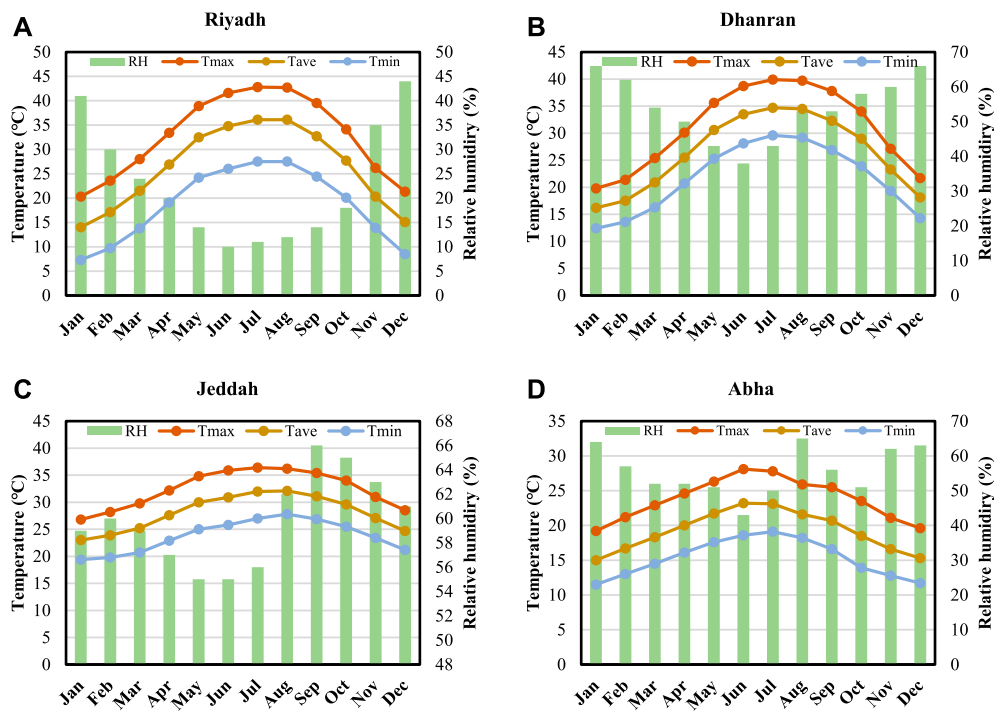


FIGURE 3

Annual weather data for representative cities of four regions: (A) Central region-Riyadh, (B) Eastern region-Dhanran, (C), Western region-Jeddah and (D) Southern region-Abha (Wunderground, 2022).

months, on the other hand, have a low ambient temperature due to the high altitude (~600 m). Therefore, in addition to cooling, there is also a need for heating.

Figure 3B shows the weather condition of Dharan, one of the biggest cities in the Eastern region. The ambient temperature varies in a similar way to that of Riyadh, i.e. hot in summer and cold in winter. However, the humidity in Dharan is higher (RH = 40%–65%), as it is close to the Persian Gulf. Therefore, it needs both cooling and dehumidification in the summer.

The Western region receives hot and humid air from the Red sea, and most cities in this region have high humidity and temperature. Figure 3C shows the monthly weather data of Jeddah, the largest city in the Western region. The ambient temperature is 20–35°C throughout the year, and the RH is always higher than 50%. The high temperature and humidity from the outdoor ambient will add substantial sensible and latent cooling loads to the buildings.

Most areas in the South region have a high altitude of >1000 m, making the ambient temperature lower than in other regions. As can be seen in Figure 3D, the ambient temperature in summer is lower than 30°C, and the need for cooling is minimum. The ambient humidity is also low, and there is little need for dehumidification.

The annual need for cooling is usually quantified by cooling degree-days (CDD). CDD is calculated by adding up the

difference between the daily-average temperature and a standard temperature (usually 18°C). One limitation of CDD is that it is calculated on a daily basis and does not account for the dynamical variation of the ambient condition. Even if the CDD is 0, there is still a need for cooling at the noon time. To overcome such a limitation, we propose to calculate the cooling needs based on the hourly data, i.e. cooling degree-hours (CDH) (Chen et al., 2022).

$$CDH = \sum (T_{hourly} - 18^{\circ}\text{C}) \text{ when } T_{hourly} > 18^{\circ}\text{C} \quad (1)$$

Both CDD and CDH consider only the sensible cooling load and neglects the latent load. To assess the latent load, we introduce the dehumidifying gram hours (DGH), which quantifies the amount of moisture that needs to be removed from the ambient air (Chen et al., 2022)

$$DGH = \sum \left(\omega_{hourly} - 9 \frac{\text{g}}{\text{kg}} \right) \text{ when } \omega_{hourly} > 9 \frac{\text{g}}{\text{kg}} \quad (2)$$

where ω_{hourly} is the humidity ratio of the ambient air.

Figure 4 summarizes the CDH and DGH for representative cities in different provinces of Saudi Arabia. It is obvious that the CDH values are very high in most cities. For example, the CDH for Riyadh is 92,248.4°C-hr/year. If averaged over the whole year (8760 h), the outdoor temperature has to be cooled

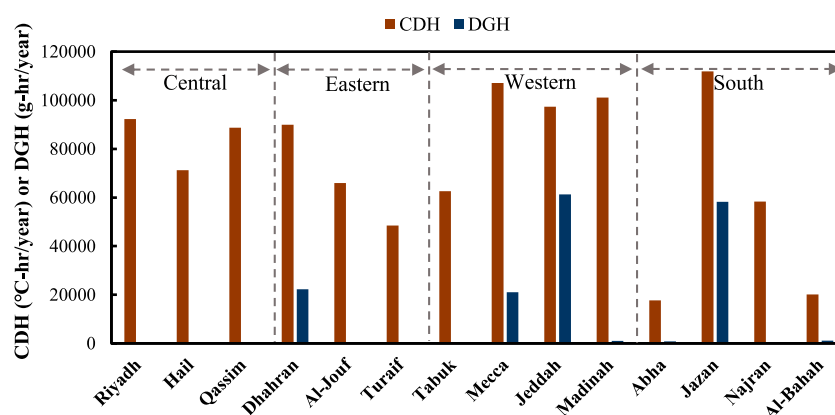


FIGURE 4
CDH and DGH for representative cities of Saudi Arabia.

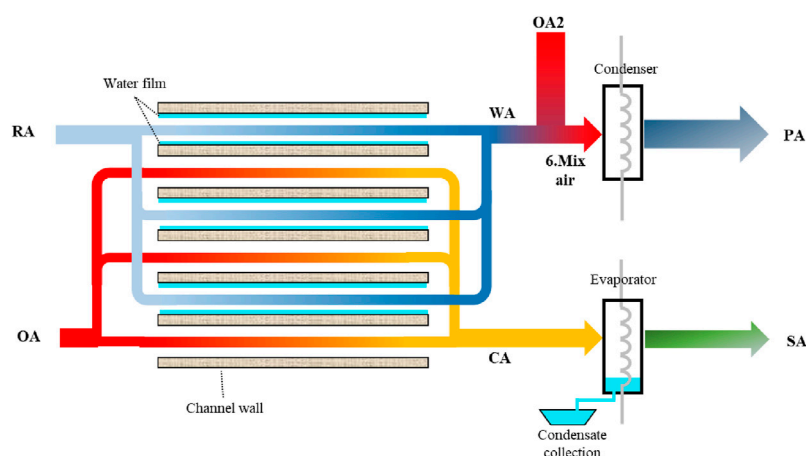


FIGURE 5
Annual weather data for representative cities of four regions.

by 10.4°C before being supplied to the room. Qassim, Dhahran, Mecca, Jeddah, Madinah, and Jazan also have CDH that are close to or higher than 9000°C-hr/year. The exception occurs in the Southern region, i.e. Abha (CDH = 175647.9°C-hr/year) and Al-Bahah (CDH = 20167.7°C-hr/year).

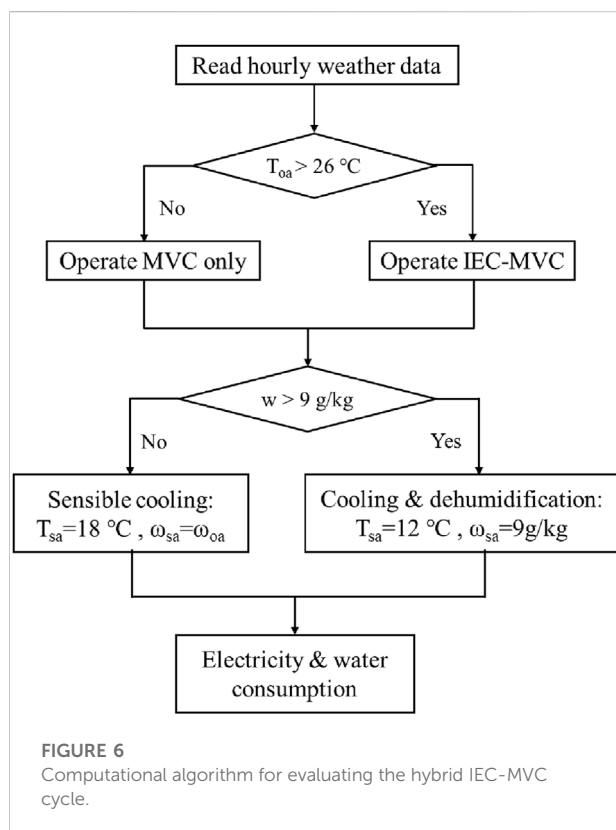
The DGH in most cities are below 1000 g-hr/year, indicating little need for dehumidification. However, there are several cities that are close to the sea (Red sea or Persian Gulf), and their DGH values are very high. These cities include Dhahran (DGH = 22,225 g-hr/kg), Jeddah (DGH = 61,307 g-hr/kg), Mecca (DGH = 22,225 g-hr/kg) and Jazan (DGH = 58,262 g-hr/kg).

3 Hybrid IEC-MVC

To improve the energy efficiency for cooling, we have proposed a novel cooling cycle combining indirect evaporative cooling (IEC) and mechanical vapor compression (MVC) (Chen et al., 2021; Chen et al., 2022). Figure 5 depicts the schematic of the hybrid IEC-MVC cycle. The IEC consists of alternating dry and wet channels. The outdoor air (OA), which is hot and sometimes humid, is supplied to the dry channels of the IEC, and the room return air (RA) passes through the wet channels. Simultaneously, water is sprayed into the wet channels from their entrances. As RA is unsaturated, the sprayed water evaporates and absorbs heat from the wet channels, which further cools OA

TABLE 1 Correlations for evaluating the IEC-MVC cycle.

Equation	No.	Comments
$\varepsilon_{IEC} = \min \left\{ \frac{h_{OA}-h_{CA}}{h_{OA}-h_{sat}(T_{RA})}, \frac{h_{WA}-h_{RA}}{h_{sat}(T_{OA})-h_{RA}} \right\}$ (3)		The effectiveness of IEC calculated from the inlet and outlet air conditions, including temperature, humidity and flowrate (Chen et al., 2021)
$\omega_{IEC} = \min \{ \omega_{OA}, \omega_s(h_{CA})_{RH=100\%} \}$ (4)		Air humidity leaving IEC
$T_{IEC} = T(h_{CA}, \omega_{IEC})$ (5)		Air temperature leaving IEC
$P_{IEC} = P_{pump} + P_{fan,IEC}$ (6)		Power consumption of IEC
$COP_{IEC} = \frac{\dot{m}_{OA}(h_{OA}-h_{CA})}{P_{IEC}}$ (7)		Energy efficiency of IEC
$P_{MVC} = P_{comp} + P_{fan,MVC}$ (8)		Power consumption of MVC
$COP_{MVC} = \frac{\dot{m}_{OA}(h_{OA}-h_{SA})}{P_{MVC,standalone}}$ (9)		Energy efficiency of MVC
$COP_{IEC-MVC} = \frac{\dot{m}_{OA}(h_{CA}-h_{SA})}{P_{IEC}+P_{MVC,hybrid}}$ (10)		Energy efficiency of hybrid IEC-MVC
$\phi_{IEC} = \frac{h_{OA}-h_{CA}}{h_{OA}-h_{SA}} \times 100\%$ (11)		Contribution of IEC to overall cooling load
$\Delta P = \frac{COP_{IEC-MVC}-COP_{MVC}}{COP_{IEC-MVC}}$ (12)		Energy-saving of IEC-MVC over MVC
$\dot{m}_{consumption} = \dot{m}_{RA}(\omega_{WA} - \omega_{RA})$ (13)		Water consumption in IEC wet channels
$\dot{m}_{collection} = \dot{m}_{OA}(\omega_{CA} - \omega_{SA})$ (14)		Condensation collection from MVC evaporator
$\dot{m}_{water} = \dot{m}_{consumption} - \dot{m}_{collection}$ (15)		Net water consumption



in the dry channels. The pre-cooled outdoor air (CA) then passes the evaporator of a conventional MVC cycle to be further processed to the desired condition before entering the room. The moisture contents formed in the evaporator are collected and reused as part of the water source for the wet channels. The air leaving the wet channels of IEC (WA) is also reused in the MVC: it is mixed with the outdoor air to function as the heat sink of the condenser.

A pilot IEC-MVC unit has been constructed and tested in our previous study (Chen et al., 2021; Chen et al., 2022). The tests cover a wide range of ambient conditions (temperature 30–45°C, humidity ratio 10–20 g/kg). Based on the test data, the performance of the system is correlated to the climatic data (temperature and humidity) and the operating conditions (air flowrate and desired supply air conditions), as summarized in Table 1. The model demonstrated high agreement with the experimental data, and the discrepancies are within 4%. The developed correlations can be used to predict the long-term performance of IEC-MVC.

Employing the developed correlations, the annual energy-saving potential of the hybrid IEC-MVC process is assessed. When the outdoor air temperature is below 26°C, IEC is bypassed as it has little energy-saving (Chen et al., 2021; Chen et al., 2022), and only MVC is operated. Otherwise, the outdoor air is pre-cooled in IEC before going to MVC. The outdoor air is finally processed to 18°C and <9 g/kg to sustain indoor thermal comfort (ANSI/ASHRAE Standard 55-2020, 2020). If the absolute humidity is below 9 g/kg, cooling the air to 18°C is sufficient. However, when the humidity is higher than that, outdoor air is cooled down to 12°C so that the moisture content can be reduced to 9 g/kg. The computational algorithm is depicted in Figure 6. Thermodynamic properties of the air are calculated based on the temperature and humidity using the equations developed by Herrmann, Kretzschmar, and Gatley (Herrmann et al., 2009).

4 Performance analysis

Employing the developed model, we evaluate the annual performance of the hybrid IEC-MVC system under the weather conditions of 14 cities in Saudi Arabia. Standalone MVC is also evaluated under the same conditions as a reference system. The analysis is performed on an hourly basis to get the energy efficiency, net water consumption, and IEC contribution. Without loss of generality, the outdoor air flowrate is assumed 1 kg/s, and the results can be extended to any air flowrate.

Figures 7A,B show the variation of air temperatures and humidity on a typical summer day (27 July 2021) in Riyadh. As described previously, Riyadh is hot and dry in the summer. The ambient temperature is 35–45°C, while the humidity ratio is below 7 g/kg. Therefore, the hybrid cooling process only needs to

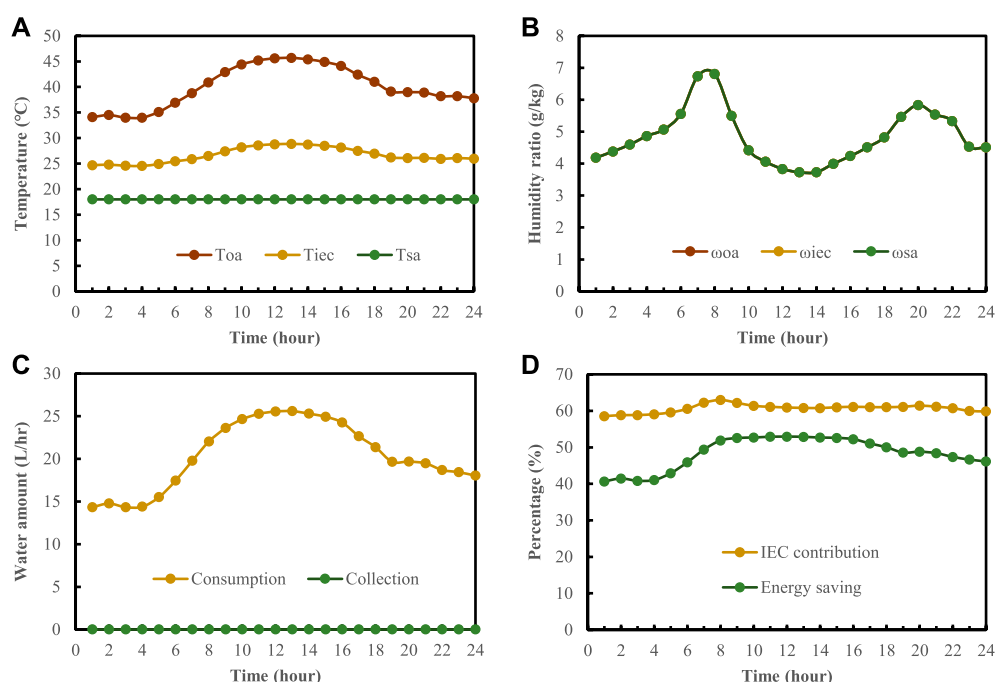


FIGURE 7

Daily performance of IEC-MVC in Riyadh on Jul-27 2021: (A) temperature change, (B) humidity change, (C) water collection and consumption, and (D) ϕ_{IEC} and energy saving.

reduce the air temperature, while the absolute humidity of the air remains the same. As IEC is a passive cooler (Chen et al., 2020; Chen et al., 2021), the air temperature leaving IEC follows the same trend as the outdoor air. The air temperature can be reduced by 9–17°C in IEC, and more temperature drop is observed during 10:00–16:00 when the ambient is hot. After pre-cooling in IEC, the air temperature is 24–29°C and is further cooled to 18°C by MVC.

Figure 7C shows the amount of water consumed by the IEC. Depending on the ambient temperature, the water consumption varies during the day and is in the range of 15–25 L/h. More water is consumed at noontime due to a higher cooling load. On the other hand, there is no water collection from the evaporator, as the outdoor air is dry. The contribution of IEC to the total cooling capacity is about 60% throughout the day, as plotted in Figure 7D. The corresponding energy saving over standalone MVC is 40%–53%, and more saving is observed at noontime. Similar observations were also reported by other studies (e.g., Cui et al. (Cui et al., 2019a)), as IEC has higher COP when the outdoor temperature is higher (Chen et al., 2020; Chen et al., 2021).

Figure 8 summarizes the performance of the system in Dharan, a hot and humid city in the Eastern region. The ambient temperature is similar to that of Riyadh, while the humidity is much higher. The absolute humidity during the daytime is 10–16 g/kg and exceeds 20 g/kg at night. Because

of the higher humidity, IEC demonstrates a different performance from the case of Riyadh, and the outlet air temperature of IEC does not follow the ambient anymore. As shown in Figure 8A, the IEC outlet temperature increases during 17:00–23:00, although the ambient temperature shows a descending trend. This is because the air temperature is lower than its dew point temperature, and condensation occurs. This can be clearly seen in Figure 8B, which shows a drop in air humidity along IEC during this period. The released condensation heat increases the air temperature. The MVC further cools down the air to a low temperature of 12°C, as opposed to 18°C in the previous case. This is to dehumidify the air to 9 g/kg.

The water consumption of IEC is in the range of 10–28 L/h, and the peak is observed at noon, as shown in Figure 8C. Such amount of water consumption can be replenished by the condensate collected from the MVC evaporator. The daily-average water consumption is 18.7 L/h, while condensate generation is 25.7 L/h due to very high humidity at night. The excessive water can be used elsewhere in the house. Figure 8D plots the contribution of IEC and the corresponding energy saving. IEC undertakes 20%–45% cooling load, much lower than the case of Riyadh. This is attributed to a latent load that is mostly handled by MVC. Due to a smaller IEC contribution, the energy saving is also less at 10%–35%.

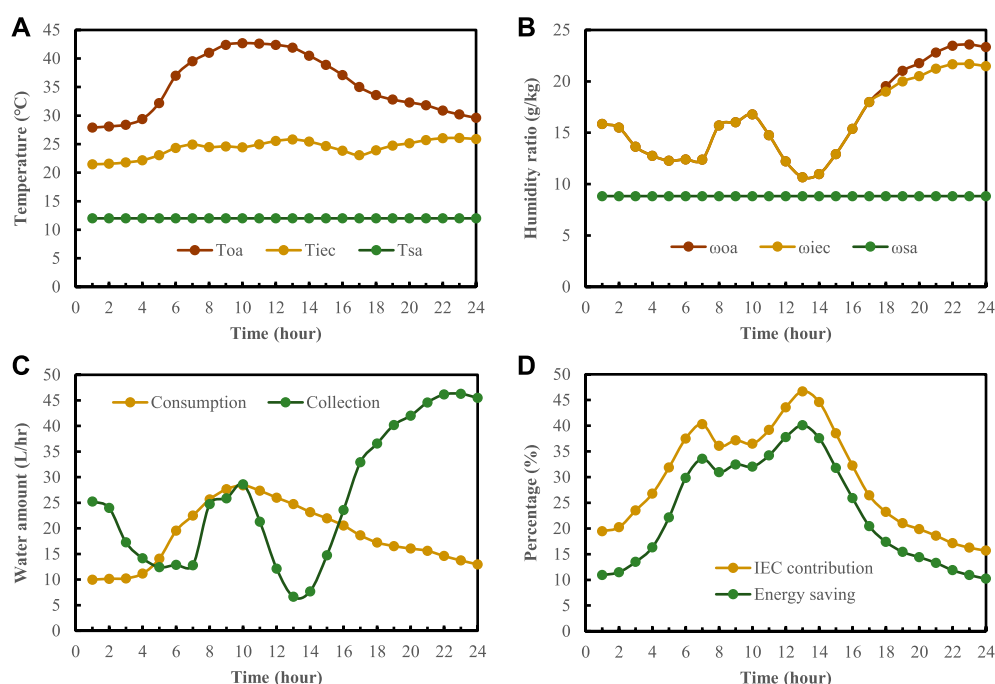


FIGURE 8

Daily performance of IEC-MVC in Dharan on Jul-15 2021: (A) temperature change, (B) humidity change, (C) water collection and consumption, and (D) ϕ_{IEC} and energy saving.

Figure 9 plots the system performance on a summer day (15 July 2021) in Jeddah. The weather condition differs from Riyadh and Dharan. Firstly, the ambient temperature is slightly lower, and the peak temperature is below 40°C. Secondly, the humidity ratio is high at 17–18 g/kg throughout the day. Due to these unique features, the outlet air temperature from IEC is relatively stable, as plotted in Figure 9A. This is because the low ambient temperature is compensated by the condensation heat released from the wet channels, which can be seen in Figure 9B. Another interesting observation is that the amount of water collection is always higher than water consumption (35.9 L/h vs. 15.5 L/h, shown in Figure 9D), and the amount of excessive water collection is significant. The contribution of IEC to the overall cooling load is lowered to 17%–30%, and the corresponding energy saving is 10%–25%.

The above analyses represent three situations for the application of IEC-MVC: 1) hot and dry weather, where IEC can handle a high portion of cooling load and the energy saving is significant, 2) hot with moderate humidity in the daytime but highly humid at night, where condensate can be collected at night to operate IEC in the daytime, and 3) high air humidity throughout the day, where there is excessive water collection for other uses.

Figure 10 summarizes the energy-saving potential of the hybrid IEC-MVC system over standalone MVC in different cities. The results are based on hour-by-hour simulations using long-term climatic data in each city. As most cities are hot and dry, IEC can meet more than 50% of the annual cooling demand and reduce energy consumption by 40%. The values are very close to the findings reported by Delfani et al. (Delfani et al., 2010), who evaluated IEC-MVC under weather conditions in Iran. For humid cities like Dhahran, Mecca, Jeddah, and Jazan, the latent load is higher and MVC has to contribute more. In this case, the contribution of IEC is smaller at 20%–30%, and the energy saving is less pronounced. Abha and Al-Bahah represent another case that has little cooling demand and little energy-saving potential.

As discussed above, a key challenge in humid areas is the need to overcool the air to remove moisture, and the contribution of IEC is small. To understand the effect of overcooling, the supply air temperature is changed between 11 and 15°C, and the system response is shown in Figure 11. For every °C increment of the supply air temperature, the contribution of IEC and the energy saving can be increased by 1%–2%. This is because a higher supply air temperature increases the evaporator temperature and reduces the thermal lift of the MVC compressor (Cui et al., 2019b).

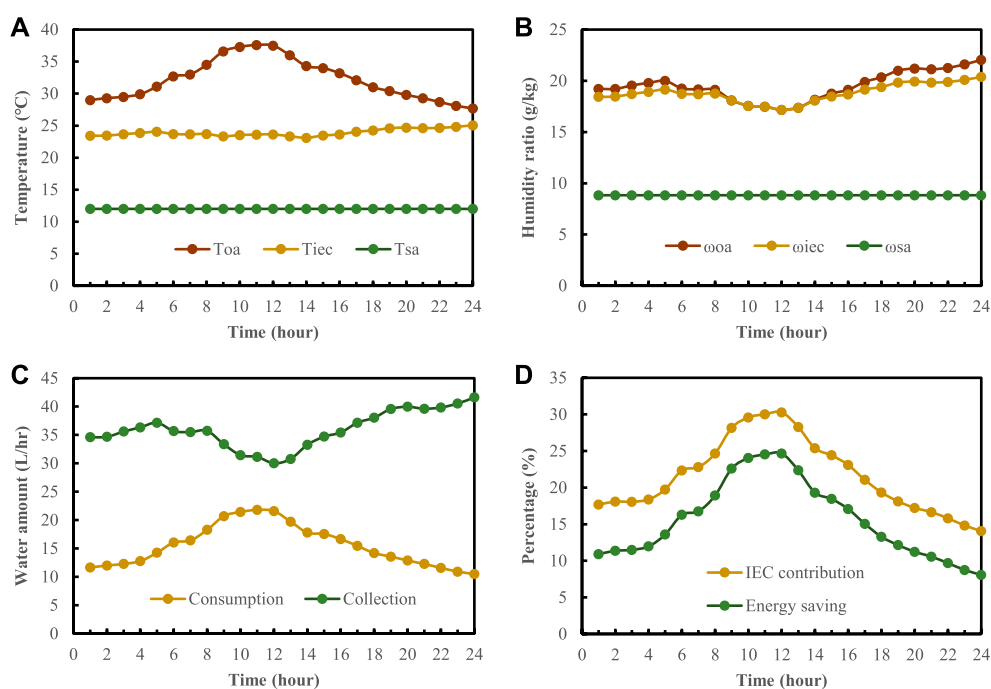


FIGURE 9

Daily performance of IEC-MVC in Jeddah on Jul-15 2021: (A) temperature change, (B) humidity change, (C) water collection and consumption, and (D) ϕ_{IEC} and energy saving.

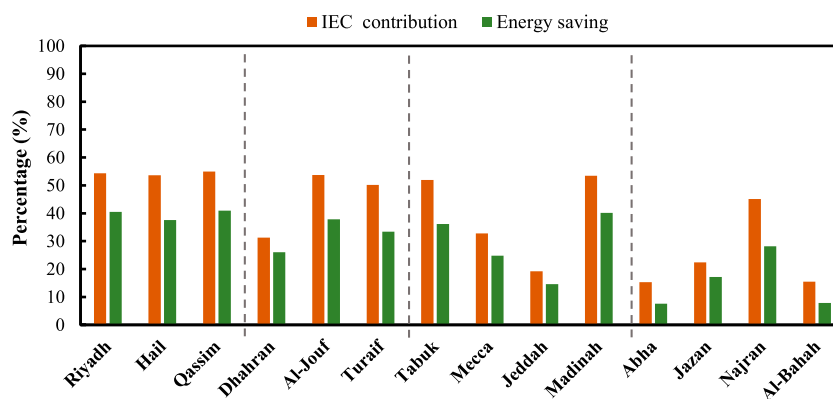


FIGURE 10

Annual energy saving and contribution of IEC in different cities.

Although the humidity ratio is also higher, the value is still below 10 g/kg until 14°C.

Figure 12 summarizes the annual water consumption of IEC and the amount of condensate collected from the MVC evaporator. For cities with certain cooling demands, the annual average water consumption is 4–12 L/h, depending on

the cooling load of IEC. More water is consumed in cities like Mecca, Jeddah, Madinah, and Jazan, where the CDH is very high, as previously shown in Figure 4. On the other hand, there is little water collection in most of the cities because of the dry ambient, and the water consumption for IEC has to be supplied by an external source. The exceptions are Dhahran, Mecca, Jeddah, and

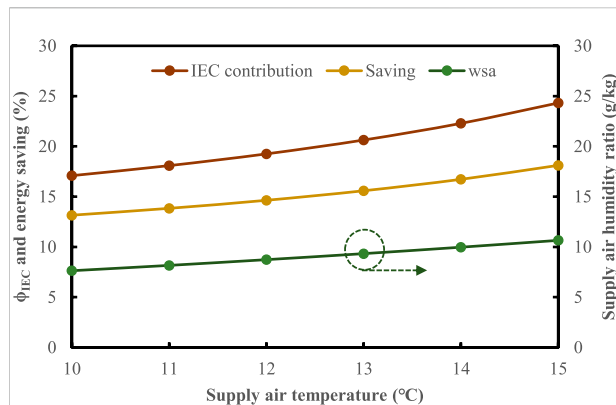


FIGURE 11

Variation of system performance in Jeddah under different set points for supply air temperature.

Jazan. In Dhahran and Mecca, the collected condensate can compensate for most of the water consumption. In the cases of Jeddah and Jazan, the amount of condensate is much higher than the water consumption, and there is excessive water to be used elsewhere.

5 Economic analysis

Based on the long-term performance, we evaluate the economic benefits of using the hybrid IEC-MVC process. Similar to the previous section, the evaluation is based on an outdoor flowrate of 1 kg/s. The annual cost is calculated as

TABLE 2 Economic parameters for IEC-MVC and standalone IEC.

Parameter	Value	Source
System lifespan (years)	20	Vargas Bautista, (2014)
Interest rate	2%	Saudi Arabia interest rate, (2022)
MVC initial cost (\$/Rton)	500	From manufacturer quotation
IEC initial cost (\$/CMH)	0.5	From manufacturer quotation
Electricity price (\$/kWh)	0.048	Electricity price in Saudi Arabia, (2022)
Water price (\$/m ³)	0.038	Saudi Arabia water price, (2022)

$$C_{\text{annual}} = C_0 \times CRF + P_{\text{elec}} \times c_{\text{elec}} + m_{\text{water}} \times c_{\text{water}} \quad (16)$$

where C_0 is the initial cost, CRF is the capital recovery factor, P_{elec} and m_{water} are the annual electricity and water consumption, respectively, and c_{elec} and c_{water} are the prices of electricity and water, respectively.

The capital recovery factor is calculated from the annual interest rate (i) and the lifespan (n)

$$CRF = \frac{i \times (1 + i)^n}{(1 + i)^n - 1} \quad (17)$$

Both systems are assumed to have a lifespan of 20 years, and the annual interest rate is 2%. The system capacities are determined by the peak load, which can be extracted from the calculations shown in the previous section. Water and electricity prices are \$0.048/kWh and \$0.04/m³, respectively. The economic parameters are summarized in Table 2.

Figure 13 summarizes the annual costs of both systems in different cities. It can be clearly seen that the costs are higher in Dhahran, Mecca, Jeddah, and Jazan, as they have very high demands for sensible cooling and dehumidification, leading to high system capacity. Other cities need only sensible cooling and the design loads are much lower. Compared

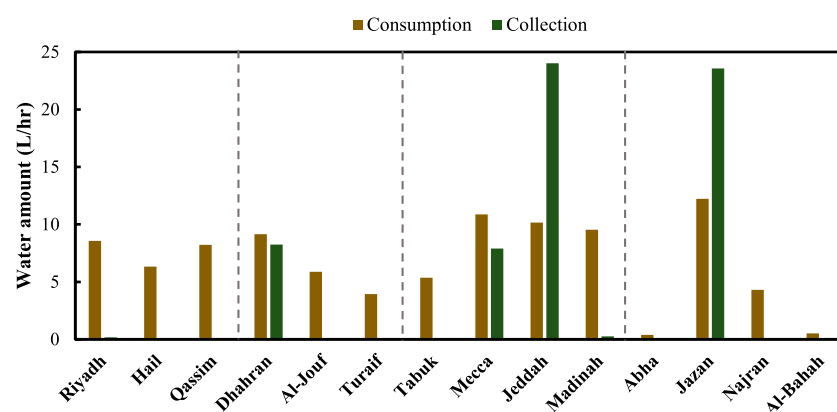


FIGURE 12

Annual water consumption and collection in different cities.

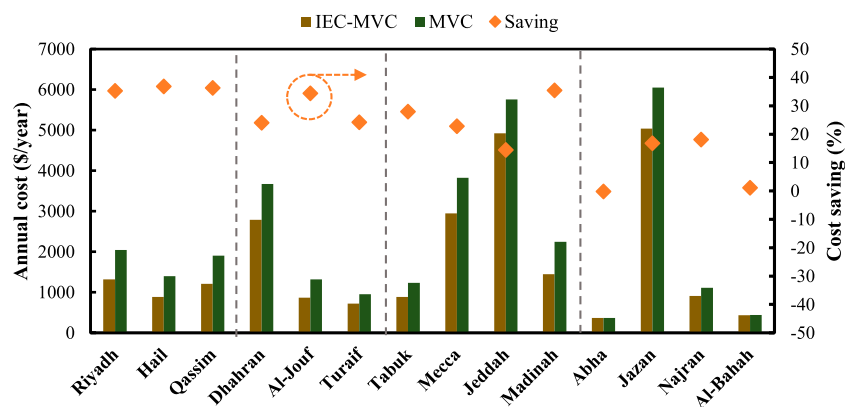


FIGURE 13

Comparison of annual cost between IEC-MVC and standalone MVC.

with standalone MVC, the hybrid IEC-MVC can reduce the annual cost by 15–35%. The cost saving is more significant in dry cities like Riyadh, Hail, Qassim, and Al-Jouf. This is because more cooling load is handled by IEC, which has lower initial costs and energy consumption.

6 Conclusion

This study evaluates the long-term performance of the hybrid IEC-MVC cycle in Saudi Arabia. The climatic and geographical conditions of different cities are firstly analyzed, followed by the daily performance profile of the system under representative cities. Afterward, the annual energy-saving potential of the hybrid system in different cities is summarized, and the economic benefits are quantified. The main takeaways from the study include:

- 1) Most of the residential houses are located in three provinces, i.e. Al-Riyadh, Eastern region, and Makkah. Al-Riyadh is characterized by hot and dry ambient in the summer, with annual CDH and DGH of 92248.4°C-hr/year and 0 g-hr/year, respectively. The other two provinces are hot and humid, and with DGH >20,000 g-hr/year;
- 2) In the summer days of Riyadh, the IEC can contribute nearly 60% of the total cooling load, reducing energy consumption by up to 50%. The savings are less significant in Dhahran and Jeddah due to a high humidity ratio, as MVC has to cool the air to a lower temperature to remove the moisture;
- 3) Over the whole year, IEC can handle >50% of cooling load in arid cities and the energy consumption is lowered by 40%. In humid cities, the contribution of IEC is reduced to 40%, and the energy saving over standalone MVC is 15–25%;
- 4) The energy consumption in humid cities can be further reduced by increasing the supply air temperature, and

every °C increment of the supply air temperature will lower the annual energy consumption by 1–2%;

- 5) The water consumption of the IEC is in the range of 4–12 L/h. In humid cities, such water consumption can be replenished by the condensate collected from the MVC evaporator, thus eliminating the need for an external water supply.
- 6) The hybrid system can reduce the annual cost by 15–35%, and the savings are more significant in arid cities.

Data availability statement

The raw data supporting the conclusion of this article will be made available by the authors, without undue reservation.

Author contributions

The contributions of the authors are summarized as follows: QC: Conceptualization, Methodology, Formal analysis, Writing—Original Draft; KM: Methodology, Software, Validation, Investigation; MB: Validation, Formal analysis; MS: Formal analysis; DY: Formal analysis; SO: Formal analysis; XC: Formal analysis; KN: Writing—Review Editing, Supervision, Project administration, Funding acquisition.

Funding

The authors gratefully acknowledge the generous funding from 1) the KAUST Cooling Initiative (KCI) project, REP/1/3988-01-01, and 2) the Water Desalination and Reuse Center (WDRC), King Abdullah University of Science and Technology (KAUST), and (3) Shenzhen

International Graduate School, Tsinghua University (07010100018).

Conflict of interest

The authors declare that the research was conducted in the absence of any commercial or financial relationships that could be construed as a potential conflict of interest.

References

- Ali, M., Ahmad, W., Sheikh, N. A., Ali, H., Kousar, R., and Rashid, T. u. (2021). Performance enhancement of a cross flow dew point indirect evaporative cooler with circular finned channel geometry. *J. Build. Eng.* 35, 101980. doi:10.1016/j.jobbe.2020.101980
- Anisimov, S., Pandelidis, D., and Danielewicz, J. (2014). Numerical analysis of selected evaporative exchangers with the Maisotsenko cycle. *Energy Convers. Manag.* 88, 426–441. doi:10.1016/j.enconman.2014.08.055
- ANSI/ASHRAE Standard 55-2020 (2020). Thermal environmental conditions for human occupancy. Available at: <https://www.ashrae.org/technical-resources/bookstore/standard-55-thermal-environmental-conditions-for-human-occupancy>.
- Boukhanouf, R., Alharbi, A., Ibrahim, H. G., Amer, O., and Worall, M. (2017). Computer modelling and experimental investigation of building integrated sub-wet bulb temperature evaporative cooling system. *Appl. Therm. Eng.* 115, 201–211. doi:10.1016/j.applthermaleng.2016.12.119
- Boukhanouf, R., Amer, O., Ibrahim, H., and Calautit, J. (2018). Design and performance analysis of a regenerative evaporative cooler for cooling of buildings in arid climates. *Build. Environ.* 142, 1–10. doi:10.1016/j.buildenv.2018.06.004
- Chen, Q., Burhan, M., Shahzad, M. W., Ybyraiymkul, D., Akhtar, F. H., and Ng, K. C. (2020). Simultaneous production of cooling and freshwater by an integrated indirect evaporative cooling and humidification-dehumidification desalination cycle. *Energy Convers. Manag.* 221, 113169. doi:10.1016/j.enconman.2020.113169
- Chen, Q., Ja, M. K., Burhan, M., Shahzad, M. W., Ybyraiymkul, D., Zheng, H., et al. (2022). Experimental study of a sustainable cooling process hybridizing indirect evaporative cooling and mechanical vapor compression. *Energy Rep.* 8, 7945–7956. doi:10.1016/j.egyr.2022.06.019
- Chen, Q., Kum Ja, M., Burhan, M., Akhtar, F. H., Shahzad, M. W., Ybyraiymkul, D., et al. (2021). A hybrid indirect evaporative cooling-mechanical vapor compression process for energy-efficient air conditioning. *Energy Convers. Manag.* 248, 114798. doi:10.1016/j.enconman.2021.114798
- Cui, X., Chua, K., Islam, M., and Ng, K. (2015). Performance evaluation of an indirect pre-cooling evaporative heat exchanger operating in hot and humid climate. *Energy Convers. Manag.* 102, 140–150. doi:10.1016/j.enconman.2015.02.025
- Cui, X., Chua, K., Islam, M., and Yang, W. (2014). Fundamental formulation of a modified LMTD method to study indirect evaporative heat exchangers. *Energy Convers. Manag.* 88, 372–381. doi:10.1016/j.enconman.2014.08.056
- Cui, X., Islam, M., and Chua, K. (2019). An experimental and analytical study of a hybrid air-conditioning system in buildings residing in tropics. *Energy Build.* 201, 216–226. doi:10.1016/j.enbuild.2019.06.028
- Cui, X., Islam, M., Mohan, B., and Chua, K. (2016). Developing a performance correlation for counter-flow regenerative indirect evaporative heat exchangers with experimental validation. *Appl. Therm. Eng.* 108, 774–784. doi:10.1016/j.applthermaleng.2016.07.189
- Cui, X., Sun, L., Zhang, S., and Jin, L. (2019). On the study of a hybrid indirect evaporative pre-cooling system for various climates. *Energies* 12 (23), 4419. doi:10.3390/en12234419
- Delfani, S., Esmaelian, J., Pasadshahri, H., and Karami, M. (2010). Energy saving potential of an indirect evaporative cooler as a pre-cooling unit for mechanical cooling systems in Iran. *Energy Build.* 42 (11), 2169–2176. doi:10.1016/j.enbuild.2010.07.009
- Dizaji, H. S., Hu, E. J., Chen, L., and Pourhedayat, S. (2020). Analytical/experimental sensitivity study of key design and operational parameters of perforated Maisotsenko cooler based on novel wet-surface theory. *Appl. Energy* 262, 114557. doi:10.1016/j.apenergy.2020.114557
- Duan, Z., Zhan, C., Zhang, X., Mustafa, M., Zhao, X., Alimohammadisagvand, B., et al. (2012). Indirect evaporative cooling: Past, present and future potentials. *Renew. Sustain. Energy Rev.* 16 (9), 6823–6850. doi:10.1016/j.rser.2012.07.007
- Duan, Z., Zhao, X., Liu, J., and Zhang, Q. (2019). Dynamic simulation of a hybrid dew point evaporative cooler and vapour compression refrigerated system for a building using EnergyPlus. *J. Build. Eng.* 21, 287–301. doi:10.1016/j.jobbe.2018.10.028
- Electricity price in Saudi Arabia (2022). Globalpetrolprices. Available at: https://www.globalpetrolprices.com/Saudi-Arabia/electricity_prices (Accessed on May 20, 2022).
- Eveloy, V., and Ayoud, D. S. (2019). Sustainable district cooling systems: Status, challenges, and future opportunities, with emphasis on cooling-dominated regions. *Energies* 12 (2), 235. doi:10.3390/en12020235
- Heidarinejad, G., and Moshari, S. (2015). Novel modeling of an indirect evaporative cooling system with cross-flow configuration. *Energy Build.* 92, 351–362. doi:10.1016/j.enbuild.2015.01.034
- Herrmann, S., Kretschmar, H.-J., and Gatley, D. P. (2009). Thermodynamic properties of real moist air, dry air, steam, water, and ice (RP-1485). *HVAC&R Res.* 15 (5), 961–986. doi:10.1080/10789669.2009.10390874
- Housing GStat (2018a). Survey data, general authority for statistics, Riyadh, kingdom of Saudi Arabia. Available at: <http://www.stats.gov.sa> (Accessed May 2nd, 2022).
- Housing GStat (2018b). Survey data, general authority for statistics, Riyadh, kingdom of Saudi Arabia. Available at: <http://www.stats.gov.sa> (Accessed April 30th, 2022).
- Jia, L., Liu, J., Wang, C., Cao, X., and Zhang, Z. (2019). Study of the thermal performance of a novel dew point evaporative cooler. *Appl. Therm. Eng.* 160, 114069. doi:10.1016/j.applthermaleng.2019.114069
- Jradi, M., and Riffat, S. (2014). Experimental and numerical investigation of a dew-point cooling system for thermal comfort in buildings. *Appl. Energy* 132, 524–535. doi:10.1016/j.apenergy.2014.07.040
- Kabeel, A., and Abdelgaied, M. (2016). Numerical and experimental investigation of a novel configuration of indirect evaporative cooler with internal baffles. *Energy Convers. Manag.* 126, 526–536. doi:10.1016/j.enconman.2016.08.028
- Kabeel, A., Bassuoni, M., and Abdelgaied, M. (2017). Experimental study of a novel integrated system of indirect evaporative cooler with internal baffles and evaporative condenser. *Energy Convers. Manag.* 138, 518–525. doi:10.1016/j.enconman.2017.02.025
- Krarti, M., Dubey, K., and Howarth, N. (2017). Evaluation of building energy efficiency investment options for the Kingdom of Saudi Arabia. *Energy* 134, 595–610. doi:10.1016/j.energy.2017.05.084
- Lee, J., and Lee, D.-Y. (2013). Experimental study of a counter flow regenerative evaporative cooler with finned channels. *Int. J. Heat Mass Transf.* 65, 173–179. doi:10.1016/j.ijheatmasstransfer.2013.05.069
- Lopez-Ruiz, H. G., Blazquez, J., and Hasanov, F. (2018). Estimating the Saudi arabian regional GDP using satellite nighttime light images. *SSRN Electron. J.* doi:10.2139/ssrn.3382748
- Mikayilov, J. I., Darandary, A., Alyamani, R., Hasanov, F. J., and Alatawi, H. (2020). Regional heterogeneous drivers of electricity demand in Saudi Arabia: Modeling regional residential electricity demand. *Energy Policy* 146, 111796. doi:10.1016/j.enpol.2020.111796
- Moshari, S., and Heidarinejad, G. (2017). Analytical estimation of pressure drop in indirect evaporative coolers for power reduction. *Energy Build.* 150, 149–162. doi:10.1016/j.enbuild.2017.05.080
- Pandelidis, D., Niemierka, E., Pacak, A., Jadwiszczak, P., Cichon, A., Drag, P., et al. (2020). Performance study of a novel dew point evaporative cooler in the

Publisher's note

All claims expressed in this article are solely those of the authors and do not necessarily represent those of their affiliated organizations, or those of the publisher, the editors and the reviewers. Any product that may be evaluated in this article, or claim that may be made by its manufacturer, is not guaranteed or endorsed by the publisher.

climate of central Europe using building simulation tools. *Build. Environ.* 181, 107101. doi:10.1016/j.buildenv.2020.107101

Park, J.-Y., Kim, B. J., Yoon, S. Y., Byon, Y. S., and Jeong, J. W. (2019). Experimental analysis of dehumidification performance of an evaporative cooling-assisted internally cooled liquid desiccant dehumidifier. *Appl. Energy* 235, 177–185. doi:10.1016/j.apenergy.2018.10.101

Provinces of Saudi Arabia (2015). Wikipedia subdivisions of Saudi Arabia. Available at: https://en.wikipedia.org/wiki/Subdivisions_of_Saudi_Arabia (Accessed April 25th, 2022).

Rashidi, S., Kashefi, M. H., Kim, K. C., and Samimi-Abianeh, O. (2019). Potentials of porous materials for energy management in heat exchangers—A comprehensive review. *Appl. Energy* 243, 206–232. doi:10.1016/j.apenergy.2019.03.200

Riffat, S., and Zhu, J. (2004). Mathematical model of indirect evaporative cooler using porous ceramic and heat pipe. *Appl. Therm. Eng.* 24 (4), 457–470. doi:10.1016/j.applthermaleng.2003.09.011

SAMA (2019). S.A.M.A., ANNUAL STATISTICS 2018. Available at: <http://www.sama.gov.sa/en-US/EconomicReports/Pages/YearlyStatistics.aspx> (Accessed April 24th, 2022).

Saudi Electricity Company. (2015) *Annual report*. Available at: <https://www.se.com.sa/en-us/Pages/AnnualReports.aspx> (Accessed April 24th, 2022).

Saudi Arabia interest rate (2022). Tradingeconomics. Available at: <https://tradingeconomics.com/saudi-arabia/interest-rate> (Accessed on May 20, 2022).

Saudi Arabia water price (2022). Globalproductprices. Available at: https://www.globalproductprices.com/Saudi-Arabia/mineral_water_prices/ (Accessed on May 20, 2022).

Shahzad, M. W., Burhan, M., Ybyraiymkul, D., Oh, S. J., and Ng, K. C. (2019). An improved indirect evaporative cooler experimental investigation. *Appl. Energy* 256, 113934. doi:10.1016/j.apenergy.2019.113934

Shahzad, M. W., Lin, J., Xu, B. B., Dala, L., Chen, Q., Burhan, M., et al. (2021). A spatiotemporal indirect evaporative cooler enabled by transiently interceding water mist. *Energy* 217, 119352. doi:10.1016/j.energy.2020.119352

Vargas Bautista, J. P. (2014). Heat recovery system in an industrial furnace to generate air conditioning through an absorption chiller. *I&E&D* 1 (14), 117–134. doi:10.23881/idebo.014.1-7i

Wang, F., Sun, T., Huang, X., Chen, Y., and Yang, H. (2017). Experimental research on a novel porous ceramic tube type indirect evaporative cooler. *Appl. Therm. Eng.* 125, 1191–1199. doi:10.1016/j.applthermaleng.2017.07.111

Wunderground (2022). Wunderground. Available at: <https://www.wunderground.com/history/daily/sa/jeddah/OEJN/date/2021-12-10> (Accessed Apr 24th, 2022).

Zanchini, E., and Naldi, C. (2019). Energy saving obtainable by applying a commercially available M-cycle evaporative cooling system to the air conditioning of an office building in North Italy. *Energy* 179, 975–988. doi:10.1016/j.energy.2019.05.065

Zhao, X., Liu, S., and Riffat, S. B. (2008). Comparative study of heat and mass exchanging materials for indirect evaporative cooling systems. *Build. Environ.* 43 (11), 1902–1911. doi:10.1016/j.buildenv.2007.11.009

Zhu, G., Chow, T.-T., and Lee, C. (2017). Performance analysis of counter-flow regenerative heat and mass exchanger for indirect evaporative cooling based on data-driven model. *Energy Build.* 155, 503–512. doi:10.1016/j.enbuild.2017.09.053

Nomenclature

Abbreviations

CDD Cooling degree days, °C-day/year

CDH Cooling degree hours, °C-hr/year

COP Coefficient of performance

DGH Dehumidifying gram hours, g-hr/year

IEC Indirect evaporative cooler

MVC Mechanical vapor compressor

RH Relative humidity, %

Symbols

h Enthalpy, kJ/kg

m Mass flowrate, kg/s

P Power, W

T Temperature, °C

Greek letters

ϵ Enthalpy effectiveness of IEC, %

ϕ Contribution of IEC to overall cooling load, %

ω Humidity ratio, g/kg

Subscripts

OA Outdoor air

CA Pre-cooled air from IEC

SA Supply air

RA Return air

WA Wet air

PA Purge air

sat Saturation

pump Water pump

fan Fan

comp Compressor



OPEN ACCESS

EDITED BY
Arianna Astolfi,
Politecnico di Torino, Italy

REVIEWED BY
Tapio Lokki,
Aalto University, Finland
Reza Soleimanpour,
Australian College of Kuwait, Kuwait
Jonathan Hargreaves,
University of Salford, United Kingdom

*CORRESPONDENCE
Takeshi Okuzono,
okuzono@port.kobe-u.ac.jp

SPECIALTY SECTION
This article was submitted to Indoor
Environment,
a section of the journal
Frontiers in Built Environment

RECEIVED 29 July 2022
ACCEPTED 22 November 2022
PUBLISHED 02 December 2022

CITATION
Okuzono T and Yoshida T (2022), High
potential of small-room acoustic
modeling with 3D time-domain finite
element method.
Front. Built Environ. 8:1006365.
doi: 10.3389/fbuil.2022.1006365

COPYRIGHT
© 2022 Okuzono and Yoshida. This is an
open-access article distributed under
the terms of the [Creative Commons
Attribution License \(CC BY\)](#). The use,
distribution or reproduction in other
forums is permitted, provided the
original author(s) and the copyright
owner(s) are credited and that the
original publication in this journal is
cited, in accordance with accepted
academic practice. No use, distribution
or reproduction is permitted which does
not comply with these terms.

High potential of small-room acoustic modeling with 3D time-domain finite element method

Takeshi Okuzono^{1*} and Takumi Yoshida^{1,2}

¹Environmental Acoustic Laboratory, Department of Architecture, Graduate School of Engineering, Kobe University, Kobe, Japan, ²Technical Research Institute, Hazama Ando Corporation, Tsukuba, Japan

Applicability of wave-based acoustics simulation methods in the time domain has increased markedly for performing room-acoustics simulation. They can incorporate sound absorber effects appropriately with a local-reaction frequency-dependent impedance boundary condition and an extended-reaction model. However, their accuracy, efficiency and practicality against a standard frequency-domain solver in 3D room acoustics simulation are still not known well. This paper describes a performance examination of a recently developed time-domain FEM (TD-FEM) for small-room acoustics simulation. This report first describes the significantly higher efficiency of TD-FEM against a frequency-domain FEM (FD-FEM) via acoustics simulation in a small cubic room and a small meeting room, including two porous-type sound absorbers and a resonant-type sound absorber. Those sound absorbers are modeled with local-reaction frequency-dependent impedance boundary conditions and an extended-reaction model. Then, the practicality of time-domain FEM is demonstrated further by simulating the room impulse response of the meeting room under various sound absorber configurations, including the frequency component up to 6 kHz. Results demonstrated the high potential and computational benefit of time-domain FEM as a 3D small room acoustics prediction tool.

KEYWORDS

frequency-domain finite element method, room acoustics simulation, small-room acoustics, acoustic design, time-domain finite element method, wave-based method

1 Introduction

Computational room-acoustics simulation methods (Vorländer, 2013; Sakuma et al., 2014) are crucially important technologies for designing comfortable indoor sound environments in architectural spaces such as concert halls and classrooms. Two acoustic simulation methods are available to compute room-impulse responses (RIR): wave-acoustics and geometrical-acoustics methods. The RIRs are essential quantities for room-acoustics evaluation and room-acoustics auralization, but the two simulation methods have their respective and opposite strengths and weaknesses. Wave-acoustics

methods are a rigorous simulation technology offering higher reliability for prediction accuracy because they solve wave equations or Helmholtz equations using numerical methods such as finite element method (FEM) and boundary element method (BEM). Wave-acoustics methods are adversely affected by their high computational loads for practical applications, but their applicable scale of space and frequency range is expanding dramatically with advances in computational technology. Conversely, geometrical-acoustics methods (Savioja and Svensson, 2015) such as ray tracing methods have high capability for practical room-acoustics design with low computational loads because they deal with sound wave propagation as ray propagation where wave effects such as diffraction are neglected. This simplification naturally reduces the prediction accuracy, but a continuous effort has been undertaken to increase their accuracy. This report presents a discussion of the applicability of a recently developed wave-acoustics method in time-domain to 3D room-acoustics simulation.

Room acoustics simulation using wave-acoustics methods has been performed respectively in both the frequency-domain and time-domain, solving the Helmholtz and wave equations. Both methods in a different domain also have unique strengths and weaknesses. FEM (Otsuru et al., 2000; Otsuru et al., 2001; Okamoto et al., 2007; Aretz and Vorländer, 2014; Okuzono and Sakagami, 2018; Murillo et al., 2019; Hoshi et al., 2020; Yatabe and Sugahara, 2022) and BEM (Yasuda et al., 2016; Yasuda et al., 2020; Gumerov and Duraiswami, 2021; Cardoso Soares et al., 2022) are standard selection as a numerical method in the former frequency-domain simulations. Frequency-domain (FD) methods have an inherent benefit for use in modeling sound absorbers (Cox and Peter, 2017) such as porous-type and resonant-type materials accurately: they can deal naturally with complex-valued frequency-dependent quantities such as specific acoustic admittance. This capability is an important advantage in computing accurate RIR, including sound absorber effects. However, FD methods need multi-frequency analyses that solve linear system equations at each pure tone analysis for RIR calculations. The solution is still quite time-consuming for large-scale room-acoustic problems at higher frequencies.

A wide variety of numerical methods are available for time-domain simulations: finite-difference time-domain (FDTD) (Sakamoto, 2007; Kowalczyk and van Walstijn, 2008; Sakamoto et al., 2008; Kowalczyk and van Walstijn, 2011; Hamilton and Bilbao, 2017; Toyoda and Eto, 2019; Cingolani et al., 2021; Toyoda and Sakayoshi, 2021) or finite-volume time-domain (FVTD) methods (Bilbao, 2013; Bilbao et al., 2016), time-domain BEM (TD-BEM) (Hargreaves and Cox, 2008), time-domain FEM (TD-FEM) (Okuzono et al., 2019; Yoshida et al., 2022), time-domain discontinuous Galerkin FEM (DG-FEM) (Simonaho et al., 2012; Wang et al., 2019; Wang and Hornikx, 2020; Pind et al., 2021), time-domain spectral element

method (TD-SEM) (Pind et al., 2019), pseudospectral time-domain (PSTD) method (Hornikx et al., 2015; Hornikx et al., 2016), and adaptive rectangular decomposition (ARD) method (Mehra et al., 2012; Morales et al., 2015; Rabisse et al., 2019). They respectively offer several benefits in terms of ease of coding and applicability of complex geometries and so on according to fundamental algorithms of numerical methods. Time-domain (TD) methods are particularly useful for computing RIR because they can obtain time responses that include a broad frequency range with a single computational run. Moreover, they can be designed as a faster explicit solver, although more stable and accurate implicit methods are available. An inherent shortcoming of TD methods is their difficulty in addressing frequency-dependent quantities. To address this inefficiency, accurate sound absorber modeling in the time domain is an active research topic which, if resolved, can increase the methods' applicability to room-acoustics simulation. Consequently, some TD methods which can deal accurately with effects of sound absorbers have been developed by incorporating local-reaction frequency-dependent impedance boundary conditions (Sakamoto et al., 2008; Bilbao, 2013; Pind et al., 2019; Rabisse et al., 2019; Wang and Hornikx, 2020; Okuzono et al., 2021). Extended-reaction models, which are naturally available in FD methods, have also been presented to deal further with the sound incidence-angle dependence effect for some porous sound materials (Okuzono et al., 2019; Zhao et al., 2019; Pind et al., 2020; Yoshida et al., 2020). Therefore, current TD methods are becoming attractive simulation technologies for room acoustics simulation.

Nevertheless, the applicability of current TD methods to 3D room-acoustics simulation considering realistic sound absorbers configurations has not been discussed well. More specifically, the accuracy, efficiency, and utility of recent TD methods against FD methods remain unclear. To elucidate several aspects of these methods, this study specifically examines a recently developed TD-FEM (Okuzono et al., 2019; Okuzono et al., 2021) for 3D room-acoustics simulation among earlier described TD methods and discusses the question with some case studies of small room-acoustics scenarios. Because TD-FEM is generally regarded as computationally expensive compared to the most used FDTD method, a case study will demonstrate a practical room acoustic simulation scenario with various sound absorber configurations at a broad frequency range beyond 4 kHz, where human auditory sensitivity has its peak.

The purpose of this study is to discuss the potential of the recently-developed TD-FEM on 3D room-acoustics simulation. To this end, this paper examines the efficiency and accuracy of TD-FEM by the performance comparison with a 3D frequency-domain FEM (FD-FEM) that uses the same finite elements for spatial discretization. The examination is performed *via* room acoustic simulations in a small cubic room and a small meeting room. The practicality of TD-FEM is evaluated through a case study of room acoustics simulation in a small meeting room up to

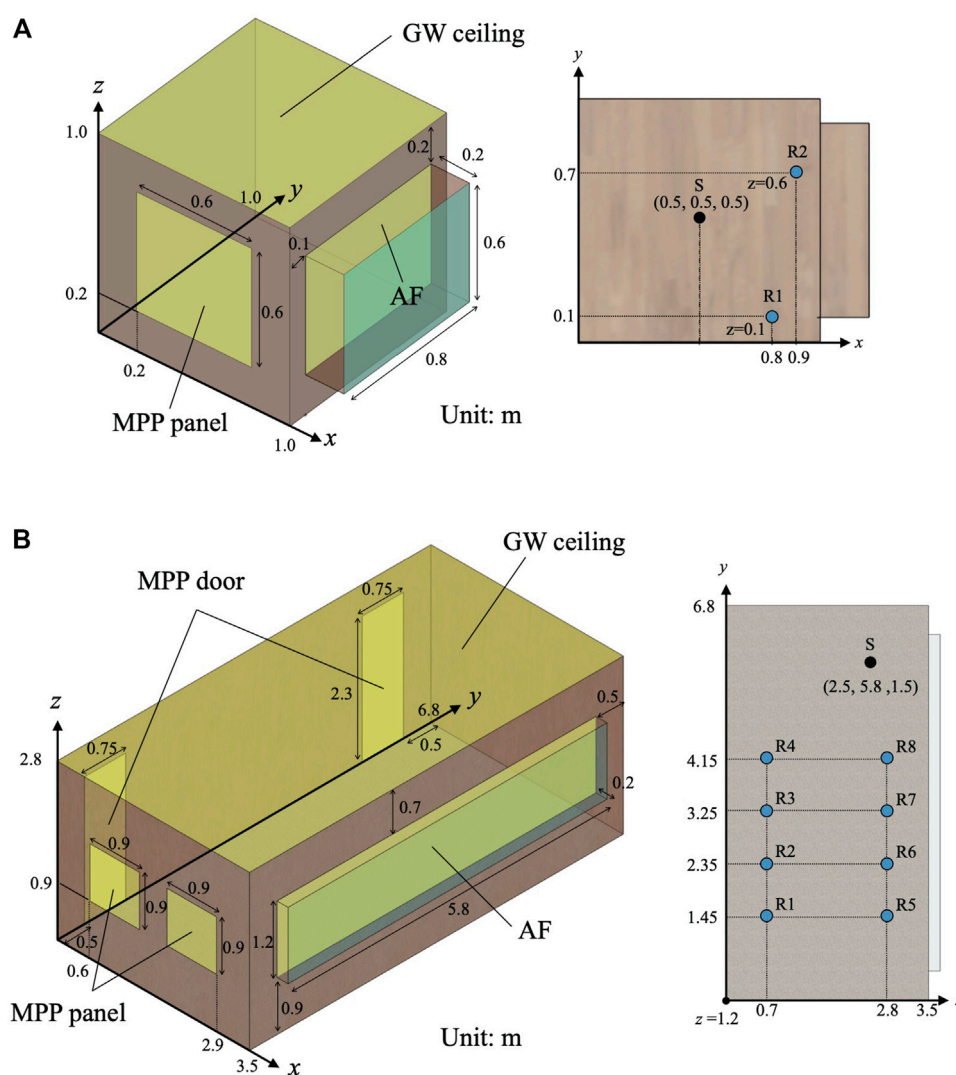


FIGURE 1

Room models: (A) Small room of 1.01 m³ with a source S and two receivers R1 and R2; and (B) Meeting room of 68 m³ with a source S and eight receivers R1–R8. Both rooms include GW absorber on ceiling, MPP absorber on walls, and AF absorber in front of a window. The Meeting room further includes MPP absorbers as doors.

6 kHz under realistic sound absorber configurations. The present paper deals with three sound absorbers: a local-reaction glass wool (GW) and extended-reaction acoustic fabric curtains (AF) as porous sound absorbers and a local-reaction microperforated panel (MPP) absorber as resonant-type sound absorbers. This study is an extension of our earlier work (Okuzono et al., 2021) on 2D room-acoustics simulation. In the previous study, we examined the performance of TD-FEM against FD-FEM *via* acoustics simulations of a 2D office and a concert hall with GW absorbers modeled by the frequency-dependent impedance boundary conditions. The result revealed that TD-FEM has higher efficiency with about 18 times faster computational speed than FD-FEM on 2D room-acoustics simulation.

However, whether or not 2D simulation results hold to 3D simulations is unclear. Therefore, it is extremely important to show evidence of the higher efficiency of TD-FEM on 3D room-acoustics simulation. The present study also includes an accuracy examination of room-acoustics parameters from a practical aspect, which are not tested in the previous study. As the salient point of novelty of the present work, we reveal that 3D TD-FEM engenders a substantial performance gain on room-acoustics simulation compared to 3D FD-FEM-based prediction and its practicality as a prediction tool for designing the acoustics of small rooms. Notably, the performance gain is one magnitude greater than that in 2D simulations. To the best of the authors' knowledge, the present paper is the first to reveal the high

potential of TD-FEM against FD-FEM in 3D room-acoustics simulations with realistic sound absorber modeling that uses a complex-valued specific acoustic admittance and an extended-reaction model. Since TD-FEM can be extended from a standard FD-FEM code, the presented results give FD-FEM users an alternative way to perform room-acoustics simulation more efficiently.

2 Room acoustic simulation using FEM

This report presents a dispersion-reduced TD-FEM and FD-FEM with a frequency-dependent local-reaction boundary condition and an extended-reaction model for permeable membrane absorbers such as AF (Okuzono and Sakagami, 2015; Okuzono and Sakagami, 2018; Okuzono et al., 2019; Okuzono et al., 2021). The spatial domain is discretized with dispersion-reduced eight-node hexahedral finite elements (Hex8), which uses Gauss–Legendre rules with modified integration points (Guddati and Yue, 2004; Yue and Guddati, 2005) to reduce spatial discretization error. As a notable feature, the dispersion-reduced FEMs can provide a more accurate solution than FEMs using conventional Hex8 for a coarser mesh (Okuzono and Sakagami, 2018; Okuzono et al., 2019). [Supplementary Section S1](#) explains this aspect from theoretical discretization error evaluation as a fundamental. For the convenience of the reader, we briefly describe the basic equations of TD-FEM and FD-FEM used here. The sound absorber model used for the frequency-dependent local-reaction boundary condition is also given. Detailed formulations of the dispersion-reduced TD-FEM and FD-FEM are available in the literature (Okuzono and Sakagami, 2015; Okuzono and Sakagami, 2018; Okuzono et al., 2019; Okuzono et al., 2021).

2.1 Time-domain FEM

Time-domain room acoustics simulation solves the following inhomogeneous acoustic wave equation to simulate sound propagation in a 3D enclosed space Ω as

$$\nabla^2 p(\mathbf{r}, t) - \frac{1}{c^2} \ddot{p}(\mathbf{r}, t) = -\rho \dot{q}(t) \delta(\mathbf{r} - \mathbf{r}_a) \text{ in } \Omega, \quad (1)$$

where p stands for the sound pressure at the position vector $\mathbf{r} = (x, y, z)$ in Cartesian coordinate system at time t , c denotes the speed of sound in air, ρ expresses the air density. The symbol ∇^2 is the Laplacian; $\ddot{(\cdot)}$ and $\dot{(\cdot)}$ respectively represent the second-order and the first-order derivatives with respect to t , i.e., $\ddot{(\cdot)} = \frac{\partial^2}{\partial t^2}$ and $\dot{(\cdot)} = \frac{\partial}{\partial t}$. The delta function is denoted by δ . A monopole sound source having volume source strength density q is placed at the position $\mathbf{r}_a = (x_a, y_a, z_a)$.

As described earlier, the present paper presents consideration of three sound absorbers. The GW and MPP absorbers are modeled by the local-reaction (LR) frequency-dependent absorbing boundary condition (BC), which is defined on the sound absorbing surface Γ_a as

$$\frac{\partial p(\mathbf{r}, t)}{\partial n} = -\frac{1}{c} \int_{-\infty}^t \tilde{y}(\mathbf{r}, t - \tau) \dot{p}(\mathbf{r}, \tau) d\tau \text{ on } \Gamma_a, \quad (2)$$

where \tilde{y} denotes the specific acoustic admittance ratio in the time domain, which is the inverse Fourier transformed value of frequency domain specific acoustic admittance ratio of $\hat{y}(\omega)$ denoting the angular frequency as ω . The auxiliary differential equation (ADE) method (Dragna et al., 2015; Troian et al., 2017) is used to implement the BC of Eq. 2. Here, LR models only frequency-dependence of sound absorbers at a specific sound incidence angle. However, AF models, as an extended-reaction (ER) BC, can account for both frequency-dependence and sound incidence angle dependence of sound absorbers. The interior BC presented hereinafter is imposed on both sides of AF as (Okuzono et al., 2019)

$$\frac{\partial p(\mathbf{r}, t)}{\partial n} = \begin{cases} -\rho \dot{v}_f(\mathbf{r}, t) & \text{on } \Gamma_{AF,1} \\ \rho \dot{v}_f(\mathbf{r}, t) & \text{on } \Gamma_{AF,2}, \end{cases} \quad (3)$$

where $\Gamma_{AF,1}$ and $\Gamma_{AF,2}$ respectively represent boundaries in both sides of curtain, and where v_f represents the particle velocity on and inside the AF, which is defined as

$$\dot{v}_f(\mathbf{r}, t) = \frac{1}{\sigma t_{AF}} \Delta \dot{p}(\mathbf{r}, t) + \frac{1}{M_{AF}} \Delta p(\mathbf{r}, t), \quad (4)$$

where σ , t_{AF} , and M_{AF} respectively represent the flow resistivity, and the thickness and the surface density of AF, and Δp is the sound pressure difference between both sides of AF.

By applying finite element discretization to the weak form of Eq. 1 with those 2 BCs, we obtain the following semi-discretized matrix equation as

$$\begin{aligned} & M\ddot{\mathbf{p}} + c^2 \mathbf{K}\mathbf{p} + c y_{\infty} \mathbf{C}' \dot{\mathbf{p}} + \frac{\rho}{m} \mathbf{S}\mathbf{p} + \frac{\rho c^2}{\sigma t_{AF}} \mathbf{S} \dot{\mathbf{p}} \\ & = \mathbf{f} - c \mathbf{C}' \left[\sum_{i=1}^{N_p} A_i \phi_i + 2 \sum_{i=1}^{N_{cp}} \left(B_i \psi_i^{(1)} + C_i \psi_i^{(2)} \right) \right], \end{aligned} \quad (5)$$

where three matrices \mathbf{M} , \mathbf{K} , and \mathbf{C}' respectively stand for the global mass matrix, the global stiffness matrix, and the global dissipation matrix without the admittance term. A matrix \mathbf{S} denotes the global matrix related to AF. Two vectors \mathbf{p} and \mathbf{f} represent the sound pressure vector and the external force vector. Parameters y_{∞} , A_i , B_i , and C_i are the real-valued coefficients for the following rational function approximation of $\hat{y}(\omega)$ as

$$\hat{y}(\omega) \approx y_{\infty} + \sum_{i=1}^{N_p} \frac{A_i}{\lambda_i + j\omega} + \sum_{i=1}^{N_{cp}} \left(\frac{B_i \pm jC_i}{\alpha_i \pm j\beta_i + j\omega} \right), \quad (6)$$

with N_p real poles λ_i and N_{cp} complex conjugate poles $\alpha_i \pm j\beta_i$. The vectors ϕ_i , $\psi_i^{(1)}$, and $\psi_i^{(2)}$ in the right-hand side of Eq. 5

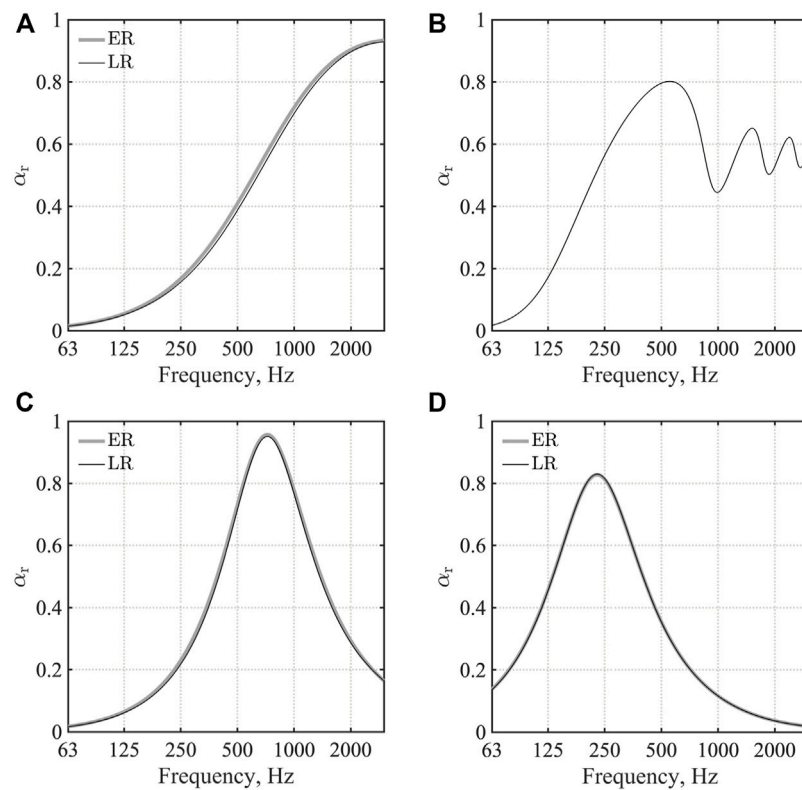


FIGURE 2

Random incidence sound absorption coefficient: (A) GW ceiling; (B) AF; (C) MPPGW panel; and (D) MPPGW door. ER and LR respectively denote extended reaction model and local reaction model.

call accumulators, which are computed solving the simultaneous first-order ordinary differential equations (ODEs) as below.

$$\dot{\phi}_i + \lambda_i \phi_i = \dot{p}, \quad (7)$$

$$\dot{\psi}_i^{(1)} + \alpha_i \psi_i^{(1)} + \beta_i \psi_i^{(2)} = \dot{p}, \quad (8)$$

$$\dot{\psi}_i^{(2)} + \alpha_i \psi_i^{(2)} - \beta_i \psi_i^{(1)} = 0. \quad (9)$$

We use Crank–Nicolson method with a high stability as the ODE solver. The sound pressure is computed by solving the second-order ODE of Eq. 5. We use the high-accuracy Fox–Goodwin method (Hughes, 2000) for the solution of Eq. 5. The present TD-FEM formulation has an implicit algorithm. Therefore, the linear system of equations at each time step is solved using a Krylov subspace iterative method called Conjugate Gradient (CG) method (Barrett et al., 1994) with diagonal scaling preconditioning. The convergence tolerance, which determines the resulting accuracy on solutions, is set as 10^{-4} . The rational function models of GW and MPP absorbers are constructed using normal-incidence specific acoustic admittance ratio calculated using the transfer matrix method. As for numerical operations of

TD-FEM, all computations are performed with real-valued operations, i.e., all matrices and vectors have real-valued components. An efficient sparse matrix storage format, namely the compressed row storage format, is used for storing matrices, which requires the largest memory consumption in FEM. The most time-consuming operation in TD-FEM is real-valued sparse matrix-vector products, which mainly appear in the linear system solution process by CG method at each time step. CG method has one sparse matrix-vector product per iteration. Therefore, the fast convergence of iterative solvers with small iteration numbers is an essential factor in achieving higher computational performance. Also, the iteration number required for convergence becomes a good quantity for the performance evaluation of the present TD-FEM.

2.2 Frequency-domain FEM

Frequency-domain room acoustics simulation solves the following inhomogeneous Helmholtz equation to simulate complex-valued sound pressure \hat{p} in 3D enclosed space Ω as

TABLE 1 Parameters y_{∞} , A_i , B_i , C_i , λ_i , α_i , and β_i for MPPGW panel. The parameters were fitted at 10 Hz–10 kHz.

y_{∞}	0.024				
i	1	2	3	4	5
A_i	-2.93	10.85	-41.89	362.19	-11310.93
B_i	944.86	32.65			
C_i	355.75	-13.59			
λ_i	1225.74	4410.71	12663.86	20634.68	441062.01
α_i	1435.26	15302.04			
β_i	-4247.19	-23308.79			

$$(\nabla^2 + k^2)\hat{p}(\mathbf{r}, \omega) = -j\omega\rho\hat{q}(\omega)\delta(\mathbf{r} - \mathbf{r}_a) \text{ in } \Omega, \quad (10)$$

where k represents the wavenumber in air and the symbol $\hat{(\cdot)}$ represents variables in frequency domain. Similarly to time-domain formulation, GW and MPP absorbers can be modeled by LR BC as

$$\frac{\partial \hat{p}(\mathbf{r}, \omega)}{\partial n} = -jk\hat{y}(\mathbf{r}, \omega)\hat{p}(\mathbf{r}, \omega) \text{ on } \Gamma_a. \quad (11)$$

In FD-FEM, we also use the normal-incidence specific acoustic admittance ratio calculated using the transfer matrix method to GW and MPP absorbers.

The following interior boundary condition is also used to model AF as

$$\frac{\partial \hat{p}(\mathbf{r}, \omega)}{\partial n} = \begin{cases} -j\omega\rho\hat{y}_{AF}(\mathbf{r}, \omega)\Delta\hat{p}(\mathbf{r}, \omega) & \text{on } \Gamma_{AF,1} \\ j\omega\rho\hat{y}_{AF}(\mathbf{r}, \omega)\Delta\hat{p}(\mathbf{r}, \omega) & \text{on } \Gamma_{AF,2}, \end{cases} \quad (12)$$

with the transfer admittance \hat{y}_{AF} of AF as

$$\hat{y}_{AF} = \frac{1}{\sigma t_{AF}} + \frac{1}{j\omega M_{AF}}. \quad (13)$$

Applying finite element discretization to the weak form of Eq. 10 produces the following linear system of equations as (Okuzono and Sakagami, 2015)

$$[\mathbf{K} - k^2\mathbf{M} + jk\hat{\mathbf{C}} + \rho\hat{\mathbf{L}}]\hat{\mathbf{p}} = \hat{\mathbf{f}}, \quad (14)$$

where $\hat{\mathbf{C}}$ and $\hat{\mathbf{L}}$ respectively denote the global dissipation matrix and the global matrix related to AF. Both matrices are complex-valued. The sound pressure is computed by solving the linear system of equations at each frequency. We use two linear system solvers called PARDISO (Included in Intel Math Kernel Library) and CSQMOR method (Zhang and Dai, 2015) with diagonal scaling preconditioning. The convergence tolerance of the CSQMOR method is set as 10^{-4} . The former PARDISO is a sparse direct solver, which is robust with higher memory consumption than iterative solvers. The latter CSQMOR is a recently-developed Krylov subspace iterative solver. An iterative solver can expect faster computation time with less memory

consumption than direct solvers when its convergence is rapid. We selected the two solvers because whether direct or iterative solvers are more efficient in FD-FEM is problem-dependent. We show a performance comparison of them in the next section. As for numerical operations of FD-FEM, complex-valued computations are necessary for the most time-consuming process of linear system solution at each frequency. The compressed row storage format is also used for the coefficient matrix of Eq. 14, but complex-valued components are stored, which is different from TD-FEM. The most time-consuming operation in FD-FEM with an iterative solver is complex-valued sparse matrix-vector products, which appear in the linear system solution process by CSQMOR method at each frequency. CSQMOR method has one sparse matrix-vector product per iteration as in CG method. Therefore, the iteration number required for convergence is also an essential measure for the performance evaluation of the present FD-FEM. However, it is crucial to remember that a complex-valued sparse matrix-vector product is more expensive than a real-valued sparse matrix-vector product.

2.3 Sound absorber modeling with transfer matrix method

When using LR BCs, the complex-valued specific acoustic admittance ratio of the sound absorber must be known. Both theoretical and measurement-based approaches are available to obtain the specific acoustic admittance ratio of materials. Measurement-based approaches include an impedance tube measurement (ISO 10534-2, 1998) and *in-situ* measurements (Brandão et al., 2015; Sakamoto et al., 2018; Sugahara et al., 2019). The transfer matrix method is a general way to theoretically compute the sound absorption characteristics of materials, and well-developed models are available for GW and MPP absorbers. This report presents computation of the specific acoustic admittance ratio by the transfer matrix method (Allard and Atalla, 2009) to model GW and MPP absorbers as frequency-dependent LR BCs. Here, the MPP absorber is a single-leaf MPP backed by a GW. We designate this absorber as MPPGW. For plane wave incidence at the angle θ , the transfer matrix T^p of the porous material is

$$T^p = \begin{bmatrix} T_{11}^p & T_{12}^p \\ T_{21}^p & T_{22}^p \end{bmatrix} = \begin{bmatrix} \cos(k_n L) & j\frac{\omega\rho_e}{k_n}\sin(k_n L) \\ j\frac{k_n}{\omega\rho_e}\sin(k_n L) & \cos(k_n L) \end{bmatrix}, \quad (15)$$

with $k_n = (k_e^2 - k^2 \sin^2 \theta)^{1/2}$, denoting k_e and ρ_e respectively as the complex wavenumber and complex effective density of porous materials. It is noteworthy that k_n can be written as $k_n = k_e \cos \theta_t$ with transmission angle θ_t . The LR model includes the assumption that $\theta_t = 0$ for any angle of plane wave incident to sound absorbers. We use the Miki model (Miki, 1990) to

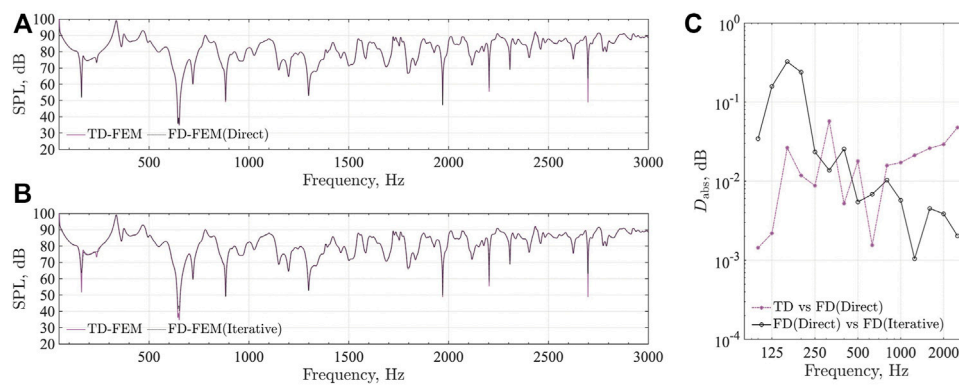


FIGURE 3

Comparison of frequency responses at R1 between TD-FEM and FD-FEM using sparse direct solver and iterative solver, and the absolute difference between them in $\frac{1}{3}$ octave band SPL: (A) TD-FEM vs. FD-FEM(Direct); (B) TD-FEM vs. FD-FEM(Iterative); and (C) Absolute difference between TD-FEM and FD-FEM(Direct). The absolute difference between FD-FEM(Direct) and FD-FEM(Iterative) is also shown.

compute these two fluid properties k_e and ρ_e . With matrix T^P , the specific acoustic admittance ratio \hat{y}^{GW} of the GW absorber having a rigid termination is computed as

$$\hat{y}^{GW} = \frac{T_{21}^P}{T_{11}^P} \rho c. \quad (16)$$

However, the transfer matrix T^M of MPP is represented by a lumped element as

$$T^M = \begin{bmatrix} T_{11}^M & T_{12}^M \\ T_{21}^M & T_{22}^M \end{bmatrix} = \begin{bmatrix} 1 & Z_t \\ 0 & 1 \end{bmatrix}, \quad (17)$$

where Z_t is the transfer impedance of MPP. For a limp MPP, the transfer impedance is defined as (Sakagami et al., 2005)

$$Z_t = \left(\frac{1}{Z_{mpp}} + \frac{1}{j\omega M_{mpp}} \right)^{-1}, \quad (18)$$

where Z_{mpp} denotes the specific acoustic impedance of rigid MPP and M_{mpp} represents the surface density of MPP. We use Maa's impedance model (Maa, 1987) as Z_{mpp} . The total transfer matrix T of MPPGW absorber is calculated as

$$T = T^M T^P = \begin{bmatrix} T_{11} & T_{12} \\ T_{21} & T_{22} \end{bmatrix}. \quad (19)$$

Assuming rigid termination, the specific acoustic admittance ratio \hat{y}^{MPPGW} of MPPGW is calculable as

$$\hat{y}^{MPPGW} = \frac{T_{21}}{T_{11}} \rho c. \quad (20)$$

Those \hat{y}^{GW} and \hat{y}^{MPPGW} at normal incidence are used to construct the rational function model of Eq. 6 for the frequency-dependent LR BCs in TD-FEM. For FD-FEM we use those \hat{y}^{GW} and \hat{y}^{MPPGW} to the frequency-dependent LR BCs in FD-FEM expressed by Eq. 11.

3 Accuracy and efficiency of TD-FEM against FD-FEM

This section presents a discussion of how accurate and efficient 3D TD-FEM is against 3D FD-FEM with two case studies. As notable results, we report the marked performance gain of the time-domain solver against the frequency-domain solver on room-acoustics simulation. The first case study, described in Section 3.1, performs the accuracy and efficiency examination *via* sound field analysis in a small cubic room of 1.01 m³ including three sound absorbers. Figure 1A depicts the small cubic room model. The accuracy examination is based on comparison of frequency responses computed using both methods under the same spatial resolution meshes. One can expect TD-FEM to have a similar level of accuracy as in FD-FEM when time-domain LR BCs model the frequency-dependence of sound absorbers successfully because both methods have almost identical discretization error characteristics to those shown in our earlier work (Okuzono et al., 2021) and Supplementary Section S1. The computational cost comparison evaluates their efficiency. Then, the second case study in Section 3.2 uses a more realistic meeting room model of 68 m³ as presented in Figure 1B. In the meeting room model study to show the practical accuracy of impulse responses computed by TD-FEM, we further compare four room-acoustic parameters computed by both methods: reverberation time (T_{20}), early decay time (EDT), clarity of speech (C_{50}), and sound strength (G). As described in the preceding section, we also compared the computational cost between PARDISO and CSQMOR methods. All computations were done using a computer (Mac Pro 2020; Apple Inc., Xeon CPU W 2.7 GHz, 24 cores; Intel Corp.) with a Fortran compiler (ver. 2020; Intel Corp.). The FEM programs used for this study were created by the authors using in-house code.

TABLE 2 Parameters y_{∞} , A_i , B_i , C_i , λ_i , α_i , and β_i for MPPGW door. The parameters were fitted at 50 Hz–2 kHz.

y_{∞}	0.024											
i	1	2	3	4	5	6	7	8	9	10	11	12
A_i	−77.52	9339.51	−10116.22	8671.99	−8433.63	522.17	6072.70	−11800.19	19648.67	−22188.60	83987.81	−80994.15
B_i	176.59	2015.62										
C_i	97.65	3525.05										
λ_i	211.87	409.55	421.54	762.98	817.96	1530.72	2383.82	2867.10	4344.27	5589.12	11059.06	12606.25
α_i	653.26	11420.49										
β_i	−1261.53	−7440.71										

3.1 Small cubic room model

3.1.1 Problem description and numerical setup

We computed the sound field generated by sound radiation from a monopole source in a small cubic room, as shown in Figure 1A at frequencies up to 3 kHz, with TD-FEM and FD-FEM. This room has three sound absorbers: a GW absorber on the ceiling, an AF in front of the window, and an MPPGW absorber on a wall. The GW absorber has flow resistivity $R = 55,000 \text{ Pa s/m}^2$ with 25 mm thickness. MPPGW absorber uses the same GW behind an MPP leaf with 1.13 kg/m^3 surface density, 1 mm hole diameter, 1 mm panel thickness, and 9 mm plate pitch. The AF has surface density of 0.5 kg/m^2 and flow resistance of 416 Pa s/m . Figures 2A–C show their random incidence sound absorption coefficient α_r computed using the transfer matrix method. This figure includes both α_r computed assuming LR and ER for GW and MPPGW absorbers to show how the LR assumption used for the numerical analysis fits the exact ER model. The other surfaces assigned the specific acoustic admittance ratio $\tilde{y} = \hat{y} = \frac{1}{71.52}$ as reflective surfaces. The rational function parameter of GW absorber was presented in Table A.3 of our earlier work (Okuzono et al., 2021). For MPPGW, we newly designed its rational function form using the vector fitting method (Gustavsen and Semlyen, 1999). It is presented in Table 1.

For spatial discretization, we used Hex8 with dispersion reduced TD-FEM and FD-FEM. The resulting FE mesh has 146,632 degrees of freedom (DOF), using cubic elements of 0.02 m edge length for the air domain and rectangular elements of $0.001 \text{ m} \times 0.02 \text{ m} \times 0.02 \text{ m}$ for AF. The spatial resolution of FE mesh is 5.7 elements per wavelength at the upper-limit frequency of 3 kHz, where the spatial resolution is defined as the ratio between the wavelength and the maximum edge length. There exist a well-used rule of thumb, i.e., ten elements per wavelength, for the spatial discretization using linear elements. As described in Supplementary Section S1, compared to the standard FEMs using a mesh that follows the rule of thumb, the dispersion-reduced FEMs can provide a more accurate solution with a coarser mesh with about five elements per wavelength. According to the fact, the present paper created

the FE mesh. A source S and two receivers R1 and R2 are placed respectively at positions (0.5, 0.5, 0.5), (0.8, 0.1, 0.1), and (0.9, 0.7, 0.6). For time-domain simulation, we used the impulse response of an optimized FIR filter based on the Parks–McClellan algorithm as a sound source signal $\hat{q}(t)$, having a flat spectrum at 70 Hz–3 kHz. This source signal can design easily with a MATLAB function, “firpm.” Note that although any source function is available according to the user’s purpose, it is important for RIRs computation to use a volume source strength density with a flat spectrum because the resulting sound pressure’s spectrum is proportional to the spectrum of volume source strength density. Earlier work (Okuzono et al., 2019) has used this source to simulate the reverberation absorption coefficient measurement, and the computed absorption coefficient showed a good agreement with measured values. Computations were performed up to the time length of 1 s with the time interval $\Delta t = \frac{1}{31000} \text{ s}$. The value of Δt is a slightly smaller value than the stability limit value. With this time interval, we must solve a linear system of equations at 31,000 time steps in total. However, for FD-FEM, a source signal is given as $j\omega\hat{q}(\omega) = 1$. The computation was performed up to 3 kHz with 1 Hz interval. Using this frequency interval, we must solve a linear system of equations at 3,000 pure tones in total. For the computational cost comparison, computations by both methods were performed respectively with serial computation and OpenMP parallel computation using 12 threads. In TD-FEM, the time marching scheme, which solves the second-order ODE of Eq. 5 and the first-order ODEs of Eqs 7–9, was parallelized, whereas FD-FEM uses parallelized linear system solvers. In neither method was the coefficient matrix construction process parallelized. Also, we need to set an arbitrary initial value to the iterative solvers when using them, which might affect their convergence characteristics. According to the preliminary study results described in Supplementary Section S2, we used an initial value of zeros for TD-FEM and previous solution values for FD-FEM. They respectively showed faster convergence characteristics for each method. The initial value setup was also used for all subsequent numerical experiments.

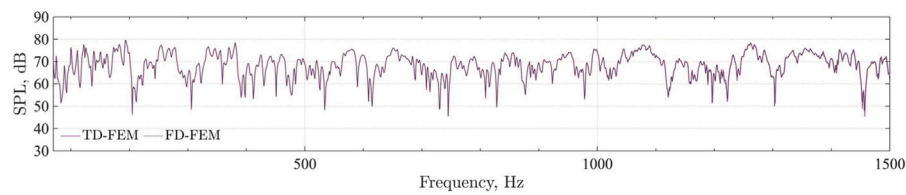


FIGURE 4
Frequency responses at R1 of TD-FEM and FD-FEM using sparse direct solver.

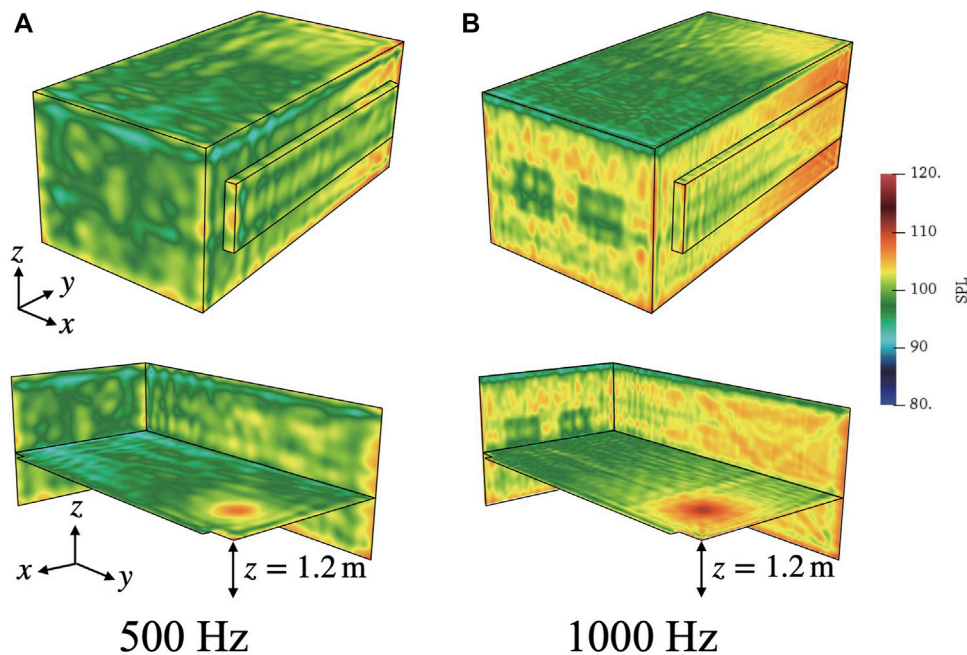


FIGURE 5
Octave band SPL distributions at 500 Hz and 1 kHz: (A) 500 Hz and (B) 1 kHz.

To compare the frequency responses $SPL(\mathbf{r}, \omega)$ computed by both methods, for TD-FEM results, we compute its transfer function value using the following equation, removing the sound source characteristics

$$SPL(\mathbf{r}, \omega) = 20 \log_{10} \frac{|\hat{p}_t(\mathbf{r})/\hat{p}_s|}{\sqrt{2}p_0} \quad [\text{dB}], \quad (21)$$

where $\hat{p}_t(\mathbf{r})$ and \hat{p}_s respectively denote the Fourier transformed values of time response by TD-FEM and the source signal, and p_0 stands for the reference sound pressure. We use the absolute difference $D_{\text{abs}}(f_c)$ between the frequency responses by both methods as an accuracy measure with the 1/3 octave band SPLs. The $D_{\text{abs}}(f_c)$ is given as

$$D_{\text{abs}}(f_c) = \frac{1}{n_{\text{receiver}}} \sum_{i=1}^{n_{\text{receiver}}} |L^{\text{FD}}(f_c, \mathbf{r}_i) - L^{\text{TD}}(f_c, \mathbf{r}_i)| \quad [\text{dB}], \quad (22)$$

where $L^{\text{FD}}(f_c, \mathbf{r}_i)$ and $L^{\text{TD}}(f_c, \mathbf{r}_i)$ respectively represent the 1/3 octave band SPLs at center frequency f_c at receiver's position \mathbf{r}_i computed by FD-FEM and TD-FEM, and where n_{receiver} is the number of receivers.

3.1.2 Results

Figures 3A,B respectively present comparisons of frequency responses at R1 computed using TD-FEM and FD-FEM. For FD-FEM results, we designated the case using the sparse direct solver PARDISO as FD-FEM(Direct) and the case using the iterative solver CSQMOR as FD-FEM(Iterative). As a fundamental

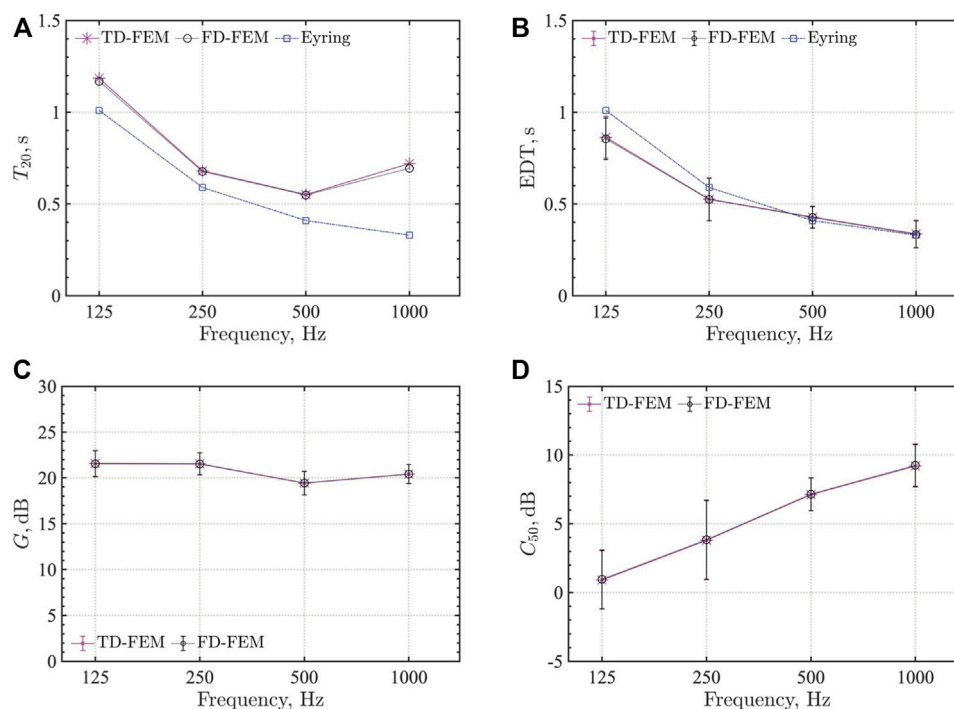


FIGURE 6

Four room-acoustic parameters of TD-FEM and FD-FEM compared using sparse direct solver: (A) T_{20} , (B) EDT, (C) G , and (D) C_{50} .

TABLE 3 Accuracy measures on four room-acoustic parameters at each frequency: $D_{T_{20}}$, D_{EDT} , D_G , and $D_{C_{50}}$.

Frequency, Hz	$D_{T_{20}}$, %	D_{EDT} , %	D_G , dB	$D_{C_{50}}$, dB
125	1.4	0.14	0.04	0.05
250	0.5	0.07	0.03	0.04
500	0.5	0.05	0.01	0.03
1,000	3.6	0.10	0.01	0.06

feature, we find that frequency responses become flattened at higher frequencies because of the higher sound absorption of porous type sound absorbers GW and AF. Two frequency responses by TD-FEM and FD-FEM show excellent agreement irrespective of the type of linear system solvers in FD-FEM. These results indicate that TD-FEM can accurately model the sound absorption characteristics of GW, MPPGW, and AF absorbers. The TD-FEM result fits better with the FD-FEM result obtained using the direct solver, which has better accuracy than those of iterative solvers. Some discrepancies can be found in SPL dips at frequencies below 700 Hz when using the iterative solver in FD-FEM. These discrepancies at dips were discussed in earlier reports of the literature (Okamoto et al., 2007) describing the performance of another iterative solver applied to high-order

FD-FEM. We infer that FD-FEM using an iterative solver has difficulty computing a converged solution at dips in SPL, although this error property is unimportant from a practical perspective. It is particularly interesting that the TD-FEM result shows good agreement with FD-FEM(Direct), even when using an iterative solver. The discrepancy between TD-FEM and FD-FEM at a dip around 2,700 Hz is attributable to their slight differences in discretization error characteristics.

Figure 3C shows the absolute difference D_{abs} in 1/3 octave band SPL between TD-FEM and FD-FEM(Direct). This figure also includes D_{abs} between FD-FEM(Direct) and FD-FEM(Iterative) to emphasize the differences in accuracies of the different linear system solvers. Results revealed that the 1/3 octave band SPL between TD-FEM and FD-FEM(Direct) match well within the absolute difference of 0.06 dB, showing that the two methods have comparable accuracy. Regarding the two FD-FEM results obtained using different linear system solvers, 1/3 octave band SPL between FD-FEM(Direct) and FD-FEM(Iterative) also agree well below $D_{abs} = 0.3$ dB, which indicates that the iterative solver has sufficient accuracy from a practical perspective. Slightly larger absolute differences at 125 Hz–200 Hz are attributable to discrepancies at the dips.

Computational cost comparisons revealed TD-FEM as the fastest method for serial and parallel computations, with noteworthy performance. Actually, in terms of serial

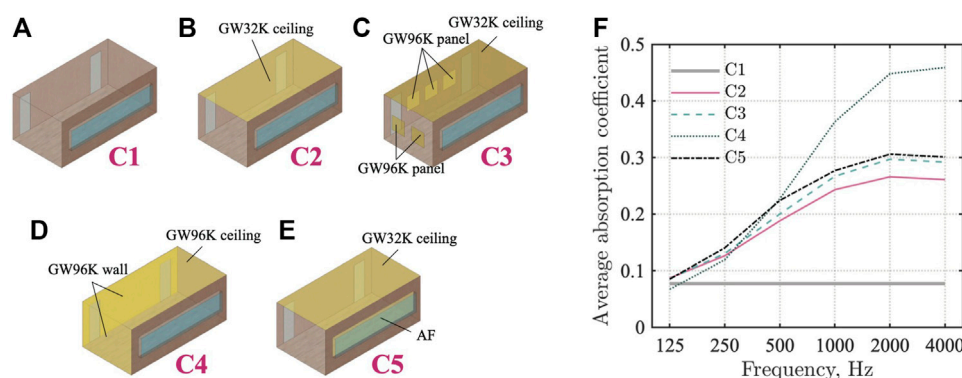


FIGURE 7

Five sound absorber configurations C1–C5 and comparison of their average absorption coefficient: (A) C1, (B) C2, (C) C3, (D) C4, (E) C5, and (F) average absorption coefficient.

computation, TD-FEM is, respectively about 68 and 27 times faster than FD-FEM(Direct) and FD-FEM(Iterative). Results show that TD-FEM, FD-FEM(Direct) and FD-FEM(Iterative) took, respectively 1,067 s, 72,279 s, and 28,632 s to produce a solution. This marked performance benefit provided by TD-FEM derives from an iterative solver's markedly better convergence property for a linear system solution. Actually, TD-FEM required only a mean iteration number of 5.6 per time step, whereas FD-FEM(Iterative) required 965.7 iterations per frequency. The TD-FEM only required the iteration of $\mathcal{O}(1)$ for the problem size of $\mathcal{O}(10^5)$. As mentioned in Sections 2.1, 2.2, the number of iterations is directly related to the number of sparse matrix-vector products, which is the most expensive operation in both FEMs. The total iterations of TD-FEM is 173,684, 1/17 of the total iteration number 2,898,407 of FD-FEM. Also, the sparse matrix-vector product of TD-FEM is a real-valued operation, which is faster than the complex-valued sparse matrix-vector product in FD-FEM. For the case using parallel computation, TD-FEM required 132 s computational time, which is, respectively, 133 and 51 times faster than FD-FEM(Direct) and FD-FEM(Iterative), with 17,604 s and 6,708 s. The performance gain in the parallel computation against serial computation is attributable to the relative increase in the contribution of computational time of the matrix construction process, which is a non-parallel process, against all computational processes in FD-FEM at each pure tone analysis. For example, FD-FEM(Iterative) required 3.0 s computational time at 3 kHz, 1.3 s for the non-parallel matrix construction process, and 1.7 s for the linear system solution process by parallel CSQMOR method. The computational time for the matrix construction process is of the same order as in the solution process, although the matrix construction process only required about 1 s. It is noteworthy that FD-FEM(Iterative) under the parallel computation was 9.2 times faster than the serial computation, focusing only on the linear system solution

process. Furthermore, results show further that FD-FEM has much better performance for the case using the iterative solver, which is a different result for 2D room acoustics simulation presented in an earlier work (Okuzono et al., 2021). Regarding the required memory, TD-FEM needed 0.14 GByte, which is 1/20 smaller than 2.73 GByte in FD-FEM(Direct) and 1.4 times larger than 0.1 GByte in FD-FEM(Iterative). In fact, FD-FEM(Iterative) has the best performance in terms of memory requirements.

3.2 Meeting room model

3.2.1 Problem description and numerical setup

We computed the sound field in a meeting room (Figure 1B) at frequencies up to 1.6 kHz. This room includes four sound absorbers: a GW ceiling absorber, an AF in front of the window, two MPPGW wall panels, and two MPPGW doors. It is noteworthy that MPPGW panels and MPPGW doors have different resonant frequencies. The GW, AF, and MPPGW panels have the same sound absorption characteristics used in earlier small room model studies. The MPPGW doors comprise a rigid MPP leaf with 1 mm hole diameter, 2 mm plate thickness, 15 mm pitch, and a backing 50-mm-thick GW absorber with the flow resistivity $R = 55,000 \text{ Pa s/m}^2$. Figure 2D shows the random incidence sound absorption coefficient α_r computed using the transfer matrix method. Results show that the LR assumption is also valid for MPPGW door. Its rational function form for TD-FEM is shown in Table 2. Other surfaces were treated as reflective surfaces with $\tilde{y} = \hat{y} = \frac{1}{91.16}$. With those sound absorption conditions, the estimated reverberation times by Eyring formula are 1.0 s, 0.6 s, 0.41 s and 0.33 s at 125 Hz, 250 Hz, 500 Hz and 1 kHz.

Spatial discretization was performed with cubic Hex8 of 0.05 m edge length. The resulting FE mesh has 569,064 DOF,

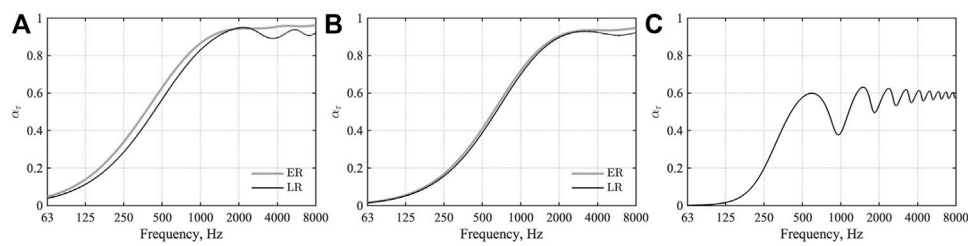


FIGURE 8

Random incidence sound absorption coefficient: (A) GW32K, (B) GW96K, (C) AF. ER and LR respectively denote the extended reaction model and local reaction model.

TABLE 4 Parameters y_{∞} , A_i , B_i , C_i , λ_i , α_i , and β_i for GW32K. The parameters were fitted at 10 Hz–10 kHz.

y_{∞}	0.87				
i	1	2	3	4	5
A_i	0.45	−2.96	−35.84	−3.56	2096.57
B_i	3395.57	5327.05	5759.46	4513.76	−8320.54
C_i	3466.69	1978.86	1452.42	1594.70	34639.47
λ_i	498.79	592.44	1826.43	3244.58	14769.66
α_i	4374.04	8099.11	10318.47	11688.27	49798.90
β_i	−5906.16	−25345.53	−45586.45	−65414.81	−77117.69

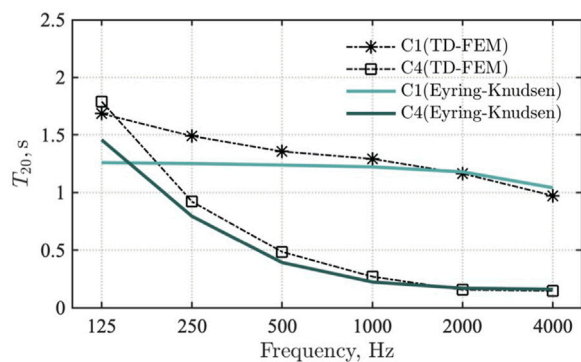


FIGURE 9

Comparison of reverberation times computed by Eyring–Knudsen formula and TD-FEM for cases C1 and C4.

with spatial resolution of 4.9 elements per wavelength at 1.4 kHz. Sound source placement was at a point S (2.5, 5.8, 1.5). Also, eight receivers were placed at positions R1–R8, as shown in Figure 1B. TD-FEM uses an impulse response of optimized FIR filter based on the Parks–McClellan algorithm as the sound source signal $\hat{q}(t)$ with the flat spectrum at 70 Hz–1.5 kHz. The computation

was performed up to the time length of 1 s with the time interval of $\Delta t = \frac{1}{13000}$ s. However, for FD-FEM, a source signal is given as $j\omega\hat{q}(\omega) = 1$ at frequencies up to 1.6 kHz with 1 Hz interval.

Four room-acoustic parameters were calculated from RIRs using TD-FEM and FD-FEM according to ISO 3382-1 (ISO 3382-1, 2009): T_{20} , EDT, G , and C_{50} . For FD-FEM, the RIR is computed using the inverse Fourier transform with the source spectrum $\hat{q}(t)$ in TD-FEM. We define the following measures for the four room-acoustic parameters to show how the RIRs by TD-FEM fit those by FD-FEM in practical respects. For T_{20} , the relative difference $D_{T_{20}}(f_c)$ is defined as

$$D_{T_{20}}(f_c) = \frac{|T_{20}^{\text{FD}}(f_c) - T_{20}^{\text{TD}}(f_c)|}{T_{20}^{\text{FD}}(f_c)} \times 100 [\%], \quad (23)$$

with the spatial averaged $T_{20}(f_c)$ computed using FD-FEM and TD-FEM at each octave band center frequency, respectively denoting $T_{20}^{\text{FD}}(f_c)$ and $T_{20}^{\text{TD}}(f_c)$. The relative difference is also used to EDT as $D_{\text{EDT}}(f_c)$, but it is evaluated with the receiver-dependent values as

$$D_{\text{EDT}}(f_c) = \frac{1}{n_{\text{receiver}}} \sum_{i=1}^{n_{\text{receiver}}} \frac{|\text{EDT}^{\text{FD}}(f_c, \mathbf{r}_i) - \text{EDT}^{\text{TD}}(f_c, \mathbf{r}_i)|}{\text{EDT}^{\text{FD}}(f_c, \mathbf{r}_i)} \times 100 [\%], \quad (24)$$

where $\text{EDT}^{\text{FD}}(f_c, \mathbf{r}_i)$ and $\text{EDT}^{\text{TD}}(f_c, \mathbf{r}_i)$ respectively denote EDT computed using FD-FEM and TD-FEM at receiver's position \mathbf{r}_i . For G and C_{50} , we defined the absolute difference as

$$D_G(f_c) = \frac{1}{n_{\text{receiver}}} \sum_{i=1}^{n_{\text{receiver}}} |G^{\text{FD}}(f_c, \mathbf{r}_i) - G^{\text{TD}}(f_c, \mathbf{r}_i)| [\text{dB}], \quad (25)$$

$$D_{C_{50}}(f_c) = \frac{1}{n_{\text{receiver}}} \sum_{i=1}^{n_{\text{receiver}}} |C_{50}^{\text{FD}}(f_c, \mathbf{r}_i) - C_{50}^{\text{TD}}(f_c, \mathbf{r}_i)| [\text{dB}], \quad (26)$$

where $G^{\text{FD}}(f_c, \mathbf{r}_i)$, and $G^{\text{TD}}(f_c, \mathbf{r}_i)$ represents G values computed by FD-FEM and TD-FEM, and $C_{50}^{\text{FD}}(f_c, \mathbf{r}_i)$ and $C_{50}^{\text{TD}}(f_c, \mathbf{r}_i)$ represents C_{50} values computed by FD-FEM and TD-FEM.

3.2.2 Results

Figure 4 presents a comparison of frequency responses at R1, as computed by TD-FEM and FD-FEM using PARDISO. The two frequency responses mutually match well at all frequency

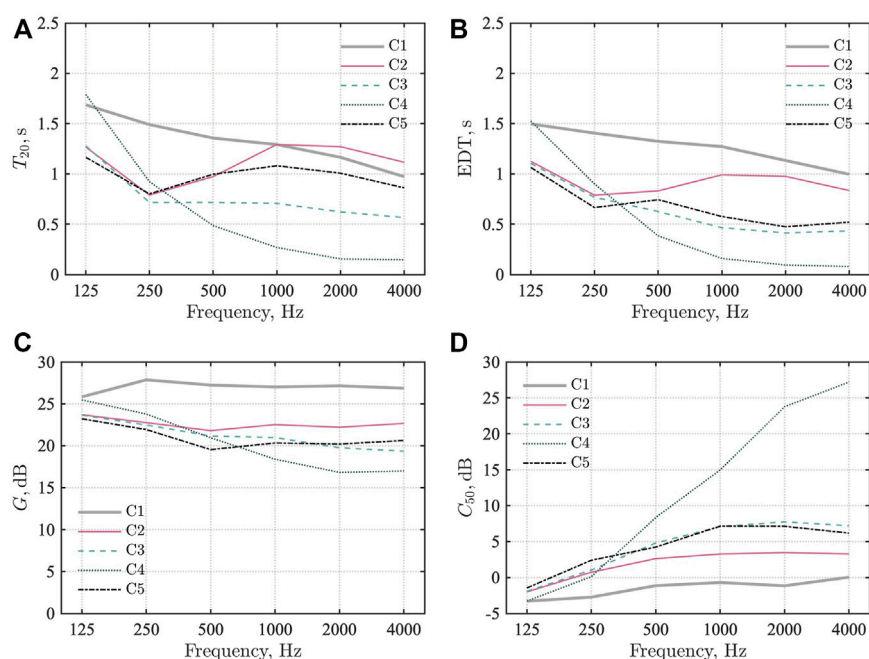


FIGURE 10

Comparison of room-acoustic parameters for cases C1–C5: (A) T_{20} , (B) EDT, (C) G , and (D) C_{50} .

ranges. Regarding the reference, Figure 5 depicts 1 octave band SPL distributions at 500 Hz and 1 kHz in the meeting room. At the room's boundaries, SPL is lower on surfaces of sound absorbers.

Figures 6A–D present comparisons of four room-acoustic parameters computed by TD-FEM and FD-FEM using PARDISO. The results presented with markers (* in TD-FEM and ° in FD-FEM) represent spatially averaged values against the eight receiver's results. The error bars shown in EDT, G and C_{50} express their standard deviation. For T_{20} , EDT, we also show the reverberation times calculated using the Eyring formula as a reference. Overall, TD-FEM results agree well with FD-FEM results for all room-acoustic parameters. Compared to the Eyring values, T_{20} s values computed by FEMs are longer for all frequencies. At 1000 Hz, the FEM results show a different trend as in the Eyring values, i.e., the Eyring values decrease as frequency increases, but the FEM results do not follow the trend at 1 kHz. However, EDT values of the Eyring formula and FEMs match well at 500 Hz and 1 kHz, which indicates that the sound field in the room is still non-diffuse.

Table 3 lists four accuracy measures $D_{T_{20}}$, D_{EDT} , D_G and $D_{C_{50}}$ at 125 Hz–1 kHz. Results revealed that the four room-acoustic parameters calculated using TD-FEM have almost identical accuracy with FD-FEM, quantitatively, with small differences less than the respective JND values (ISO 3382-1, 2009). The values of T_{20} computed using TD-FEM agree well with those of FD-FEM with $D_{T_{20}}$ less than 3.6%. Three other room-acoustic

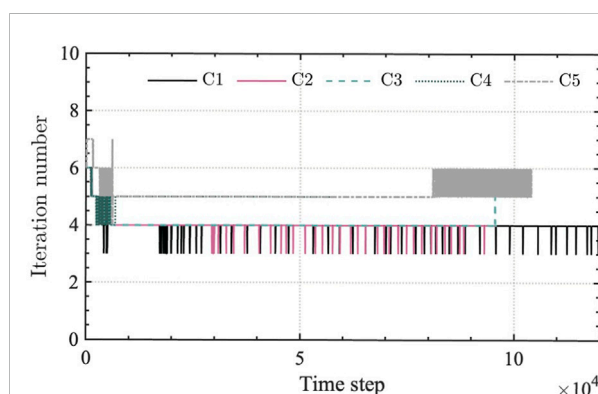


FIGURE 11

Comparison of iteration numbers among cases C1–C5.

parameters of EDT, G , and C_{50} computed using TD-FEM show excellent agreement with those of FD-FEM: $D_{EDT} \leq 0.14\%$, $D_G \leq 0.04$ dB and $D_{C_{50}} \leq 0.06$ dB. These values indicate that TD-FEM can model sound fields in a realistic room with complex sound absorber configurations with comparable accuracy to that of FD-FEM under the use of the same FE mesh.

Regarding computational costs, the realistic meeting room model results showed that TD-FEM has markedly higher performance than that of FD-FEM. The computational time

of TD-FEM is only 248 s when given a 0.52 GByte memory requirement when using 12 threads on OpenMP parallel computations. For the same parallel computation conditions, FD-FEM using PARDISO and CSQMOR respectively consume 78,698 s with 16.5 GByte and 39,002 s with 0.39 GByte. FD-FEM using CSQMOR is twice as fast, and with 1/42 less memory than that necessary for using PARDISO, revealing the effectiveness of using iterative solver for 3D FD-FEM at this frequency range. More importantly, TD-FEM has 157 times faster computational speed with 1.3 times larger memory requirement than FD-FEM using CSQMOR. Even in serial computation with the computational time of 2,137 s, TD-FEM is still fast: it is 18 times faster than FD-FEM using CSQMOR. This marked performance gain is attributable to its much better convergence of iterative solver in TD-FEM compared to that in FD-FEM. TD-FEM requires a mean iteration number of 5.7 per time step, but FD-FEM using CSQMOR needs mean iterations of 3985 per frequency. The total iteration of TD-FEM is 74,530, which is 1/86 of the total iteration of 6,375,544 in FD-FEM. The real-valued sparse matrix-vector product in TD-FEM further enhances the performance compared to FD-FEM with the complex-valued sparse matrix-vector product. The present result revealed that 3D TD-FEM has more attractive computational performance for room acoustics simulation than that of 3D FD-FEM. The present TD-FEM formulation can apply any type of finite elements for spatial discretization. Therefore, a similar performance gain can be expected against FD-FEM using the same finite elements. In this context, constructing higher-order TD-FEM is a subject to be addressed in future research.

4 Simulation under various sound absorber configurations

This section presents the practicality of TD-FEM for room acoustics simulation *via* a case study with a large-scale model having 35 million DOFs. We use the same small meeting room model in Figure 1B, but compute RIRs, which include the frequency component up to 6 kHz, under five sound absorber configurations. The five configurations include a case with no sound absorber. The remaining four use two glass wool absorbers having two characteristics and an AF absorber to control the acoustics inside the room. This demonstration will present the use of the wave-acoustics method can be a realistic selection for the room-acoustics design of small rooms.

4.1 Sound absorbers configuration

Figures 7A–E show the five sound absorber configurations C1–C5. Their details are explained below:

C1 The case with reflective interior finish: All boundary surfaces have reflective materials. Walls, the floor, the ceiling, and window frames were treated as reflective surfaces with $\alpha_r = 0.08$. The window and door surfaces have $\alpha_r = 0.05$.

C2 The case with a ceiling absorber: This case installed a GW32K absorber, the glass wool absorber with 32 kg/m³ density, to the meeting room's ceiling. Other conditions are the same as in C1. The GW32K absorber has flow resistivity of 13,900 Pa s/m² with 50 mm thickness.

C3 The case with a ceiling absorber and five absorbing panels on two walls: This case installed a GW32K absorber, the same as in C1, to the meeting room's ceiling. In addition, five GW96K absorbing panels were installed on two walls of the *zx* plane at *y* = 0 and the *yz* plane at *x* = 0. Other conditions are the same as those in C1. The GW96K absorbing panels have dimensions of 0.9 m × 0.9 m × 0.025 m. Either one surface of the opposing boundary surfaces is treated with sound-absorbing material.

C4 The case with a ceiling absorber and wall absorbers on two walls: This case installed a GW96K absorber with 25 mm thickness to the meeting room's ceiling. The GW96K absorber was installed further on two walls of the *zx* plane at *y* = 0 and *yz* plane at *x* = 0. As in C3, either one surface of the opposing boundary surfaces is treated with sound-absorbing material, but this case has a larger sound-absorbing area. Other conditions are the same as those in C1.

C5 The case with a ceiling absorber and acoustic fabric in front of a window: This case installed a GW32K absorber, the same as in C1, to the meeting room's ceiling. An AF with the flow resistance of 462 Pa s/m and surface density of 0.12 kg/m² was installed further with backing air cavity depth of 0.2 m in front of the windows. Other conditions are the same as those presented in C1.

Figure 7F presents a comparison of average absorption coefficient $\bar{\alpha}$ among C1–C5: Of them, C4 is the highest acoustic treatment case. Also, C3 and C5 have a comparable $\bar{\alpha}$ with different sound absorber configurations. C2 has the lowest $\bar{\alpha}$ among the acoustic treatment cases, but $\bar{\alpha}$ exceeds 0.24 above 1 kHz. It is noteworthy that C2, C3, and C5 can be expected to create a non-diffuse sound field (Nilsson, 2004) according to their non-uniform sound absorber distributions. Figures 8A–C show random-incidence sound absorption coefficients of GW32K, GW96K, and AF calculated using the transfer matrix method. For GW32K and GW96K, their α_r with the ER model is also depicted. The LR model results approximate the ER model well, although the LR model of GW32K shows a slight discrepancy from the ER model. With this comparison result, we judged to use the LR model for GW absorbers. The rational function form of GW32K is available in Table 4.

4.2 Numerical setup

The small meeting room models with sound absorber configurations C1–C5 were spatially discretized with cubic Hex8 of 0.0125 m edge length. The resulting FE meshes have about 35 million DOFs. Their spatial resolutions are 4.6 elements per wavelength at the upper-limit frequency of 6 kHz. The RIRs were computed with a sound source signal: an impulse response of an optimized FIR filter based on the Parks–McClellan algorithm. The source signal has a flat spectrum at 70 Hz–6 kHz. The analyzed time lengths differ among cases: C1 computed RIR up to 2.5 s. For C2, C3, and C5, RIRs were computed up to 2.0 s. We computed an RIR of 1.2 s for C4. The time intervals were set to $\Delta t = \frac{1}{48,000}$ s for C1–C4, and $\Delta t = \frac{1}{52,000}$ s for C5. Because this demonstration computes RIR up to high frequency, we considered air absorption to the RIRs with an IIR filter having time-varying filter coefficients proposed in the literature (Kates and Brandewie, 2020). This air absorption filter fits the pure-tone sound attenuation coefficient described in ISO 9613-1 (ISO 9613-1, 1993) with the cascade of three time-varying low pass filters. We considered for our demonstration that the atmospheric conditions are air temperature of 20°C and 50% relative humidity at standard atmospheric pressure. All computations were performed using a supercomputer system with 2000 nodes at Kyushu University: ITO, Subsystem A, Fujitsu Primergy CX2550/CX2560M4. Each node has two Intel Xeon Gold 6154 (3.0 GHz) with 18 cores. We used Intel Fortran compiler ver. 2020 and performed OpenMP parallel computations with 36 cores.

4.3 Results

First, we explain how the reverberation time computed by TD-FEM fits the classical reverberation theory by the Eyring–Knudsen formula for cases C1 and C4 having uniform sound-absorbing surfaces in the room. We judged that those cases can better meet the reverberation theory assumption than the remaining cases. Figure 9 presents the comparison result, showing that TD-FEM results represent better agreement with the Eyring–Knudsen formula values at higher frequencies for both cases. At lower frequencies, TD-FEM results show longer reverberation times than Eyring–Knudsen formula values because of the lower diffuseness of the sound field.

Then, we discuss the characteristics of sound fields for the cases based on their average absorption coefficient magnitude relation and existing knowledge. Figures 10A–D show comparisons of the four room-acoustic parameters for cases C1–C5. In the case of C2 with a ceiling absorber, T_{20} does not decrease above 500 Hz despite the average absorption coefficient $\bar{\alpha}$ increases concomitantly with increasing frequency because rectangular rooms with a ceiling absorber and the reflective materials on the remaining surfaces become a

typical non-diffuse sound field, as presented in the literature (Nilsson, 2004). The reverberation times of such a rectangular room show a long value because of the slower decay of sound waves traveling parallel to the ceiling absorber. Results show that C3 and C5 have comparable $\bar{\alpha}$, but T_{20} of C5 is longer than that of C3. The C5 has a greater number of untreated opposite surfaces with sound absorbers. The sound corresponding to the axial modes in y direction show slower attenuation, which engenders T_{20} larger than that of C3. Additionally, AF can not absorb the grazing incidence sound wave effectively because of the effect of the non-locally reacting backing air cavity (Okuzono et al., 2020). These results presented herein are consistent with the characteristics of the decay process of a non-diffuse rectangular room with a ceiling absorber discussed in the literature (Nilsson, 2004) as obtained from a Statistical Energy Analysis model. The comparison of EDT among C1, C2, and C5 shows that cases C2 and C5 reduce the reverberance with installing the sound absorbers. Mainly, C5 shows a similar level of EDT as in C3, presenting the effectiveness of the additional sound-absorbing curtain. Comparison of G among C1–C5 revealed that the resulting G value is proportional to $\bar{\alpha}$ of the room. The larger $\bar{\alpha}$ of the room is associated with a lower G value. The same trend is apparent for C_{50} : Higher speech clarity is obtained for larger $\bar{\alpha}$ of the room. Regarding G and C_{50} , their magnitude relations are consistent with the average absorption coefficient magnitude relation among the five cases. These observations further show the plausibility of the TD-FEM results. In future studies, we expect to examine the validity of the TD-FEM for small room-acoustics simulation under various sound absorber configurations by comparison with measurement results. Among the presented cases, C4 has the highest speech clarity but shows the smallest loudness. C3 can be the most attractive sound absorber configuration, satisfying both high loudness and speech clarity. Actually, C5 has similar speech clarity and loudness as that of C3, but it can perceive longer reverberance. Because the optimum configurations of sound absorbers and acoustic diffusers to improve room acoustic quality in meeting rooms are still active research areas (Cucharero et al., 2019; Arvidsson et al., 2020; Labia et al., 2020), the present 3D TD-FEM will become an attractive prediction tool to explore the optimum acoustic materials' configurations in small rooms.

Regarding the computational performance, the computational times were 17–20 h per unit time length for C1–C4. We required the longest time of 25 h for the case C5 having AF because C5 must use a smaller time interval according to its stability condition. The memory requirements are about 32 GByte for all cases. Note that only one node with 36 cores out of 2000 nodes on the supercomputer was used for the present computations. Also, the 32 GByte memory requirements are only 1/6 of the memory capacity of one node. Therefore, the present computations can perform on current standard workstations thoroughly. We also find the

notable property of the convergence of iterative solver in TD-FEM for the sound field up to 6 kHz under various sound absorber configurations. Figure 11 presents a comparison of iteration numbers in TD-FEM among C1–C5. The iterative solver applied to TD-FEM shows a robust and stable convergence at all time steps. The convergence is markedly fast, with 4–5.2 mean iterations per time step despite those large-scale models have 35 million DOFs. Therefore, the order of iterations is $\mathcal{O}(1)$ for the problem of $\mathcal{O}(10^7)$. It is a noteworthy property that the number of iterations is independent of the sound field and degrees of freedom, despite the use of classical iterative solver with and the simplest preconditioning. Those results clearly demonstrated the practicality of TD-FEM to compute RIRs in small spaces up to high frequencies.

5 Conclusion

This paper presents the applicability of a wave-based solver using the recently developed TD-FEM on 3D room-acoustic simulations of small rooms within volume on the order 10 m^3 . Three sound absorbers of GW, AF, and MPPGW were modeled using a frequency-dependent LR BCs and an ER model. For GW and MPPGW absorbers, the simpler LR BCs, which only consider the frequency-dependence of complex-valued specific acoustic admittance ratio, were used once confirming their consistency to ER models computed using the transfer matrix method. In the first part of this report, we explained our examination of the accuracy and efficiency of TD-FEM with the comparison of FD-FEM using two linear system solvers, PARDISO and CSQMOR. The two case studies examined herein respectively simulate RIRs of a small cubic room and a small meeting room with GW and AF porous-type sound absorbers and MPPGW resonant-type sound absorbers. The study results revealed that, compared to FD-FEMs using the two linear system solvers, TD-FEM has a high benefit for 3D small room acoustics simulation with markedly less computational time while maintaining the same accuracy as that obtained using FD-FEM. The small meeting room result showed that the computational time of FD-FEM using CSQMOR is 157 times that of TD-FEM. Moreover, the four room-acoustic parameters, T_{20} , EDT, C_{50} , and G , have comparable accuracies of less than the respective JND values.

Then, based on the accuracy examination with FD-FEM, the practicality of TD-FEM as a room acoustic prediction tool was demonstrated further with the large-scale acoustic simulation in the small meeting room under five sound absorber configurations up to 6 kHz. How room acoustics among the five meeting rooms change was presented by comparison of four room-acoustic parameters. The plausibility of results was demonstrated in three respects: 1) comparison of reverberation times between TD-FEM and the Eyring–Knudsen formula for cases with the most live and

dead sound absorber configurations, 2) a consistency check of the results with existing knowledge related to non-diffuse rectangular rooms, and 3) a consistency check of results with the magnitude relation of average sound absorption coefficients. The computational cost results revealed that 3D TD-FEM has a remarkably appealing property for large-scale room-acoustic simulation with rapid convergence characteristics of the iterative solver. The iterative solver converged with iterations of $\mathcal{O}(1)$ for problems having DOFs of $\mathcal{O}(10^7)$. Considering the results from the small cubic room and the small meeting room models, the convergence is independent of sound fields and DOFs of FE models despite use of the simplest preconditioned CG solver. To conclude, TD-FEM can be an attractive design tool for the acoustics of small spaces, with the ability of accurate sound absorber modeling.

However, an experimental examination is still necessary to show the reliability of 3D TD-FEM on room-acoustics prediction of real rooms. We therefore show experimental examination results for real rooms with various sound absorber configurations in future studies.

Data availability statement

The original contributions presented in the study are included in the article/[Supplementary Material](#), further inquiries can be directed to the corresponding author.

Author contributions

TO contributed to the conception and design of the study, conducted the numerical simulations, and prepared the draft of the manuscript. TY contributed to give feedback about the research design and numerical simulations, analyzed the results, and supported writing of the manuscript and coding used for the study. All authors contributed to manuscript revision, reading, and approval of the submitted version.

Funding

This work was supported in part by a Kajima Foundation Scientific Research Grant and Ono charitable Trust for Acoustics.

Conflict of interest

Author TY was employed by the company Hazama Ando Corporation.

The remaining author declares that the research was conducted in the absence of any commercial or financial

relationships that could be construed as a potential conflict of interest.

Publisher's note

All claims expressed in this article are solely those of the authors and do not necessarily represent those of their affiliated organizations, or those of the publisher, the editors and the reviewers. Any product that may be

evaluated in this article, or claim that may be made by its manufacturer, is not guaranteed or endorsed by the publisher.

Supplementary material

The Supplementary Material for this article can be found online at: <https://www.frontiersin.org/articles/10.3389/fbuil.2022.1006365/full#supplementary-material>

References

- Allard, J., and Atalla, N. (2009). "Modeling multilayered systems with porous materials using the transfer matrix method," in *Propagation of sound in porous media: Modeling sound absorbing materials* (Chichester: John Wiley & Sons), 243–281.
- Aretz, M., and Vorländer, M. (2014). Combined wave and ray based room acoustic simulations of audio systems in car passenger compartments, Part II: Comparison of simulations and measurements. *Appl. Acoust.* 76, 52–65. doi:10.1016/j.apacoust.2013.07.020
- Arvidsson, E., Nilsson, E., Hagberg, D. B., and Karlsson, O. J. I. (2020). The effect on room acoustical parameters using a combination of absorbers and diffusers: An experimental study in a classroom. *Acoustics* 2, 505–523. doi:10.3390/acoustics2030027
- Barrett, R., Berry, M., Chan, T., Demmel, J., Donato, J., Dongarra, J., et al. (1994). "Nonstationary iterative methods," in *Templates for the solution of linear systems: Building blocks for iterative methods* (Philadelphia: SIAM), 14–20.
- Bilbao, S., Hamilton, B., Botts, J., and Savioja, L. (2016). Finite volume time domain room acoustics simulation under general impedance boundary conditions. *IEEE/ACM Trans. Audio Speech Lang. Process.* 24, 161–173. doi:10.1109/TASLP.2015.2500018
- Bilbao, S. (2013). Modeling of complex geometries and boundary conditions in finite difference/finite volume time domain room acoustics simulation. *IEEE Trans. Audio Speech Lang. Process.* 21, 1524–1533. doi:10.1109/TASLP.2013.2256897
- Brandão, E., Lenzi, A., and Paul, S. (2015). A review of the *In Situ* impedance and sound absorption measurement techniques. *Acta Acustica united Acustica* 101, 443–463. doi:10.3813/AAA.918840
- Cardoso Soares, M., Brandão Carneiro, E., Aizik Tenenbaum, R., and Mareze, P. H. (2022). Low-frequency room acoustical simulation of a small room with BEM and complex-valued surface impedances. *Appl. Acoust.* 188, 108570. doi:10.1016/j.apacoust.2021.108570
- Cingolani, M., Fratoni, G., Barbaresi, L., D'Orazio, D., Hamilton, B., and Garai, M. (2021). A trial acoustic improvement in a lecture hall with MPP sound absorbers and ftdt acoustic simulations. *Appl. Sci.* 11, 2445. doi:10.3390/app11062445
- Cox, T. J., and Peter, D. (2017). *Acoustic absorbers and diffusers: Theory, design and application, third edition*. London: Taylor & Francis.
- Cucharero, J., Hänninen, T., and Lokki, T. (2019). Influence of sound-absorbing material placement on room acoustical parameters. *Acoustics* 1, 644–660. doi:10.3390/acoustics1030038
- Dragna, D., Pineau, P., and Blanc-Benon, P. (2015). A generalized recursive convolution method for time-domain propagation in porous media. *J. Acoust. Soc. Am.* 138, 1030–1042. doi:10.1121/1.4927553
- Guddati, M. N., and Yue, B. (2004). Modified integration rules for reducing dispersion error in finite element methods. *Comput. Methods Appl. Mech. Eng.* 193, 275–287. doi:10.1016/j.cma.2003.09.010
- Gumerov, N. A., and Duraiswami, R. (2021). Fast multipole accelerated boundary element methods for room acoustics. *J. Acoust. Soc. Am.* 150, 1707–1720. doi:10.1121/1.0006102
- Gustavsen, B., and Semlyen, A. (1999). Rational approximation of frequency domain responses by vector fitting. *IEEE Trans. Power Deliv.* 14, 1052–1061. doi:10.1109/61.772353
- Hamilton, B., and Bilbao, S. (2017). FDTD methods for 3-D room acoustics simulation with high-order accuracy in space and time. *IEEE/ACM Trans. Audio Speech Lang. Process.* 25, 2112–2124. doi:10.1109/TASLP.2017.2744799
- Hargreaves, J. A., and Cox, T. J. (2008). A transient boundary element method model of schroeder diffuser scattering using well mouth impedance. *J. Acoust. Soc. Am.* 124, 2942–2951. doi:10.1121/1.2982420
- Hornikx, M., Hak, C., and Wenmaekers, R. (2015). Acoustic modelling of sports halls, two case studies. *J. Build. Perform. Simul.* 8, 26–38. doi:10.1080/19401493.2014.959057
- Hornikx, M., Krijnen, T., and van Harten, L. (2016). openPSTD: The open source pseudospectral time-domain method for acoustic propagation. *Comput. Phys. Commun.* 203, 298–308. doi:10.1016/j.cpc.2016.02.029
- Hoshi, K., Hanyu, T., Okuzono, T., Sakagami, K., Yairi, M., Harada, S., et al. (2020). Implementation experiment of a honeycomb-backed MPP sound absorber in a meeting room. *Appl. Acoust.* 157, 107000. doi:10.1016/j.apacoust.2019.107000
- Hughes, T. (2000). "Algorithms for hyperbolic and parabolic-hyperbolic problems," in *The finite element method linear static and dynamic finite element analysis* (New York: Dover), 490–569.
- ISO 10534-2 (1998). *Acoustics – determination of sound absorption coefficient and impedance in impedance tubes—Part 2: Transfer-function method*. Geneva: International Organization for Standardization.
- ISO 3382-1 (2009). *Acoustics – measurement of room acoustic parameters – Part 1: Performance spaces*. Geneva: International Organization for Standardization.
- ISO 9613-1 (1993). *Acoustics – attenuation of sound during propagation outdoors – Part 1: Calculation of the absorption of sound by the atmosphere*. Geneva: International Organization for Standardization.
- Kates, J. M., and Brandewie, E. J. (2020). Adding air absorption to simulated room acoustic models. *J. Acoust. Soc. Am.* 148, EL408–EL413. doi:10.1121/10.002489
- Kowalczyk, K., and van Walstijn, M. (2008). Formulation of locally reacting surfaces in FDTD/K-DWM modelling of acoustic spaces. *Acta Acustica united Acustica* 94, 891–906. doi:10.3813/AAA.918107
- Kowalczyk, K., and van Walstijn, M. (2011). Room acoustics simulation using 3-D compact explicit FDTD schemes. *IEEE Trans. Audio Speech Lang. Process.* 19, 34–46. doi:10.1109/TASLP.2010.2045179
- Labia, L., Shtrepi, L., and Astolfi, A. (2020). Improved room acoustics quality in meeting rooms: Investigation on the optimal configurations of sound-absorptive and sound-diffusive panels. *Acoustics* 2, 451–473. doi:10.3390/acoustics2030025
- Maa, D.-Y. (1987). Microperforated-panel wideband absorbers. *Noise Control Eng. J.* 29, 77–84. doi:10.3397/1.2827694
- Mehra, R., Raghuvanshi, N., Savioja, L., Lin, M. C., and Manocha, D. (2012). An efficient GPU-based time domain solver for the acoustic wave equation. *Appl. Acoust.* 73, 83–94. doi:10.1016/j.apacoust.2011.05.012
- Miki, Y. (1990). Acoustical properties of porous materials – modifications of Delany–Bazley models. *J. Acoust. Soc. Jpn. E* 11, 19–24. doi:10.1250/ast.11.19
- Morales, N., Mehra, R., and Manocha, D. (2015). A parallel time-domain wave simulator based on rectangular decomposition for distributed memory architectures. *Appl. Acoust.* 97, 104–114. doi:10.1016/j.apacoust.2015.03.017
- Murillo, D. M., Fazi, F. M., and Astley, J. (2019). Room acoustic simulations using the finite element method and diffuse absorption coefficients. *Acta Acustica united Acustica* 105, 231–239. doi:10.3813/AAA.919304
- Nilsson, E. (2004). Decay processes in rooms with non-diffuse sound fields Part I: Ceiling treatment with absorbing material. *Build. Acoust.* 11, 39–60. doi:10.1260/1351010041217220

- Okamoto, N., Tomiku, R., Otsuru, T., and Yasuda, Y. (2007). Numerical analysis of large-scale sound fields using iterative methods part II: Application of Krylov subspace methods to finite element analysis. *J. Comp. Acous.* 15, 473–493. doi:10.1142/S0218396X07003512
- Okuzono, T., and Sakagami, K. (2015). A finite-element formulation for room acoustics simulation with microperforated panel sound absorbing structures: Verification with electro-acoustical equivalent circuit theory and wave theory. *Appl. Acoust.* 95, 20–26. doi:10.1016/j.apacoust.2015.02.012
- Okuzono, T., and Sakagami, K. (2018). A frequency domain finite element solver for acoustic simulations of 3D rooms with microperforated panel absorbers. *Appl. Acoust.* 129, 1–12. doi:10.1016/j.apacoust.2017.07.008
- Okuzono, T., Shimizu, N., and Sakagami, K. (2019). Predicting absorption characteristics of single-leaf permeable membrane absorbers using finite element method in a time domain. *Appl. Acoust.* 151, 172–182. doi:10.1016/j.apacoust.2019.03.006
- Okuzono, T., Uenishi, K., and Sakagami, K. (2020). Experimental comparison of absorption characteristics of single-leaf permeable membrane absorbers with different backing air cavity designs. *Noise Control Eng. J.* 68, 237–245. doi:10.3397/1/376820
- Okuzono, T., Yoshida, T., and Sakagami, K. (2021). Efficiency of room acoustic simulations with time-domain FEM including frequency-dependent absorbing boundary conditions: Comparison with frequency-domain FEM. *Appl. Acoust.* 182, 108212. doi:10.1016/j.apacoust.2021.108212
- Otsuru, T., Tomiku, R., Okamoto, N., and Ichikawa, Y. (2000). “Accuracy of finite element sound field analysis of an irregular shaped reverberation room,” in *Proceedings of the seventh international congress on acoustics* (Garmisch-Partenkirchen, 2093–2100).
- Otsuru, T., Tomiku, R., Toyomasu, M., and Takahashi, Y. (2001). “Finite element sound field analysis of rooms in built environment,” in *Proceedings of the eighth international congress on acoustics* (Hong Kong, 765–772).
- Pind, F., Engsig-Karup, A. P., Jeong, C.-H., Hesthaven, J. S., Mejlum, M. S., and Strømman-Andersen, J. (2019). Time domain room acoustic simulations using the spectral element method. *J. Acoust. Soc. Am.* 145, 3299–3310. doi:10.1121/1.5109396
- Pind, F., Jeong, C.-H., Engsig-Karup, A. P., Hesthaven, J. S., and Strømman-Andersen, J. (2020). Time-domain room acoustic simulations with extended-reacting porous absorbers using the discontinuous galerkin method. *J. Acoust. Soc. Am.* 148, 2851–2863. doi:10.1121/10.0002448
- Pind, F., Jeong, C.-H., Hesthaven, J. S., Engsig-Karup, A. P., and Strømman-Andersen, J. (2021). A phenomenological extended-reaction boundary model for time-domain wave-based acoustic simulations under sparse reflection conditions using a wave splitting method. *Appl. Acoust.* 172, 107596. doi:10.1016/j.apacoust.2020.107596
- Rabisse, K., Ducourneau, J., Faiz, A., and Trompette, N. (2019). Numerical modelling of sound propagation in rooms bounded by walls with rectangular-shaped irregularities and frequency-dependent impedance. *J. Sound Vib.* 440, 291–314. doi:10.1016/j.jsv.2018.08.059
- Sakagami, K., Morimoto, M., and Yairi, M. (2005). A note on the effect of vibration of a microperforated panel on its sound absorption characteristics. *Acoust. Sci. Technol.* 26, 204–207. doi:10.1250/ast.26.204
- Sakamoto, S., Nagatomo, H., Ushiyama, A., and Tachibana, H. (2008). Calculation of impulse responses and acoustic parameters in a hall by the finite-difference time-domain method. *Acoust. Sci. Technol.* 29, 256–265. doi:10.1250/ast.29.256
- Sakamoto, N., Otsuru, T., Tomiku, R., and Yamauchi, S. (2018). Reproducibility of sound absorption and surface impedance of materials measured in a reverberation room using ensemble averaging technique with a pressure-velocity sensor and improved calibration. *Appl. Acoust.* 142, 87–94. doi:10.1016/j.apacoust.2018.08.009
- Sakamoto, S. (2007). Phase-error analysis of high-order finite difference time domain scheme and its influence on calculation results of impulse response in closed sound field. *Acoust. Sci. Technol.* 28, 295–309. doi:10.1250/ast.28.295
- Sakuma, T., Sakamoto, S., and Otsuru, T. (2014). *Computational simulation in architectural and environmental acoustics: Methods and applications of wave-based computation*. Tokyo: Springer Japan.
- Savioja, L., and Svensson, U. P. (2015). Overview of geometrical room acoustic modeling techniques. *J. Acoust. Soc. Am.* 138, 708–730. doi:10.1121/1.4926438
- Simonaho, S.-P., Lähivaara, T., and Huttunen, T. (2012). Modeling of acoustic wave propagation in time-domain using the discontinuous galerkin method: A comparison with measurements. *Appl. Acoust.* 73, 173–183. doi:10.1016/j.apacoust.2011.08.001
- Sugahara, A., Lee, H., Sakamoto, S., and Takeoka, S. (2019). Measurements of acoustic impedance of porous materials using a parametric loudspeaker with phononic crystals and phase-cancellation method. *Appl. Acoust.* 152, 54–62. doi:10.1016/j.apacoust.2019.03.019
- Toyoda, M., and Eto, D. (2019). Prediction of microperforated panel absorbers using the finite-difference time-domain method. *Wave Motion* 86, 110–124. doi:10.1016/j.wavemoti.2019.01.006
- Toyoda, M., and Sakayoshi, Y. (2021). Filter and correction for a hybrid sound field analysis of geometrical and wave-based acoustics. *Acoust. Sci. Technol.* 42, E2111–E2180. doi:10.1250/ast.42.170
- Troian, R., Dagna, D., Bailly, C., and Galland, M.-A. (2017). Broadband liner impedance eduction for multimodal acoustic propagation in the presence of a mean flow. *J. Sound Vib.* 392, 200–216. doi:10.1016/j.jsv.2016.10.014
- Vorländer, M. (2013). Computer simulations in room acoustics: Concepts and uncertainties. *J. Acoust. Soc. Am.* 133, 1203–1213. doi:10.1121/1.4788978
- Wang, H., and Hornikx, M. (2020). Time-domain impedance boundary condition modeling with the discontinuous galerkin method for room acoustics simulations. *J. Acoust. Soc. Am.* 147, 2534–2546. doi:10.1121/10.0001128
- Wang, H., Sihar, I., Muñoz, R. P., and Hornikx, M. (2019). Room acoustics modelling in the time-domain with the nodal discontinuous galerkin method. *J. Acoust. Soc. Am.* 145, 2650–2663. doi:10.1121/1.5096154
- Yasuda, Y., Ueno, S., Kadota, M., and Sekine, H. (2016). Applicability of locally reacting boundary conditions to porous material layer backed by rigid wall: Wave-based numerical study in non-diffuse sound field with unevenly distributed sound absorbing surfaces. *Appl. Acoust.* 113, 45–57. doi:10.1016/j.apacoust.2016.06.006
- Yasuda, Y., Saito, K., and Sekine, H. (2020). Effects of the convergence tolerance of iterative methods used in the boundary element method on the calculation results of sound fields in rooms. *Appl. Acoust.* 157, 106997. doi:10.1016/j.apacoust.2019.08.003
- Yatabe, K., and Sugahara, A. (2022). Convex-optimization-based post-processing for computing room impulse response by frequency-domain fem. *Appl. Acoust.* 199, 108988. doi:10.1016/j.apacoust.2022.108988
- Yoshida, T., Okuzono, T., and Sakagami, K. (2020). Time-domain finite element formulation of porous sound absorbers based on an equivalent fluid model. *Acoust. Sci. Technol.* 41, 837–840. doi:10.1250/ast.41.837
- Yoshida, T., Okuzono, T., and Sakagami, K. (2022). A parallel dissipation-free and dispersion-optimized explicit time-domain FEM for large-scale room acoustics simulation. *Buildings* 12, 105. doi:10.3390/buildings12020105
- Yue, B., and Guddati, M. N. (2005). Dispersion-reducing finite elements for transient acoustics. *J. Acoust. Soc. Am.* 118, 2132–2141. doi:10.1121/1.2011149
- Zhang, J., and Dai, H. (2015). A new quasi-minimal residual method based on a biconjugate a-orthonormalization procedure and coupled two-term recurrences. *Numer. Algorithms* 70, 875–896. doi:10.1007/s11075-015-9978-5
- Zhao, J., Chen, Z., Bao, M., Lee, H., and Sakamoto, S. (2019). Two-dimensional finite-difference time-domain analysis of sound propagation in rigid-frame porous material based on equivalent fluid model. *Appl. Acoust.* 146, 204–212. doi:10.1016/j.apacoust.2018.11.004

Nomenclature

Boundary conditions

ER Extended-reaction

LR Local-reaction

Numerical methods

ADE Auxiliary differential equation

ARD Adaptive rectangular decomposition

BEM Boundary element method

CG Conjugate gradient

CSQMOR Complex symmetric quasi-minimal residual method based on coupled two-term biconjugate A-orthonormalization procedure

DG-FEM Discontinuous Galerkin FEM

FD-FEM Frequency-domain FEM

FDTD Finite-difference time-domain

FEM Finite element method

FVTD Finite-volume time-domain

PSTD Pseudospectral time-domain

TD-BEM Time-domain BEM

TD-FEM Time-domain FEM

TD-SEM Time-domain spectral element method

Other symbols

FD Frequency-domain

JND Just noticeable difference

RIR Room impulse response

TD Time-domain

Sound absorbers

AF Acoustic fabric curtain

GW Glass wool

MPP Microperforated panel

MPPGW MPP absorber backed by GW



OPEN ACCESS

EDITED BY

Young Ki Kim,
United Arab Emirates University, United
Arab Emirates

REVIEWED BY

Hossein Omrany,
University of Adelaide, Australia
Haowei Yao,
Zhengzhou University of Light Industry,
China

*CORRESPONDENCE

Ahmed Agiel,
a.agiel@uaeu.ac.ae

[†]These authors have contributed equally
to this work and share first authorship

[†]This author has senior authorship

[§]This author has last authorship

SPECIALTY SECTION

This article was submitted to
Indoor Environment,
a section of the journal
Frontiers in Built Environment

RECEIVED 28 October 2022

ACCEPTED 24 November 2022

PUBLISHED 06 December 2022

CITATION

Rahman R, Bidoun D, Agiel A and
Albdour A (2022), Advancing the use of
the repertory grid technique in the built
environment: A systematic review.
Front. Built Environ. 8:1082149.
doi: 10.3389/fbuil.2022.1082149

COPYRIGHT

© 2022 Rahman, Bidoun, Agiel and
Albdour. This is an open-access article
distributed under the terms of the
[Creative Commons Attribution License](#)
(CC BY). The use, distribution or
reproduction in other forums is
permitted, provided the original
author(s) and the copyright owner(s) are
credited and that the original
publication in this journal is cited, in
accordance with accepted academic
practice. No use, distribution or
reproduction is permitted which does
not comply with these terms.

Advancing the use of the repertory grid technique in the built environment: A systematic review

Rawan Rahman[†], Dana Bidoun[†], Ahmed Agiel^{*†} and Ala' Albdour[§]

Architectural Engineering Department, United Arab Emirates University, Al-Ain, United Arab Emirates

Since the development of personal construct theory, the repertory grid technique (RGT) has been the most recognized tool to elicit personal constructs. Although RGT was found to be a viable scientific and practical method in different fields, its utilization in the built environment has been extremely limited. Therefore, this study aimed to explore RGT as a research method and advance its use in the built environment field. Following Preferred Reporting Items for Systematic Reviews and Meta-Analyses guidelines, this study conducted a systematic review to identify studies on Scopus that have used RGT before 2021. These studies were investigated according to subject area, location, year of publication, aim, and research design. Among the 782 studies contributing to more than 24 subject areas, 30 used RGT within the built environment scope. Results indicated the validity of RGT to the built environment by exploring different ways it may be employed. This review strongly recommends advancing the use of RGT in the built environment and taking advantage of its potential.

KEYWORDS

personal construct theory, repertory grid technique, built environment, systematic review, repgrid, architecture, engineering, design

1 Introduction

In the last 2 decades with the development of the technology and science, the research about human and built environment interaction has increased and developed interestingly. The Sustainable Development Goals' (SDGs) most topics are related to the subjective human well-being (De Neve and Sachs, 2020). New fields have emerged such as neuroarchitecture by combining the architecture field with the neuroscience to understand the interaction between human and built environment by exploring the unconscious mind of people (Choo et al., 2017; Albdour et al., 2022; Lee et al., 2022). The development in bioinformatics, computer devices, virtual reality, artificial intelligence and other technologies has supported the development of research about this interaction (Karakas and Yildiz, 2020). On the other hand, from epistemological and ontological perspective, studying and understanding the human cognition and perception of the built environment is more complex than directly asking people about them or neglecting their

opinion. Therefore in psychology, Personal construct theory (PCT) is a personality and cognition theory developed in the 1950s by the American psychologist George Kelly which can deal with this cognitive complexity with its Repertory Grid Technique (RGT). It concerns the psychological reasons for actions and suggests that variations among individuals arise from the various ways in which they predict and experience events in the world around them. Kelly (2003) explained, personal constructs are tools that each person uses to gather information and evaluate and interpret it. This theory has significantly influenced the history of the human science movement of constructivism (Butt, 2008). It has been first developed to be used for medical diagnosing. Later on, it has been used to contribute in various fields. Recent examples of this use, Sewell (2020) who used the PCP to investigate the children's own view about the educational experience as a better method to collect the Voice of the Child. In contrary, Nowruzi and Amerian (2020) tried to gain insight into the teachers' grading process and factors. Winter and Reed (2021) used the PCP to understand the employees' career shock caused by COVID-19 in Serbia. Also, Kawaf and Istanbuluoglu (2019) used the PCT in marketing to investigate the relevance of online fashion shopping. Additionally, Mullineux et al. (2019) used it to understand the mechanism of experts' judgement on the re-offending likelihood. While Samonas et al. (2020) used it to investigate the understanding of different stakeholders to the security policy. Walker and Winter (2007) found that people create personal constructs of how the environment works to understand their observations and perceptions. This method has a great potential to be used in many fields because it is providing the researcher with a theoretical base to understand how people's conscious and unconscious cognition and perception are working. The potential and applicability of PCT was the use of the repertory grid technique (RGT). Kelly developed RGT as an analytical compound to manage and understand the data elicited from each individual or a group of individuals. Therefore, in this study we investigated the use of this theory in the built environment field by conducting a systematic literature review for the papers which used this method to study the human-built environment interaction.

The use of RGT is not limited to researchers and practitioners within psychology; it is rather common across different disciplines and approaches. Jankowicz (2005) provided a brief list of applications of RGT. This was also evident in several systematic and bibliographic reviews. The most recent bibliographic review of RGT in 2012 covered the scientific production with or about RGT between 1998 and 2007 (Saúl et al., 2012). It evaluated the types of documents found, the evolution of the number of publications, the fields of application, and the degree of openness to other disciplines. However, no recent systematic review has been found on the use of RGT as a scientific research method.

Meanwhile, research on the built environment shares the concerns of PCT regarding human behavior, needs, actions, interactions, experiences, and social and cultural occurrences. Psychologists argue that people's perceptions of places and their plans to respond to them are determined by how they "construe" place (Kelly, 2003). Safiullah and Sharma (2017) defined the built environment as "everything humanly made, arranged, or maintained; to fulfill human purposes (needs, wants, and values); to mediate the overall environment; and with result that affect the environmental context". As a result, each aspect of the built environment has some psychological effect, creating contact with the user and influencing cognition, which in turn shapes human behavior. The observed lack of knowledge about human behaviors, attitudes, and values is an important problem in built environment design.

PCT and repertory grids are theoretical and methodological approaches that have been successfully applied in the area of the built environment. In the 1970s, Honikman (1970; Honikman, 1972; Honikman, 1973) studied the relation between the PCT approach and built environmental evaluation. He concluded with a discussion about the potential of this approach and its possible applications in developing humans' understanding of how people use and interpret the environment. Afterward, Harrison and Sarre (1975) assessed and highlighted the effectiveness of the repertory grid in measuring urban residents' environmental images. Their findings suggested possible significant links between these images and behavior in the urban environment.

Building on Honikman's work on the potential and application of PCT in environmental evaluation, Agiel et al. (2019) adopted the personal construct methodology to assess perceptions of traditional architectural images and strengthen the field of meaning in architecture. The results demonstrated the existence of architectural "brand images," "inherent images," and "ideal images" of the built environment in the perceptions of its inhabitants. Moreover, Agiel and Kutty (2019) analyzed and evaluated the visual aesthetics of contemporary architectural images of mosque designs and the influence of emotional, symbolic, and formal building qualities applied to them based on PCT. Although RGT was found to be a viable scientific and practical method in determining the cognitive features of participants and processes and assessing individuals' response to their environment, the utilization of this technique was extremely limited.

Because RGT last underwent a bibliometric review in 2007 (Saúl et al., 2012) and because of the evident limitations of its use in the built environment, this paper aims to explore RGT as a research method and advance its use in the built environment field. This is achieved by 1) systematically mapping the use of RGT as a scientific research method in terms of subject area, location, and year of publication; 2) reporting and exploring RGT as an effective scientific research method in the built environment field, and 3) forming a theoretical framework to

help advance its use in built environment research. This study intends to answer the following questions:

- 1) What is the current state of scientific research on RGT as a method in terms of subject area, location, and year of publication?
- 2) Within the scope of the built environment, what were the research aims of the studies that have adopted RGT?
- 3) Within the scope of the built environment, in what way was RGT methodologically practiced in terms of research design and procedure?
- 4) How can researchers in the built environment field advance RGT as a research method?

Before answering the research questions, we tried to explain more about the RGT in the following section and the major terms and components of this method to make it easier for built environment researchers to understand it and be able to use it.

1.1 Repertory grid technique

Since the development of PCT, RGT has been the most recognized instrument for generating personal constructs. Originally designed by Kelly (2003), this technique was a systematic method of using his theory of personal constructs. RGT combines elements, constructs, and rating scales to create an idiographic measure of one's personality. It deals with the reduction of human thoughts into basic understandable elements while perceiving any stimuli. Unlike other research approaches, the repertory grid allows for structured conversations by assigning mathematical values to the constructs and elements associated with the issue being investigated (Fransella, 2005).

The repertory grid is a matrix that was manually constructed at its early stages and then developed into digital forms to make it more accessible and easier to use. Among these forms are DOS-based software such as CIRCUMGRIDS, GRIDSTAT, GRIDSCAL, FLEXIGRID, and OMNIGRID, which were later replaced by Windows/Web-based software including Gridcor, GridSuite, Idiogrid, OpenRepGrid, Rep Plus, rep:grid, and Sci:vesco. As continuing developing technology, there are attempts to involve the artificial intelligence (AI) in data elicitation process in the RGT (Rosenberger, 2022).

RGT is a primarily quantitative and statistical technique, but it also offers great potential for qualitative work (Fransella, 2005). Qualitative grids may contain words or pictures rather than numbers and are conceptually straightforward but rich in their ability to capture interpersonal situations. Their usefulness has been observed when working with families, teams, and other groups (Procter, 2005; Procter, 2007; Bannister and Fransella, 2019). Studies have discussed and further elaborated on these qualitative grids (Procter, 2014). However, this paper focuses on promoting the use of the

original quantitative repertory grids in the field of the built environment as a method for data elicitation.

The design of a grid can be a delicate process that requires a high level of skill and understanding of the nature of research problem being studied. While it can be quite easy to design new forms of a grid, they will not yield relevant information unless their design is appropriate. Furthermore, the design of a grid must consider the manner in which it will be interpreted as well as the available analysis methods. Kelly (2003) demonstrated the utility of the repertory grid in psychological settings; meanwhile, several researchers discussed the use of RGT in other different fields (Honikman, 1970; Honikman, 1972; Honikman, 1973; Easterby-Smith, 1980; Rozenszajn and Yarden, 2015; Gardiner et al., 2021; Berghoefer and Vollrath, 2022).

This section summarizes the relevant findings on the main components of RGT and the elicitations accompanying its use. These components are as follows:

- 1) Elements refer to "the things or events which are abstracted by a construct" (Kelly, 2003) (p. 137); that is, they pertain to the stimuli that a research study considers significant.
- 2) Constructs are discriminations made between people, events, or things in life. Each construct, however, applies to a regulated number of people, events, or things (Fransella, 2005). They differ from elements in terms of their properties. They are considered bipolar dimensions that each person has created and formed into a system through which they interpret their experiences of the world (Fransella, 2005).

1.1.1 Element selection

Fransella (2005) argued that the nature of elements depends on the context being explored. Elements must be "within the range of convenience of the constructs used" and "representative of the area being investigated" (Fransella, 2005) (p. 18). They must also be discrete, evaluative (Stewart et al., 1981), homogenous, and relevant to all participants (Easterby-Smith, 1980). The selection of elements has two feasible alternatives:

- 1) Supplied elements, which are provided by the researcher;
- 2) Elicited elements, in which participants provide their own elements.

According to Reger (1990), several factors support a researcher's decision to supply elements. First, elements may be provided if a researcher's aim is to learn about a given set of elements from several participants. Second, elements may be supplied if a researcher wants an existing theory to guide the selection. Third, elements may be given if the researcher is interested in comparing the responses of different participants to a standard set of elements. Such comparison could be within a homogenous group of participants or across different ones.

Meanwhile, researchers can ask participants to elicit elements that they themselves consider relevant. Elements can be elicited in different ways (Easterby-Smith, 1980):

- 1) Researchers can define role or situation descriptions in which participants provide their own specific examples that fit these descriptors.
- 2) Researchers can define a “pool” in which participants list certain elements that fit the description, such as “name three effective and three ineffective managers.”
- 3) Researchers can help participants elicit elements through discussions.

1.1.2 Construct elicitation

A “good” construct expresses participants’ meaning precisely and completely, has a clear contrast, is detailed appropriately, and has a direct link to the research topic (Jankowicz, 2005). RGT supports several construct elicitation methods. Minor variations and combinations can be applied to some of these methods depending on the research aim (Easterby-Smith, 1980; Beail, 1985; Reger, 1990). The triadic sort method is believed to be the most convenient when exploring participants’ constructs (Kelly, 2003).

- 1) Supplied constructs, in which the researcher provides the constructs.
- 2) Minimum context form (triadic sort method), in which each elicitation entails the selection of three random elements from the full set. Here, participants identify how two elements are similar yet different from the third. Researchers may provide participants with contextual cues to facilitate their attention toward a specific research problem. The researcher repeats the elicitation process until all relevant constructs are identified. Research has shown that in most domains, the required number of triads to elicit constructs from participants is usually 7–10 (Reger, 1990). Dyads can also be used if participants find it difficult to generate constructs from the triadic method or if the elements themselves are complex (Easterby-Smith, 1980).
- 3) Full context form, in which participants are presented with the full set of elements and are asked to sort them into an unlimited number of piles based on similarities they identify (Easterby-Smith, 1980). Afterward, participants are asked to provide short descriptive titles for each group of elements.
- 4) Group construct elicitation (Stewart et al., 1981), in which the researcher facilitates a group of participants involved in the research. These participants collaboratively reach an agreement on the elements of the repertory grid. The minimum context form, or any other construct elicitation method, may then be employed to elicit bipolar constructs. In this process, the researcher collects the constructs from the participants and randomly selects them. After completing this

phase, the researcher assists all the participants in the group to connect elements to constructs. However, eliciting the individual grids then analyzing multiple grids to understand a group of participants’ views is more supported as no biased ideas is expected as in the group discussions.

- 5) Laddering may be used with any of the above elicitation methods. This process allows participants to further build on the elicited constructs through a series of probing questions, such as how or what and why (Easterby-Smith, 1980).

1.1.3 Linking elements to constructs

As with all methods for eliciting personal constructs, the resulting constructs are not required to be used in some form of repertory grid (Fransella, 2005). The obtained information can be of sufficient use in itself. However, elements are linked to constructs in three ways: dichotomizing, ranking, and rating (Easterby-Smith, 1980; Tan and Hunter, 2002).

- 1) In dichotomizing, elements are either close to the left construct pole or the right construct pole and are labeled accordingly.
- 2) In ranking, elements are placed in order between two construct poles. This method allows for more discrimination and gives participants possibility to exclude elements that are not relevant to the scale.
- 3) In rating, participants have no reference to make discriminations between elements and exercise more freedom when sorting them might not in line with original method of Kelly. When the range of rating values is larger than the number of elements, participants’ freedom is maximized. Research suggests that anything higher than a five-point scale is considered quite complex to assess visually and that seven-point scales are considered the limit for most participants. This process of evaluation, however, is advanced with the new rep:grid and no need to use values to determine differences. The system requires sorting the elements visually on a scale while the rep:grid identify statistical values based on programmed algorithms.
- 4) No linking.

1.1.4 Sample size

The intensive nature of RGT often means the sample size is relatively small but it can be also large using the new rep:grid systems. This helps in generating quantitative data to understand a large population. However for qualitative data, a sample size of 15–25 within a population will frequently generate sufficient constructs to approximate the “Universe of meaning” regarding a given domain of discourse (Dunn, 1986; Ginsberg, 1989). That is, no new constructs are normally added despite an increase in sample size. Studies using RGT with a small sample size can develop items for larger sample instruments such as closed-ended preprepared constructs.

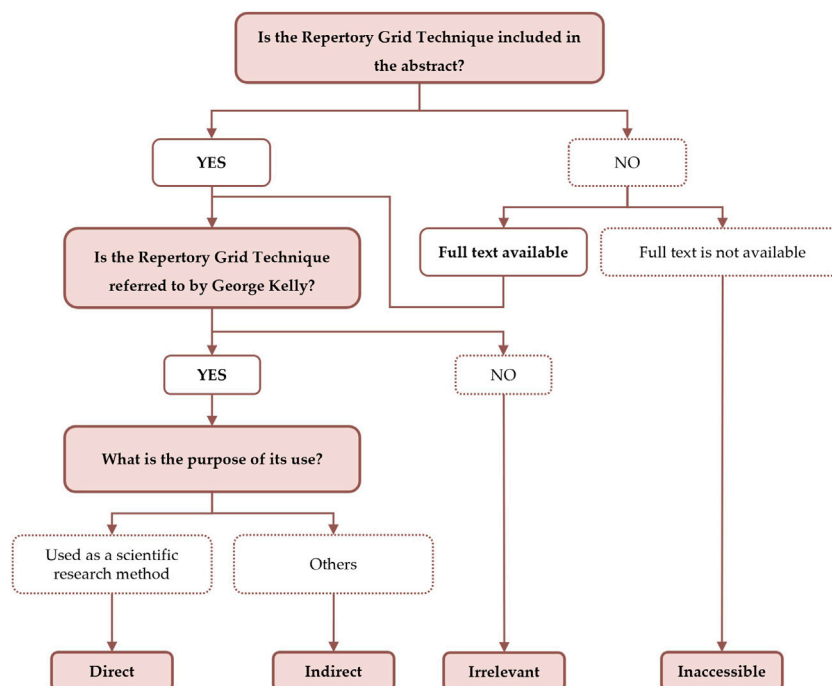


FIGURE 1
Second and third exclusion stages and validation processes.

TABLE 1 Descriptions of the validation process categories.

Category	Description
Direct	Studies that used repertory grid technique (RGT) as a scientific research method solely or in conjunction with other methods
Indirect	Studies that investigated the potential of RGT as a tool without using it as a scientific research method; studies that described or explained RGT; studies that compared RGT to other methods without using it as a scientific research method
Inaccessible	Studies in which RGT was not cited in the abstract and full text is not available on UAEU's online library or open-access databases
Irrelevant	Studies in which the discussed RGT was not by George Kelly

2 Materials and methods

This study was conducted as a systematic review to answer the above research questions. It followed the Preferred Reporting Items for Systematic Reviews and Meta-Analyses (PRISMA) guidelines (Tricco et al., 2018).

2.1 Eligibility criteria

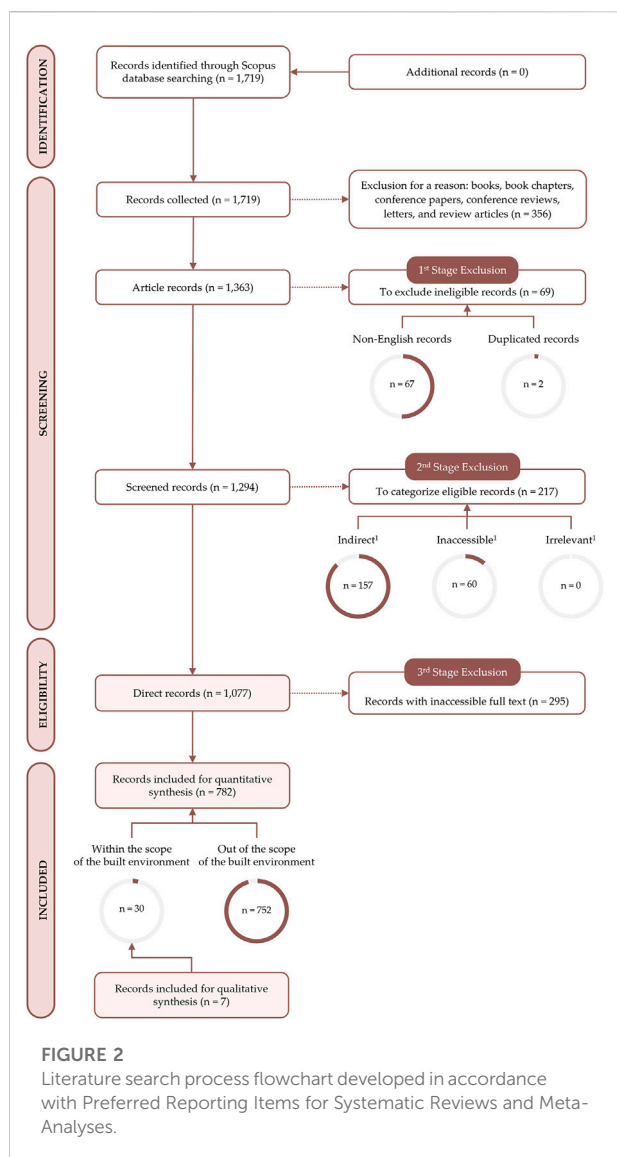
To be eligible for inclusion in this systematic review, the studies must be peer-reviewed articles published before 2021. The analysis excluded books, book chapters, conference papers, conference reviews, letters, and review articles (such as scoping reviews, systematic reviews and bibliographic reviews, meta-

analyses, etc.). Only articles written in English or those with available English translation were included.

Articles were required to use RGT as a research method or any of its derived tools or extensions to be eligible. Studies were included if RGT was used solely or in conjunction with other methods but excluded if it was not used as a research method or if the full text was not accessible.

2.2 Information sources

A structured literature search during the first quarter of 2021 was conducted to identify relevant studies found in the Scopus database. The final search results were exported into CSV format on 16 April 2021 (provided as supplementary material).



This feature allowed Scopus to be an effective search tool for the purpose of this study unlike other databases such as Google Scholar, ResearchGate, or JSTOR, where data exportation was not possible. Given that the Scopus content was checked and revised by an independent Content Selection and Advisory Board, the publications on this database were considered reputable. Also when compared to Web of Science, Scopus database is the largest database which contains 20% more journals than Web of Science (Falagas et al., 2008). However, for this topic we found it 70% more (1817 Scopus/ 1064 Web of Science). However, because of time limitation we couldn't scan multidatabases, we relied on Scopus database. The exported database consisted of citation information, bibliographical information, abstracts, keywords, funding details, and other information. In the further stages of this research, where the full text of the records was required, the United Arab Emirates

University (UAEU) online library and open-access databases were used to retrieve the full text.

2.3 Search strategy

This review selected search terms based on the main concepts of the research question: RGT and method. To find records in Scopus, Boolean operators were used to develop the following search string: "TITLE-ABS-KEY ("RepGrid" OR "repgrid technique" OR "repertory grid technique" OR "repertory grid method" OR "repertory grid") AND PUBYEAR <2021" (without quotation marks). All records from this search had to comply with the condition expressed, and at least one keyword from each OR operator was required in the title, abstract, or keywords.

2.4 Selection and data collection process

To define the current state of scientific research utilizing RGT and answer the first research question, the final database search results identified several records, and the screening process was performed in three exclusion stages. In the first exclusion stage, all non-peer-reviewed articles, non-English articles, and articles with no abstracts were removed, in that order. Duplicates were later removed through an Excel command that highlights cells with identical values. To decide whether the highlighted publications were duplicates, the titles, document types, years of publication, and abstracts had to be the same as well. For further verification, an additional free online tool was used to compare the abstracts of the duplicated records. Before starting any of the screening processes for this review, two reviewers filtered 33 random publications and discussed the results to develop and amend a standardized validation process illustrated in Figure 1. Disagreements on study selection and data validation were resolved by discussion and consensus with other reviewers if needed. The aim of this stage was to prepare the data for validation.

In the second exclusion stage, the validation process for identifying direct records involved screening RGT in the abstract alone. If cited, the technique had to be related to Kelly's PCT and used as a scientific research method. Whether used solely as the main research method or in conjunction with other methods, the record was defined as **direct**. If cited and if RGT was used for description or comparison, literature review, or part of a case study, the record was defined as **indirect**. If cited but the technique was unrelated to Kelly's PCT, the record was defined as **irrelevant**. In case the abstract did not cite RGT or any of the terms used in the search string, the full text was retrieved using the previously stated information sources, screened, and categorized. If the full text was not accessible to the reviewers, the record was excluded and deemed **inaccessible**. Excluded records at this stage had to meet both conditions, in which

key terms were not cited in the abstract and the full text was not accessible for screening. This stage sought to identify direct records and exclude indirect, irrelevant, and inaccessible ones.

In the third exclusion stage, the direct records were screened for eligibility where their full texts were required. Excluded records needed to comply with three conditions, that is, key terms were cited in the abstract, the technique was related to Kelly's PCT and used as a scientific research method, but the full text was not accessible for screening. The aim of this stage was to identify eligible records for quantitative synthesis.

A data-charting Excel form was developed to determine which variables to extract and store the records obtained from the reviewed studies. Following an iterative process, reviewers independently charted the data, discussed the results, and continuously updated the data-charting form. To increase consistency among themselves, the reviewers sequentially validated the titles, abstracts, and keywords of the eligible publications. Using the same validation process, they classified each study according to their purpose into one of the following categories: 1) direct, 2) indirect, 3) inaccessible, and 4) irrelevant. **Table 1** summarizes the category descriptions.

To report on and explore the use of RGT in the built environment, relevant studies in the previous stage were further screened in two phases. In the first phase, titles and abstracts were filtered to categorize studies 1) within or 2) out of the built environment scope according to the definition of the built environment stated earlier. In the second phase, the full texts of the studies classified within scope were retrieved, carefully reviewed, and listed with their use of RGT.

2.5 Data items

The data-charting elements were as follows:

- 1) Author(s): first author's last name, first author's first name, etc.;
- 2) Document title: as specified in the data-charting Excel form;
- 3) Publication year: as specified in the data-charting Excel form;
- 4) Document type: as specified in the data-charting Excel form;
- 5) Country: manually extracted from the first author's affiliation;
- 6) Subject area: manually extracted from Scopus;
- 7) Use of RGT: manually extracted from research papers.

2.6 Synthesis methods

The figures and tables in this study were created using both automated and manual processes. The data-charting Excel form included the author(s), document title, publication year, and document type. However, the publication country was manually

extracted by reviewers from the first author's affiliation. The study's subject area was exported from Scopus into a CSV format sheet and merged back into the original Excel form.

3 Results

This section should concisely and precisely describe the experimental results, their interpretation, as well as the experimental conclusions that can be drawn from them.

3.1 Study selection

Figure 2 illustrates the PRISMA flowchart used to answer the first research question. To define the current state of scientific research utilizing RGT, the review team started with a total of 1,719 records for screening. The first exclusion stage removed books, book chapters, conference papers, conference reviews, letters and review articles ($n = 356$), non-English articles ($n = 67$), and duplicates ($n = 2$), in that order. Afterward, 425 of the 1,719 studies were eliminated; hence, 1,294 publications were eligible for validation in the second exclusion stage. After the second exclusion stage, a further 217 studies were removed, resulting in 1,077 eligible publications for validation in the third exclusion stage. After the third exclusion stage, a further 295 studies were excluded, resulting in a total of 782 publications eligible for quantitative synthesis.

In the second exclusion stage, studies that cited the terms "RepGrid," "repgrid technique," "repertory grid technique," "repertory grid method," or "repertory grid" in their abstracts and referred to the technique discussed by Kelly were screened and categorized. If RGT or any of these terms were not cited in the abstract, the full text was retrieved, screened, and categorized. As a result, 1,077 of 1,294 studies were categorized as "direct," as they used RGT as a scientific research method. Then, 157 of the 1,294 studies were categorized as "indirect," as they described, explained, compared, cited, or studied the grid without using it as a scientific research method. A total of 60 of the 1,294 studies were inaccessible. No records were identified as irrelevant.

In the final exclusion stage, the full texts of 295 of 1,077 "direct" studies were inaccessible; consequently, 782 were included for quantitative synthesis. Among these papers, reviewers identified 30 records within the scope of the built environment and 752 out of scope.

3.2 Study characteristics

Figures 3–5 present the characteristics of the 782 studies using RGT as a scientific research method and simultaneously highlight the characteristics of the 30 studies within the built environment field.

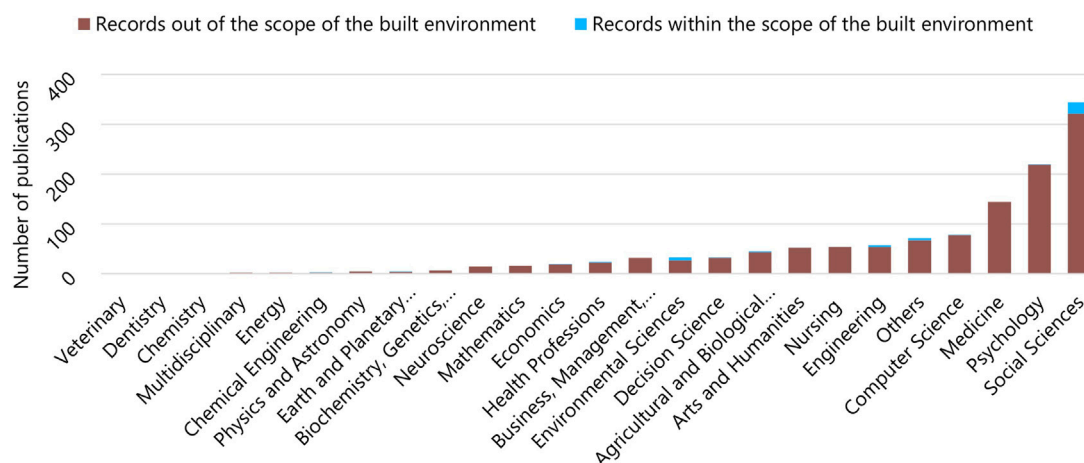


FIGURE 3
Number of publications according to subject area in the included studies.

3.2.1 Subject area

According to Scopus, more than half of the studies in our sample (432 of 782) were published in more than one subject area. One record contributed to six different subject areas: social sciences, health professions, agriculture and biological sciences, arts and humanities, psychology, and nursing. Another contributed to five different subject areas. Of the 432 records, 14 contributed to four subject areas, 36 three subject areas, and 315 two subject areas. The remaining 350 of the 782 records contributed to only one subject area, in which the subject areas of 72 studies were classified as “others.” Figure 3 illustrates the distribution of these studies among subject areas defined by Scopus.

As highlighted in Figure 3, a total of 30 records identified within the built environment scope also contributed to one or more subject areas such as social sciences ($n = 19$), environmental science ($n = 2$), engineering ($n = 2$), agricultural and biological sciences, decision sciences, and economics ($n = 1$ each). The subject areas of four studies were classified as “others.”

3.2.2 Location

The included records were published in several parts of the world as indicated in Figure 4. To a greater extent, and since 1967, research has been conducted in the United Kingdom ($n = 290$), the United States ($n = 77$), Australia ($n = 67$), Spain ($n = 36$), Canada and Germany ($n = 35$ each), Taiwan ($n = 28$), Italy ($n = 21$), Sweden ($n = 20$), the Philippines ($n = 14$), New Zealand and Turkey ($n = 12$ each), China and Netherlands ($n = 11$ each), and Hong Kong and Switzerland ($n = 10$ each).

On a smaller scale, studies have been published in Belgium ($n = 9$); Denmark, Ireland, and Japan ($n = 6$ each); India and South Africa ($n = 5$ each); France, Malaysia, and the Russian Federation ($n = 4$ each); Norway ($n = 3$); Argentina, Brazil, Czech Republic, Finland, Greece, Pakistan, Portugal, and other

countries ($n = 2$ each); and Bahrain, Bangladesh, Chile, Cyprus, Iceland, Indonesia, Iran, Luxembourg, Mexico, Namibia, Singapore, South Korea, Thailand, and the United Arab Emirates ($n = 1$ each).

As for the records within the built environment field, research has been conducted in the United Kingdom ($n = 10$); Australia ($n = 5$); Malaysia ($n = 3$); Japan and Switzerland ($n = 2$ each); and Bahrain, Greece, Hong Kong, Luxembourg, Taiwan, Turkey, Spain, and the United States ($n = 1$ each). One record was classified as “others.”

3.2.3 Year of publication

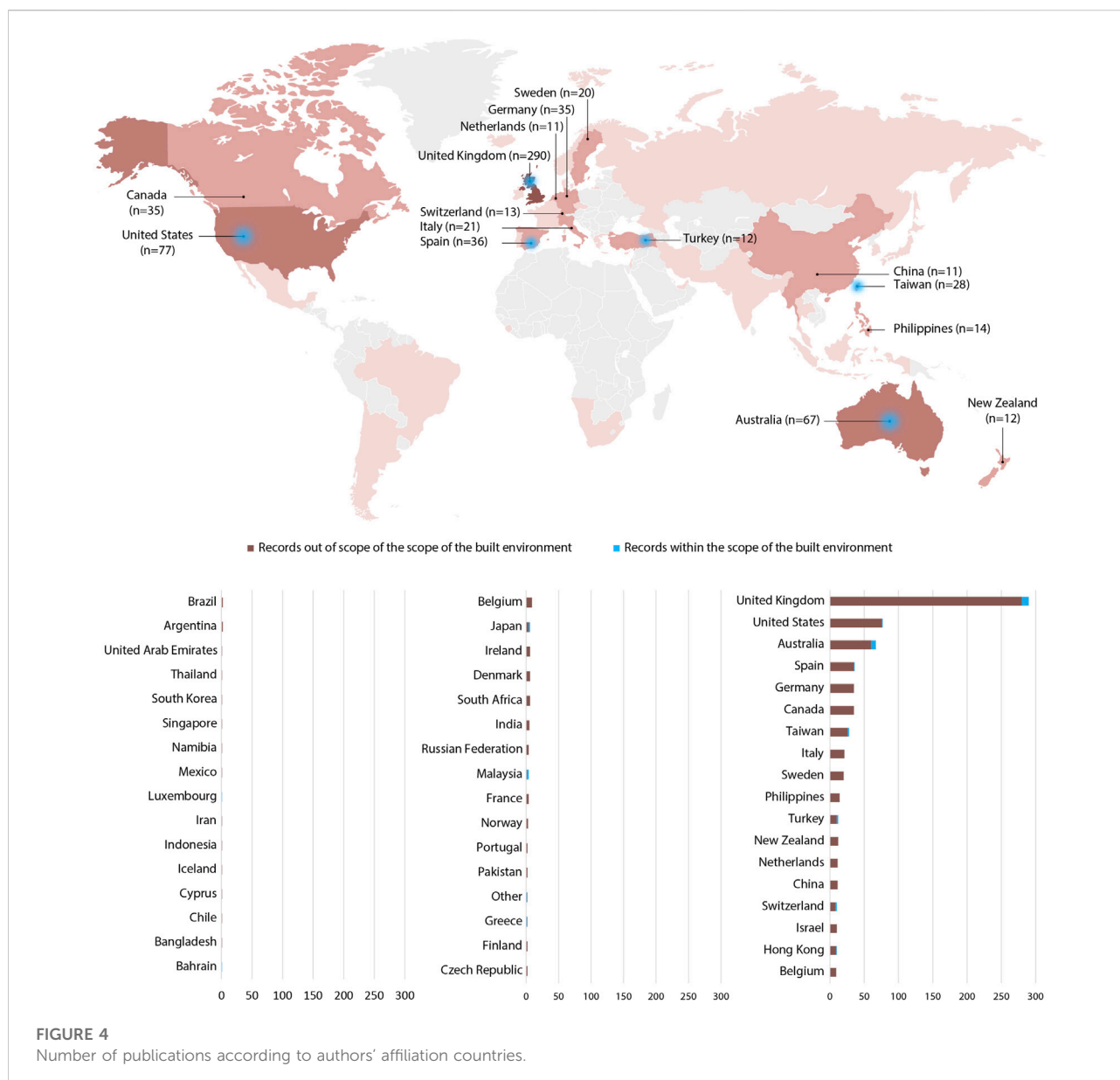
Figure 5 illustrates the 782 studies published between 1967 and 2020 as a line graph. Overall, the publication rate improved during that period. From 1967 to 1994, the publication rate remained consistent, from one to seven publications per year. The rate increased dramatically afterward, peaking at 36 publications in 1997 and again in 2000. Between 2001 and 2015, the publication rate fluctuated, reaching a low of 17 studies published in 2003 and 2008 and a high of 31 studies published in 2012 and 2014. Later, the number of publications increased to 44 in 2017 but slightly fell to 38 in 2020. Meanwhile, studies within the built environment field emerged in 1978. Studies published in 2012 and 2014 peaked at four (out of 30).

3.3 Results of individual studies

3.3.4 Research aim

Within the built environment scope, Table 2 lists the research aims of studies that have adopted RGT.

Based on the definition of the built environment cited earlier, these studies can be classified as either direct or indirect



contributors to the field. Direct contributors included record 234 (Dayaratne, 2016), which used RGT to examine the applicability of physiological techniques in a housing project, and records 133 (Tu et al., 2018) and 135 (Cheah et al., 2018), which adopted RGT to promote sustainable behavior practices or avoid extra energy consumption. Additionally, records 26 (Ratnasingam et al., 2020), 209 (Lallemant and Koenig, 2017), 712 (Vassiliadis and Fotiadis, 2007), 1078 (Mitchell and Kiral, 1999), and 1088 (Mitchell and Kiral, 1998) used RGT to explore human–space interaction, user experience, and spatial experience; assess images of space, or determine material selection. Records 301 (Wan and Shen, 2015), 541 (Abdul-Rahman et al., 2011), 606 (Home et al., 2010), 740 (Home et al., 2007), 875 (Selby, 2004), 1503 (Potter,

1986), 1505 (Potter and Coshall, 1986), and 1652 (Taylor and Stough, 1978) used RGT to elicit users' perceptions of key attributes of urban green spaces, understand the meanings of urban green spaces, provide planners with the necessary tools, identify spatial inequalities, or perform multivariate analysis in geography.

Meanwhile, indirect contributors included record 1062 (Okoroh and Torrance, 1999), which used RGT to analyze the subcontractor's risk elements in constructing refurbishment projects, and records 24 (Kislali et al., 2020), 736 (Byrne and Skinner, 2007), 745 (Pike, 2007), 751 (Naoui et al., 2007), 797 (Naoui et al., 2006), 885 (Hankinson, 2004), 917 (Pike, 2003), 922 (Waite et al., 2003), 933 (Caldwell and Coshall, 2002), 1025

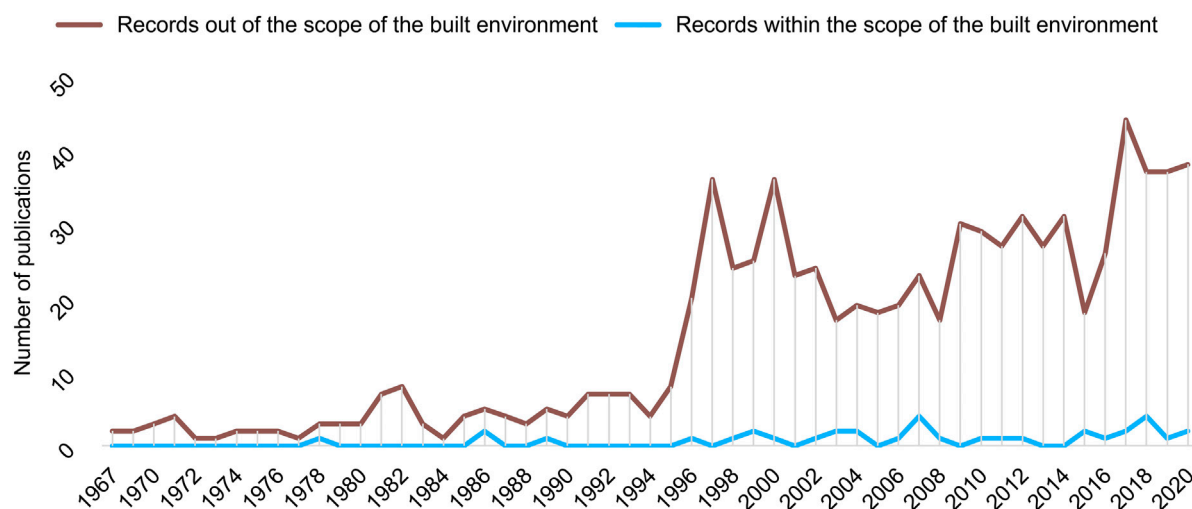


FIGURE 5
Number of publications according to year of publication.

(Coshall, 2000), 1174 (Botterill and Crompton, 1996), and 1411 (Embacher and Buttle, 1989), which adopted RGT to evaluate users' experience, perception, and destination image and its assessment. Finally, the reviewers grouped 30 records into six main topics according to the research aim and keywords: architecture and meaning, building sciences, interior architecture, management and decision-making, tourism and city branding, and urban planning and design. Table 3 summarizes these topics and their typologies.

3.1.5 Repertory grid technique design and procedure

To explain how RGT can be methodologically practiced within the built environment field, this section presents the results of the seven records categorized as direct contributors to the field and published after 2010. The main components of RGT are reported for each record. Table 4 summarizes the use of RGT design components for these records.

Records in the above table used RGT to explore the personal constructs of end users, subcontractors, managers, architects, and urban designers with the aim to evaluate users' experience, perception, and destination image; promote sustainable behavior practices; manage energy consumption; and elicit key attributes of urban green spaces.

3.1.6 Repertory grid technique in architecture and meaning of space

To develop and construct a housing neighborhood in Sri Lanka (Dayaratne, 2016), residents' input was used over two tasks. The first sorting task was conducted with 12 families to achieve a profound understanding of their existential

consciousness and conceptualization of their setting. The authors asked participants to elicit elements by writing the locations they recognize of the present setting on sorting cards. These sorting cards were then presented to each participant as elements to sort into several groups and elicit 10 positive and negative constructs. The sorting process was conducted until no further groups could be generated. The second sorting task was conducted with 20 participants to divulge their conceptualizations and fantasies about the places they wished to see in the new neighborhood. The previous process was repeated, and 28 spatially relevant constructs were used.

3.1.7 Repertory grid technique in building sciences

In (Tu et al., 2018), two phases were used to promote sustainable behavior practices. The first phase used RGT to understand participants' views of the Design for Sustainable Behavior (DfSB) approach, develop an assessment tool in the form of a grid, and propose design strategies for improving the sustainable behavior of household appliances. The second phase used a questionnaire to verify the developed tool. In the first phase, four designers were given six design approaches written on cards as elements. The participants were asked to randomly select three cards, elicit the similarities between two cards, and elicit the difference between those and the third card. The participants repeated the process until no new constructs could be extracted or a certain period had elapsed. A total of 187 constructs falling under 23 typologies were obtained. The 10 most common constructs elicited and the six supplied elements were used to build a 6×10 grid tool for understanding the perceptions and

TABLE 2 List of records within the scope of the built environment.

Rec. No.	Research aim	Author
24	To develop a holistic framework of destination image formation capturing the dynamic nature of the image and incorporating information sources and sociocultural factors	Kislali et al. (2020)
26	To determine the most preferred attributes of overlay materials used in wood-based panel furniture	Ratnasingam et al. (2020)
133	To explore opportunities for promoting sustainable behavior practices	Tu et al. (2018)
135	To investigate the motivations and impediments in avoiding electricity wastage	Cheah et al. (2018)
178	To investigate the decision-making process of travelers	Keshavarzian and Wu, (2017)
209	To explore students' perceptions of learning environments	Lallemand and Koenig, (2017)
234	To examine the applicability of two psychological techniques in a housing project	Dayaratne, (2016)
301	To elicit users' perceptions of key attributes of urban green spaces	Wan and Shen, (2015)
541	To extract a set of core factors in site planning focusing on the tacit knowledge acquisition process to develop a tacit-based decision support system	Abdul-Rahman et al. (2011)
606	To understand the meanings of urban green spaces and provide planners a tool to match urban natural resource management with the needs of residents	Home et al. (2010)
712	To demonstrate the importance of the analysis of constructs in relation to management (local authorities or private institutions) suggestions concerning the museums of a specific area	Vassiliadis and Fotiadis, (2007)
736	To understand the brand of Dublin and explore the way the marketing of a national capital city for business tourism both influences and is influenced by the marketing of the nation itself	Byrne and Skinner, (2007)
740	To reveal a dominant anthropocentric attitude toward urban green spaces	Home et al. (2007)
745	To report the first trial of RGA in eliciting salient destination image attributes using group settings	Pike, (2007)
751	To illustrate the complex nature of visitors' evaluation of historical districts as tourism destinations	Naoi et al. (2007)
797	To discuss the complex nature of visitors' evaluation of a historical district	Naoi et al. (2006)
875	To study tourists' knowledge of Cardiff	Selby, (2004)
885	To elicit attributes associated with 25 destination images in the United Kingdom.	Hankinson, (2004)
917	To identify salient attributes for New Zealanders when differentiating domestic short-break holiday destinations	Pike, (2003)
922	To report on how tourists discriminate between their perception of human artifacts as attractions and the region's gorges, rivers, billabongs, flora, and fauna	Waite et al. (2003)
933	To focus on visitor motivation in the field of museums and galleries	Caldwell and Coshall, (2002)
1025	To analyze tourists' images of London's museums and art galleries	Coshall, (2000)
1062	To analyze the subcontractor's risk elements in constructing refurbishment projects	Okoroh and Torrance, (1999)
1078	To explore the prima facie case for using perceived-risk theory in analyzing store perceptions and set out definitions of store risks in this context	Mitchell and Kiral, (1999)
1088	To assess store images of three United Kingdom grocery retailers	Mitchell and Kiral, (1998)
1174	To explore Kelly's PCT to better understand the nature of tourists' experience	Botterill and Crompton, (1996)
1411	To investigate English vacationers' images of Austria as a summer destination	Embacher and Buttle, (1989)
1503	To present a method to identify, analyze, and monitor spatial inequalities in developing countries	Potter, (1986)
1505	To use repertory grids as a general method of multivariate analysis in geography	Potter and Coshall, (1986)
1652	To assess the empirical validity of Altman's typology of human territories	Taylor and Stough, (1978)

TABLE 3 Categorization of records using RGT in the built environment according to topic.

Contribution	Topic	Record number
Direct	Architecture and Meaning of Space	234
	Building Sciences	133, 135
	Interior Architecture	26, 209, 712, 1078, 1088
	Urban Planning and Design	301, 606, 740, 875, 1503, 1505, 1652
Indirect	Management and Decision-Making	541, 1062
	Tourism and City Branding	24, 178, 736, 745, 751, 797, 885, 917, 922, 933, 1025, 1174, 1411

TABLE 4 Summary of the use of RGT design components.

Topic	Record no. (ref)	Element selection			Construct elicitation			Linking elements to constructs			
		Supplied	Elicited	Supplied constructs	Minimum context form	Group construct elicitation	Full context form	Dichotomizing	Ranking	Rating	No linking
Architecture and Meaning of Space Building Sciences	234 Dayaratne, (2016)		•				•				•
	133 Tu et al. (2018)	•	•		•				•		
	135 Cheah et al. (2018)		•		•				•		
Interior Architecture	026 Ratnasingam et al. (2020)	•			•				•		
	209 Lallemand and Koenig, (2017)	•			•						•
Urban Planning and Design	301 Wan and Shen, (2015)		•		•						•
	606 Home et al. (2010)	•			•					•	

experiences of 38 new young designers, who rated each element based on the construct poles using a five-point Likert scale. To establish the basic concepts of DfSB approaches among participants in the two parts of the first phase, the participants read a short descriptive essay before the interview sessions.

To investigate motives and challenges in preventing electricity wastage, the participants in (Cheah et al., 2018) were asked to list up to six household electricity users. They were supplied with two additional elements and were then asked to randomly select three cards representing three household members and group two cards that were similar but different from the third. The selection criteria were based on members' motivations for not wasting electricity. Once the participants began answering, the constructs were elicited. In every triad process, the participants rated family members according to the constructs in the grid and using a seven-point scale. The elements were placed back into the pile and reshuffled once the participant could no longer elicit new constructs from the same set of cards. Laddering was used, and the process was repeated until the participants either could not generate new constructs or became visibly tired.

3.1.8 Repertory grid technique in interior architecture

To determine the most preferred attributes of overlay materials used in wood-based panel furniture, the participants examined three wood samples (Ratnasingam et al., 2020) by describing the characteristics and attributes in which one sample was different from the other two. The participants rated all three samples with regard to the elicited constructs on a five-point Likert scale.

To explore students' perception of learning environments, 26 students were given 37 printed Web pictures representing different learning spaces during three focus sessions (Lallemand and Koenig, 2017). They followed standardized instructions on how to compare triads and elicit constructs and had 20 min to complete this task individually and repeat the process until saturation was reached. The authors then clustered all contract pairs into six distinct and relevant categories under an affinity diagram format.

3.1.9 Repertory grid technique in urban planning and design

To elicit users' perceptions and assessments of key attributes of urban green spaces (UGS) in Hong Kong, 21 participants were asked to elicit nine UGS that fit a given set of descriptors (Wan and Shen, 2015). Eight descriptors were assigned to a UGS they recall visiting in a certain period, and a ninth descriptor labeled "ideal urban green space" was not assigned but was for their imagination. Each participant was presented with at least six different triad combinations of the elicited elements to generate 131 constructs, which were later used to develop a questionnaire.

To understand the meanings of UGS and provide planners with a tool to match urban natural resource management with residents' needs (Home et al., 2010), 17 participants were supplied with nine photographs of UGS representing different green spaces in Zurich and one imaginary ideal landscape. They were presented with random groups of three elements to elicit construct pairs. A total of 118 constructs were generated and linked using a Likert scale.

4 Discussion

4.1 Interpretation

This systematic review identified a total of 782 studies that used RGT as a scientific research method. According to Scopus, these studies contributed to more than 24 subject areas, with more than half being listed under two or more areas together. Higher contribution rates were identified in three main areas—social sciences, psychology, and medicine, in which PCT was initially introduced.

Regarding location, the highest number of publications was 290 in the United Kingdom, followed by the United States, Australia, Spain, Germany, and Canada, in that order. The high publication rate in these countries is expected because of the international congresses and conferences taking place in these regions. The United Kingdom alone is home to several regional “interest groups” working in personal construct psychology. Nevertheless, publications were not limited to these countries but were spread throughout more than 43 other countries.

In terms of period, the publication rate increased between 1967 and 2020. From 1967 to 1994, the rate of publication remained almost consistent, especially during the evolution of PCT and RGT as tools. Afterward, rates increased dramatically, peaking in 1997 and again in 2000, and then fluctuated between 2001 and 2015 before increasing again in 2017 and finally dropping slightly in 2020. These rates do not necessarily reflect publications on RGT as a tool; instead, they reflect its use as a scientific method in the research field.

Out of the 782 included studies, this review identified only 30 within the scope of the built environment. According to Scopus, these records also contributed to one or more subject areas, such as social sciences, environmental science, engineering, agricultural and biological sciences, chemical engineering, decision sciences, Earth and planetary sciences, health professions, and psychology. In terms of location, the highest number of publications was 10 in the United Kingdom, followed by Australia, Malaysia, Japan, Switzerland, Taiwan, Turkey, Bahrain, Greece, Hong Kong, Luxembourg, Spain, and the United States, in that order. While studies using RGT had a high rate of publication over the period 1967–2020, RGT in the built environment was noticeably absent. Studies started emerging in 1978 and increased to a maximum of four publications between 2007 and 2018.

Studies within the built environment scope used RGT to examine the applicability of physiological techniques in a housing project (Dayaratne, 2016), promote sustainable behavior practices (Tu et al., 2018), and avoid energy consumption (Cheah et al., 2018). RGT was also used to elicit users' perceptions of key attributes of UGS, understand the meanings of UGS (Taylor and Stough, 1978; Potter and Coshall, 1986; Selby, 2004; Home et al., 2007; Wan and Shen, 2015), provide planners with necessary tools (Home et al., 2010), identify spatial inequalities, and integrate it with multivariate analysis in geography (Potter, 1986). In general, RGT was used to explore and evaluate human–space interactions, user experience, spatial experience, perception, and images of space—factors that designers consider important in architectural engineering.

These studies were categorized into direct and indirect topics based on their contributions to the built environment field. Topics included architecture and meaning, building sciences, interior architecture, management and decision-making, tourism and city branding, and urban planning and design. This categorization indicates how RGT contributed to the divergent fields of the built environment.

4.2 Theoretical framework: Using repertory grid technique in the built environment

This analysis provides a broader discussion of what built environment research should consider when designing the RepGrid. Because the decision and elicitation of a repertory grid can be a delicate process that requires high levels of skill and sensitivity, researchers must select among several design alternatives described below.

4.2.1 Element selection

Elements can be supplied if the research aim is to learn about a given set of elements from several participants. For example, in (Ratnasingham et al., 2020), the researcher provided participants with a set of overlay materials to learn more about their characteristics and attributes from the participants' perspectives. In (Lallemant and Koenig, 2017), the researcher supplied participants with 37 printed Web pictures of learning spaces to explore their perceptions of learning environments. In (Lallemant and Koenig, 2017), the researcher presented participants with nine photographs of UGS that represent different green spaces in Zurich. Elements can also be given if the researcher is interested in allowing an existing theory guide element choice or in comparing the responses of several respondents given a standard set of elements. None of the seven records followed these criteria. Meanwhile, elements can be elicited if they are implied by the study or if they must be relevant to the participants (Easterby-Smith, 1980). This method is particularly effective if the researcher's aim is to involve laypeople's perceptions in the

design process. For example, in (Dayaratne, 2016), the researcher (designer) asked participants to elicit places they recall in their current neighborhood and places they wish to have in a future development. In (Wan and Shen, 2015), because of the large number of elements that meet the research criteria and their relevance to the participants, researchers asked participants to elicit places they have visited relying on their real-life experience. They were provided with descriptors to guide their elicitation process. However, in (Cheah et al., 2018), because the research sought to study specific behaviors toward energy consumption, participants were asked to elicit names of household users as elements for the experiment.

Whether supplied or elicited, elements refer to stimuli that are significant in a research study. They can be in the form of printed or digital photographs (Home et al., 2010; Lallemand and Koenig, 2017), text, people (Cheah et al., 2018), or objects (Ratnasingam et al., 2020) or any other suitable format based on research purpose. In cases where real experiences are difficult to reproduce, researchers can use pictures or objects without introducing particular biases. When a large number of elements is relevant to the study or when the identification of a common list for all participants is difficult, researchers can provide participants with a set of descriptors, roles, or situations from which they can elicit their own specific examples that fit these categories. For cases where participants might be unfamiliar with the topic, researchers can provide them with short descriptive essays before interview sessions as in (Tu et al., 2018).

4.2.2 Construct elicitation

RGT supports several methods for eliciting constructs to which minor variations and combinations can be applied. The minimum context form, also known as the triadic sort method, is considered the most convenient and common method for exploring a participant's constructs. This method involves the selection of three random elements from a full set of elements. Participants then identify how two elements are similar yet different from a third. In (Home et al., 2010; Wan and Shen, 2015; Lallemand and Koenig, 2017; Cheah et al., 2018; Tu et al., 2018; Ratnasingam et al., 2020), researchers asked participants to elicit constructs through the minimum context form.

Dyads can also be used to elicit constructs if participants find it difficult to generate constructs *via* the triadic method or if the elements themselves are complex (Easterby-Smith, 1980; Keen and Bell, 1980). None of the records in Table 4 implemented this approach.

Another method to elicit constructs is the full context form. In this method, participants sort a full set of elements into groups using any similarity criteria of their choice (Easterby-Smith, 1980). In (Dayaratne, 2016), the full context form was adopted, and the participants were asked to elicit constructs in the form of short descriptive titles for each pile of elements. Other methods include supplied constructs or group construct elicitation. Again, none of the studies in Table 4 used group

construct elicitation or supplied the constructs, as the methods did not elicit the required data to answer the research question.

4.2.3 Linking elements to constructs

As with all methods for eliciting personal constructs, the resulting constructs are not required to be used in some form of repertory grid (Fransella, 2005); the information gained can be deemed sufficient in itself. Therefore, not all researchers will perform linking. As Table 4 indicates, in (Wan and Shen, 2015; Dayaratne, 2016; Lallemand and Koenig, 2017), researchers were satisfied with the information they obtained and did not use any linking method.

In most cases, elements are linked to constructs through ratings. When rating elements, participants exercise greater freedom and are not compelled to make discriminations where none exist. In (Home et al., 2010; Cheah et al., 2018; Tu et al., 2018; Ratnasingam et al., 2020), ratings were used. When the range of rating values exceeds the number of elements, participants' freedom is maximized. For example, in (Ratnasingam et al.), the participants rated three samples on a five-point scale; in (Tu et al., 2018), the participants rated six elements using a five-point scale; and in (Cheah et al., 2018), the participants rated eight elements on a seven-point scale.

It is important to mention that not all the practice of RGT is responding effectively to the original theory of Kelly especially in the case of group elicitation and rating approaches.

4.2.4 Other considerations

It is important to note that RGT can be used as a scientific research method solely or in conjunction with other approaches. It can also help validate other methods or serve as a preliminary phase for further research. This was evident in most studies such as (Wan and Shen, 2015), where researchers used the construct elicitation results as a base to develop a closed-ended constructs for their research purpose.

Furthermore, Dayaratne (2016) believed that in conventional surveys, participants mostly express negativity. However, RGT allows participants to freely express both negative and positive conceptualizations that are real and strongly experienced.

Also worth noting is that in some cases, elements and constructs can be elicited by a participant group and then supplied to another participant group for research purposes. For example, in (Tu et al., 2018), four designers elicited elements and constructs that were then rated by another group of 38 young designers. However, the data analysis of individual RGT can be studied in groups of individuals to understand how they perform in a certain task.

4.3 Limitations

To make this review more sufficient we considered Scopus data as a benchmark. Therefore, only Scopus was used for the initial identification of records. The scope of this study is to

review articles that were published before 2021. However, there are 60 new articles have been published from 2021 until 22nd of December 2022 which passed the second stage of exclusion on Scopus. Further as acknowledged earlier in the literature search process flowchart, only the UAEU online open-access databases were used to retrieve the full text of the records.

5 Conclusion

This study explored the use of RGT as a research method and advance its use in the built environment field. Following PRISMA guidelines, this research conducted a systematic review to identify studies from Scopus that have adopted RGT before 2021.

The scientific community has become increasingly aware of the potential of RGT in the social sciences, arts, and humanities, but the technique remains underused in the built environment, especially given that the latter field shares several attributes with the former ones in terms of user experience.

Results also indicate that 70 years after RGT was formulated, extended efforts in the development of George Kelly's PCT and the current state of scientific research utilizing RGT as a method are evidently substantial despite the large number of existing evaluation tools. Simply put, widespread research conducted worldwide since the discovery of this theory, especially in the United Kingdom, illustrates its importance and value for research. However, the limited number of publications in the Middle East suggests the need to further investigate RGT. With the growing interest of the MENA region in sustainability and user-centered design, a promising direction for future studies could focus on integrating RGT into the design process. The RGT is in a study work exploring the potential of artificial intelligence as a technique for facilitating data elicitation which can be interesting to deal with human needs with the built environment.

Finally, this review provides insights for scholars and practitioners who want to learn more about applying RGT as a scientific research method in the built environment field. By

providing a theoretical framework for design decisions, this review recommends advancing the use of RGT in the built environment and developing future innovations in this fast-paced field especially by involving the artificial intelligence and machine learning field which might reduce the time and efforts of conducting the interviews for RGT for huge number of participants.

Author contributions

All authors listed have made a substantial, direct, and intellectual contribution to the work and approved it for publication.

Funding

This research was funded by United Arab Emirates University, grant number G00003445, and the APC was funded by United Arab Emirates University.

Conflict of interest

The authors declare that the research was conducted in the absence of any commercial or financial relationships that could be construed as a potential conflict of interest.

Publisher's note

All claims expressed in this article are solely those of the authors and do not necessarily represent those of their affiliated organizations, or those of the publisher, the editors and the reviewers. Any product that may be evaluated in this article, or claim that may be made by its manufacturer, is not guaranteed or endorsed by the publisher.

References

- Abdul-Rahman, H., Wang, C., and Eng, K. S. (2011). Repertory grid technique in the development of Tacit-based Decision Support System (TDSS) for sustainable site layout planning. *Automation Constr.* 20 (7), 818–829. doi:10.1016/j.autcon.2011.02.004
- Aguel, A., and Kutty, N. (2019). "Using repertory grid technique (RGT) to analyze the aesthetics of contemporary architectural images of mosques," in *Mosque architecture: Present issues and future ideas*, eds. M. A. Al Naim, H. M. Al Huneidi, and N. H. Abdul Majid. Eds ed (Kuala Lumpur, Malaysia: ITBM), 625–658.
- Aguel, A., Lang, J., and Caputi, P. (2019). Assessing perceptions of di fausto's neo-traditional architecture based on personal construct methodology. *Personal Constr. Theory Pract.* 16, 111–132.
- Albdour, A., Aguel, A., and Ghoudi, K. (2022). Assessing the emotional affordance of brand image and foreign image based on a physiological method using examples from dubai: Exploratory study. *Build. (Basel)*. 12 (10), 1650. doi:10.3390/buildings12101650
- Bannister, D., and Fransella, F. (2019). *Inquiring man: The psychology of personal constructs*. 3rd Edition. London, England: Routledge.
- Beail, N. (1985). "An introduction to repertory grid technique," in *Repertory grid technique and personal constructs: Applications in clinical & educational settings* (Cambridge, MA: Brookline Books), 1–26.
- Berghoefer, F. L., and Vollrath, M. (2022). Cyclists' perception of cycling infrastructure—A Repertory Grid approach. *Transp. Res. Part F Traffic Psychol. Behav.* 87, 249–263. doi:10.1016/j.trf.2022.04.012
- Botterill, T. D., and Crompton, J. L. (1996). Two case studies exploring the nature of the tourist's experience. *J. Leis. Res.* 28 (1), 57.
- Butt, T. (2008). Kelly's legacy in personality theory: Reasons to be cheerful. *Personal. Constr. theory Pract.* 5, 51–59.
- Byrne, P., and Skinner, H. (2007). International business tourism: Destination dublin or destination Ireland? *J. Travel & Tour. Mark.* 22 (3–4), 55–65. doi:10.1300/j073v22n03_05

- Caldwell, N., and Coshall, J. (2002). Measuring brand associations for museums and galleries using repertory grid analysis. *Manag. Decis.* 40 (4), 383–392. doi:10.1108/00251740210426376
- Cheah, S. K., Yeow, P. H., Nair, S. R., and Tan, F. B. (2018). Behavioural modification framework to address wastage in household electricity consumption. *Ergonomics* 61 (5), 627–643. doi:10.1080/00140139.2017.1397200
- Choo, H., Nasar, J. L., Nikrahei, B., and Walther, D. B. (2017). Neural codes of seeing architectural styles. *Sci. Rep.* 7, 40201–40209. doi:10.1038/srep40201
- Coshall, J. T. (2000). Measurement of tourists' images: The repertory grid approach. *J. Travel Res.* 39 (1), 85–89. doi:10.1177/004728750003900111
- Dayaratne, R. (2016). Creating places through participatory design: Psychological techniques to understand people's conceptions. *J. Hous. Built Environ.* 31 (4), 719–741. doi:10.1007/s10901-016-9497-2
- De Neve, J.-E., and Sachs, J. D. (2020). The SDGs and human well-being: A global analysis of synergies, trade-offs, and regional differences. *Sci. Rep.* 10 (1), 15113. doi:10.1038/s41598-020-71916-9
- Dunn, W. N. (1986). Policy analysis: Perspectives, concepts, and methods.
- Easterby-Smith, M. (1980). The design, analysis and interpretation of repertory grids. *Int. J. Man-Machine Stud.* 13 (1), 3–24. doi:10.1016/s0020-7373(80)80032-0
- Embacher, J., and Buttle, F. (1989). A repertory grid analysis of Austria's image as A summer vacation destination. *J. Travel Res.* 27 (3), 3–7. doi:10.1177/004728758902700302
- Falagas, M. E., Pitsouni, E. I., Malietzis, G. A., and Pappas, G. (2008). Comparison of PubMed, Scopus, Web of science, and Google scholar: Strengths and weaknesses. *FASEB J.* 22 (2), 338–342. doi:10.1096/fj.07-9492LSF
- Fransella, F. E. (2005). *The essential practitioner's handbook of personal construct psychology*. John Wiley & Sons.
- Gardiner, I. A., Littlejohn, A., and Boye, S. (2021). Researching learners' perceptions: The use of the repertory grid technique. *Lang. Teach. Res.* 13621688211013623, 136216882110136. doi:10.1177/13621688211013623
- Ginsberg, A. (1989). Construing the business portfolio: A cognitive model of diversification. *J. Manag. Stud.* 26 (4), 417–438. doi:10.1111/j.1467-6486.1989.tb00737.x
- Hankinson, G. (2004). The brand images of tourism destinations: A study of the saliency of organic images. *J. Prod. Brand Manag.* 13 (1), 6–14. doi:10.1108/10610420410523803
- Harrison, J. N., and Sarre, P. (1975). Personal construct theory in the measurement of environmental images. *Environ. Behav.* 7 (1), 3–58. doi:10.1177/001391657500700101
- Home, R., Bauer, N., and Hunziker, M. (2007). Constructing urban green spaces: An application of Kelly's repertory grid. *Tour. Rev.* 62 (3/4), 47–52. doi:10.1108/16605370780000321
- Home, R., Bauer, N., and Hunziker, M. (2010). Cultural and biological determinants in the evaluation of urban green spaces. *Environ. Behav.* 42 (4), 494–523. doi:10.1177/0013916509338147
- Honikman, B. C. (1972). *An investigation of the relationship between the construing of the environment and its physical form*. London, England: University College London.
- Honikman, B. (1973). "Personal construct theory and environmental evaluation," in Fourth international EDRA conference: *Dowden* (Blacksburg: Hutchison & Ross Stroudsburg), 242–253.
- Honikman, B. (1970). "The investigation of a method of relating the personal construing of the built environment to the designer, AP 70," in *Proceedings of architectural psychology conference* (RIBA Publications and Kingston Polytechnic).
- Jankowicz, D. (2005). *The easy guide to repertory grids*. John Wiley & Sons.
- Karakas, T., and Yildiz, D. (2020). Exploring the influence of the built environment on human experience through a neuroscience approach: A systematic review. *Front. Archit. Res.* 9 (1), 236–247. doi:10.1016/j.foar.2019.10.005
- Kawaf, F., and Istanbuloglu, D. (2019). Online fashion shopping paradox: The role of customer reviews and Facebook marketing. *J. Retail. Consumer Serv.* 48, 144–153. doi:10.1016/j.jretconser.2019.02.017
- Keen, T. R., and Bell, R. C. (1980). One thing leads to another: A new approach to elicitation in the repertory grid technique. *Int. J. Man-Machine Stud.* 13 (1), 25–38. doi:10.1016/s0020-7373(80)80033-2
- Kelly, G. A. (2003). *The psychology of personal constructs*. London, England: Routledge.
- Keshavarzian, P., and Wu, C.-L. (2017). A qualitative research on travellers' destination choice behaviour. *Int. J. Tour. Res.* 19 (5), 546–556. doi:10.1002/jtr.2128
- Kislali, H., Kavaratzis, M., and Saren, M. (2020). Destination image formation: Towards a holistic approach. *Int. J. Tour. Res.* 22 (2), 266–276. doi:10.1002/jtr.2335
- Lallemant, C., and Koenig, V. (2017). The vocabulary of learner-space interactions-understanding learning spaces experience through the repertory grid method. *Interact. Des. Archit.*, 32. (s)
- Lee, S., Shin, W., and Park, E. J. (2022). Implications of neuroarchitecture for the experience of the built environment: A scoping review. *Archmet-IJAR* 16 (2), 225–244. doi:10.1108/arch-09-2021-0249
- Mitchell, V. W., and Kiral, R. H. (1998). Primary and secondary store-loyal customer perceptions of grocery retailers. *Br. Food J.* 100 (7), 312–319. doi:10.1108/00070709810242109
- Mitchell, V. W., and Kiral, H. R. (1999). Risk positioning of UK grocery multiple retailers. *Int. Rev. Retail, Distribution Consumer Res.* 9 (1), 17–39. doi:10.1080/09593699342660
- Mullineux, J. C., Taylor, B. J., and Giles, M. L. (2019). Probation officers' judgements: A study using personal construct theory. *J. Soc. Work* 19 (1), 41–59. doi:10.1177/1468017318757384
- Naoi, T., Airey, D., Iijima, S., and Niininen, O. (2007). Towards a theory of visitors' evaluation of historical districts as tourism destinations: Frameworks and methods. *J. Bus. Res.* 60 (4), 396–400. doi:10.1016/j.jbusres.2006.09.023
- Naoi, T., Airey, D., Iijima, S., and Niininen, O. (2006). Visitors' evaluation of an historical district: Repertory grid analysis and ladder analysis with photographs. *Tour. Manag.* 27 (3), 420–436. doi:10.1016/j.tourman.2004.11.008
- Nowruz, M., and Amerian, M. (2020). Exploring the factors Iranian EFL institute teachers consider in grading using personal construct theory. *Teach. Engl. as a Second Lang. Q.* 38 (4), 123–164.
- Okoroh, M. I., and Torrance, V. B. (1999). A model for subcontractor selection in refurbishment projects. *Constr. Manag. Econ.* 17 (3), 315–327. doi:10.1080/014461999371529
- Pike, S. (2007). Repertory grid analysis in group settings to elicit salient destination image attributes. *Curr. issues Tour.* 10 (4), 378–392. doi:10.2167/citmp010.0
- Pike, S. (2003). The use of repertory grid analysis to elicit salient short-break holiday destination attributes in New Zealand. *J. Travel Res.* 41 (3), 315–319. doi:10.1177/0047287502239054
- Potter, R. B. (1986). Spatial inequalities in Barbados, west indies. *Trans. Inst. Br. Geogr.* 11 (2), 183. doi:10.2307/622005
- Potter, R. B., and Coshall, J. T. (1986). Nonparametric factor analysis in urban geography: Method and validation. *Urban Geogr.* 7 (6), 515–529.
- Procter, H. G. (2007). "Construing within the family," in *The child within: Taking the young person's perspective by applying personal construct theory* (Chichester, UK: Wiley), 190–206.
- Procter, H. G. (2005). "Techniques of personal construct family therapy," in *Personal construct psychotherapy: Advances in theory, practice research*. Editors D. Winter and L. Viney (London: Whurr), 94–108.
- Procter, H. (2014). Qualitative grids, the relationality corollary and the levels of interpersonal construing. *J. Constr. Psychol.* 27 (4), 243–262. doi:10.1080/10720537.2013.820655
- Ratnasingham, J., Ioras, F., Ark, C. K., and Ab Latib, H. (2020). Success factors of wood veneer as an overlay material for panel-based furniture manufacturing in Malaysia. *BioResources* 15 (1), 1311–1322.
- Roger, R. K. (1990). "The repertory grid technique for eliciting the content and structure of cognitive constructive systems," in *Mapping strategic thought* (Chichester, UK: Wiley), 301–309.
- Rosenberger, M. (2022). *Resonance Economy: How resonances arise, how we can identify them and use them to our benefit*. Nordstedt: BoD—Books on Demand.
- Rozenszajn, R., and Yarden, A. (2015). Exposing biology teachers' tacit views about the knowledge that is required for teaching using the repertory grid technique. *Stud. Educ. Eval.* 47, 19–27. doi:10.1016/j.stueduc.2015.06.001
- Safiullah and Sharma, A. S. (2017). Built environment psychology A complex affair of buildings and user. *Int. J. Eng. Technol.* 9 (3S), 503–509. doi:10.21817/ijet/2017/v9i3/170903s077
- Samonas, S., Dhillon, G., and Almusharraf, A. (2020). Stakeholder perceptions of information security policy: Analyzing personal constructs. *Int. J. Inf. Manag.* 50, 144–154. doi:10.1016/j.jinfomgt.2019.04.011
- Saúl, L. A., López-González, M. A., Moreno-Pulido, A., Corbella, S., Compañ, V., and Feixas, G. (2012). Bibliometric review of the repertory grid technique: 1998–2007. *J. Constr. Psychol.* 25 (2), 112–131. doi:10.1080/10720537.2012.651065
- Selby, M. (2004). Consuming the city: Conceptualizing and researching urban tourist knowledge. *Tour. Geogr.* 6 (2), 186–207. doi:10.1080/1461668042000208426
- Sewell, A. (2020). Utilising personal construct psychology and the repertory grid interview method to meaningfully represent the voice of the child in their social relationships. *Pastor. Care Educ.* 38 (2), 93–115. doi:10.1080/02643944.2020.1713869

- Stewart, V., Stewart, A., and Fonda, N. (1981). *Business applications of repertory grid*. London: McGraw-Hill.
- Tan, F. B., and Hunter, M. G. (2002). The repertory grid technique: A method for the study of cognition in information systems. *MIS Q.* 26 (1), 39. doi:10.2307/4132340
- Taylor, R. B., and Stough, R. R. (1978). Territorial cognition: Assessing Altman's typology. *J. Personality Soc. Psychol.* 36 (4), 418–423. doi:10.1037/0022-3514.36.4.418
- Tricco, A. C., Lillie, E., Zarin, W., O'Brien, K. K., Colquhoun, H., Levac, D., et al. (2018). PRISMA extension for scoping reviews (PRISMA-ScR): Checklist and explanation. *Ann. Intern. Med.* 169 (7), 467–473. doi:10.7326/m18-0850
- Tu, J.-C., Nagai, Y., and Shih, M.-C. (2018). Establishing design strategies and an assessment tool of home appliances to promote sustainable behavior for the new poor. *Sustainability* 10 (5), 1507. doi:10.3390/su10051507
- Vassiliadis, C., and Fotiadis, T. A. (2007). Multiple museum construct motivators: A multivariable analysis with repertory grid analysis (RGA) approach. *Tour. Int. Multidiscip. Refereed J. Tour.* 3 (1), 12–35.
- Waitt, G., Lane, R., and Head, L. (2003). The boundaries of nature tourism. *Ann. Tour. Res.* 30 (3), 523–545. doi:10.1016/s0160-7383(02)00104-4
- Walker, B. M., and Winter, D. A. (2007). The elaboration of personal construct psychology. *Annu. Rev. Psychol.* 58 (1), 453–477. doi:10.1146/annurev.psych.58.110405.085535
- Wan, C., and Shen, G. Q. (2015). Salient attributes of urban green spaces in high density cities: The case of Hong Kong. *Habitat Int.* 49, 92–99. doi:10.1016/j.habitatint.2015.05.016
- Winter, D. A., and Reed, N. (2021). Unprecedented times for many but not for all: Personal construct perspectives on the COVID-19 pandemic. *J. Constr. Psychol.* 34 (3), 254–263. doi:10.1080/10720537.2020.1791291



OPEN ACCESS

EDITED BY

Xiaolin Wang,
University of Tasmania, Australia

REVIEWED BY

Muhammad Wakil Shahzad,
Northumbria University, United Kingdom
Siamak Hoseinzadeh,
Sapienza University of Rome, Italy

*CORRESPONDENCE

Seung Jin Oh,
✉ ohs8680@kitech.re.kr

SPECIALTY SECTION

This article was submitted to Indoor Environment, a section of the journal Frontiers in Built Environment

RECEIVED 05 October 2022

ACCEPTED 19 December 2022

PUBLISHED 30 December 2022

CITATION

Kim JW, Kim Y-M, Ko YJ, Chen Q, Xin C and Oh SJ (2022), Study on an advanced borehole heat exchanger for ground source heat pump operating in volcanic island: Case study of Jeju island, South Korea.
Front. Built Environ. 8:1061760.
doi: 10.3389/fbuil.2022.1061760

COPYRIGHT

© 2022 Kim, Kim, Ko, Chen, Xin and Oh. This is an open-access article distributed under the terms of the [Creative Commons Attribution License \(CC BY\)](#). The use, distribution or reproduction in other forums is permitted, provided the original author(s) and the copyright owner(s) are credited and that the original publication in this journal is cited, in accordance with accepted academic practice. No use, distribution or reproduction is permitted which does not comply with these terms.

Study on an advanced borehole heat exchanger for ground source heat pump operating in volcanic island: Case study of Jeju island, South Korea

Jong Woo Kim^{1,2}, Yeong-Min Kim³, Yoon Jung Ko³, Qian Chen⁴, Cui Xin⁵ and Seung Jin Oh^{3*}

¹Department of Mechanical Engineering, Jeju National University, Jeju City, Jeju Special Self-Governing Province, South Korea, ²Research and Development Division, Intertech Co., Ltd., Jeju City, Jeju Special Self-Governing Province, South Korea, ³Korea Institute of Industrial Technology, Cheonan, Jeju Special Self-Governing Province, South Korea, ⁴Institute for Ocean Engineering, Shenzhen International Graduate School, Tsinghua University, Shenzhen, China, ⁵Institute of Building Environment and Sustainable Technology, Xi'an Jiaotong University, Xi'an, China

This paper presents an advanced borehole heat exchanger that has been developed in order to apply a ground source heat pump to a volcanic island where the existing borehole heat exchangers are inapplicable by local ordinance. The advanced borehole heat exchanger was fabricated and installed at a verification-test site to evaluate its heat capacity in terms of refrigeration ton (RT). The proposed heat exchanger was also compared with the conventional heat exchanger that was made of high-density polyethylene (HDPE) heat exchanger. The thermal response test was carried out by flowing water at various temperatures into the heat exchangers at the fixed flow rate of 180 L/min. The results revealed that the maximum heat capacity for the developed heat exchanger was measured at 63.9 kW, which is 160% higher than that of the high-density polyethylene heat exchanger (39.9 kW). It was also found that the developed HX has the highest heat gain achieving 94 kW as compare to 21 kW for high-density polyethylene-Hx.

KEYWORDS

borehole heat exchanger, ground-source heat pump, volcanic island, renewable energy, thermal response test

1 Introduction

Fossil fuel-based power generation has achieved economies of scale through large-scale power generation complexes and, thus, has contributed to the policy goal of an inexpensive and stable power supply (Lanzi et al., 2011; Bogdanov et al., 2021). Fossil fuels, however, are also the cause of environmental pollution, in particular, carbon dioxide and particulate matter emissions, which exacerbate climate change (Shahzad et al., 2017; Alrowais et al., 2020; Gani, 2021; Martins et al., 2021). Accordingly, interest in the development of renewable energy industries and eco-friendly power generation has increased worldwide, focusing on the social, environmental, and technological aspects of renewables (Oh et al., 2012; 2019; Chen et al., 2020a; 2020b; 2021; Hoseinzadeh and Heyns, 2020; Jamil et al., 2021; Hoseinzadeh and Stephan Heyns, 2022).

Jeju self-governing province is promoting the expansion of renewable energy by conducting the “Carbon Free Island Jeju 2030” project, which is a low carbon green growth model to cope

with climate change as well as to establish zero net energy island (Lee et al., 2021; Mun et al., 2021). Although the installed capacities of solar and wind energy are 130 MW and 270 MW, which is account for 60.7% of the total electricity demand of Jeju, their annual utilization rates are only 23% and 13%, respectively due to unstable weather conditions (Ko et al., 2019).

Geothermal heat pump systems tend to have higher energy efficiency than conventional air source heat pump systems, having no equipment exposed to the atmosphere, and are more stable than other heat sources in heating and cooling cycles throughout the year (Tye-Gingras and Gosselin, 2014). Most of the existing geothermal cooling and heating facilities in Korea were installed in the early 2000s, and ground heat exchanger technologies (e.g., vertical closed-loop type and open-loop type) suitable for domestic soil structures have been continuously developed (Yearbook of Regional Energy Statistics, 2022). It is difficult, however, to apply these technologies to high-density subsoils such as the porous basalt foundation (similar to granite) found on Jeju Island. The geology of the island, which was formed by volcanic activity, is characterized by repeated basalt and pyroclastic layers (clinker, scoria). In addition, small-scale rocks have accumulated—rather than extensive rock formation—in many areas due to volcanic eruptions and lava flows (Park et al., 2021). Consequently, structures that allow surface air or water to be easily introduced into the ground are prevalent, allowing for the relatively free flow of water and air.

The Hydrogeologic characteristic of the island hinders the employment of the existing borehole heat exchanger such as a vertical closed-loop geothermal heat exchanger and a horizontal closed-loop heat exchanger that extract geothermal energy by conduction heat transfer with the ground. Furthermore, the drilling cost is relatively high compared to inland areas since the thickness of the soil layer is thin as well as the ground is mainly composed of rocks. It is also banned to use an open-loop geothermal system on Jeju Island due to regulations that prohibits the use of groundwater as an energy source.

For such reasons, Jeju Island has been recognized as an area where the use of geothermal energy is inappropriate. To address this problem, underground air in basalt layers has been utilized as the heat source in systems installed in agricultural facilities on Jeju Island (Kang and Lim, 2016). The geothermal energy harvested by such method, however, has not been certified as a renewable energy source for the reason that it is different from the existing geothermal energy utilization method. Adoption of the technology has been hampered due to the high relative humidity of the underground air as well as the claim that radon exists (in trace amounts) and that the process releases underground CO₂.

Recently, the land use ordinances of Jeju Island have been revised to allow the installation of heat exchangers in groundwater, given that geothermal energy based on groundwater has a very high heat capacity, the feasibility of such systems is expected to be high. Although cooling and heating systems that use groundwater heat sources were supplied after the ordinance revision, the heat exchangers used in these systems are made of high-density polyethylene (HDPE), which has also been used in underground air source systems.

Many studies have been conducted both theoretically and experimentally in order to improve the thermal energy system's efficiency (Ng et al., 2021; Alizadeh et al., 2022; Hossein Zolfagharnasab et al., 2022). Hossein Zolfagharnasab et al. (2022) applied porous materials to a shell and tube heat exchanger and

TABLE 1 Dimensions of borehole.

Borehole depth (m)	65
Grout depth (m)	35
Borehole diameter (mm)	250
Underground water level (m)	35

investigated the heat transfer rate. They concluded that the proposed porous-filled heat exchanger exhibits 60% higher efficiency compared to the conventional heat exchanger. Ng et al. (2021) developed a thermodynamic platform that can be used to assess the energy efficiency of combined power generation and desalination plants. The proposed platform was evaluating the energy efficiency of any thermal system by introducing the primary energy concept. Alizadeh et al. (2022) experimentally investigated heat pipes in order to improve the energy performance of a heat-recovery system. Their result revealed that the heat-pipe heat exchanger could reduce the consumption of natural gas by 510,132 SCM a year.

In this study, an advanced heat exchanger made of a stainless with high thermal conductivity was developed to increase the utilization of geothermal heat, including groundwater heat. In addition, the heat capacities of the developed heat exchangers were compared with HDPE heat exchanger in order to assess the feasibility of geothermal energy systems suitable for the particular geology of Jeju Island.

2 Experimental apparatus

2.1 Borehole construction

A borehole was excavated using the method stipulated in the ordinance of Jeju Island. Based on the excavation point, concrete is poured into the area of at least 3 m (horizontal) by 3 m (vertical) at a thickness of 30 cm or more and cured for at least 24 h. Excavation to a certain depth (35 m by the ordinance) is then performed with a diameter of 450 mm, and grouting is performed to prevent groundwater pollution caused by the collapse of the perforation area. Afterward, the second perforation is performed to the required depth with a 250 mm borehole. In addition, a corrosion-resistant casing must be installed at the top of the borehole to prevent water pollution and damage to the perforation area.

In Table 1, we present the dimensions of the borehole constructed for the experiment. The borehole was constructed in accordance with the regulations of the ordinance, and the total borehole depth was 65 m due to the underground water level.

2.2 Heat exchanger

The flow velocity of the groundwater varies depending on the altitude difference. Due to the presence of pyroclastic layers, upper groundwater also falls from the top to the bottom of the borehole. The largest problem with the commonly used HDPE heat exchangers is that they are lost from the inlet/outlet headers due to the flow of groundwater and the impact of falling upper groundwater. This inhibits the function of the exchanger and causes groundwater

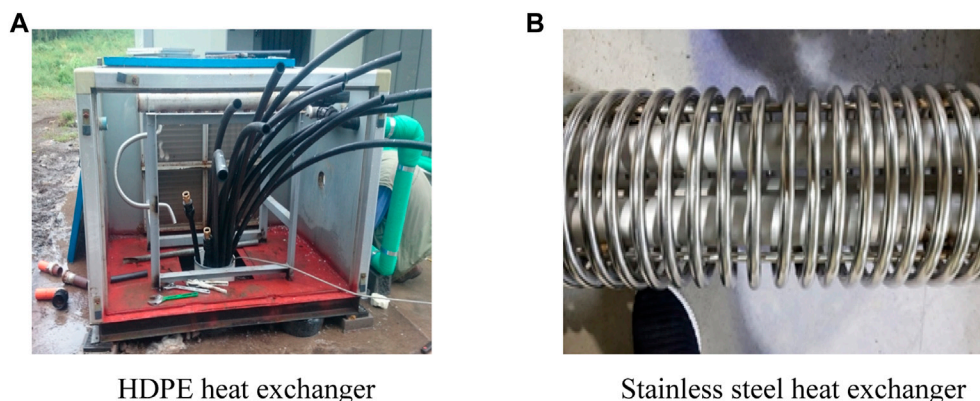


FIGURE 1

Borehole heat exchangers used in Jeju island. (A) HDPE heat exchanger, (B) Stainless steel heat exchanger.

TABLE 2 Dimensions of the heat exchangers.

HDPE heat exchanger		
Diameter (mm)	34	
Thickness (mm)	3.5	
Total length (m)	560(35*2*8)	
Stainless steel heat exchanger		
Diameter (mm)	Main	Coil
	48.6	16
Thickness (mm)	2.8	2.1
Total length (m)	70	810

pollution. It is also difficult to insert the exchangers into the borehole during the installation because of the high buoyancy and low thermal conductivity of the plastic units. Owing to the low thermal conductivity, it is also questionable whether such units can acquire sufficient thermal energy from the groundwater.

To address these problems, a heat exchanger with pipes made of STS316 (stainless steel) was developed. The new unit enables the use of welding or flanges, is applicable to a site where a longer heat exchanger is needed due to the high altitude, causes little concern over the separation caused by the pressure of upper groundwater, and has high thermal conductivity and corrosion resistance. The largest benefit of this type of heat exchanger is that it is possible to remove it for repair or replacement without damage to the borehole. The geometry of the two different heat exchangers is shown in Figure 1. In the case of the HDPE heat exchanger (Figure 1A), eight U-tubes from the heat exchanger supply header inside the casing at the top of the borehole are connected to the return header. A U-tube has an outer diameter of 34 mm, a thickness of 3.5 mm, and a length of 70 m. The newly developed STS316 heat exchanger is shown in Figure 1B.

The two main pipes (inlet and return pipes) with a diameter of 48.6 mm and a thickness of 2.8 mm are surrounded by the coil-type

pipe, with a diameter of 16 mm and a thickness of 2.1 mm, to increase the heat transfer area. The heat exchanger comprises 15 coil heat exchangers as it is distributed to three coil heat exchangers per 6 m of the main pipe. The circulating water descends to the location of groundwater through the inlet pipe and passes through the coil-type pipe and the return pipe, resulting in heat exchange. The total length of the main pipe is 70 m, and that of the coil-type pipe is 810 m. The dimensions of each heat exchanger are given in Table 2.

3 Experimental method

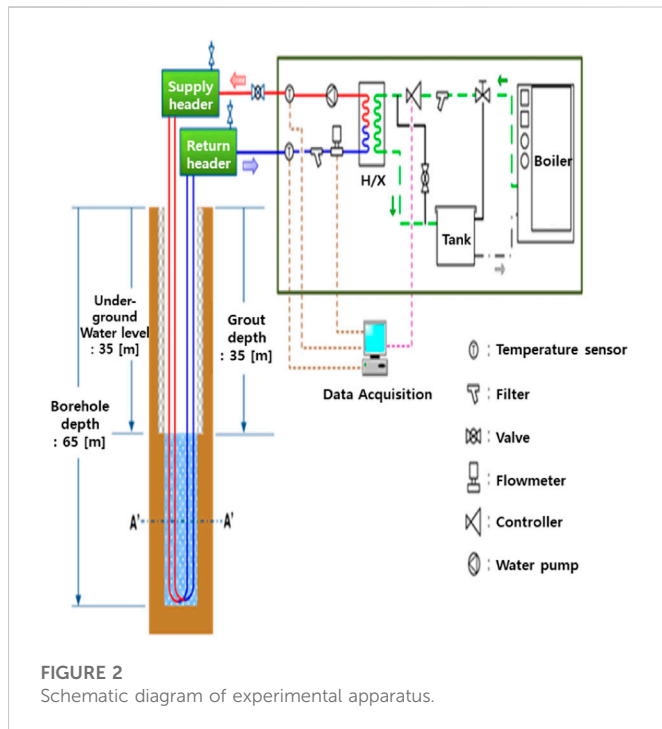
A facility cultivation farm located in Doryeon-dong, Jeju-si, was selected as the experimental site at which we compared the performance of the heat exchangers. After drilling two holes according to the dimensions in Table 1, the HDPE and STS316 heat exchangers were inserted, and their thermal characteristics were compared and analyzed.

The borehole heat exchangers are generally evaluated by thermal response testing, which is a method for determining the thermal properties of ground materials, mainly the thermal conductivity and ground temperature. The heat transfer fluid (HTF) circulates inside the heat exchanger while it either absorbs or releases heat from/to the grout and the surrounding soil depending on the operation mode (heating or cooling). Thus, the rate of heat transfer (W/m) that can be extracted by the heat transfer is approximated by measuring the thermal conductivity. In this study, however, thermal response testing is unable to use since the heat transfer between HFT in the heat exchanger and the groundwater mainly takes place by convection mechanism. Hence, it is difficult to find out the rate of heat transfer for the proposed borehole heat exchangers without measuring the conductivity.

In this study, therefore, we calculated the rate of heat transfer in the unit of Watt by measuring the temperature of the outlet water that passed through the heat exchanger while inputting constant energy into the heat exchanger.

The rate of heat transfer can be expressed using Eq. 1 and the mean temperature with Eq. 2.

$$Q = \dot{m} \times c_p \times (T_i - T_o) \quad (1)$$



$$T_m = \frac{(T_i + T_o)}{2} \quad (2)$$

where Q is the heat transfer rate (kW), m is the mass flow rate of the circulating water (kg/min), c_p is the specific heat of the circulating water (kJ/kg·°C), and T (°C) is the temperature of the circulating water. The subscripts i , o , and m represent the temperature of the circulating water at the inlet, outlet, and the mean, respectively.

In the experimental apparatus of this study, the inlet temperature (T_i) was increased by inputting energy through an electric hot water boiler while maintaining the flow rate of the working fluid flowing into the heat exchange at a constant level, and the temperature difference from the outlet temperature (T_o) was measured to compare and analyze the amount of heat exchanged for each heat exchanger (made of different materials).

Figure 2 shows a schematic of the experimental apparatus. The main devices include a 100 kW hot water boiler to increase the temperature of the influent, a circulating water pump, sensors to measure the temperature and flow rate, and the data-recording device. First, each ground heat exchanger was filled with water (the circulating water). The circulation pump was operated with no energy input until the temperature of the groundwater and circulating water was maintained at a steady state. The initial temperature of the circulating water was then determined.

The flow rate was maintained at a constant level, approximately 180 LPM. The inlet temperature of the circulating water was increased by operating the boiler. A steady state was assumed to have been reached when the mean temperature of the inlet and outlet temperatures (T_m) showed no change for more than 10 min, at which point the next experiment was performed by inputting additional energy. Through this stepwise input of energy, three experiments were performed for the HDPE heat exchanger and four experiments for the stainless steel heat exchanger.

4 Results and discussion

Because the heat release capacity of the portable experimental apparatus could not exceed 100 kW, all experiments were carried out within this range. The experimental conditions for the HDPE heat exchanger and the newly developed STS316 heat exchanger are shown in Table 3. In the case of the HDPE heat exchanger, three experiments were performed while changing the inlet temperature of the circulating water from 21.6°C to 36.2°C. As for the STS316 heat exchanger, experiments were performed in four cases while changing the inlet temperature from 19.7°C to 27.1°C. A constant flow rate of approximately 180 LPM was maintained. The surface area was 59.8 m² for the HDPE heat exchanger and 51.4 m² for the STS316 heat exchanger.

Figures 3, 4 show the inlet/outlet temperatures, mean temperature, and heat gain obtained from Eq. 1 for the HDPE and STS316 heat exchangers, respectively. The inlet/outlet temperatures of the HDPE heat exchanger continuously and gradually increased, and it took considerable time to reach a steady state. In the case of STS316, however, a steady state was reached rapidly—within approximately 25 min after the temperature rise.

In Figure 3, CASE 1 represents the experimental data when the mean inlet temperature of the circulating water in the HDPE exchanger was set to 21.6°C. The mean outlet temperature was 20.7°C, and the heat gain was approximately 11.2 kW. In CASE 2, the mean inlet temperature of the circulating water was set to 28.7°C. The mean outlet temperature was 26.7°C, and the heat gain was approximately 25.2 kW. In CASE 3, the mean inlet temperature of the circulating water was set to 36.2°C. The mean outlet temperature was 33.1°C, and the heat gain was approximately 39.9 kW.

In Figure 4, CASE 4 represents the experimental data when the mean inlet temperature of the circulating water in the STS316 exchanger was set to 19.7°C. The mean outlet temperature was 18.1°C, and the heat gain was approximately 20.4 kW. In CASE 5, the mean inlet temperature of the circulating water was set to 21.6°C. The mean outlet temperature was 19.2°C, and the heat gain was approximately 30.7 kW. In CASE 6, the mean inlet temperature of the circulating water was set to 23.4°C. The mean outlet temperature was 20.2°C, and the heat gain was approximately 40.9 kW. In CASE 7, the mean inlet temperature of the circulating water was set to 27.1°C. The mean outlet temperature was 22.1°C, and the heat gain was approximately 63.9 kW.

TABLE 3 Test conditions.

H/X	Test	Flow	T _i	T _o	T _m
Type	Code	Rate (L/min)	(°C)	(°C)	(°C)
HDPE	CASE 1	180.8	21.6	20.7	21.2
	CASE 2	180.9	28.7	26.7	27.7
	CASE 3	180.9	36.2	33.1	34.7
STS316	CASE 4	182.6	19.7	18.1	18.9
	CASE 5	183.1	21.6	19.2	20.5
	CASE 6	183.2	23.4	20.2	21.8
	CASE 7	183.3	27.1	22.1	24.6

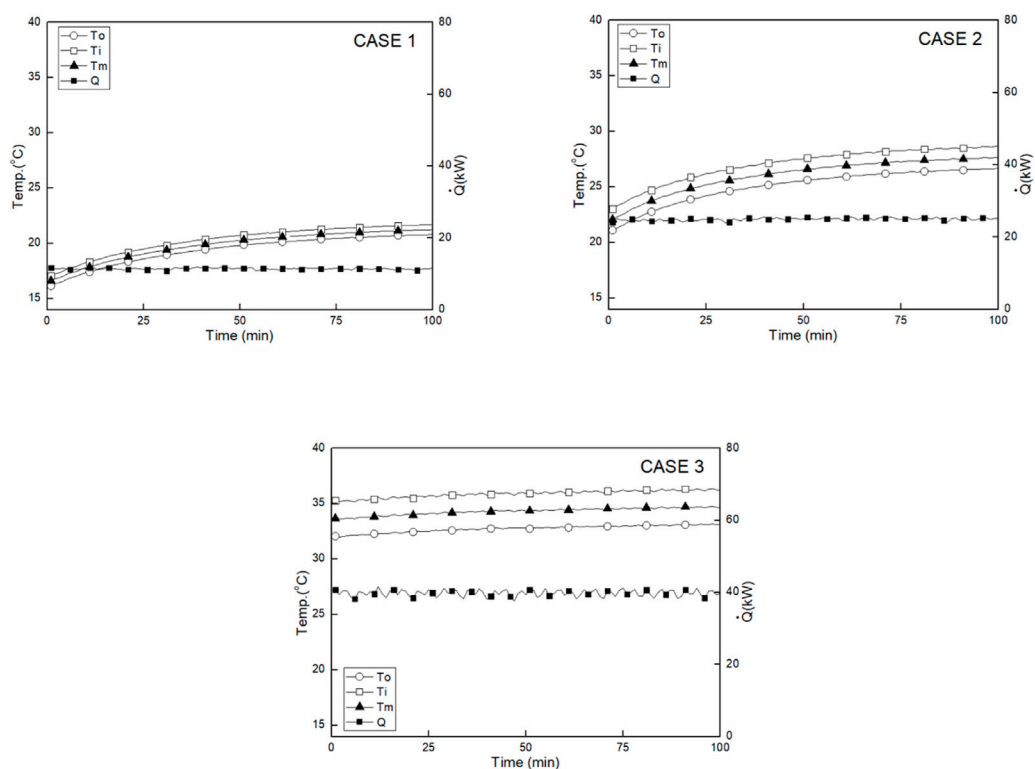


FIGURE 3

Variation of the T_i , T_o , T_m and power consumption (HDPE H/X).

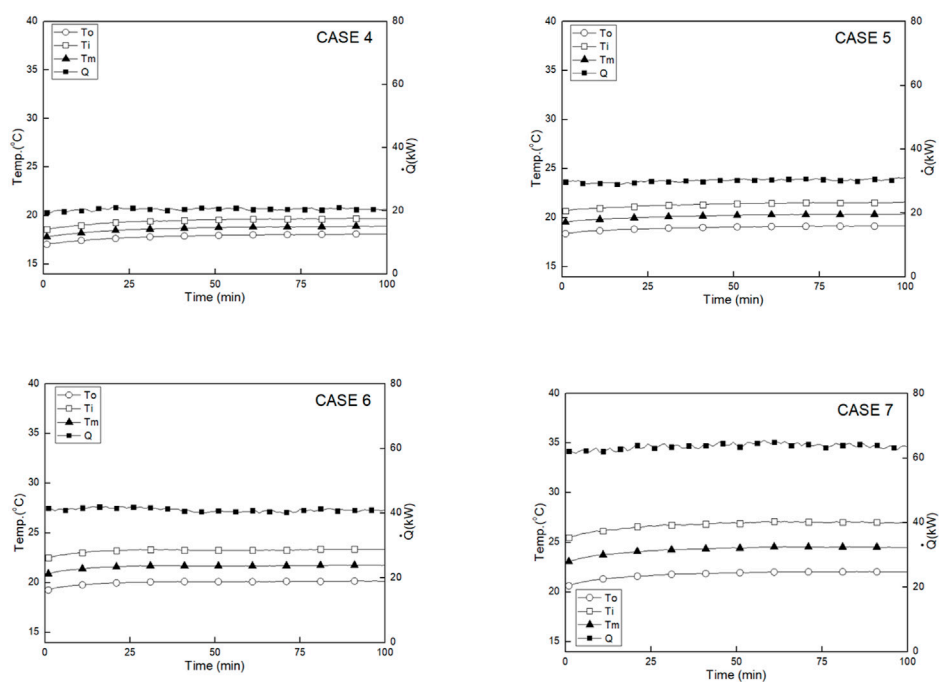
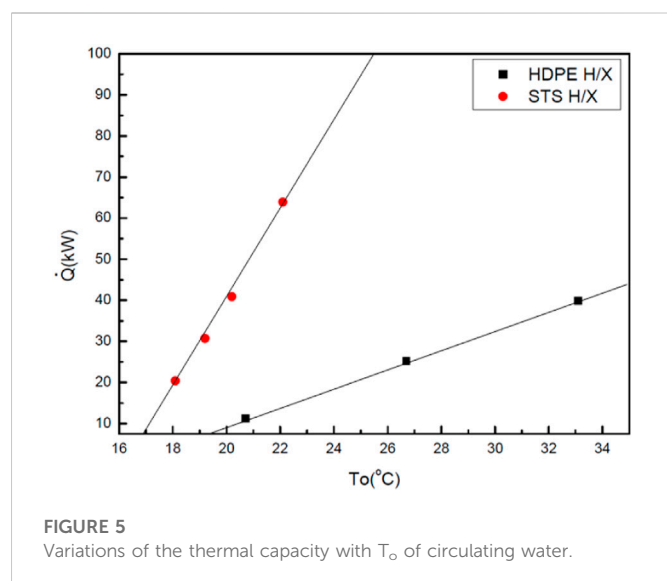


FIGURE 4

Variation of the T_i , T_o , T_m and power consumption (STS H/X).



In the heat capacity test, the maximum heat capacity was found to be approximately 39.9 kW for the HDPE pipe and 63.9 kW for the STS316 pipe, indicating that the heat gain of the STS316 heat exchanger can be approximately 160% higher than that of the HDPE heat exchanger.

Figure 5 shows the variations of the heat gain for two different heat exchangers with the outlet temperatures of circulating water. It is noteworthy that in the cooling mode, the circulating water enters in to the condenser of a water-to-water heat pump and its temperature rises by the refrigerant that circulate the loop of heat pump and then it flows back to the borehole heat exchanger to release the heat to the groundwater. From this graph, we can predict the heat gain for the heat exchangers at any given outlet temperature. For instance, when the inlet temperature to the condenser of a heat pump is at 25°C which is a test condition under KS B 8292 standards for a water-to-water geothermal heat pump unit, the heat gain for STS heat exchanger is equal to 94 kW. It can be easily inferred that the performance of STS heat exchanger is four times higher than that of the HDPE heat exchanger.

5 Conclusion

In this study, an advanced borehole exchanger was developed and investigated by comparing its performance with a conventional high-density polyethylene (HDPE) exchanger. The key findings from this study include:

- 1) The heat gain of the STS heat exchanger was found to be approximately four times higher than that of the HDPE heat exchanger under the same borehole conditions and ground loop system test conditions (KS B 8292; water-to-water geothermal heat pump unit), notwithstanding that the heat transfer area of the STS exchanger is approximately 15% smaller.
- 2) When the outlet temperature was measured while changing the inlet temperature of the circulating water in each heat exchanger, it was found that considerable time was required for the HDPE heat exchanger to reach a steady state. In contrast, the STS316 heat

exchanger reached a steady state approximately 25 min after the temperature rise.

- 3) The difference in performance is probably due to the difference in thermal properties of the HDPE and STS heat exchangers; the STS unit has a relatively higher thermal conductivity, which is favorable for acquiring heat from the ground. Thus, the STS heat exchanger has a higher heat gain.

It is expected that the results of this study will be useful in designing new heat exchangers in the Jeju area. Further research should be carried out on ground heat exchangers made of different materials other than STS and HDPE heat exchangers. Furthermore, it is expected that the COP can be improved up to five when a water-to-water heat pump uses the proposed bore hole heat exchanger in Jeju island.

Data availability statement

The original contributions presented in the study are included in the article/supplementary material, further inquiries can be directed to the corresponding author.

Author contributions

JK: data collection and draft manuscript. Y-MK: data analysis. YK: figures. QC: study conception. CX: result interpretation. SO: manuscript preparation and funding.

Funding

This work was supported by the Renewable Surplus Sector Coupling Technology Program of the Korea Institute of Energy Technology Evaluation and Planning (KETEP) granted financial resource from the Ministry of Trade, Industry and Energy, Republic of Korea (No. 20226210100050) and supported by Korea Institute of Planning and Evaluation for Technology in food and Planning (IPET) funded by Ministry of Agriculture, Food and Rural Affairs (MAFRA) (No. 320048-3).

Conflict of interest

JK was employed by Intertech Co., Ltd.

The remaining authors declare that the research was conducted in the absence of any commercial or financial relationships that could be construed as a potential conflict of interest.

Publisher's note

All claims expressed in this article are solely those of the authors and do not necessarily represent those of their affiliated organizations, or those of the publisher, the editors and the reviewers. Any product that may be evaluated in this article, or claim that may be made by its manufacturer, is not guaranteed or endorsed by the publisher.

References

- Alizadeh, A., Ghadamian, H., Aminy, M., Hoseinzadeh, S., Khodayar Sahebi, H., and Sohani, A. (2022). An experimental investigation on using heat pipe heat exchanger to improve energy performance in gas city gate station. *Energy* 252, 123959. doi:10.1016/j.energy.2022.123959
- Alrowais, R., Qian, C., Burhan, M., Ybyraiymkul, D., Shahzad, M. W., and Ng, K. C. (2020). A greener seawater desalination method by direct-contact spray evaporation and condensation (DCSEC): Experiments. *Appl. Therm. Eng.* 179, 115629. doi:10.1016/j.applthermaleng.2020.115629
- Bogdanov, D., Ram, M., Aghahosseini, A., Gulagi, A., Oyewo, A. S., Child, M., et al. (2021). Low-cost renewable electricity as the key driver of the global energy transition towards sustainability. *Energy* 227, 120467. doi:10.1016/j.energy.2021.120467
- Chen, Q., Alrowais, R., Burhan, M., Ybyraiymkul, D., Shahzad, M. W., Li, Y., et al. (2020a). A self-sustainable solar desalination system using direct spray technology. *Energy* 205, 118037. doi:10.1016/j.energy.2020.118037
- Chen, Q., Muhammad, B., Akhtar, F. H., Ybyraiymkul, D., Muhammad, W. S., Li, Y., et al. (2020b). Thermo-economic analysis and optimization of a vacuum multi-effect membrane distillation system. *Desalination* 483, 114413. doi:10.1016/j.desal.2020.114413
- Chen, Q., Burhan, M., Shahzad, M. W., Ybyraiymkul, D., Akhtar, F. H., Li, Y., et al. (2021). A zero liquid discharge system integrating multi-effect distillation and evaporative crystallization for desalination brine treatment. *Desalination* 502, 114928. doi:10.1016/j.desal.2020.114928
- Gani, A. (2021). Fossil fuel energy and environmental performance in an extended STIRPAT model. *J. Clean. Prod.* 297, 126526. doi:10.1016/j.jclepro.2021.126526
- Hoseinzadeh, S., and Heyns, P. S. (2020). Thermo-structural fatigue and lifetime analysis of a heat exchanger as a feedwater heater in power plant. *Eng. Fail. Anal.* 113, 104548. doi:10.1016/j.engfailanal.2020.104548
- Hoseinzadeh, S., and Stephan Heyns, P. (2022). Development of a model efficiency improvement for the designing of feedwater heaters network in thermal power plants. *J. Energy Resour. Technol.* 144, 072102. doi:10.1115/1.4054196
- Hossein Zolfagharnasab, M., Zamani Pedram, M., Hoseinzadeh, S., and Vafai, K. (2022). Application of Porous-Embedded shell and tube heat exchangers for the Waste heat Recovery Systems. *Appl. Therm. Eng.* 211, 118452. doi:10.1016/j.applthermaleng.2022.118452
- Jamil, M. A., Goraya, T. S., Ng, K. C., Zubair, S. M., Xu, B. B., and Shahzad, M. W. (2021). Optimizing the energy recovery section in thermal desalination systems for improved thermodynamic, economic, and environmental performance. *Int. Commun. Heat Mass Transf.* 124, 105244. doi:10.1016/j.icheatmasstransfer.2021.105244
- Kang, Y.-K., and Lim, T.-S. (2016). The Analysis of heating performance of heat pump system for agricultural facility using underground air in Jeju area - focused on the Jeju Area -. *KIEAE J.* 16, 109–114. doi:10.12813/kieae.2016.16.6.109
- Ko, W., Lee, J., and Kim, J. (2019). The effect of a renewable energy certificate incentive on mitigating wind power fluctuations: A case study of Jeju island. *Appl. Sci.* 9, 1647. doi:10.3390/app9081647
- Lanzi, E., Verdolini, E., and Haščič, I. (2011). Efficiency-improving fossil fuel technologies for electricity generation: Data selection and trends. *Energy Policy* 39, 7000–7014. doi:10.1016/j.enpol.2011.07.052
- Lee, J., Lee, J., and Wi, Y.-M. (2021). Impact of revised time of use tariff on variable renewable energy curtailment on Jeju island. *Electron. (Basel)* 10, 135. doi:10.3390/electronics10020135
- Martins, T., Barreto, A. C., Souza, F. M., and Souza, A. M. (2021). Fossil fuels consumption and carbon dioxide emissions in G7 countries: Empirical evidence from ARDL bounds testing approach. *Environ. Pollut.* 291, 118093. doi:10.1016/j.envpol.2021.118093
- Mun, H., Moon, B., Park, S., and Yoon, Y. (2021). A study on the economic feasibility of stand-alone microgrid for carbon-free island in Korea. *Energies (Basel)* 14, 1913. doi:10.3390/en14071913
- Ng, K. C., Burhan, M., Chen, Q., Ybyraiymkul, D., Akhtar, F. H., Kumja, M., et al. (2021). A thermodynamic platform for evaluating the energy efficiency of combined power generation and desalination plants. *NPJ Clean. Water* 4, 25. doi:10.1038/s41545-021-00114-5
- Oh, S. J., Lee, Y. J., Chen, K., Kim, Y. M., Lim, S. H., and Chun, W. (2012). Development of an embedded solar tracker for the enhancement of solar energy utilization. *Int. J. Energy Res.* 36, 249–258. doi:10.1002/er.1813
- Oh, S. J., Shahzad, M. W., Burhan, M., Chun, W., Kian Jon, C., Kumja, M., et al. (2019). Approaches to energy efficiency in air conditioning: A comparative study on purge configurations for indirect evaporative cooling. *Energy* 168, 505–515. doi:10.1016/j.energy.2018.11.077
- Park, J. B., Koh, G. W., Jeon, Y., Park, W. B., Moon, S. H., and Moon, D. C. (2021). Geology and volcanism of hyeongjeseom (islet) volcano, Jeju island. *Econ. Environ. Geol.* 54, 187–197. doi:10.9719/EEG.2021.54.2.187
- Shahzad, M. W., Burhan, M., Ang, L., and Ng, K. C. (2017). Energy-water-environment nexus underpinning future desalination sustainability. *Desalination* 413, 52–64. doi:10.1016/j.desal.2017.03.009
- Tye-Gingras, M., and Gosselin, L. (2014). Generic ground response functions for ground exchangers in the presence of groundwater flow. *Renew. Energy* 72, 354–366. doi:10.1016/j.renene.2014.07.026
- Yearbook of Regional Energy Statistics (2022). *Yearbook of regional energy statistics*. Available at: <http://www.kesis.net>.

Nomenclature

HDPE high-density polyethylene

RT refrigeration ton

STS stainless steel

Q heat transfer rate (kW)

\dot{m} mass flow rate (kg/s)

T temperature (°C)

c_p specific heat (kJ/kg°C)



OPEN ACCESS

EDITED BY

N. Emekwuru,
Coventry University, United Kingdom

REVIEWED BY

Michele Rocca,
University of Pisa, Italy
Roberto Alonso González-Lezcano,
CEU San Pablo University, Spain

*CORRESPONDENCE

Mpho Ndou,
✉ jrndou@gmail.com

[†]These authors have contributed equally
to this work and share first authorship

SPECIALTY SECTION

This article was submitted
to Indoor Environment,
a section of the journal
Frontiers in Built Environment

RECEIVED 14 December 2022

ACCEPTED 23 March 2023

PUBLISHED 14 April 2023

CITATION

Ndou M and Aigbavboa C (2023),
Exploring environmental policy adoption
enablers for indoor air quality
management in higher educational
institutions in South Africa.
Front. Built Environ. 9:1124248.
doi: 10.3389/fbuil.2023.1124248

COPYRIGHT

© 2023 Ndou and Aigbavboa. This is an
open-access article distributed under the
terms of the [Creative Commons
Attribution License \(CC BY\)](#). The use,
distribution or reproduction in other
forums is permitted, provided the original
author(s) and the copyright owner(s) are
credited and that the original publication
in this journal is cited, in accordance with
accepted academic practice. No use,
distribution or reproduction is permitted
which does not comply with these terms.

Exploring environmental policy adoption enablers for indoor air quality management in higher educational institutions in South Africa

Mpho Ndou^{*†} and Clinton Aigbavboa[†]

CIDB Centre of Excellence and Sustainable Human Settlement and Construction Research Centre,
Faculty of Engineering and the Built Environment, University of Johannesburg, Johannesburg, South
Africa

Purpose: This study seeks to investigate the extent to which the indoor air quality (IAQ) management of higher educational institutions (HEIs) in South Africa could be improved through the appropriate implementation of environmental policy adoption enablers. Multiple challenges have been documented to the improvement of IAQ standards in HEIs. However, an alternative to the management of IAQ is possible through environmental behavioral change.

Research Methodology: A philosophical stance of post-positivism influences the adoption of a quantitative research approach for this study. Primary data on the views shared by various academic and administrative staff employed by HEIs across South Africa were collected using a closed-ended questionnaire survey. A literature review uncovered 16 influential environmental policy adoption enablers that could further the objective of the study. A four-phase data analytical approach was adopted to interpret the empirical data through screening and reliability assessment, together with descriptive and inferential statistical evaluations, to ascertain the influence held by the surveyed policy adoption enablers on improving the management of IAQ in HEIs.

Results: The inferential statistical evaluation using exploratory factor analysis revealed three crucial environmental policy adoption metrical approaches (stakeholder dialogue, institutional commitment, and policy composition) to the management of IAQ in HEIs.

Discussion: From a practical perspective, the administrative council of HEIs could consider the identified policy adoption enablers as a catalyst for pro-environmental behavior and the management of IAQ in all respective institutions. Theoretically, this study contributes to the body of knowledge by providing factors associated with environmental policy adoptions for IAQ management and laying the groundwork for future research in environmental behavior, this has been lacking in previous IAQ studies and current environmental management discourse. As an instrumental enabler, the identified policy adoption approaches could inform any existing or new institutional policy adoption initiative aimed at improving current individuals' perception of workplace comfort, satisfaction, and performance directly associated with their indoor environmental conditions.

KEYWORDS

environment, indoor air quality (IAQ), policy, quality education, well-being

1 Introduction

Higher educational institutions (HEIs) are key to developing any country's social, political, and economic systems. Alemu (2019) described HEIs as a collective of institutions administering teaching, learning, and content creation in a conducive environment at the tertiary level. Due to their important role, the failure of HEIs to meet their objective function—education in its entirety—would delay any transformative goal a country might have for its development (economic growth, social dynamics, and policies). Since most people spend most of their time indoors, challenges associated with health issues experienced by occupants have become a growing concern since worsening climate change influences human well-being and performance in various ways (Al Horr et al., 2016; Mohamed et al., 2021). Furthermore, the continuous decay of environmental conditions has been fueled by industrialization's quest to develop “archaic” environments. However, the opposite is true, as the very environmental development activities now threaten their beneficiaries (Alam and Paramati, 2015; Shahbaz et al., 2019). A conducive facility for teaching and learning is necessary for the pursuit of occupant well-being, optimal productivity, and quality education; this can be achieved through adequate indoor environmental quality (IEQ) management of HEIs (Sadick, 2018).

The first initiative in addressing IEQ inadequacies is to understand the elements that affect it and its effect on the occupants of indoor spaces. The phenomenon of IEQ encompasses four main environmental conditions: air quality (constituents, odors, and pollutants), thermal environment (temperature and humidity), acoustics (sound), and luminance (light) (Sakhare and Ralegaonkar, 2014; Godish, 2016). The current study focused mainly on indoor air quality (IAQ) since multiple studies have been conducted on empirical IEQ assessment modeling and indexing, together with the overall influence of IEQ and its impact on energy performance (Sakhare and Ralegaonkar, 2014; Leccese et al., 2021). To date, there have been limited efforts to create a legislative directive that addresses the well-being of occupants specifically in relation to their IAQ environment. However, environmental regulatory standards and/or legislative policies aimed at alleviating pollution are in place and are used as a form of IAQ guidelines by the European Union (Bluyssen, 2010). It must be noted that, for an ideal indoor environment in any country, guidelines and standards are necessary and should reflect internal (political, economic, and social status) and external (geographical disposition and climate regime) factors.

There is limited information on the overall satisfaction with IAQ management in HEIs, especially in developing countries. Mendell and Heath (2005) emphasized the lack of empirical data on the influence of thermal conditions in academic environments. Although most countries have adopted the benchmarked and accepted international standards or guidelines from ASHRAE (American Society of Heating, Refrigerating, and Air-Conditioning Engineers), the European Commission (EC), the World Health Organization (WHO), and the International Organization for Standardization (ISO), not all environmental

parameters have been adopted by all countries (Bluyssen, 2010; Abdul-Wahab et al., 2015; Mujeebu and Bano, 2022). Thus, it is necessary to review how these policies can be better implemented and adopted in key public indoor spaces such as HEIs. The current study, therefore, seeks to investigate critical enablers that will allow for better IAQ management in HEIs in South Africa through the adoption of environmental policies. Practically, the study contributes to the body of knowledge on IAQ by identifying crucial policy adoption enablers in the quest for a conducive teaching and learning environment. The study begins with a review of the literature and an outline of the research methodology adopted. The data collected are analyzed, followed by conclusions and recommendations drawn from the study's findings.

2 Literature review

Respiration is the pathway to life, but while we breathe every second, not every breath is clean. WHO (2015) advocates that every human should have access to healthy indoor air within their indoor environments, as the air we breathe affects our health, which in turn influences our quality of life and well-being. The inadequacy of IAQ control can be linked to various factors associated with ambient conditions, indoor and outdoor contaminants, construction materials, and poor building design and maintenance. Similarly, thermal comfort is affected by various mediating variables such as the season, age, gender, ethnicity, geographical climate, and location (Mohamed et al., 2021; Hormigos-Jimenez et al., 2018). Awareness of health and its significance for adequate IAQ is limited in many developing societies, including South Africa (Brits, 2012). Although efforts have been made to establish environmental policies that have human interests at heart, limited development has been seen in creating IAQ legislation specific to South Africa. The first initiative in combating any poor IAQ environment is to introduce an IAQ-specific policy that deals with the underlying elements that affect the IAQ environment and the required adoption appetite to ensure its implementation.

Increasing environmental concerns over global warming, environmental decay, and pollution (both external and internal) cannot be resolved in isolation, owing to the complex direct and indirect interactions of stakeholders. Behavioral change toward any normative environmental standard requires a collective effort to shape and encourage a commitment to change (Yu and Yu, 2017). Thus, for effective change management toward any new innovative transition, such as IAQ management, the synchronization of the attitude and knowledge of an individual or group (HEIs' stakeholders) is affected by the innovation (Boudreau and MacKenzie, 2014). This study identified its stakeholders as institutional management (departmental schools, the academic senate, and facilities and operational management), the institutional community (professional and administrative staff), and the government (the Department of Education and the Department of Higher Education and Training, both nationally and locally). There is only limited literature that recognizes the

TABLE 1 Policy adoption enablers.

Enablers	Literature
Stakeholder salience (coherent engagement)	Zardo et al. (2014); Daddi et al. (2016)
Transparency (procedures and regulations)	Westerheijden and Kohoutek (2014)
Transformative regulations	Westerheijden and Kohoutek (2014)
Institutional environment (economic and political conditions)	Institute of Medicine (IOM) (2011); Sebri and Ben-Salha (2014)
Alleviate environmental concerns (pollution, etc.)	Institute of Medicine (IOM). (2011)
Defined economic benefits	Bornstein and Thalmann (2008); Chitescu and Lixandru (2016)
Institutional support (environmental guidance and counseling)	Bell et al. (2013); Westerheijden and Kohoutek (2014); Dermont et al. (2017)
Pro-environmental behavior (individual attitude and knowledge)	Boudreau and MacKenzie (2014); Colombo and Kriesi (2017)
Societal values and norms	Nolan et al. (2008); Eggins (2014)
Institutional structure	Taweekaw (2014)
Qualification of the proposal (simple or complex)	Van Rijnsoever et al. (2015); Dermont et al (2017)
Risk management (environmental, market, etc.)	Institute of Medicine (IOM) (2011)
Availability of policy information	Boudreau and MacKenzie (2014)
Complementing institutional goals (compatibility)	Eggins (2014)
Policy intention (translatable policy design)	Benoit (2013)
Type of policy instrument (rule- or incentive-based)	Feng and Chen (2018)

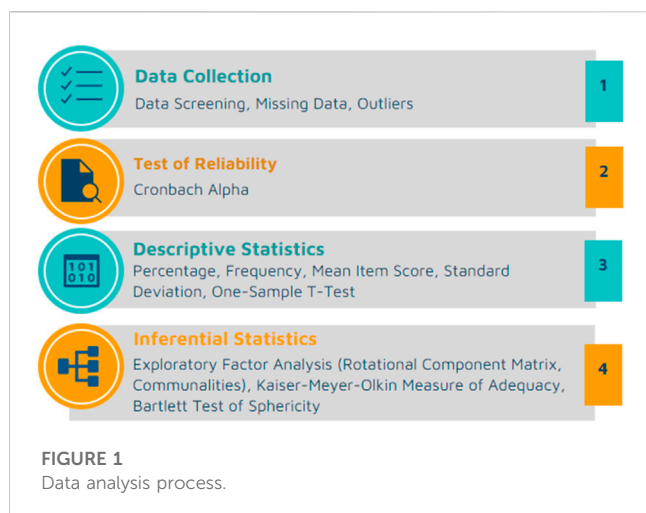
institutional community as a key stakeholder in IAQ management in HEIs. At face value, institutional management is seen as fulfilling a “collective” managerial and leadership function, while the institutional community contributes an “individual” or career-focused role within the broader sense of HEI stakeholders (Marshall, 2018).

Similarly, Zardo et al. (2014) add that the coherency of the stakeholders who drive the change is crucial when establishing an instrument of change (policy model). Benoit (2013) observed that introducing a form of change requires a policy instrument that may be adopted as a guiding tool toward the desired change. In the same vein, Bornstein and Thalmann (2008) also revealed that the envisaged economic benefits of adopting an environmental policy needed to be defined or outlined during its developmental stages to emphasize its importance. Moreover, the type of policy instrument that is driving the change is a key factor in its adoption by various stakeholders (Stadelmann-Steffen, 2011): an incentive-based policy instrument requires a reward-based approach to ensure change, while a rule- or ban-based policy tends to be less favored. However, the availability of information on the intended environmental policy is fundamental to providing environmental guidance and counseling on how to transform ideas about regulation into enforceable instruments (Westerheijden and Kohoutek, 2014). Through environmental knowledge, a policy's compatibility with addressing some of the institutional objectives can be assessed (Dill, 2012; Eggins, 2014).

Failure to provide reliable and accurate value engineering exercises related to the design and constructability of new buildings and the renovation of older buildings costs employers far less than the cost of poor productivity and the ill health of employees (Alrazni, 2016). Mohamed et al. (2021) argued that maintaining adequate IAQ is the most profitable strategy for any public or private institution. Many office buildings, such as academic

institutions utilized for commercial purposes, require more energy to efficiently maintain their IAQ through traditional HVAC units, which in turn increases operational costs and reduces expected profits (Mendell and Heath, 2005). On the other hand, adequate IAQ reduces absenteeism due to airborne illnesses (Hormigos-Jimenez et al., 2018) and increases productivity (Mohamed et al., 2021) due to a comfortable indoor environment; this ultimately translates into quality education and overall environmental satisfaction experienced by the institutional community.

In the context of a developing nation where poverty and unemployment are urgent areas of concern, a proposed environmental policy to aid IAQ management would most likely receive poor attention unless it addressed the main economic issues faced by that country. Grymonpre et al. (2016) pointed out the complexities associated with any green adoption model and how interactions and processes are influenced by internal and external factors. Eggins (2014) cautioned that policies to improve education stall in their implementation due to the organizational, cultural, and social norms to which the stakeholders are exposed. Also, the Institute of Medicine (IOM) (2011) mentioned that consideration of environmental, economic, and political conditions together with their associated risks should be considered when developing an environmental policy for any institution. Once these risks and conditions have been identified, a qualified policy instrument, whether simple or complex, should be adopted in response to the identified environmental concerns the policy intends to resolve (IOM, 2011; Alrazni, 2016). To better understand these policy guidelines, Table 1 details the identified critical enablers that promote policy adoption for IAQ management in HEIs in South Africa (Bell et al., 2013; Sebri and Ben-Salha, 2014; Van Rijnsoever et al., 2015; Dermont et al., 2017).



3 Research methodology

To better comprehend its quantitative objective, this study adopted a post-positivist philosophical stance. According to Bryman (2012), post-positivism is suited to an action-oriented study that yields primary data through empirical probing. A closed-ended questionnaire structured survey compiled in the English language was adopted due to its ability to reliably measure the study's objective across a varied population. In support, Flick (2011) highlighted that a well-structured survey collection instrument yields a higher measure of reliability when dealing with a larger sample. The questionnaire surveyed 16 variables derived from the literature review and was randomly distributed using an online survey platform (Google Forms) in an effort to reach a wider group. The target population of the study was the institutional community, defined as the academic and administrative staff in HEIs, as opposed to existing studies on IEQ in educational facilities, which mainly considered end-users (students) (Wargocki et al., 2020; Sadrizadeh et al., 2022). A total of 26 public HEIs were surveyed, mainly South African universities (technical, comprehensive, and traditional). Section 1 of the questionnaire gathered the demographics of the respondents, while the respondent's views on the influence of the identified enablers in encouraging the adoption of IAQ-driven policies in their respective institutions were covered in Section 2. To adequately measure the respondent's views, Section 2 was guided by a five-point Likert scale, with 1 being "no influence" and 5 being "a very high influence". Since the population size of the study was 61,242, Cochran's sample size equation was adopted to derive a sample size of 413 based on a 90% confidence level and a $\pm 7\%$ margin of error. A questionnaire response rate of 51.3% was achieved for the collected data, which was more than the minimum 50% of the estimated proportion of the sample size (Kline, 2016). This resulted in 212 completed surveys being deemed acceptable for the study, in line with Kline's recommendations.

The data analysis process of the study was guided by a sequential, phased approach (Figure 1). The collected data were screened for missing information during the initial phase of the data analysis process. Phase 2 of the data analysis framework involved the employment of Cronbach's alpha test, which determined the reliability of the variables adopted by the questionnaire survey. An alpha value of 0.907 was derived for all 16 enabling variables for IAQ policy adoption. This was deemed acceptable for the current

study, as Hair et al. (2010) recommended a threshold alpha value of 0.70. Descriptive statistics formed part of the third phase of the data analysis process, in which the demographic data together with the views of the respondents relating to the influence of the identified enablers of policy adoption were interpreted by percentage and frequency. Additional descriptive statistical measures were adopted to further ascertain the influence of the identified policy adoption enablers from the respondent's perspective. These included standard deviation (SD), mean item score (MIS), and a one-sample *t*-test using SPSS Statistics, version 28. The last phase of data analysis involved the use of exploratory factor analysis (EFA) as a supplementary inferential statistical tool to determine the variability of the identified policy adoption enablers together with the factorial loading of the gathered data measured through a rotation matrix, Bartlett's test of sphericity (BTS), and the Kaiser-Meyer-Olkin (KMO) (Tabachnick and Fidell, 2007; Kline, 2014). Kaiser (1974) and Kline (2014) suggested a KMO value between 0 and 1, with 0.60 being a minimum acceptable value for a meaningful group of components or factors, while a BTS value of ($\alpha < 0.05$) was deemed significant for satisfactory factor analysis (Bartlett, 1954). Furthermore, to better understand the factorial loadings of the rotated matrix, the categorization of similarly characterized policy adoption enablers in each cluster was adopted.

4 Findings and discussion

4.1 Background information about the respondents

Table 2 presents the respondent's demographic information. More than 30 working hours per week were spent indoors by over 75% of the academic and administrative staff. These findings were analogous to those of Kecorius et al. (2018), who found that more than 50% of occupants spent around 45 working hours per week indoors. Interestingly, the majority of respondents worked in an enclosed, single-occupancy office, while less than 10% shared a common open-plan office layout divided by cubicles. Respondents were largely in both academic teaching and research roles (27.4%)—academic research roles were the least represented (13.7%). It is noteworthy that less than 5% of respondents highlighted a below-average health status, while the majority, 47.6%, reported very good health. Of these findings, a group average of 28 working hours was derived from the data. This translates into a fair representation of the respondent's overall census, making them representative of the general population who shares their views on the study's objective of how influential the identified policy adoption enablers are in improving the IAQ management of their respective HEI in South Africa.

4.2 Influence of enabling factors in motivating IAQ policy adoption in institutions of higher learning

4.2.1 Descriptive statistics

Table 3 presents 16 influential policy adoption enablers. All SD values were below the threshold of 1, which translates to a relatively

TABLE 2 Background information of the respondents.

Demographic category	Category description	Frequency	Percentage (%)
Average working hours	< 10	7	3.3
	11–20	13	6.1
	21–30	30	14.2
	> 30	162	76.4
	Total	212	100.0
Workstation setup	Enclosed office—single occupancy	93	43.9
	Enclosed office—multiple occupancies	54	25.5
	Open-plan office—cubicles	19	9.0
	Open-plan office—desks	46	21.7
	Total	212	100.0
Institutional role	Academic teaching	49	23.1
	Academic research	29	13.7
	Both academic teaching and research	58	27.4
	Academic support	35	16.5
	Administrative support services	41	19.3
	Total	212	100.0
General health status	Excellent	57	26.9
	Very good	101	47.6
	Good	47	22.2
	Fair	7	3.3
	Total	212	100.0

low deviation in the view of the respondents (Nolan et al., 2008). Although the sample size of the academic and administrative staff of HEIs was smaller than their overall population, its generalization was true since all variables had a standard error of the mean value closer to zero. Most of the respondents believed that all 16 identified variables were influential in enabling IAQ management of their respective HEIs through environmental policy adoption since a mean value of 3.0 or above was derived (Lee et al., 2015). The type of policy instrument—whether rule- or incentive-based (MIS = 3.89)—compatibility with their institutional goals (MIS = 3.85), and providing environmental guidance and counseling (MIS = 3.70) were the three most influential policy adoption enablers. The study's findings were analogous to those of Yu and Yu (2017) since an individual's preference for the type of policy—whether an incentive- or market-based policy or a ban- or rule-oriented policy influenced their overall support for any new environmental policy adoption. In other words, institutional stakeholders such as institutional academic and administrative staff would be more willing to appraise an incentive-based policy instrument due to the associated “cost illusion” rather than a “motiveless” rule- or ban-based policy instrument (Feng and Chen, 2018).

The findings of Eggins (2014) were corroborated by the current study, as the ability of a policy instrument to meet institutional goals was key to its adoption by the very same institution. Colombo and

Kriesi (2017) added that individual attitudes concerning environmental issues improved the systematic processing of policies aimed at alleviating these concerns. However, individual attitudes and knowledge were ranked 11th by respondents due to their perception of the environmental concerns facing South Africa. Although general support for the aim of the policies is expected, it is notable that individual behavior can lead to the adoption or rejection of a policy based on the available information on environmental issues (Daddi et al., 2016). However, the current study noted that variations in strong attitudes and environmental knowledge can influence the support or rejection of environmental policies. There are economic and political complexities that may constrain the development and adoption of any public policy (IOM, 2011). These submissions were to some extent analogous to those of the study, as the demographic, economic, and political conditions were perceived to have some influence on the adoption of an environmental instrument.

The characterized organizational management or structure has been identified as one of the key attributes of environmental policy adoption by the current study. Taweekaew (2014) supported this finding by also submitting that organizations with favorable organizational structures are more likely to adopt policies in a timely manner than those with unfavorable structures. Similarly, Taweekaew (2014) and Zardo et al. (2014) argued, in harmony with

TABLE 3 Environmental policy adoption descriptive results.

Policy adoption enablers	MIS	SD	R	Std. error mean
Type of policy instrument (rule- or incentive-based)	3.89	0.690	1	0.047
Complementing institutional goals (compatibility)	3.85	0.669	2	0.046
Provide environmental guidance and counseling	3.70	0.668	3	0.046
Availability of policy information	3.67	0.731	4	0.050
Transparency (procedures and regulations)	3.62	0.695	5	0.048
Stakeholder salience (coherent engagement)	3.52	0.698	6	0.048
Alleviate environmental concerns (pollution, etc.)	3.52	0.692	7	0.047
Institutional environment (economic and political conditions)	3.52	0.698	8	0.048
Risk management (environmental, market, etc.)	3.45	0.737	9	0.051
Institutional structure	3.45	0.717	10	0.049
Pro-environmental behavior (individual attitude and knowledge)	3.42	0.772	11	0.053
Qualification of the proposal (simple or complex)	3.25	0.831	12	0.057
Societal values and norms	3.24	0.744	13	0.051
Transformative regulations	3.20	0.766	14	0.053
Policy intention (translatable policy design)	3.19	0.756	15	0.052
Defined economic benefits	3.00	0.773	16	0.053
Overall Cronbach's alpha (α)	0.907			

Note: MIS = mean item score; SD, standard deviation, R = rank.

the study's findings, that the persistent coherency of institutional and community stakeholders generates the sustained pressure necessary to trigger their institutions to effectively consider and incorporate sustainable environmental policies. Chitescu and Lixandru (2016) stressed that the defined economic benefits of any sustainable policy are crucial to its adoption. However, the opposite is true for the current study, as the academic and administrative staff of various HEIs ranked it as the least influential policy adoption enabler among societal values and norms, together with the translation of policy design into intentional instruments.

To further ascertain the extent of the influence of the surveyed policy adoption enablers on improving the IAQ management of HEIs, a one-sample *t*-test was also conducted. Where the identified policy adoption enablers were non-influential, they formed a null hypothesis and were set at ($H_0: U \leq U_0$), while influential enablers formed an alternative hypothesis set at ($H_a: U > U_0$), with U_0 being the population mean of 3.0 (De Winter 2013). The confidence coefficient interval of 95% guided the study, with a base *p*-value of 0.05. All influential policy adoption enablers were analyzed under a two-sided (two-tailed) significance measure that derived a *p*-value = 0.00, thus rejecting the null hypothesis and adopting the latter hypothesis (Table 4). The analysis also revealed that no major outliers in relation to deviation were noticed in the views of respondents, as a *p*-value lower than 0.05 was derived. Therefore, the collective views of the surveyed variables can be generalized to the overall population and adopted for studies of a similar nature.

4.2.2 Exploratory Factor Analysis

The study adopted the Principal component analysis (PCA) technique using the varimax rotation method to identify their commonalities. Table 5 indicates that all the identified policy adoption enablers had a rotated component matrix factor of 0.362–0.785, which was above the acceptable threshold of 0.3, thus qualifying the variables for factor analysis (Hair et al., 2006). The KMO analysis was performed to better understand the sampling adequacy of each policy adoption enabler; it yielded a value of 0.923, which exceeds the acceptable threshold of 0.6 (Tabachnick and Fidell, 2007). The BTS analysis was also conducted to further reveal an acceptable approximate chi-squared (X^2) value of 1340.525 while yielding a rotatable *p*-value of 0.000, which is significant and adequate for sampling since the *p*-value was < 0.5 (Tabachnick and Fidell, 2007). A scree plot diagram was adopted as a confirmatory tool to better represent the number of factors yielded by the rotational matrix. Figure 2 shows a curved line diagram where three components can be seen in a linear pattern before the scree plot curves in a linear swing to depict all other components with an eigenvalue <1. Similarly, the PCA method further yielded the total variance explained (Table 5) which depicted three extractions with an eigenvalue >1 and a cumulative variance value of 55.66%. All extracted components were recommended to yield a threshold value > 50% (Pallant, 2013). Three factorial clusters were derived from the pattern of correlations observed among all 16 policy adoption enablers. Thus, the kinship relationship between all extracted variables in each cluster is :

TABLE 4 Statistical results of one-sample t-test.

Policy adoption enablers	Test value = 3.0			95% confidence interval of the difference	
	t	df	Sig. (two-tailed)	Lower	Upper
Stakeholder salience (coherent engagement)	10.918	211	0.000	0.43	0.62
Transparency (procedures and regulations)	12.937	211	0.000	0.52	0.71
Transformative regulations	3.768	211	0.000	0.09	0.30
Institutional environment (economic and political conditions)	10.817	211	0.000	0.42	0.61
Qualification of the proposal (simple or complex)	4.380	211	0.000	0.14	0.36
Defined economic benefits	3.752	211	0.000	0.10	0.32
Institutional support (environmental guidance and counseling)	15.309	211	0.000	0.61	0.79
Pro-environmental behavior (individual attitude and knowledge)	7.921	211	0.000	0.32	0.52
Societal values and norms	4.709	211	0.000	0.14	0.34
Institutional structure	9.102	211	0.000	0.35	0.55
Alleviate environmental concerns (pollution, etc.)	10.924	211	0.000	0.43	0.61
Risk management (environmental, market, etc.)	8.949	211	0.000	0.35	0.55
Policy intention (translatable policy design)	3.636	211	0.000	0.09	0.29
Complementing institutional goals (compatibility)	18.579	211	0.000	0.76	0.94
Availability of policy information	13.333	211	0.000	0.57	0.77
Type of policy instrument (rule- or incentive-based)	18.808	211	0.000	0.80	0.98

Note: t, t-statistic; df, degrees of freedom; Sig., significance (p-value < 0.05).

- Cluster 1—Stakeholder dialogue: The initial extracted component yielded a cumulative variance of 42.07%, comprising seven variable loadings extracted into this cluster. These include policy adoption enablers such as alleviating environmental concerns (0.785), defining economic benefits (0.737), transforming regulations (0.707), pro-environmental behavior (0.634), stakeholder salience (0.558), institutional environment (0.542), and risk management (0.488). Although maintaining an adequate IAQ environment demands more time and resources to manage, its long-term benefits outweigh the initial costs (Pedrosa Ortega et al., 2019). Thus, having a sound stakeholder dialogue is imperative in advocating for the adoption of an environmentally friendly policy that increases institutional awareness of pro-environmental behavior while demystifying any misconceptions about environmental risks and restrictions that might prevent its development and implementation (Van Hoof and Thiel, 2014; Mohamed et al., 2021).
- Cluster 2—Institutional commitment: Five variable loadings that translated into a cumulative variance of 49.07% of the total variance explained constitute this cluster. These variables included institutional structure (0.413), complementary institutional goals (0.718), institutional support (0.711), societal values and norms (0.649), and transparency (0.647). It is noteworthy that, in recent literature examining the successful adoption of innovative and sustainable environments, there has been no consistency in the findings of various studies (Grymonpre et al., 2016). Past

and recent studies that evaluate the adoption of policies in the education sector have repeatedly stressed organizational structure, leadership commitment, faculty heads, awareness of policy, committed resources, and student engagement as leading factors in the development of sound educational policy (Barnsteiner et al., 2007; Evans et al., 2011; MacKenzie and Merritt, 2013; Leccese et al., 2021).

- Cluster 3—Policy composition: The third extracted component derived a cumulative variance of 55.66% of the total variance explained, which included four variable loadings. These variables were Qualification of the proposal (0.362), policy intention (0.475), availability of policy information (0.776), and the type of policy instrument (0.679). The literature reveals several stages in the creation of any public policy. These include problem identification, agenda setting, policy formation, adoption, implementation, and evaluation, which agree with the policy composition of this cluster's variables (Helbig et al., 2015).

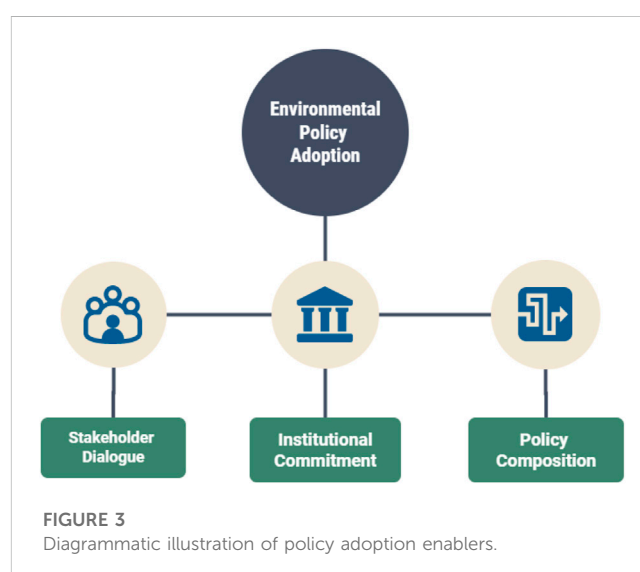
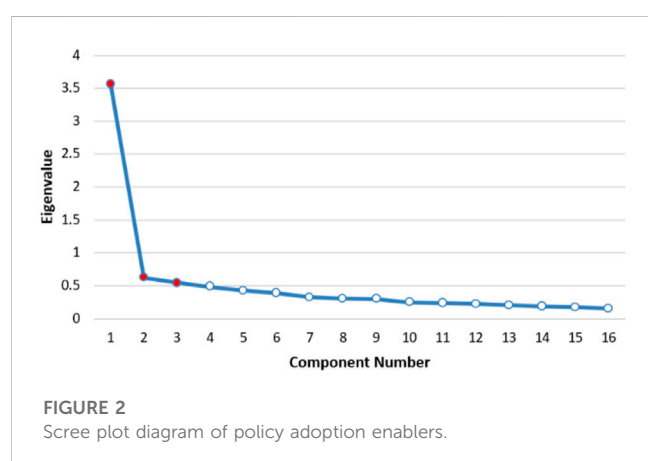
To better understand the categorized clusters in the context of IAQ management, Figure 3 provides a diagrammatic illustration of how each policy adoption enabler contributes to the adoption of an environmental policy that will improve the adequacy of IAQ management in HEIs in South Africa. Thus, to improve the state of IAQ in an institution, three fundamental policy adoption enablers should be considered before introducing an environmental policy aimed at achieving

TABLE 5 Rotated component matrix and communality results.

Policy adoption enablers	Cumulative	Component			Communality	
	% of variance	1	2	3	Initial	Extraction
Alleviate environmental concerns (pollution, etc.)	42.069	0.785			1.000	0.691
Defined economic benefits	49.212	0.737			1.000	0.489
Transformative regulations	55.657	0.707			1.000	0.586
Pro-environmental behavior (individual attitude and knowledge)	61.454	0.634			1.000	0.595
Stakeholder salience (coherent engagement)	66.680	0.558			1.000	0.486
Institutional environment (economic and political conditions)	71.315	0.542			1.000	0.488
Risk management (environmental, market, etc.)	75.278	0.488			1.000	0.543
Institutional structure	78.911		0.413		1.000	0.514
Complementing institutional goals (compatibility)	82.382		0.718		1.000	0.448
Institutional support (environmental guidance and counseling)	85.495		0.711		1.000	0.439
Societal values and norms	88.457		0.649		1.000	0.553
Transparency (procedures and regulations)	91.234		0.647		1.000	0.484
Qualification of the proposal (simple or complex)	93.785			0.362	1.000	0.478
Policy intention (translatable policy design)	96.090			0.475	1.000	0.535
Availability of policy information	98.156			0.776	1.000	0.571
Type of policy instrument (rule- or incentive-based)	100.000			0.679	1.000	0.476
Kaiser–Meyer–Olkin measure of sampling adequacy		0.923				
Bartlett's Test of Sphericity	<i>Approx. X^2</i>	1340.525				
	<i>Df</i>	120				
	<i>Sig.</i>	0.000				

Note: Extraction method: principal component analysis; rotation method: Varimax with Kaiser normalization.

*Rotation converged in 11 iterations.



holistic IAQ management in HEIs. Although earlier models have suggested that these pathways were progressively linear, more recent literature argues that the relationship between the stages is somewhat simultaneous, inverse, or interlinked (Benoit, 2013). It is noteworthy that the trilateral relationship between policy

adoption enablers is directional in nature, since all three fundamental policy clusters cannot be implemented in isolation but rather as a collective instrument.

5 Conclusion and recommendations

The study investigated the critical enablers for the adoption of environmental policies for the management of IAQ in South African HEIs. From the reviewed literature and surveyed data, it can be concluded that institutional goals, environmental guidance, and the availability of environmental information must be aligned to resolving IAQ issues that influence the overall quality of education and the wellbeing of staff. From a theoretical perspective, since growth is inclusive, HEIs would be able to adopt pro-environmental policies that improve their IAQ management principles at minimal cost due to the progressive nature of said policies. This is to say, the use of pro-environmental policy in managing IAQ in HEIs is expected to show lower signs of adoption in the initial stages, while a significant increase in the rate of implementation is expected when most stakeholders are driven by current social support to adopt it.

It is recommended that adopting a new policy to improve IAQ management in HEIs requires more than just passive stakeholder salience, but a rather active stakeholder dialogue, institutional commitment, and sound policy. The empirical views of academic and administrative staff also support a consideration of the institution's external influences, such as economic and political conditions, together with the proposed policy's capacity to respond to the identified environmental concerns of pollution that affect the working environments of HEI staff. Similarly, the institutional structure, together with individual attitudes and knowledge of the effects of IAQ on teaching and learning, influences the overall adoptability of environmental policies geared toward adequate IAQ management. Hence, adequate IAQ management not only benefits staff members of HEIs through improved psychological and physiological well-being but also benefits the institution through improved quality of education since a conducive working environment also stimulates better cognition in students.

Unlike the current *modus operandi* of implementing solutions using a formative framework, while some grounds have been established, there remains little empirical evidence that can support a sustainable movement within the education sector and its interdependence with environmental sciences, with a particular focus on the indoor environment in developing countries. Thus, more research is needed on how HEIs can benefit from IAQ policy adoption within and between the institutional community and its management.

Data availability statement

The original contributions presented in the study are included in the article/**Supplementary Material**, further inquiries can be directed to the corresponding author.

References

- Abdul-Wahab, S. A., En, S. C. F., Elkamel, A., Ahmadi, L., and Yetilmezsoy, K. (2015). A review of standards and guidelines set by international bodies for the parameters of indoor air quality. *Atmos. Pollut. Res.* 6 (5), 751–767. doi:10.5094/apr.2015.084
- Al Horr, Y., Arif, M., Kaushik, A., Mazroei, A., Katafygiotou, M., and Elsarrag, E. (2016). Occupant productivity and office indoor environment quality: A review of the literature. *Build. Environ.* 105, 369–389. doi:10.1016/j.buildenv.2016.06.001
- Alam, M. S., and Paramati, S. R. (2015). Do oil consumption and economic growth intensify environmental degradation? Evidence from developing economies. *Appl. Econ.* 47 (48), 5186–5203. doi:10.1080/00036846.2015.1044647
- Alemu, S. K. (2019). African higher education and the bologna process. *Eur. J. High. Educ.* 9 (1), 118–132. doi:10.1080/21568235.2018.1561313
- Alrazni, W. (2016). Improving indoor air quality (IAQ) in Kuwaiti housing developments at design, construction, and occupancy stages. Doctoral dissertation. Salford: University of Salford.
- Barnsteiner, J. H., Disch, J. M., Hall, L., Mayer, D., and Moore, S. M. (2007). Promoting interprofessional education. *Nurs. Outlook* 55, 144–150. doi:10.1016/j.outlook.2007.03.003
- Bartlett, M. S. (1954). A note on the multiplying factors for various χ^2 approximations. *J. R. Stat. Soc. B* 16, 296–298. doi:10.1111/j.2517-6161.1954.tb00174.x

Author contributions

MN contributed to the drafting of the introduction, literature review, conclusion, and recommendations together with referencing the study citations. CA compiled the research methodology and data analysis sections of the study and provided a general review of the draft manuscript.

Funding

This research was funded by a National Research Foundation (NRF) Scarce Skills and Innovation Grant (No.113002) in collaboration with the CIDB Centre of Excellence and Sustainable Human Settlement and Construction. The study was fully supported by the University of Johannesburg's Faculty of Engineering and Built Environment, South Africa.

Acknowledgments

All primary and secondary information that contributed to this study is cited and acknowledged appropriately.

Conflict of interest

The authors declare that the research was conducted in the absence of any commercial or financial relationships that could be construed as a potential conflict of interest.

Publisher's note

All claims expressed in this article are solely those of the authors and do not necessarily represent those of their affiliated organizations, or those of the publisher, the editors and the reviewers. Any product that may be evaluated in this article, or claim that may be made by its manufacturer, is not guaranteed or endorsed by the publisher.

Supplementary material

The Supplementary Material for this article can be found online at: <https://www.frontiersin.org/articles/10.3389/fbuil.2023.1124248/full#supplementary-material>

- Bell, D., Gray, T., Haggett, C., and Swaffield, J. (2013). Re-visiting the 'social gap': Public opinion and relations of power in the local politics of wind energy. *Environ. Polit.* 22 (1), 115–135. doi:10.1080/09644016.2013.755793
- Benoit, F. (2013). *Public policy models and their usefulness in public health: The Stages Model*. Montréal, Québec: National Collaborating Centre for Healthy Public Policy.
- Bluyssen, P. M., (2010). *Product policy and indoor air quality. Indoor sources and health effects: Background information and ways to go*. Belgium: Directorate General for Environment, Brussels.
- Bornstein, N., and Thalmann, P. (2008). 'I pay enough taxes already!' Applying economic voting models to environmental referendums. *Soc. Sci. Q.* 89 (5), 1336–1355. doi:10.1111/j.1540-6237.2008.00580.x
- Boudreau, C., and MacKenzie, S. A. (2014). Informing the electorate? How party cues and policy information affect public opinion about initiatives. *Am. J. Political Sci.* 58 (1), 48–62. doi:10.1111/ajps.12054
- Brits, P. J. (2012). Assessment of indoor air quality in an office building in South Africa. [Master's Dissertation]. Witwatersrand: [University of the Witwatersrand (WITS)].
- Bryman, A. (2012). *Social research methods*. New York: Oxford University Press.
- Chitescu, R. I., and Lixandru, M. (2016). The influence of the social, political and economic impact on human resources, as a determinant factor of sustainable development. *Procedia Econ. Finance* 39, 820–826. doi:10.1016/s2212-5671(16)30259-3
- Colombo, C., and Kriesi, H. (2017). Party, policy—or both? Partisan-Biased processing of policy arguments in direct democracy. *J. Elections, Public Opin. Parties* 27 (3), 235–253. doi:10.1080/17457289.2016.1254641
- Daddi, T., Testa, F., Frey, M., and Iraldo, F. (2016). Exploring the link between institutional pressures and environmental management systems effectiveness: An empirical study. *J. Environ. Manag.* 183, 647–656. doi:10.1016/j.jenvman.2016.09.025
- De Winter, J. C. (2013). Using the Student's t-test with extremely small sample sizes. *Pract. Assess. Res. Eval.* 18 (1), 10.
- Dermont, C., Ingold, K., Kammermann, L., and Stadelmann-Steffen, I. (2017). Bringing the policy making perspective in: A political science approach to social acceptance. *Energy policy* 108, 359–368. doi:10.1016/j.enpol.2017.05.062
- Dill, D. D. (2012). "The management of academic culture revisited: Integrating universities in an entrepreneurial age," in *Managing reform in universities* (London: Palgrave Macmillan), 222–237.
- Eggs, H. (2014). *Drivers and barriers to achieving quality in higher education*. United Kingdom: Springer Science & Business Media.
- Evans, C. H., Cashman, S. B., Page, D. A., and Garr, D. R. (2011). Model approaches for advancing interpersonal prevention education. *Am. J. Prev. Med.* 40, 245–260. doi:10.1016/j.amepre.2010.10.014
- Feng, Z., and Chen, W. (2018). Environmental regulation, green innovation, and industrial green development: An empirical analysis based on the Spatial Durbin model. *Sustainability* 10 (1), 223. doi:10.3390/su10010223
- Flick, U. (2011). *Mixing methods, triangulation, and integrated research*. New York: Qualitative inquiry and global crises, 132.
- Godish, T. (2016). *Indoor environmental quality*. USA: CRC Press.
- Grymonpre, R. E., Ateah, C. A., Dean, H. J., Heinonen, T. I., Holmqvist, M. E., MacDonald, L. L., et al. (2016). Sustainable implementation of interprofessional education using an adoption model framework. *Can. J. High. Educ.* 46 (4), 76–93. doi:10.47678/cjhe.v46i4.186571
- Hair, J. F., Black, W. C., Babin, B. J., Anderson, R. E., and Tatham, R. L. (2006). *Multivariate data analysis*. 6th Edition. New Jersey: Pearson Prentice Hall.
- Hair, J. F., Jr, Black, W. C., Babin, B. J., and Anderson, R. E. (2010). *Multivariate data analysis*. 7th edn. Upper Saddle River, NJ: Pearson Prentice Hall.
- Helbig, N., Dawes, S., Dzhusupova, Z., Klievink, B., and Mkude, C. G. (2015). "Stakeholder engagement in policy development: Observations and lessons from international experience," in *Policy practice and digital science* (Cham: Springer), 177–204.
- Hormigos-Jimenez, S., Padilla-Marcos, M. A., Meiss, A., Gonzalez-Lezcano, R. A., and Feijó-Muñoz, J. (2018). Experimental validation of the age-of-the-air cfd analysis: A case study. *Sci. Technol. Built Environ.* 24 (9), 994–1003. doi:10.1080/23744731.2018.1444885
- Institute of Medicine (IOM) (2011). *Committee on the effect of climate change on indoor air quality and public health*. Washington, DC: National Academies Press.
- Kaiser, H. F. (1974). An index of factorial simplicity. *Psychometrika* 39, 31–36. doi:10.1007/bf02291575
- Kecorius, S., Tamayo, E. G., Galvez, M. C., Madueño, L., Betito, G., Gonzaga-Cayetano, M., et al. (2018). Activity pattern of school/university tenants and their family members in Metro Manila-Philippines. *Aerosol Air Qual. Res. (AAQR)* 18, 2412–2419. doi:10.4209/aaqr.2018.02.0069
- Kline, P. (2014). *An easy guide to factor analysis*. UK: Routledge.
- Kline, R. B. (2016). *Principles and practice of structural equation modeling*. 4th ed. New York: Guilford Press.
- Leccese, F., Rocca, M., Salvadori, G., Belloni, E., and Buratti, C. (2021). Towards a holistic approach to indoor environmental quality assessment: Weighting schemes to combine effects of multiple environmental factors. *Energy Build.* 245, 111056. doi:10.1016/j.enbuild.2021.111056
- Lee, D. K., In, J., and Lee, S. (2015). Standard deviation and standard error of the mean. *Korean J. Anesthesiol.* 68 (3), 220–223. doi:10.4097/kjae.2015.68.3.220
- MacKenzie, D., and Merritt, B. K. (2013). Making space: Integrating meaningful interprofessional experiences into an existing curriculum. *J. Interprofessional Care* 27, 274–276. doi:10.3109/13561820.2012.751900
- Marshall, S. J. (2018). *Shaping the university of the future*. Singapore: Springer.
- Mendell, M. J., and Heath, G. A. (2005). Do indoor pollutants and thermal conditions in schools influence student performance? A critical review of the literature. *Indoor air* 15 (1), 27–52. doi:10.1111/j.1600-0668.2004.00320.x
- Mohamed, S., Rodrigues, L., Omer, S., and Calautit, J. (2021). Overheating and indoor air quality in primary schools in the UK. *Energy Build.* 250, 111291. doi:10.1016/j.enbuild.2021.111291
- Mujeeb, M. A., and Bano, F. (2022). Integration of passive energy conservation measures in a detached residential building design in warm humid climate. *Energy* 255, 124587. doi:10.1016/j.energy.2022.124587
- Nolan, J. M., Schultz, P. W., Cialdini, R. B., Goldstein, N. J., and Griskevicius, V. (2008). Normative social influence is underdetected. *Personality Soc. Psychol. Bull.* 34 (7), 913–923. doi:10.1177/0146167208316691
- Pallant, J. (2013). *SPSS survival manual: A step by step guide to data analysis using ibm SPSS*. 5th edn. Crows Nest, Australia: Allen & Unwin.
- Pedrosa Ortega, C., Hernández-Ortiz, M., García Martí, E., and Vallejo Martos, M. C. (2019). The stakeholder salience model revisited: Evidence from agri-food cooperatives in Spain. *Sustainability* 11 (3), 574. doi:10.3390/su11030574
- Sadick, A. M. (2018). Assessment of school buildings' physical conditions and indoor environmental quality in relation to teachers' satisfaction and wellbeing. [Doctoral thesis]. Canada: University of Manitoba.
- Sadrizadeh, S., Yao, R., Yuan, F., Awbi, H., Bahnfleth, W., Bi, Y., et al. (2022). Indoor air quality and health in schools: A critical review for developing the roadmap for the future school environment. *J. Build. Eng.* 57, 104908. doi:10.1016/j.jobte.2022.104908
- Sakhare, V. V., and Ralegaonkar, R. V. (2014). Indoor environmental quality: Review of parameters and assessment models. *Archit. Sci. Rev.* 57 (2), 147–154. doi:10.1080/00038628.2013.862609
- Sebri, M., and Ben-Salha, O. (2014). On the causal dynamics between economic growth, renewable energy consumption, CO2 emissions and trade openness: Fresh evidence from BRICS countries. *Renew. Sustain. Energy Rev.* 39, 14–23. doi:10.1016/j.rser.2014.07.033
- Shahbaz, M., Haouas, I., and Van Hoang, T. H. (2019). Economic growth and environmental degradation in vietnam: Is the environmental kuznets curve a complete picture? *Emerg. Mark. Rev.* 38, 197–218. doi:10.1016/j.ememar.2018.12.006
- Stadelmann-Steffen, I. (2011). Citizens as veto players: Climate change policy and the constraints of direct democracy. *Environ. Polit.* 20 (4), 485–507. doi:10.1080/09644016.2011.589577
- Tabachnick, B. G., and Fidell, L. S. (2007). *Using multivariate statistics*. 5th edn. Boston: Allyn & Bacon.
- Taweekae, K. (2014). An analysis of the factors affecting the success of environmental policy implementation: A study of the tambon administration organization (TAO). *Sci. Res. J. (SCIRJ)* 2 (10), 20–25.
- Van Hoof, B., and Thiell, M. (2014). Collaboration capacity for sustainable supply chain management: Small and medium-sized enterprises in Mexico. *J. Clean. Prod.* 67, 239–248. doi:10.1016/j.jclepro.2013.12.030
- Van Rijnsoever, F. J., van Mossel, A., and Broecks, K. P. F. (2015). Public acceptance of energy technologies: The effects of labeling, time, and heterogeneity in a discrete choice experiment. *Renew. Sustain. Energy Rev.* 45 (5), 817–829. doi:10.1016/j.rser.2015.02.040
- Wargocki, P., Porras-Salazar, J. A., Contreras-Espinoza, S., and Bahnfleth, W. (2020). The relationships between classroom air quality and children's performance in school. *Build. Environ.* 173, 106749. doi:10.1016/j.buildenv.2020.106749
- Westerheijden, D. F., and Kohoutek, J. (2014). "Implementation and translation: From European standards and guidelines for quality assurance to education quality work in higher education institutions," in *Drivers and barriers to achieving quality in higher education* (Netherlands: Brill Sense), 1–11.
- World Health Organization (2015). *School environment: Policies and current status*. Copenhagen: WHO Regional Office for Europe.
- Yu, T. Y., and Yu, T. K. (2017). The moderating effects of students' personality traits on pro-environmental behavioral intentions in response to climate change. *Int. J. Environ. Res. Public Health* 14 (12), 1472. doi:10.3390/ijerph14121472
- Zardo, P., Collie, A., and Livingstone, C. (2014). External factors affecting decision-making and use of evidence in an Australian public health policy environment. *Soc. Sci. Med.* 108, 120–127. doi:10.1016/j.socscimed.2014.02.046



OPEN ACCESS

EDITED BY

Hasim Altan,
Prince Mohammad bin Fahd University,
Saudi Arabia

REVIEWED BY

Yorgos Spanodimitriou,
University of Campania Luigi Vanvitelli,
Italy
Giacomo Salvadori,
University of Pisa, Italy

*CORRESPONDENCE

Paul Fowler,
✉ paul.fowler@keene.edu

RECEIVED 09 April 2023

ACCEPTED 09 May 2023

PUBLISHED 24 May 2023

CITATION

Fowler P, Del Ama Gonzalo F, Newell S,
Poolman J, Montero Burgos MJ and
González Lezcano RA (2023), Assessment
of indoor air quality and comfort by
comparing an energy simulation and
actual data in Native American shelters.
Front. Built Environ. 9:1202965.
doi: 10.3389/fbuil.2023.1202965

COPYRIGHT

© 2023 Fowler, Del Ama Gonzalo,
Newell, Poolman, Montero Burgos and
González Lezcano. This is an open-
access article distributed under the terms
of the [Creative Commons Attribution
License \(CC BY\)](#). The use, distribution or
reproduction in other forums is
permitted, provided the original author(s)
and the copyright owner(s) are credited
and that the original publication in this
journal is cited, in accordance with
accepted academic practice. No use,
distribution or reproduction is permitted
which does not comply with these terms.

Assessment of indoor air quality and comfort by comparing an energy simulation and actual data in Native American shelters

Paul Fowler^{1*}, Fernando Del Ama Gonzalo¹, Sarah Newell¹,
James Poolman¹, Maria J. Montero Burgos² and
Roberto Alonso González Lezcano³

¹Department of Sustainable Product Design and Architecture, Keene State College, Keene, NH, United States, ²Energy Simulation Department, Ineria Management (S.L.), Cochabamba, Madrid, Spain, ³Escuela Politécnica Superior, Universidad San Pablo-CEU, Montepríncipe Campus, Madrid, Spain

Introduction: This research will determine if a native American shelter (wigwam) can create comfort and if while doing so can provide healthy indoor air quality (IAQ) levels as defined by current standards. Concurrent to this research a technique to digitally model the outcomes of comfort created within the shelter was developed.

Methods: A fullsize example of a wigwam was built and data from inside and outside the wigwam monitored for comparison. Data collected both inside and outside was temperature and relative humidity of the air, collected inside the wigwam were CO₂, VOC, and PM2.5 levels. The wigwam allowed us to compare the accuracy of a digital model created in Design Builder. The Design Builder model was made to the specific size, materials, and location of the actual wigwam. This allowed an accurate comparison of temperature and relative humidity levels. Design-Builder accurately recreated the attributes of the full-size wigwam.

Results and Discussion: It was found that comfort can be achieved to modern standards in this native shelter; as temperature, relative humidity, and rainfall exposure can all be controlled to acceptable levels. Indoor air quality is always at an acceptable level when a fire isn't active. When an open fire is introduced, the particulates and VOC released into the interior of the wigwam are at dangerous levels. A woodstove with flue pipe allowed for comfort to be maintained at healthier air quality levels but did not reach acceptable levels for particulate matter.

KEYWORDS

native American shelter, indoor air quality (IAQ), building energy simulation, building environment, monitoring

1 Introduction

Before the settlers moved to North America, the indigenous woodland people, or the Algonquian tribes such as the Wampanoag, Abenaki, and Narragansett ([Native American Houses, 2022](#)), constructed a specific type of shelter called a wigwam. This shelter style was pervasive wherever tree branches were abundant and located in the northeastern region of America. Although more permanent than a tipi, this dwelling was still used as temporary or

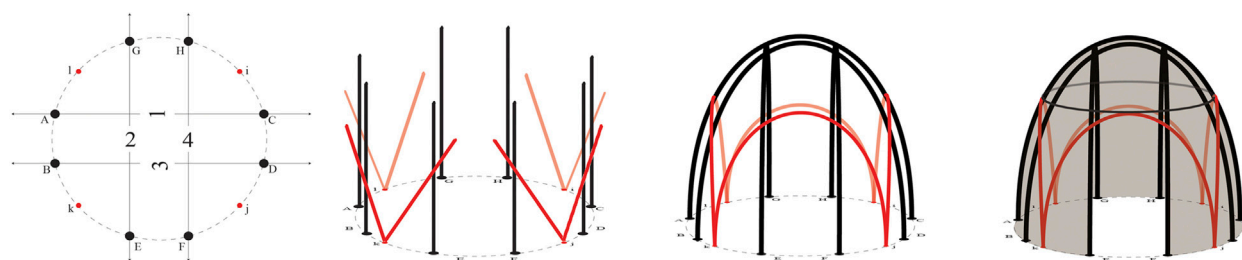


FIGURE 1
An illustrated simplification of the construction of a wigwam.

semi-permanent residency (Nabokov & Easton, 1989; Mayrl, 2022). Historically, constructing a wigwam could take one to 3 weeks. A uniform curved shape of the wigwam and wetu allowed the interior space to be evenly cooled or heated while withstanding precipitation effects (Morgan, 1881; Montgomery, 2000). The more traditional circular wigwam was typically 6–10 ft tall and 10–14 ft in diameter (Kalman, 2000; Kidadl, 2022). Steps to construct this shelter in real-life were carried out in a straightforward procedure: Traditionally, a relatively flat site would be surveyed. Next, the wigwam's mainframe was built with young red maple, swamp maple, or even red willow saplings (The Building of a Wigwam, 2022). These flexible pieces would often be straight, no thicker than two inches in diameter, and 10–16 ft long (Bushnell, 1922). Twelve to sixteen points for holes would be plotted around the circle (Speck, 1922). The saplings would then get bent into arches. Where the arches intersected, bark fibers would be used to lash the saplings together (Nyholm, 1981). Layers of “hoops” or “bands” made of saplings would be added and be equally spaced apart from one another (Wigwam, 2022). Two lower bands on the frame would not connect on the eastern side to ensure room for an entrance. One of the last steps was to situate the “coverings” over the frame but leave a hole at the top to allow fire-generated smoke to escape. Overlapping birchbark pieces created watertight, impenetrable skin (Holley, 2007). In the summer, woven rushes would be used instead of bark for the outside layer (Montero Burgos et al., 2020). A sufficient correlation exists between the health complications experienced by the Native American population and the unhealthy level of exposure to damaging particles from birth to death. Much of the harmful particulate matter in these communities originated from burning biomass freely in a compact living area, such as a wigwam, with only a small opening to release the generated smoke (Ghio, 2017). Native Americans would employ fire burning for heating and cooking purposes. However, subjecting inhabitants to an elevated concentration of damaging particles is shown to cause health concerns analogous to the effects of desert dust storms, cigarette, and tobacco smoke. These consequences increase susceptibility to lower respiratory tract infections in Native American communities. Conversely, higher particulate matter concentrations can contribute to an increased rate of asthma, chronic bronchitis, heart disease and cardiovascular/respiratory mortality, and hospital admissions (NY State Gov., 2022). Some authors have shown that chronic bronchitis was reported in Native American people living in rural areas. Due to biomass fires and stove emissions, the severe cough cases were comparable to those

diagnosed in highly populated industrial areas. The prevalence of those cases among Native Americans was more significant in women than in men, unlike the cases reported in industrial areas (Gold et al., 2000). Noting that air quality is integral to how a building performs efficiently, assessments were done measuring the concentration of VOC (volatile organic compounds), PM 2.5 (Particulate Matter 2.5), and CO₂ levels when a fire is burning within the wigwam. According to the World Health Organization, a healthy PM 2.5 concentration is around 10 µg/m³, with a slightly dangerous accumulation at 25 µg/m³ (Gonzalo et al., 2022). According to the U.S. Environmental Protection Agency 2022 standards, 35 µg/m³ is considered the standard limit within a 24-h standard period. Hazardous conditions gather at 250–500 µg/m³ (EPA, 2022). Although some researchers stated that it is not possible to give a unique CO₂ threshold valid for every building type, some studies recommend keeping indoor CO₂ concentration below 1000 ppm to reduce airborne transmission, (Fantozzi et al., 2020). Zero–220 ppb (parts per billion) is considered healthy for VOC levels. Anything between 220–660 ppb, one can start to experience uncomfortable symptoms such as nausea, dizziness, or irritation of the eyes. Longer exposure with levels surpassing 2,200 ppb can cause health compromises such as liver and kidney damage, cardiovascular diseases, and cancers (Getuhoo, 2022; IBM, 2022).

Human comfort can be evaluated through different methods. Fanger's Predicted Mean Vote (PMV) method was developed to consider the different variables that influence the comfort assessment for an indoor environment. (Fanger, 1970; Fanger, 1973). It allows the thermal sensation prediction from the heat-balance equation in which six main factors must be considered: metabolic rate, clothing insulation, air temperature, radiant temperature, airspeed, and humidity. On the other hand, the adaptive model approach considers people as active subjects who can interact with and adapt to the environment. Fanger's heat balance model might be unsuitable for assessing the actual thermal sensation that people may experience, especially in naturally ventilated buildings. Conversely, the adaptive model does not include several parameters implicated in thermal perception. Despite its limitations, Fanger's Predicted Mean Vote remains the most used worldwide (Lamberti, 2021). ISO 7730 (2005), ASHRAE Handbook (2012), and ASHRAE standard 55 (2017) defined local thermal comfort as satisfaction with the thermal environment that must be evaluated by subjective means. Open or closed fires inside the wigwam generate radiant heat at a

TABLE 1 Characteristics of the measurement devices.

Device	Temperature range (°C)	Temperature accuracy (°C)	Relative humidity range at 25°C (%)	Relative humidity accuracy (m ³)	CO ₂ concentration (ppm)
Elitech RC-51	−30°C–70°C	+/−0.5°C (−20°C–40°C) ± 1.0°C (<20°C or >40°C)	10%–95%	+/− 3% (20%–90%) ± 5% (<20% or >90%)	-
AWAIR	−40°C–125°C	-	0%–100%	-	400 to 5000

high temperature that affects the comfort of occupants due to convective airflows generated by the heat source and the top opening, so inhomogeneity in indoor air temperatures must be studied (De la Torre, 2014). A method to assess indoor comfort must consider the position of occupants, ceiling height, the room's shape, radiant asymmetry, and the angle factor, which depends on the occupant's position (Fawwaz et al., 2022).

The lack of thermal mass in the wigwam's envelope and the fluctuations in outdoor conditions make the simulation of the indoor environment a challenging task (Ruiz et al., 2017). Thus, it is essential to validate the models to gain trust in the building simulation. Many studies have been published on the validation of energy simulation results, and interest in this subject has increased significantly over the last few years (Lezcano and Burgos, 2021). The literature review included scientific articles by other authors who have analyzed these criteria to standardize the calibration process of modeling a building and to clarify the typical errors that can occur in such modeling (Bozkaya et al., 2018; Mazzeo et al., 2020). Evaluating shelters' energy efficiency and indoor comfort under extreme weather conditions has been one of the topics of former research articles. Pilsworth (1978) proposed a straightforward procedure for calculating shelters' heat losses based on envelope parameters and air infiltrations. Several factors influence the thermal performance of the shelters. Firstly, the form factor of the shelter impacts the heat exchange between indoors and outdoors. Secondly, the envelope color can help optimize the inhabitants' comfort conditions. Finally, the construction method affects the air leakage and the cost of the structure (Dominguez et al., 2020). As energy simulation software became a common practice for modeling building thermal performance, researchers utilized digital models for temporary shelters to sustain the actual data on the thermal properties of these shelters. Crawford et al. (2005) modeled different prototype shelters and tested their performance under severe cold conditions using simulation models validated using experimentally measured data from built prototypes. Ulal et al. (2022) used OpenStudio for a soft-wall shelter unit to predict indoor thermal comfort. Finally, computational fluid dynamics (CFD) has also been used to study shelter performance under various conditions (Borge-Diez et al., 2013). Other studies addressed the users' energy performance and social context, proposing that the users' social behavior, including clothing, activities, and schedules, affect energy consumption and comfort. These studies used survey methods to assess the thermal comfort of occupants of humanitarian tents (Albadra et al., 2017). However, fewer studies have been based on shelter comfort and indoor air quality. Furthermore, most of these studies focused on current technology shelter prototypes with electric or fossil-fueled

heaters. Thus, this research's novelty lies in applying energy simulation tools and actual measurements for indoor air quality optimization and renewable fuel consumption for traditional shelters.

The main objective of this article is to assess the existing functionality and comfort parameters of the traditional wigwam and compare it to a digital version of an identical model made in Design Builder. By adjusting the properties of the virtual one, it is possible to have the results congruous to existing standards to ensure comfortability. The second parameter analyzed is the indoor air quality (IAQ) through and between the open and enclosed fire operations. The IAQ components include carbon dioxide (CO₂), volatile organic compounds (VOCs), Particulate Matter 2.5 (PM 2.5) evaluated damaging symptoms to the human body. This paper will evaluate the precision of Design Builder by analyzing any discrepancies in the data between the computerized and real-life model.

2 Materials and methods

A full-scale wigwam replica was constructed which allowed for the evaluation of human comfort and interior air quality within the environment. A digital model of this wigwam was prepared using Design Builder; which was based on the materials and size of the full-scale replica. These two models allowed us to compare data documented in real life with that produced in the digital model. This section presented the methods to evaluate the constructed wigwam's ability to adhere adequately to standards of comfortability and IAQ. Data from inside the wigwam and the surrounding local environment was collected throughout the fall and into the winter. Information from a week in October and December was used as samples to be evaluated against ASHRAE defined standards of comfort and IAQ. Finally, this empirical data was compared to the virtual rendition to verify the accuracy of the computer program.

2.1 Constructing the wigwam

Construction of a full-scale version of a traditional wigwam shelter was started in July 2022 in Winchendon Mass (42.6871°N, 72.0440°W). Wigwam was built using traditional techniques; first by scouting a flat piece of Earth and then mapping out proposed holes on the ground to dig out later. Figure 1 illustrates eight long poles that make up the mainframe, each measured to be 14' in length and between 1 1/8" and 1 1/2" in diameter. The mapped-out holes were dug into the ground, measuring about 1 1/2" in diameter and 8" to 10" deep. For each hole, one of the eight long poles was inserted. These poles would be bent in an arching fashion connecting to the

TABLE 2 Areas and volume of the wigwam.

Floor area (m ²)	Wall area (m ²)	Roof area (m ²)	Volume (m ³)	Opening area (m ²)
6.92	12.12	6.85	10.21	0.15

TABLE 3 Summary of the envelope materials (Sunforger[®] Tent Canvas, 2023).

Thickness (m)	Conductivity (W/mK)	Density (kg/m ³)	Specific heat (J/kgK)	U (W/m ² K)
0.0013	0.084	518.9	1620	0.47

opposite-facing pole by being lashed together in the middle at the highest point of the curve. These crossings would also be attached where the arches would intersect with other pairs of poles. Traditionally components would be connected using bark fibers, but in this example a non-traditional approach was used connecting members together using string as the securing mechanism (Knight, 2017). As illustrated in Figure 1, the sub-framing system was made up of two smaller poles placed into each of the four holes labeled k, j, i, l and bent into an arch facing away from each other, crossing the mainframe members 1, 2, 3, and 4 forming smaller arches when fastened together. A compression ring, adding reinforcement and resisting the arches natural tendency to compress under stress was then added to the top of these arches tying the frame together as a unified structure (Nabokov and Easton, 1989; Schwartz, 2009). The unconventional sheathing selected was cotton canvas, a biodegradable material that took the place of the traditional sheathing of bark. The canvas was then cut to specific shapes to ensure overlapping so the wigwam would be watertight. The canvas was secured using a needle and thread. A space was delegated for a doorway and included a canvas flap between holes E and F. A hole at the top was left uncovered to allow any generated smoke from a fire to escape.

2.2 Measures of comfort and air quality

Defined by engineer Povl Ole Fanger as the Predicted Mean Vote (PMV), “comfort” is considered the product of six variables: metabolic rate, thermal insulation of clothing, mean radiant temperature, air velocity, air temperature, and relative humidity (Fanger, 1973). The CBE Thermal Comfort tool established by the University of California Berkeley is an integrative tool used to assess all these factors per the standards set by ASHRAE-55 (2017). Since the latter three factors of the PMV were actively measured and assessed in real life, and the former three were not, metabolic rate, thermal insulation, and mean radiant, these variables were preset in the CBE tool: clothing set to 1 Clo (typical winter clothing), the metabolic rate set to 1.2 Met (standing, relaxed). Operative temperature is a function of the Mean Radiant Temperature. The performance goals for the wigwam to be considered as comfortable according to the standards of ASHRAE -55-2017 (Kabrein, 2017), had to retain an air temperature level of 19.4°C–27.8°C and a relative humidity range that was less than 80% with no lower limit (CBE, 2022.). The indoor relative humidity and temperature data points were

collected with an Elitech RC—51 Waterproof USB Temperature and Humidity Data logger located within Wigwam’s enclosed canvas skin. For the outdoor temperature and relative humidity, a matching datalogger was implemented 20 ft from the structure. The Elitech RC—51 Waterproof USB Data logger is a battery-operated device that measures temperature and relative humidity every 5 min and logs this information. Logged information can be transferred to a computer and exported as an EXCEL document. Measuring rainfall was done with three rain gauges. One rain gauge was placed outside directly beside the wigwam, one inside the Wigwam directly under the opening in the roof of the Wigwam, and the last off to the side inside the structure, where people would be located. At each rain event, starting from the time the Wigwam was completed to when precipitation changed from rain to snow, the amount of rain was measured and documented. Measuring air velocity was done using a handheld anemometer (Moreno-Rangel et al., 2018). These measurements were done at each fire event by measuring the air velocity directly outside the structure and inside at various times. They were then recorded and later placed into graphs. The wind velocity in the CBE tool was set to 0.1 m/s. The indoor air quality in the wigwam was monitored in this study using an AWAIR Element indoor air quality monitoring device. Relative humidity, temperature, CO₂, VOC, and PM2.5 data points were collected with an AWAIR device located within Wigwam’s enclosed canvas skin. The AWAIR is a device that can function as a stand-alone or with other Smart Home devices (Dominguez et al., 2020). Each device can accurately monitor 1000 square feet of indoor air. Relative humidity and temperature are measured by a complementary metal-oxide-semiconductor (CMOS). A Non-Dispersive Infrared Sensor (NDIR) measures the CO₂ concentration. In addition, a Multi-pixel metal oxide gas sensor and a laser-based light scattering sensor measure the VOC and PM2.5 concentration, respectively. These devices have been used lately to assess indoor air quality, especially in residential buildings. The characteristics of the measurement devices are summarized in Table 1. Typically, the indoor air quality was relatively stable when there was not a heat source introduced into the wigwam interior. Wood fires were utilized as the heat source; these fires were either “open” or “enclosed.” The “open” fires did not consist of any enclosed implementation that surrounded the active flames or any chimney directing the smoke through the top of the hole. A Guide Gear portable wood-burning stove where the chimney allowed the generated smoke to be vented out the top constituted an “enclosed” fire (Efficiency Valuation Organization, 2012).

2.3 The creation of the digital model

Design-Builder requires a climatic file to recreate the model's outdoor and indoor conditions. EnergyPlus website provides this type of file from all over the world. The one used for the wigwam simulation has been the one that contains the information regarding Keene Dillant-Hopkins Airport (WMO station 726165, 42.9065°N, 72.2726°W). This airport is located about 20 miles away from the place where the actual wigwam was built. To adapt the information contained in this file to the measured outdoor conditions of this shelter, the values for the outdoor dry-bulb temperature and its matching outdoor relative humidity were substituted by the values recorded by the data logger. This way, the accuracy of the indoor values calculated by Design-Builder was higher. Its corresponding wet bulb temperature and dew point temperature were determined using the software Elements, designed by Bigladder® software. Geometrically, Design-Builder divided the envelope of the wigwam into two groups of surfaces according to their inclination. Any surface that exceeded 70° was considered as a segment of the wall, while inclinations that were shorter constituted parts of the roof. This fact implies that their thermal transmittances (W/m²K) are different, even though their assigned material was the same, the cotton duck that covered the whole structure. In conclusion, they are slightly different because of their corresponding surface resistance values (m²K/W). The model's door was a different element, even though its material was cotton duck. This element only affected the CFD model since it let the outdoor air enter the wigwam. Measures of area and volume of the wigwam are shown in Table 2. Occupancy was not considered, so zero persons per square meter is the value introduced as an input for the simulation. Density and conductivity are two complementary parameters. The former determines the speed at which heat will transmit (diffusivity) and its ability to accumulate heat (effusivity), while the latter only indicates the ability of these materials to oppose the passage of heat. Considering that the envelope's thermal conductivity is equal to 0.084 W/mK, this material would be equivalent, in short, to a thermal transmittance coefficient of 0.47 W/m²K for 1.3 mm. The wigwam virtual model was created as a dome whose floor has twenty edges and was divided into four horizontal rows. Table 3 shows the technical characteristics of the envelope made with cotton duck. The values were taken from Lawson et al. (2005).

To take into account the influence of the hearth when it was lit up, the first option was to consider a group of people with a similar heat load. Nevertheless, that option was ruled out because it increased relative humidity. Thus, an internal sensible heat load was loaded into the model. The amount of wood used was different depending on the heating system. For open fires, the average wood was 4.6 kg per hour, whereas for the woodstove the average amount of wood was 2.1 kg per hour. On the reported days, the fire was operating for 5 h, so the total amount of wood was 23 kg for open fires and 10.5 kg for wood stoves. According to Kristak et al. (2019), the considered thermal heat capacity of wood was 3.5 kWh per kg, so an imaginary load of 8 kW was added to the model to mimic the internal sensible heat source of a wood stove at 370°C. By taking this option, the humidity levels recorded by the data logger in the wigwam were very similar to those delivered by Design-Builder. Besides, this heat source load had to be assigned a schedule in

Design-Builder. It was designed considering the moment the hearth was lit up and the last trunk was added. At that moment, it reached its highest temperature, 370°C. From then, its temperature begins to decrease. By loading the open fire with this solution, no heating set point had to be established in the model or any heating system. This way, the results obtained by Design-Builder were not manipulated to match those delivered by the data logger. Air tightness is one of the parameters that can affect the energy performance of these sorts of structures. Mazzeo et al. (2020) considered 0.6 ACH the performance of a similar tent with low wind exposure in cold climates. Ulal et al. (2022) considered 1.4 ACH in tents with high wind exposure. Persily et al. (2009) considered air change rates ranging from 0.55 to 1.08 in emergency shelters with mild and calm wind conditions. Due to the low exposure to wind due to existing constructions around the prototype, the model's airtightness was established at a constant rate of 0.7 ACH. The turbulence model corresponds to the k-ε model, which belongs to the RANS family models (Reynolds Averaged Navier-Stokes). The discretization scheme was upwind, substituting the defining set of partial differential equations with a group of finite difference equations.

2.4 Validation of the digital model

This section of the present research aimed to develop a methodology to match the measurements delivered by the data loggers with the results from the simulation. This way, the climatic data of its location and its surroundings were introduced into the model. Thus, its measurements, the technical characteristics of its envelope, and the hearth lit up inside it were considered. Design-Builder v7.02.006 software has been used in previous articles as a Building Energy Simulation tool to assess the energy performance of Native American shelters (Radhi, 2010). It is based on the "EnergyPlus" engine, allowing users to calculate the energy consumption of the building, the hourly variation of temperature and relative humidity, and the impact of supply air on temperature and velocity distribution within a room with computational fluid dynamics (CFD) (Neymark, 2002; Del Ama Gonzalo et al., 2023). In addition, the simulation process by Design-Builder has been validated with the Building Energy Simulation Test (BESTest) regarded by the American Department of Energy to assess building energy simulation programs' features. (William et al., 2021; Tan et al., 2022). Parametric analysis screens allow the user to investigate the effect of variations in design parameters on several performance criteria (Wang et al., 2012).

The experimental indoor air temperature and relative humidity were used to evaluate the precision of the simulation results. For this objective, three accuracy indices were calculated for each short-time testing campaign and each parameter, the Normalized Mean Bias Error (NMBE), the Coefficient of Variation of the Root Mean Square Error (CVRMSE), and the coefficient of determination (R^2). However, all these coefficients derive from the Mean Bias Error (MBE), shown in Eq. 1.

$$MBE = \frac{1}{n} \sum_{i=1}^n (A_i - S_i), \quad (1)$$

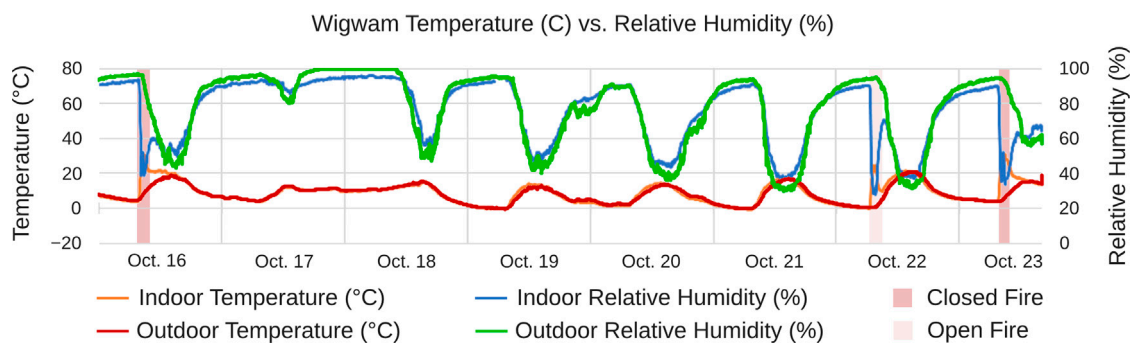


FIGURE 2
October's collected temperature and relative humidity data in and between periods of fires.

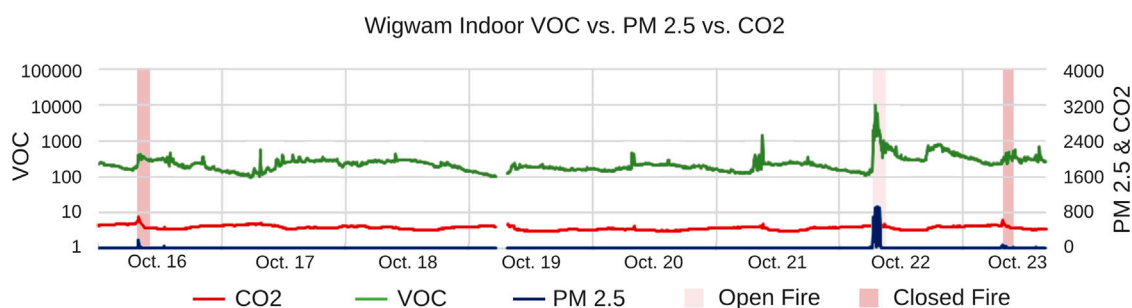


FIGURE 3
October's collected IAQ data in and between periods of fires.

where A_i represents the actual data measured, S_i is the data simulated by the tools, and n is the number of samples. RMSE varies between zero and one. A value closer to zero indicates an absence of deviations between measured and simulated data. However, the main issue with this parameter is that the sum of positive and negative values could reduce the value of MBE and, thus, the magnitude of deviations. Eq. 2 shows the Normalized Mean Bias Error (NMBE) that results from dividing MBE by the mean of measured values, \bar{A} , and p is the number of parameters included in the control volume, which, for calibration purposes, is suggested to be zero.

$$NMBE = \frac{1}{\bar{A}} \frac{1}{(n-p)} \sum_{i=1}^n (A_i - S_i) \times 100. \quad (2)$$

This parameter can also cause cancelation errors, so [ASHRAE Guideline 14, 2014](#) defines a procedure for validating the building energy model against actual data ([Fernández and Ramos, 2017](#)). In addition, the International Performance Measurement and Verification Protocol (IPMVP) and the Federal Energy Management Program (FEMP) propose a methodology to assess the accuracy of energy simulations. It proposes limits for the Root Mean Square Error (RMSE) and the Coefficient of Variation of Normalized Root Mean Square Error (CVRMSE), shown in Eqs 3, 4, using the average as a

normalization means to verify the precision of the energy model. The CVRMSE calibrates models in measured building performance and indicates instability in the observed relationship between variables in the baseline period. It is the coefficient of the variation of the simulated values relative to the measured ones.

$$RMSE = \sqrt{\frac{\sum_{i=1}^n (A_i - S_i)^2}{n}}, \quad (3)$$

$$CVRMSE = \frac{1}{\bar{A}} \sqrt{\frac{\sum_{i=1}^n (A_i - S_i)^2}{n-p}} \times 100. \quad (4)$$

Finally, Eq. 5 shows the expression of the coefficient of determination, R^2 . It displays how close simulated values are to the regression line of the measured values. It is another statistical index commonly used to measure the uncertainty of the models. It is limited to between 0.00 and 1.00 where the upper value indicates that the simulated values correspond to the measured ones correctly and the lower ones do not. It is not a prescriptive value for calibrated models, but the ASHRAE Handbook and IPVMP always recommend values >0.75 for hourly measurements.

$$R^2 = 1 - \frac{\sum_{i=1}^n (A_i - S_i)^2}{\sum_{i=1}^n (A_i - \bar{A})^2}. \quad (5)$$

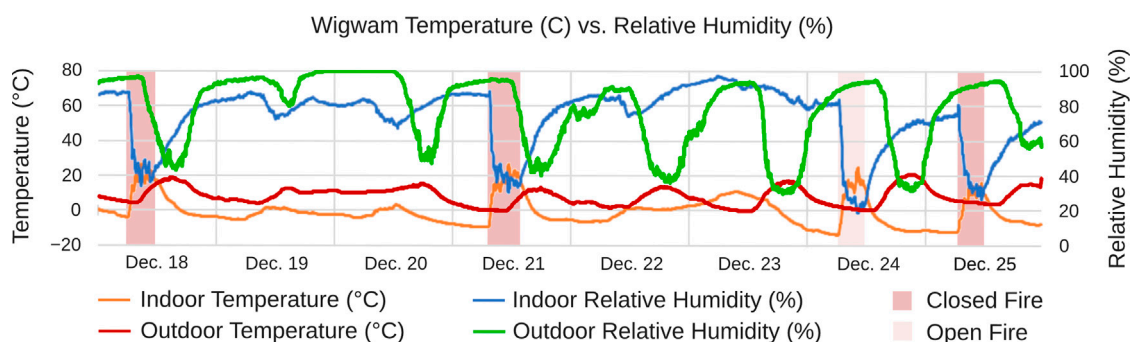


FIGURE 4
October's collected temperature and relative humidity data in and between periods of fires.

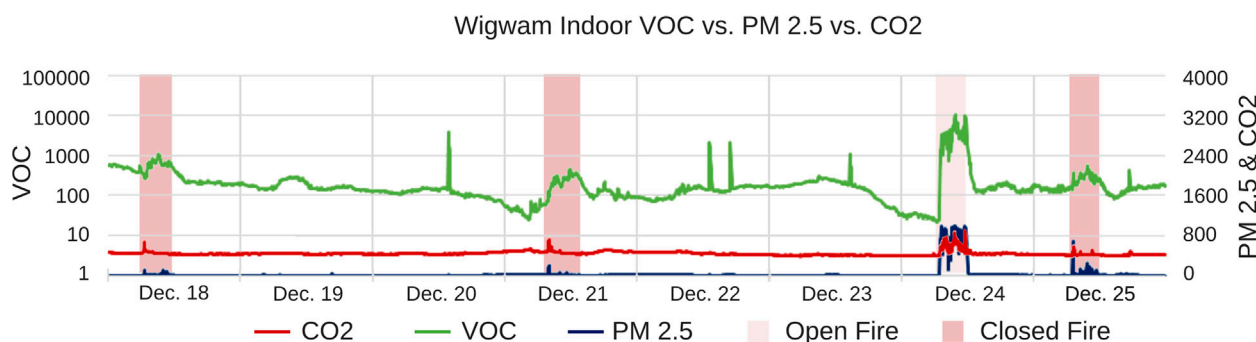


FIGURE 5
December's collected IAQ data in and between periods of fires.

3 Results

The open and enclosed fires were constructed for 3 months to analyze the performance of the wigwam in various climates. Throughout all the months tested, the data collected from October 16th to the 23rd was explicitly examined, as the environment was the most temperate week, and from December 18th to the 25th as it was the coldest.

3.1 Comparing wigwam data to comfortability and IAQ parameters

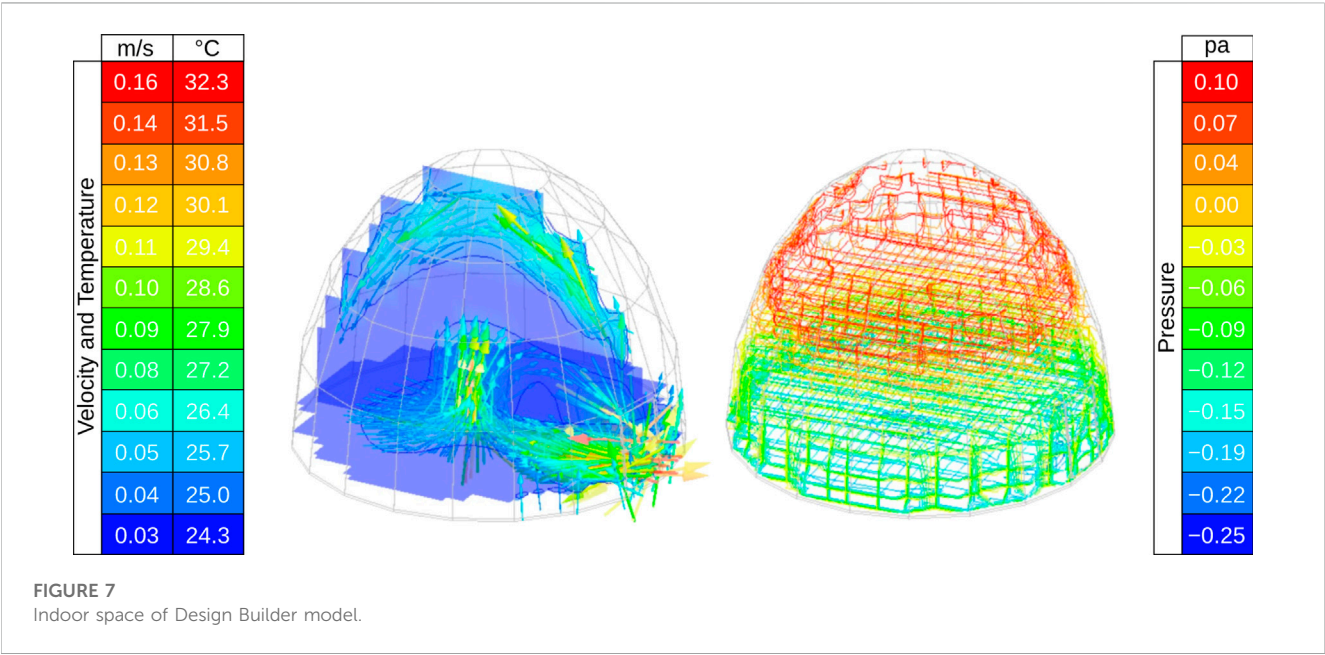
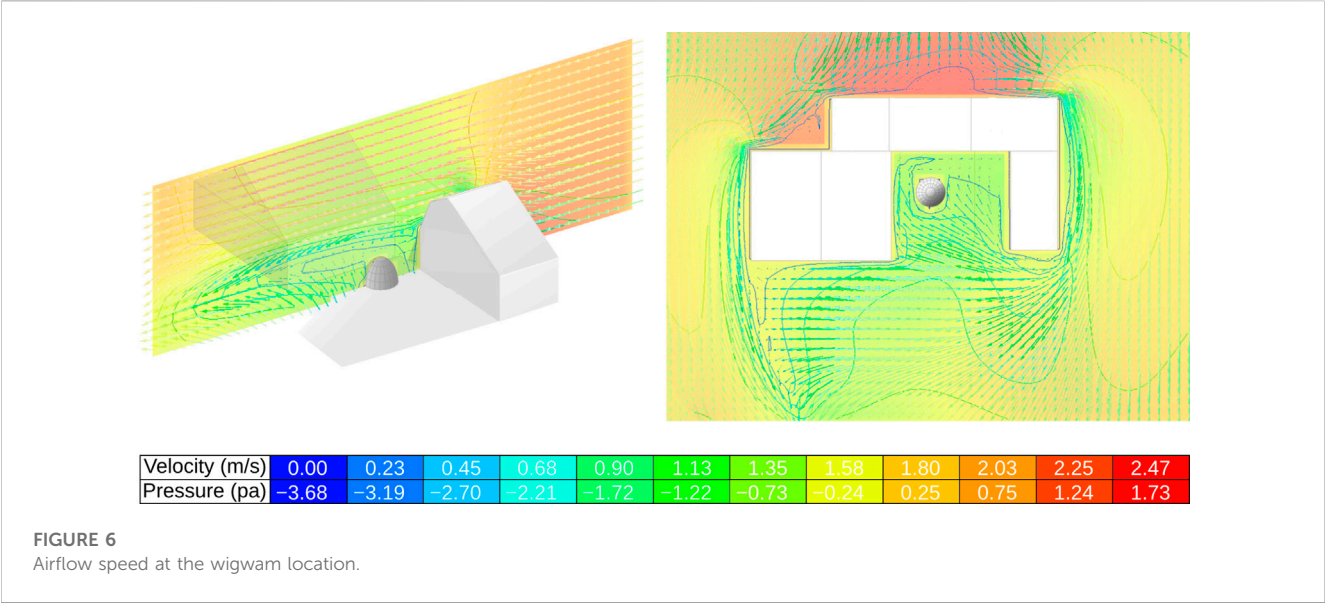
During October, two woodstove fires on the 16th and 23rd were made, with an open fire on the 22nd. For December, one open fire on the 24th with three enclosed fires on the 18th, 21st, and 25th were built. The collected data is presented in two categories: comfort and IAQ. The comfort category illustrates temperature and relative humidity trends, while the IAQ denotes CO₂ levels and harmful particulate matter such as VOCs and PM 2.5s.

Figure 2 helps delineate a steady pattern between the indoor temperature and relative humidity reminiscent of the mild weather in October, during the time when this was collected. The range of

indoor relative humidity when there was no fire operating was between 85.9% and 92.8%. However, as the temperature increases because of the interior heat source, the relative humidity subsides to 39%–67.3%. According to ASHRAE-5-2017 and CIBSE 2005&2006 guidelines, this performing range is acceptable. The indoor temperatures during the enclosed and open fire reached and maintained an ideal thermal climate between the degrees of 18.2°C–30.2°C. The outdoor temperature nearly replicates the indoor temperature when there are no external variables.

For each fire made in October, there is a significant spike in the graphs for particulate matter shown in Figure 3. During the first enclosed fire on the 16th, VOCs reached an accumulation of 472.4 ppb. The second enclosed fire on the 23rd attained 700.2 ppm. If occupants are exposed to either of these levels for an extended period, it could cause Adverse respiratory side-effects. The PM 2.5 levels were significantly elevated, with highs between 54.6–195 µg/m³. This particulate concentrate was above the dangerous threshold of 25 µg/m³. The CO₂ levels rose with the other two variables and increased to an unsafe elevated amount of 643.7–703.6 ppb. The open fire particulates exceeded the closed fire's IAQ values and hit hazardous levels for occupant exposure.

Figure 4 illustrates the indoor temperature and relative humidity levels inside the wigwam and the outdoor temperature and relative



humidity levels during the selected days in December. For indoor relative humidity, the top graph shows a range between a high of 95.8% and a low of 67% between the time of each fire operation. This number is elevated from the ASHRAE-5-2017 ideal range of 40%–60%–80%. However, with a fire, there is an observable pattern where the indoor relative humidity drops as the indoor temperature crests. When there were any fires, the relative humidity descended to around 26.3%–34.2%, a low relative humidity according to ASHRAE-5-2017. The graph presents the relative humidity tapering noticeably lower on the 24th with the open fire, even though the indoor temperature did not reach the highest of the three other fires. All the fires during this time reached and maintained temperature levels within the guidelines of

“comfortability,” according to ASHRAE -5-2017. The highest temperature reached was on the 21st with an enclosed fire that attained 26.7°C. Without any fires, the wigwam’s indoor temperature was aligned with the outdoor temperature, although slightly colder due to the lack of apricotty. The outdoor relative humidity oscillations show the relative humidity mirroring the interior with slight variation except for fire.

As the indoor temperature rose with each fire made, there was somewhat of a replicated pattern amongst the IAQ variables. The data in [Figure 5](#) suggests that having an enclosed fire significantly impacts the amount of particulate matter being projected into the indoor environment. Having an enclosed fire influences the amount of particulate matter by lowering the intensity of particulate matter.

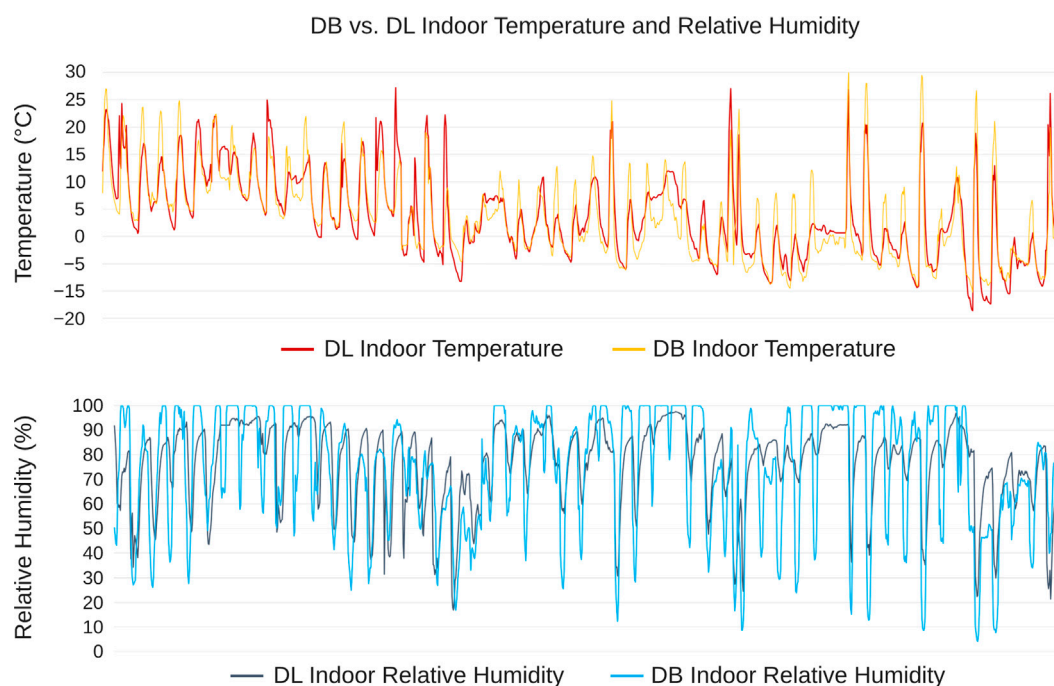


FIGURE 8

Comparison between simulated and actual values for indoor Temperature and Relative Humidity.

While analyzing the PM 2.5 levels, it is apparent that although significantly less than the open fire, the highest PM 2.5 levels for the first two enclosed fires and last fire reach around 119.8, 194, and 697.2 $\mu\text{g}/\text{m}^3$. These numbers are well above the threshold of 25 $\mu\text{g}/\text{m}^3$, which might constitute hazardous levels. As for the VOC levels, they are also all considerably higher than the amounts from PM 2.5. The VOC levels for the same enclosed fires reach 317.7, 332–391 ppb. These amounts are not at dangerous levels but could still potentially produce adverse physical symptoms. The CO₂ concentrations for the enclosed fires rose with the particulate matter and achieved levels between 574.1 ppb and 713.1 ppb. Data collected during the open fire in December shows levels that are hazardous to human health. The CO₂ levels reached peaks up to 896.4 ppb, VOC levels peaked at 10,592 ppb, and PM_{2.5} levels reached magnitudes close and up to 1000mg/m³ multiple times during the fire event. The heat source started at 8:30 on 17 December (until then, it was off). From then to 9:30, just 25% of its capacity (79°C) was on. From 9:30 to 10:45, it rose to 273°C. Finally, at noon, when no more wood was added, it reached its highest point, 370°C. From then on, its temperature decreased since no more wood was added. From 14:00 to 24:00, it went out.

It is important to acknowledge that any succeeding IAQ oscillation after each initial peak during any closed fires in October and December reflected when the woodstove door was opened to fuel the fire. Although these initial peaks failed to match the criteria of healthy air quality standards, it was essential to look at the timeline for these crests. For example, as shown on this last graph, the period when the PM 2.5 and CO₂ levels initially spiked is not continuous for any of the fires. Therefore, this would not

constitute consistent exposure. On this day, these subsequent peaks were less than the initial spike. The VOC pattern, on the hand, displayed levels rising with time and only tapering off when the fires dies down.

3.2 Compare the wigwam actual data to the Design-Builder model

The location of the wigwam under study determines the climatic conditions. Therefore, the weather file is applied by default in the Design-Builder software application. In addition, the data loggers measured on-site parameters inside and outside the prototype. The Computational Fluid Dynamics analysis (CFD) was carried out in two scenarios. The first corresponds to the wigwam's surroundings, where two buildings and several trees can be found. Wind force comes from the north, and its velocity was estimated as 2.15 m/s. This value corresponds to the average annual wind velocity for Keene Dillant-Hopkins Airport according to the EnergyPlus weather files. The solution converged in iteration number 11077. As shown in Figure 6, the airflow speed at the wigwam location was decelerated by the surrounding obstacles. Therefore, its value (2.15 m/s) decreases by approximately 50%. It works in the same way vertically and horizontally. As seen in Figure 6, its surroundings are composed of trees and two buildings, which could affect indoor temperatures and their corresponding humidity levels. Moreover, they cast shadows and impacted the wind velocity and direction in such a way that was essential to simulate the indoor values of the wigwam. Besides, wind mainly blows from the north in the wigwam location, the same orientation protected by the nearby trees and the

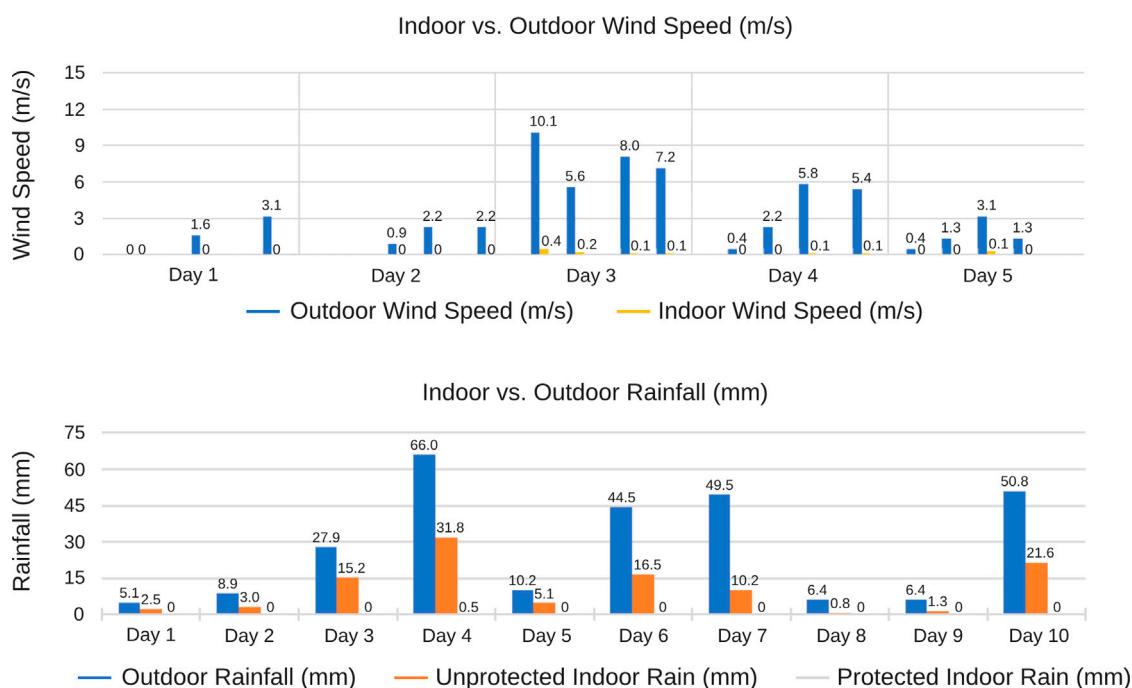


FIGURE 9
Indoor vs. outdoor windspeed and rainfall.

two constructions mentioned above. So, indoor conditions were highly influenced by them.

Figure 7 corresponds to the indoor space of the model. A hearth was placed in its center, modeled as a Design-Builder assembly component, as a radiator. Its temperature was estimated at 100°C since the indoor temperature of the wigwam was known and established as 22°C approximately when the hearth was lit. In this case, convergence was reached in iteration number 999. As can be seen, the hearth sucked the airflow that came from the entrance, triggering a little swirl that would get out the wigwam through the smoke hole when it was opened. This effectively created a little air-conditioning machine since its ventilation system started when that hearth was lit up. In this way, the wood stove installed inside the wigwam created airflow from the exterior up through the smoke hole. This airflow can be controlled by modifying the percentage of the opened area of the door. The bigger the area, the slower the airflow was, and *vice versa*.

Although at the monthly and annual level, it might seem that there are no significant differences, when entering hourly data the differences between simulation and actual values are substantial. This means that accurate comparisons cannot be made between days of the different years; so the data must be grouped, for instance, in weeks. Figure 8 illustrates the comparison between experimental and simulated trends of the internal air temperature and relative humidity for the experimental campaigns made in October and December. In particular, the difference between the simulated and measured temperature, was 10°C when the hearths were at their peak

heating load, whereas that difference was 4°C when the hearths were off. In addition to the model's ability to predict the indoor temperature, Figure 8 showed that the deviations for indoor relative humidity were more significant than the temperature. In conclusion, the hourly temperature was predicted with less error, which is a reasonable outcome since the relative humidity depended on more factors, such as the soil, the occupancy, and fuel combustion.

Some aspects require alignment to detect the accuracy of the building performance simulation tools compared with the experimental results. The deviations in results can be attributed to the accuracy of the mathematical models. However, some building simulation settings, such as the geometric representation, the outdoor climate conditions, and the heat transfer parameters, can impact the results. Design-Builder allows the user to select a gross, net, or mean internal volume of the thermal zone, so the surface areas related to a wall's inner or external side can be used. As mentioned in Section 2.2 the experimental weather data useful for the STB thermal dynamic simulation are the external air humidity and temperature, normal direct solar radiation, horizontal diffuse solar radiation, and wind speed intensity and direction. The diffuse component's Perez model was selected in Energy Plus to determine the global solar radiation on the STB surfaces differently oriented and inclined. To determine the simulation inputs, some experimental values, such as outdoor temperature, were introduced for the simulation. Nevertheless, other experimental values, such as the solar radiation on the inclined surfaces, were not measured, so verification was made on the indoor temperature and relative humidity.

TABLE 4 Indexes to calibrate errors according to international standards.

Calibration criteria	Index	FEMP criteria	ASHRAE 14	IPMVP
Hourly criteria %	NMBE	±10	±10	±5
	CVRMSE	30	30	20
	R ²	-	> 0.75	> 0.75

TABLE 5 Analysis of error between actual and simulated indoor temperature and relative humidity in October and December.

Parameter	MBE	NMBE	RMSE	CVRMSE
Tint (October)	0.18	0.06	4.40	1.55
RHint (October)	6.59	9.05	12.48	17.16
Tint (December)	1.04	0.38	4.32	1.58
RHint (December)	1.34	17.60	18.44	24.12

3.3 Results of rain and wind data collected

Whether or not a wigwam can serve as a viable shelter depends on how well it can protect its occupants from the elements. Empirical data for rainfall and wind speed were collected inside and outside the wigwam to make it possible to compare the values. Ideally, wind speed would be calm and undetectable by the wigwam's occupants, which, according to the National Weather Service, is anywhere below 4 mph (1.79 m/s). Wind speed was measured on several occasions using a handheld anemometer. In [Figure 9](#), the top graph represents five mornings from 6:00 a.m. to 11:00 a.m. when data was collected both outside and inside the wigwam. For all instances, wind speed decreased significantly on the interior. The lowest outdoor wind speed that resulted in wind registering on the anemometer was 3.1 with a 0.1 m/s reading. Any measurement below 3.1 m/s resulted in no wind inside. Day 3 experienced the strongest winds, up to 10.1 m/s. At this speed, indoor wind speed reached 0.4 m/s. Rainfall was collected both indoors and outdoors using multiple rain gauges. Due to the opening in the wigwam used for ventilating smoke, some rain entered the shelter. To be able to effectively determine the ability of the cotton duck material to keep out rain, two separate series of measurements on the interior were taken: one from the small area directly below the opening, and one underneath the covered area. The covered area is important because it's where occupants will circulate as the fire pit is directly below the opening. Both the unprotected and protected data are illustrated in the bottom graph of [Figure 9](#) along with the outdoor area. Both series of measurements saw a smaller amount of rain than the outside. The protected area received no rain except for Day 4's measurement of 0.5 mm, meaning nearly 100% of the rain was kept out of this area. The unprotected area, however, received more noticeable amount for nearly all the days. The rainfall under the opening ranged from; 0.8 mm when there was outside rain in the amount of 6.4–31.8 mm when there was outside rain in the amount of 66 mm. Across all measurements, an average of 36.9% of outdoor rain made its way into the wigwam underneath the opening.

4 Discussion

4.1 Comparison between Design-BUILDER and actual measurements

In this research, the simulated models were compared with data measured in the field. There were many challenges for the calibration process. First, the outdoor temperature data had strong fluctuations that could lead to significant discrepancies between the actual and simulated values. The second uncertainty was the evolution of the building envelope over time, for the materials might suffer a variation in their temperature. Finally, the simulated heat source had to be created as a sensible heat load that increased its temperature without adding humidity. These actual field measurements allowed adjustments to be made in the different parameters of the model to achieve an acceptable error. The digital model analyzed by Design-BUILDER included a new method to simulate the envelope parameters and characterize the heat source inside the wigwam. Therefore, after analyzing the results, it was essential to clarify the requirements to determine the accuracy of the building energy model. As it was stated in previous sections, there are several calibration criteria to assess the accuracy of simulated values against actual measurements. [Table 4](#) illustrates the indices used to calibrate errors and the thresholds proposed by the ASHRAE Guideline 14, the Federal Energy Management Program (FEMP), and the International Performance Measurement and Verification Protocol (IPMVP). The calibration criteria given by these standards are ±10% for the NMBE, 30% for the CVRMSE, and >0.75 for the coefficient of determination R².

A more extensive dataset makes evaluating the deviations more accurate. Thus, the indices were calculated over the entire month when considering hourly data. [Table 5](#) presents the outcomes of hourly calibration, where simulated indoor air temperature and relative humidity were validated against the ASHRAE and FEMP criteria. It shows the distribution of the deviation considering hourly data for a one-month simulation. The deviation range for CVRMSE for the relative humidity was 17.16% in October and 24.12% in December. Regarding indoor temperature, CVRMSE, and NMBE values were below 15% and 5%, respectively, for October and December, which can be regarded as a good agreement.

Despite the uncertainties in actual climatic conditions, the indoor temperature data obtained through the Design-BUILDER model showed a high correlation in all the comparisons made with the digital model against the actual measured data. [Figure 10](#) shows how the coefficient of determination (R²) between experimental and simulated indoor air temperature changes as a function of the indoor data of all the considered period of testing, but it is consistently above 0.75, the

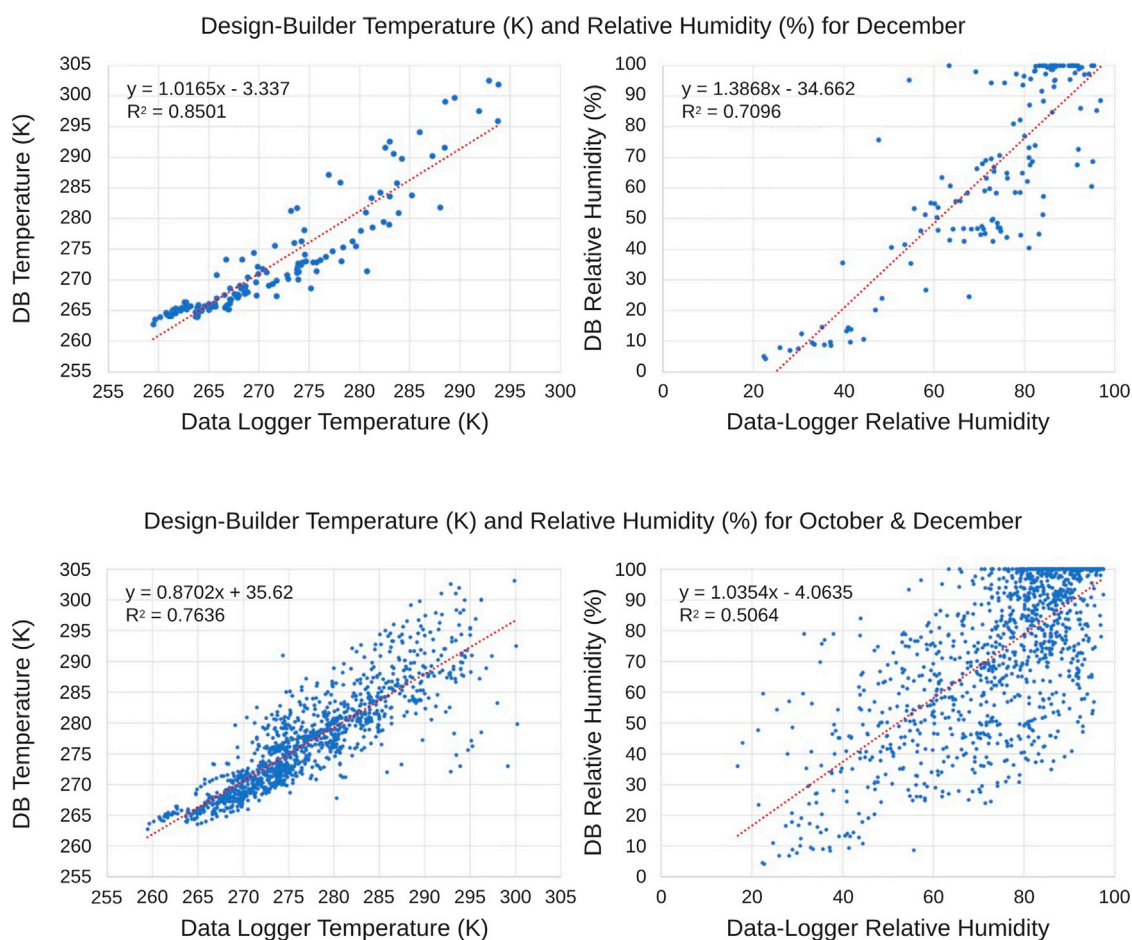


FIGURE 10

Coefficient of determination (R^2) for simulated and actual values of Temperature and Relative Humidity.

minimum calibration criteria accepted by ASHRAE and IPMVP. In contrast, the relative humidity dataset shows a value of 0.5 for the R^2 , far from the model's predictions and many points far from the best-fit line. As can be noticed, an increase in indoor temperature led to a growth of systematic errors. However, these measurements are valuable for validating the simulations. As observed in the images, the time the hearth was at its peak of thermal load showed the most significant difference between simulated and measured data. [Mazzeo et al. \(2020\)](#) analyzed the correlation between the simulated temperature by software IDA Indoor Climate and Energy 4.5. and measured internal temperature. A NRMSE equal to 11% on an hourly basis and a value of R^2 of 0.9439 was obtained, confirming that the built model can be considered calibrated. [Moran et al. \(2021\)](#) studied thermal comfort in refugee shelters in desert environments. They reported a Pearson's correlation coefficient, R^2 , ranging from 0.81 to 0.96. The main difference assessed in this article was the methodology to simulate the heating effect of open fires and wood stoves, considering the amount of renewable fuel to achieve indoor comfort in severe winter weather. Another difference from previous studies was to assess the accuracy of relative humidity simulations. The simulated indoor temperature values from December 20 to December 26 matched the trends and satisfied the required calibration criteria for

the coefficient of determination. The figures highlight that the simulated relative humidity values were more accurate over the week in December when the internal heat source controlled the temperature. However, due to uncertainties in the simulation inputs that may correspond to inaccuracies in the physical properties of the building and rates of infiltration or ventilation, the coefficient of determination is not above the acceptable threshold of 0.75.

4.2 Indoor air quality

The data revealed that thermal comfort and air quality standards showed different trends. Therefore, there is a need for a system that correlates indoor air quality factors and comfort parameters. This section discussed the results of Indoor Air Quality and comfort parameters, focusing on the correlation between temperature and the rest of indoor air quality indicators. As the weather got cold, there was a need to build either open fires or use a wood stove for short periods, increasing indoor temperature, decreasing relative humidity, and rising pollutants. [Table 6](#) shows the correlation among all Indoor Air Quality factors from October 7 to October 23. Its

TABLE 6 Analysis of the correlation factor between IAQ parameters in October.

	Tint (°C)	RHint (%)	CO2 (ppm)	VOC	PM2.5
Tint (°C)	1.00				
RHint (%)	−0.64	1.00			
CO2 (ppm)	−0.36	0.55	1.00		
VOC	0.28	−0.27	0.23	1.00	
PM2.5	0.11	−0.16	0.32	0.81	1.00

TABLE 7 Analysis of the correlation factor between IAQ parameters in December.

	Tint (°C)	RHint (%)	CO2 (ppm)	VOC	PM2.5
Tint (°C)	1.00				
RHint (%)	−0.63	1.00			
CO2 (ppm)	0.29	−0.16	1.00		
VOC	0.35	−0.24	0.89	1.00	
PM2.5	0.49	−0.37	0.61	0.70	1.00

value ranges from 0 to ± 1 , where 0 represents no correlation, and ± 1 indicates an excellent correlation. There was a high inverse correlation between the indoor temperature (Tint) and relative humidity. However, the temperature and particles did not show a high correlation, with values ranging from 0.11 between temperature and PM2.5 to 0.28 between temperature and VOC.

Table 7 shows a significant correlation between PM2.5 levels and VOCs (0.70) in December, although the highest correlation factor was shown between CO₂ and VOCs (0.89).

The correlation index increased considerably on days in which the heating source was on, either with an open fire or with a wood stove. Table 8 shows a high correlation above 0.6 between indoor temperature and both, PM2.5 and VOCs levels on December 24 and December 25. On those days, the heat source made the particle concentration rise and the relative humidity decrease. VOC and PM risk concentrations were mainly related to open fires, lack of ventilation, and occupants' unawareness of indoor air quality.

4.3 Comfort considerations

Increasing the share of radiation or conduction can increase comfort at colder air temperatures in winter. Radiant heat can make people comfortable at a lower air temperature, too. Indoors, the radiant temperature represents the total infrared radiation exchanged between all surfaces in a room. Radiant heating systems don't heat the air but the surfaces in a space, including human skin, raising the radiant temperature and providing thermal comfort at a colder air temperature. At high wind speeds, the warming effect of the heat source disappears. A wood stove in the middle of the room can be considered a longwave infrared panel. The highest radiant

TABLE 8 Analysis of the correlation factor between IAQ parameters from December 20 to December 26.

	Tint (°C)	RHint (%)	CO2 (ppm)	VOC	PM2.5
Tint (°C)	1.00				
RHint (%)	−0.90	1.00			
CO2 (ppm)	0.55	−0.32	1.00		
VOC	0.63	−0.42	0.89	1.00	
PM2.5	0.68	−0.40	0.88	0.89	1.00

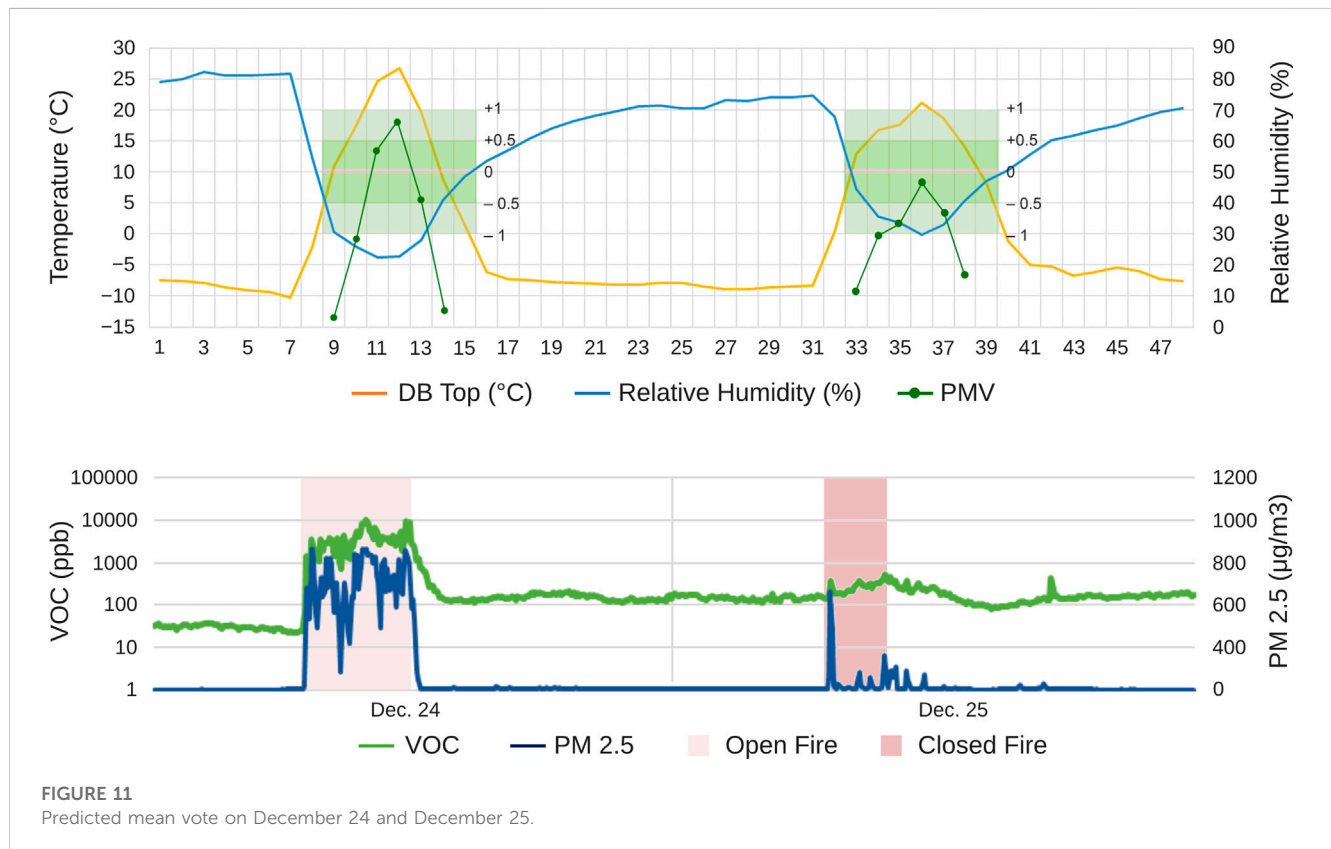
temperature would be measured in the middle of the room, right beside the heating source. The radiant temperature would decrease in concentric circles towards the envelope of the wigwam. The difference between minimum and maximum radiant temperature is more significant than in the case of an air heating system. Thus, neither a high nor low radiant air temperature guarantees thermal comfort. The best interpretation of the thermal comfort in a room is provided by the operative temperature, which is a weighted average of the air and radiant temperatures. On the vertical plane, warm air rises so that most heat ends up at the ceiling level, which is useless. Heating only the occupied space of a room is possible with a radiant heating source, such as a wood stove, no matter how high the ceiling, which is much more energy efficient. The heat only rises if the heating surface is aimed upwards. In addition, almost all the energy a radiant heating system uses is effective for heating humans. Table 9 defines the PMV range for the thermal sensation scale according to ASHRAE 55 standard.

Figure 11 summarizes all the variables that affected the comfort and indoor air quality inside the wigwam when there was a heat source. It illustrates the variations of the predicted mean vote (PMV), operative temperature, and relative humidity on two December days. The data logger measured indoor relative humidity, whereas the operative temperature was taken from the Design-Builder simulation. Hence, the open fire and the wood stove provided comfortable conditions during 4 hours of operation. The operative temperature rose from -10°C at 9:00 a.m. to 26°C at noon on December 24 and from -8°C at 9:00 a.m. to 21°C at 12 p.m. on December 25. In contrast, the relative humidity ranged from 80% to 22% on December 24 and 75%–30% on December 25. For 4 h, the PMV was between -1 and 1 . The PMV analysis showed that occupants would describe their comfort conditions as “Slightly Cool” or “Slightly Warm.” Regarding Indoor Air Quality conditions, the wood stove provided a much better indoor environment with VOC values below 500 ppb and PM2.5 levels below $10\text{ }\mu\text{g}/\text{m}^3$, except at moments in which the stove door was open to load the fuel with levels above the dangerous threshold of $25\text{ }\mu\text{g}/\text{m}^3$, which constitutes hazardous levels.

An aspect that can impact comfort is the asymmetry of radiant heating. For example, a person sitting in front of an open fire can be in thermal balance, but thermal comfort will not be obtained because the heat gain on one side equals the heat loss on the other. Thus, a solution to thermal asymmetry could be supplementing local heating with insulation to create a

TABLE 9 ASHRAE 55 thermal comfort scale^a.

Cold	Cool	Slightly cool	Neutral	Slightly warm	Warm	Hot
−3	−2	−1	0	+1	+2	+3

^aValues are taken from [39].

comfortable microclimate. One example was the hooded chair. This chair, which could be upholstered or covered with leather or wool blankets, fully exposed people to a radiant heat source while protecting their backs from the drafts and the low surface temperatures behind them. At the same time, the furniture's shape could make the occupants effectively perceive a more significant percentage of the radiant heat emitted by the source. For example, if a chair were heated directly by the fire through radiation, the heat could be transferred to the person sitting on it by conduction. Open fires are inefficient because a large share of heat escapes vertically without heating the occupants. Stoves work better but remain relatively ineffective and must be fired regularly, like a fireplace. And both options can release air pollutants significantly. Still, many options exist, such as electric and conductive heating systems. These are more efficient and safer than the heating sources of yesteryear. [Albadra et al. \(2017\)](#) addressed the problem of the actual living conditions during periods of hot and cold weather in emergency shelters. These surveys confirm that occupants lived outside of comfort thresholds stated by Fanger's Predicted Mean Vote, so other comfort models, such as adaptive models, must be considered in future studies of these structures.

In conclusion, exposure to either an open or an enclosed fire inside the wigwam for an extended period could generate adverse symptoms from the harmful particulate matter. Therefore, wigwam occupants may want to regulate their time inside the structure. In addition, for closed fires, the woodstove door should be only briefly opened to feed the fire in order to help mitigate any additional accumulation. A novelty outcome from this research was the dependence of indoor air quality on the heating system, indicating a condition to consider other heating devices that combine renewable fuels and a reduction of pollutant emissions.

5 Conclusion

This research confirmed that, by developing a digital model in Design-Builder, it is possible to get a good correlation between actual and simulated data for indoor temperature and relative humidity of wigwam. The proposed methodology offered a proper procedure to simulate the heat source of sensible heat that did not change the humidity ratio, as it was based on the data measured from the prototype. At the same time, the calibration process can be used to assess the thermal behavior of any given building.

Using Design-Builder software, the authors addressed the challenge of simulating the wigwam's indoor air temperature and relative humidity. Several iterations were necessary to simulate, first, the thermal parameters of the envelope, second, the influence of natural ventilation, and finally, a heat source that mimicked the heat source and its impact on relative humidity. Statistical analysis was used to assess the accuracy of the simulations by finding the coefficient of determination (R^2) between the simulated and actual data for daily and monthly values. Deviations were acceptable comparing the indoor air temperature with R^2 values above 0.75. However, the relative humidity results showed more uncertainties.

Real data collection showed the ability to combine comfort conditions and Indoor Air Quality within the shelter with freezing outdoor weather. The Predicted Mean Vote (PMV) on winter days ranged from -1 to $+1$ when a renewable heating system was on. However, the Indoor Air Quality levels were far from acceptable with open fires. Data collected during the open fire in December shows levels that are hazardous to human health. For example, the CO_2 levels reached 896.4 ppb, VOC levels peaked at 10,592 ppb, and $\text{PM}_{2.5}$ levels reached magnitudes close and up to $1000 \mu\text{g}/\text{m}^3$ multiple times during the fire event. In contrast, during closed fires, the VOC levels reached 391 ppb, not at dangerous levels but with the potential to produce adverse physical symptoms. The CO_2 concentrations for the enclosed fires achieved levels of 600 ppb, 30% below open fire levels. Finally, $\text{PM}_{2.5}$ levels reached $200 \mu\text{g}/\text{m}^3$, 80% below open fire levels but above the $25 \mu\text{g}/\text{m}^3$ threshold of healthy conditions.

One of the limitations encountered in the methodology was the difficulty in measuring the Mean Radiant Temperature (MRT). CBE tool can select MRT by the input box if the user selects option EN-16798. Another option was to use the Operative Temperature as a function of Mean Radiant Temperature and Indoor Air Temperature. Design Builder provides users with Operative Temperature, so those values were used as input to calculate thermal comfort using the option ASHRAE-55 in the CBE tool. Future research must include envelope temperature measurements to accurately evaluate the heat source radiation's effect. The prototype was measured in the cold season. How the model will work in other seasons with different envelopes is worth being validated in the future. [AcuRite 5, 2023](#), [Elitechlog, 2023](#), [Getawair, 2023](#).

Data availability statement

The raw data supporting the conclusion of this article will be made available by the authors, without undue reservation.

References

- AcuRite 5 (2023). Capacity easy-to-read magnifying acrylic, rain gauge. Available online: <https://www.acurite.com/shop-all/weather-instruments/rain-gauges/easy-read-5-magnifying-rain-gauge-00850.html>. (accessed Feb 12, 2023)
- Albadra, D., Vellei, M., Coley, D., and Hart, J. (2017). Thermal comfort in desert refugee camps: An interdisciplinary approach. *Build. Environ.* 124, 460–477. doi:10.1016/j.buildenv.2017.08.016
- Ashrae (2017). "ASHRAE-55 ANSI/ASHRAE standard 55," in *Thermal environmental conditions for human occupancy* (Atlanta, GA, USA: ASHRAE).
- Ashrae Guideline 14 (2014). *Measurement of energy and demand savings*. Atlanta, GA, USA: American Society of Heating, Ventilating, and Air Conditioning Engineers.
- Ashrae (2012). "Heating, ventilating, and air-conditioning systems and equipment," in *Tullie circle* (Atlanta, GA, USA: ASHRAE).
- Borge-Diez, D., Colmenar-Santos, A., Mur-Pérez, F., and Castro-Gil, M. (2013). Impact of passive techniques and clean conditioning systems on comfort and economic feasibility in low-cost shelters. *Energy Build.* 62, 414–426. doi:10.1016/j.enbuild.2013.03.032
- Bozkaya, B., Li, R., and Zeiler, W. (2018). A dynamic building and aquifer co-simulation method for thermal imbalance investigation. *Appl. Therm. Eng.* 144, 681–694. doi:10.1016/j.applthermaleng.2018.08.095
- Bushnell, D. (1922). *Villages of the algonquian, siouan, and caddoan tribes west of mississippi*. Washington, DC, USA: Government Printing Office.

Author contributions

Conceptualization, PF and FD; methodology, PF, SN, and JP; software, MM; validation, PF, RG, and FD; investigation, PF, SN, and JP; data curation, PF and SN; writing—original draft preparation, PF and SN; writing—review and editing, FD and MM; visualization, SN, JP, and MM; supervision, PF, RG, and FD; project administration, PF; funding acquisition, PF. All authors contributed to the article and approved the submitted version.

Funding

The authors wish to thank CEU San Pablo University Foundation for the funds dedicated to the ARIE Research Group, through the Project Ref. EC01/0720- MGI22RGL provided by the CEU San Pablo University. Materials and student grants for this research were funded by Keene State College, Faculty Development Grant "Wigwam made with modern materials."

Conflict of interest

The authors declare that the research was conducted in the absence of any commercial or financial relationships that could be construed as a potential conflict of interest.

Publisher's note

All claims expressed in this article are solely those of the authors and do not necessarily represent those of their affiliated organizations, or those of the publisher, the editors and the reviewers. Any product that may be evaluated in this article, or claim that may be made by its manufacturer, is not guaranteed or endorsed by the publisher.

Supplementary material

The Supplementary Material for this article can be found online at: <https://www.frontiersin.org/articles/10.3389/fbuil.2023.1202965/full#supplementary-material>

- Cbe (2022). Thermal comfort tool. Available online: <https://cbe.berkeley.edu/tool/cbe-thermal-comfort-tool/> (accessed Dec 17, 2022).
- Crawford, C., Manfield, P., and McRobie, A. (2005). Assessing the thermal performance of an emergency shelter system. *Energy Build.* 37, 471–483. doi:10.1016/j.enbuild.2004.09.001
- De la Torre, S., and Yousif, C. (2014). Evaluation of chimney stack effect in a new brewery using DesignBuilder-EnergyPlus software. *Energy Procedia* 62, 230–235. doi:10.1016/j.egypro.2014.12.384
- Del Ama Gonzalo, F., Moreno Santamaría, B., and Burgos, M. J. M. (2023). Assessment of building energy simulation tools to predict heating and cooling energy consumption at early design stages. *Sustainability* 15 (3), 1920. doi:10.3390/su15031920
- Dominguez, S., Fernandez-Aguera, J., Cesteros-García, S., and Gonzalez-Lezcano, R. (2020). Bad air can also kill: Residential indoor air quality and pollutant exposure risk during the COVID-19 crisis. *Int. J. Environ. Res. Public Health* 17, 7183. doi:10.3390/ijerph17197183
- Efficiency Valuation Organization (2012). Washington, DC, USA: Efficiency Valuation Organization. International performance measurement and verification Protocol: Concepts and options for determining energy and water savings
- Elitechlog (2023). RC-51H PDF Temperature & Humidity data logger. <http://www.elitechlog.com/rc-51h-pdf-temperaturehumidity-data-logger/> (accessed Mar 8, 2023).
- Epa (2022). Revised air quality standards for particle pollution and updates to the air quality index. https://www.epa.gov/sites/default/files/2016-04/documents/2012_aqi_factsheet.pdf (accessed Dec 17, 2022).
- Fanger, P. O. (1973). Assessment of man's thermal comfort in practice. *Occup. Environ. Med.* 30 (4), 313–324. doi:10.1136/oem.30.4.313
- Fanger, P. O. (1970). *Thermal comfort, analysis, and application in environmental engineering*. Copenhagen, Denmark: Danish Technical Press.
- Fantozzi, F., Lamberti, G., Leccese, F., and Salvadori, G. (2022). Monitoring CO₂ concentration to control the infection probability due to airborne transmission in naturally ventilated University classrooms. *Archit. Sci. Rev.* 65 (4), 306–318. doi:10.1080/00038628.2022.2080637
- Fawwaz Alrebei, O., Obeidat, L. M., Ma'bdeh, S. N., Kaouri, K., Al-Radaideh, T., and Amhamed, A. I. (2022). Window-windcatcher for enhanced thermal comfort, natural ventilation and reduced COVID-19 transmission. *Buildings* 12, 791. doi:10.3390/buildings12060791
- Fernández Bandera, C., and Ramos Ruiz, G. (2017). Towards a new generation of building envelope calibration. *Energies* 10, 2102. doi:10.3390/en10122102
- Getawair (2023). TopTes TS-301 digital anemometer, wind speed meter with 2.26-inch LCD screen, air meter. <https://www.getawair.com/products/element>.
- Getuhoo (2022). Understanding VOC's and its effects on health. Available online: <https://getuhoo.com/blog/home/understanding-vocs-and-its-effects-on-health/> (accessed Dec 17, 2022).
- Ghio, A. J. (2017). Particle exposure and the historical loss of native American lives to infections. *Am. J. Respir. Crit. Care Med.* 195, 1673. doi:10.1164/rccm.201609-1810le
- Gonzalo, F. d. A., Griffin, M., Laskosky, J., Yost, P., and González-Lezcano, R. A. (2022). Assessment of indoor air quality in residential buildings of new england through actual data. *Sustainability* 14, 739. doi:10.3390/su14020739
- Holley, L. A. (2007). *Tipis, teepees, teepees: History and design of the cloth tipi*. 1st ed. Layton, UT, United States: Gibbs Smith Publisher.
- Ibm (2022). IBM maximo worker insights. Available online: <https://www.ibm.com/docs/en/mwi?topic=shields-air-quality-shield>. (accessed Nov 28, 2022)
- ISO 7730 (2005). *Ergonomics of the thermal environment- Analytical determination and interpretation of thermal comfort using calculation of the PMV and PPD indices and local thermal comfort criteria. (reviewed and confirmed in 2015)*. Geneva, Switzerland: International Organization for Standardization ISO.
- Kabrein, H., Yusof, M. Z. M., Hariri, A., Leman, A. M., and Afandi, A. (2017). Improving indoor air quality and thermal comfort in office building by using combination filters. *IOP Conf. Ser. Mater. Sci. Eng.* 243, 012052. doi:10.1088/1757-899x/243/1/012052
- Kalman, B. (2000). *Native homes*. St. Catharines, Ontario, Canada: Crabtree Pub Co.
- Kidadl (2022). Wigwams facts learn all about the Native American homes. <https://kidadl.com/facts/wigwams-facts-learn-all-about-the-native-american-homes> (accessed Nov 10, 2022).
- Knight, P. V. (2017). *Native American homes: From longhouses to wigwams (native American cultures)*. Milwaukee, Wisconsin: Gareth Stevens Pub.
- Kristak, L., Igaz, R., and Ruziak, I. (2019). Applying the EDPS method to the research into thermophysical properties of solid wood of coniferous trees. *Adv. Mater. Sci. Eng.* 2019, 1–9. doi:10.1155/2019/2303720
- Lamberti, G. "Critical overview of heat balance, adaptive, local discomfort models to predict thermal comfort in buildings," in Proceedings of the IEEE International Conference on Environment and Electrical Engineering and 2021 IEEE Industrial and Commercial Power Systems Europe (IEEEIC/ I&CPS Europe), Bari, Italy, September 2021. doi:10.1109/IEEEIC/ICPSEurope51590.2021.9584714
- Lawson, J. R., Walton, W. D., Bryner, N. P., and Amon, F. K. (2005). *Estimates of thermal properties for fire fighters' protective clothing materials*. Gaithersburg, Maryland: U.S. Department of Commerce Building and Fire Research Laboratory National Institute of Standards and Technology.
- Lezcanoand Burgos (2021). Airflow analysis of the Haida plank house, a breathing envelope. *Energies* 14 (160), 4871. doi:10.3390/en14164871
- Mayrl, D. (2002). *The potawatomi of Wisconsin*. New York, NY, United States: PowerKids Press.
- Mazzeo, D., Matera, N., Cornaro, C., Oliveti, G., Romagnoni, P., and Santoli, L. (2020). EnergyPlus, IDA ICE and TRNSYS predictive simulation accuracy for building thermal behaviour evaluation by using an experimental campaign in solar test boxes with and without a PCM module. *Energy Build.* 212, 109812. doi:10.1016/j.enbuild.2020.109812
- Montero Burgos, M. J., Sanchiz Álvarez de Toledo, H., González Lezcano, R. A., and Galán de Mera, A. (2020). The sedentary process and the evolution of energy consumption in eight native American dwellings: Analyzing sustainability in traditional architecture. *Sustainability* 12 (5), 1810. doi:10.3390/su12051810
- Montgomery, D. (2000). "Native American crafts and skills," in *A fully illustrated Guide to wilderness living and survival*. 2nd (Essex, CT, United States: Lyons Press).
- Moran, F., Fosas, D., Coley, D., Natarajan, S., Orr, J., and Bani Ahmad, O. (2021). Improving thermal comfort in refugee shelters in desert environments. *Energy Sustain. Dev.* 61, 28–45. doi:10.1016/j.esd.2020.12.008
- Moreno-Rangel, A., Sharpe, T., Musau, F., and McGill, G. (2018). Field evaluation of a low-cost indoor air quality monitor to quantify exposure to pollutants in residential environments. *J. Sens. Sens. Syst.* 7, 373–388. doi:10.5194/jsss-7-373-2018
- Morgan, L. H. (1881). *Houses and house-life of the American aborigines*. Washington D.C, VA: Govt. Print. Off.
- Nabokov, P., and Easton, R. (1989). *Native American architecture*. New York, NY, USA: Oxford University Press.
- Native American houses (2022). Native American houses. Available online: <https://www.warpaths2peacepipes.com/native-american-houses/wigwam.htm>. (accessed Nov 10, 2022)
- Neymark, J., Judkoff, R., Knabe, G., Le, H. T., Dürig, M., Glass, A., et al. (2002). Applying the building energy simulation test (BESTEST) diagnostic method to verification of space conditioning equipment models used in whole-building energy simulation programs. *Energy Build.* 34 (9), 917–931. doi:10.1016/s0378-7788(02)00072-5
- Ny State Gov (2022). Department of health. Available online: https://www.health.ny.gov/environmental/indoors/air/pmq_a.htm. (accessed Nov 24, 2022)
- Nyholm, E. (1981). *The use of birch bark by the ojibwa Indians. Folk life festival*. Michigan, US: Crafts, Indigenous Peoples.
- Pilsworth, M. N. (1978). *The calculation of heat loss from tents*. Natick, MA, USA: United States Army Natick Research & Development Command.
- Radhi, H. (2010). On the optimal selection of wall cladding system to reduce direct and indirect CO₂ emissions. *Energy* 35, 1412–1424. doi:10.1016/j.energy.2009.11.026
- Ruiz, G. R., and Bandera, C. F. (2017). Validation of calibrated energy models: Common errors. *Energies* 10, 1587. doi:10.3390/en10101587
- Schwartz, S. (2009). *Native American housing*. New York, NY, USA: Gilder Lehrman Institute of American History.
- Speck, F. G. (1922). *Beothuk and micmac*. New York, NY, USA: Museum of the American Indian Heye foundation: NYC.
- Sunforger Tent Canvas (2023). Available online <https://www.bigduckcanvas.com/canvas-for-tents/army-duck/10-10-oz-60-sunforger-fire-retardant-tent-canvas> (accessed Feb 26, 2023).
- Tan, H., Wong, K. Y., Othman, M. H. D., Hong, Y. K., Roswanira, A. W., Garry, K. P. E., et al. (2022). Current and potential approaches on assessing airflow and particle dispersion in healthcare facilities: A systematic review. *Environ. Sci. Pollut. Res.* 29, 80137–80160. doi:10.1007/s11356-022-23407-9
- The Building of a Wigwam (2022). The building of a wigwam. Available online: <https://www.youtube.com/watch?v=4JBqBtcJlA>. (accessed Nov 10, 2022)
- Ullal, A., Aguacil, S., Vannucci, R., Yang, S., Pernot, J. G., Licina, D., et al. (2022). Comparing thermal performance of standard humanitarian tents. *Energy Build.* 264, 112035. doi:10.1016/j.enbuild.2022.112035
- Wang, S., Yan, C., and Xiao, F. (2012). Quantitative energy performance assessment methods for existing buildings. *Energy Build.* 55, 873–888. doi:10.1016/j.enbuild.2012.08.037
- Wigwam (2022). Wigwam. Available online: <https://www.newworldencyclopedia.org/entry/Wigwam>. (accessed Nov 10, 2022)
- William, M. A., Suárez-López, M. J., Soutullo, S., and Hanafy, A. A. (2021). Building envelopes toward energy-efficient buildings: A balanced multi-approach decision making. *Int. J. Energy Res.* 45, 21096–21113. doi:10.1002/er.7166



OPEN ACCESS

EDITED BY

Faming Wang,
KU Leuven, Belgium

REVIEWED BY

Jiying Liu,
Shandong Jianzhu University, China

*CORRESPONDENCE

Roberto Alonso González-Lezcano,
✉ rgonzalezcano@ceu.es

RECEIVED 10 May 2023

ACCEPTED 28 August 2023

PUBLISHED 13 September 2023

CITATION

González-Lezcano RA,
Sanglier Contreras G, Iglesias Sanz CM,
Sancho Alambillaga R and
López Fernández EJ (2023), Construction
parameters that affect the air leaks of the
envelope in dwellings in Madrid.
Front. Built Environ. 9:1220559.
doi: 10.3389/fbuil.2023.1220559

COPYRIGHT

© 2023 González-Lezcano, Sanglier
Contreras, Iglesias Sanz, Sancho
Alambillaga and López Fernández. This is
an open-access article distributed under
the terms of the [Creative Commons
Attribution License \(CC BY\)](#). The use,
distribution or reproduction in other
forums is permitted, provided the original
author(s) and the copyright owner(s) are
credited and that the original publication
in this journal is cited, in accordance with
accepted academic practice. No use,
distribution or reproduction is permitted
which does not comply with these terms.

Construction parameters that affect the air leaks of the envelope in dwellings in Madrid

Roberto Alonso González-Lezcano^{1*}, Gastón Sanglier Contreras¹,
Carlos Miguel Iglesias Sanz¹, Rocío Sancho Alambillaga² and
Eduardo José López Fernández¹

¹Escuela Politécnica Superior, Montepríncipe Campus de Boadilla del Monte, Universidad San Pablo-CEU, CEU Universities, Madrid, Spain, ²UDIT Universidad de Diseño y Tecnología, Madrid, Spain

In buildings, ventilation, or rather, a lack of airtightness facilitates air leaks, from the outside to the inside and *vice versa*, and is not controlled. Cold air enters through the enclosure, and warm air is lost to the outdoors, due to the poor hermeticity of the facades, roofs, carpentry, ducts, etc. In order to quantify the airtightness in multi-family dwellings in Madrid, 151 blower door tests have been carried out in multi-family dwellings built in different periods whose execution has been regulated by the UNE-EN 13829 standard. Through its quantification by an n_{50} value, the average values of 5.8 renovations per hour have been obtained in addition to detecting the main points where air infiltration occurs. The constant improvement in the transmittance of construction elements has indicated that the entry of outside air has a progressively greater relevance to the total energy consumed by the residential sector while facilitating the uncontrolled movement of air through the building envelope. This not only implies higher energy consumption but also generates a series of problems that affect the health of the occupants, such as a lack of thermal comfort, entry of pollutants and odours, noise, inadequate operation of ventilation systems, and less protection against fire.

KEYWORDS

residential buildings, natural ventilation, air infiltration, building envelope airtightness, energy leakage, indoor air quality monitoring

1 Introduction

Building energy demand has become one of the most important concerns in the construction sector. The European Energy Performance of Buildings Directive (EPBD) is committed to achieving a highly efficient and decarbonized building stock, considering that almost 50% of the final energy consumption is used for heating and cooling, 80% of which is used in buildings (European Parliament, 2018).

Concerns about the airtightness of dwellings have been taken into account in the United States since before 1995 (Sherman, 1995), in view of the fact that EU member states have committed themselves to reducing the primary energy consumption by 20% by 2020. The energy consumption in residential and commercial buildings accounts for approximately 40% of the total final energy consumption (Darvish et al., 2020), 52% of which accounts for the main heat losses in dwellings due to ventilation and therefore infiltration (Almarzouq and Sakhrieh, 2018).

A lot of documentation of air infiltration is available in European countries with cold climates but little, or almost nothing, in warm countries, such as Spain, and it is important to

know the main causes for the controlled and uncontrolled air infiltration through the study of houses in Madrid, in warm climates (Lozinsky and Touchie, 2018).

Leakage is a current of air that circulates through cracks, interstices, and unwanted openings, which is produced by a pressure difference, due to wind, temperature differences, or the mechanical ventilation system itself (Goubran et al., 2017). This uncontrolled flow of air can move from the outside to the inside (infiltration, which is a common form in buildings) or in the opposite direction (exfiltration, which is rare, due to unique external and internal conditions) (Sherman, 1987; Jokisalo et al., 2009).

In this field of study, airtightness is understood as the quality of the building envelope capable of preventing the entry of air or other elements, such as water, noise, and pollutants, from an external environment to an internal environment (González-Lezcano and Hormigos-Jiménez, 2016; Bhandari et al., 2018). In order to achieve good acoustics and thermal insulation, airtightness is considered necessary for the building envelope. This is one of the necessary conditions for energy savings (Hamby, 1994; Fernandez-Antolin et al., 2019a).

The lack of airtightness of the dwelling leads to other causes in addition to the energy cost, and important among them is the quality of the air, which determines that these infiltrations cannot be considered natural ventilation due to the quality of the surrounding air (Villi et al., 2013). According to Sherman (1987), the causes of leakage in a dwelling are height, area, and age. He sets the height coefficient at 1.15, i.e., adding one storey in height increases leakage rates by 15%. The greater the area, the higher the ratio of openings to the total volume of the building. The older they get, the higher the leakage will be, at a rate of 1% per year (Sadineni et al., 2011; Bramiana et al., 2016).

This paper focuses on the characterization of the residential building stock in the Madrid area. Despite the fact that no evidence was found to justify that climate is a significant variable in terms of airtightness (Synnefa et al., 2007; Fernandez-Antolin et al., 2019b), it seems clear that there are different aspects associated with the region where the building is located such as differences in construction quality, dwelling design or materials, or due to differences in the building size or age (Lee et al., 2011; Fernandez-Antolin et al., 2021). The aim of this study is to delve into the main causes of the lack of airtightness of multi-family dwellings through 151 blower door tests in the Community of Madrid.

2 Materials and methods

A blower door is the measurement technique used to determine the level of infiltration in the dwellings studied. It consists of a fan placed on an exterior door or window that generates a pressure difference, either by pressurizing or depressurizing the room, by injecting or extracting a flow of air. The number of renovations per hour of the building is calculated by dividing the flow rate at a pressure of 50 Pa by the volume of indoor air, as a way of measuring the airtightness. Once the leakage rate for a building has been measured, it is useful to estimate the total size of all leaks or openings in the building envelope (Sfakianaki et al., 2008; Fernandez-Antolin et al., 2020). TECTITE Express airtightness

test analysis software is used to calculate two separate leakage areas, based on different assumptions about the physical shape of the hole. The equivalent leakage area (EqLA) is defined by Canadian researchers at the National Research Council of Canada as the area of a sharp-edged opening through which the same amount of air will leak as that measured at a pressure difference of 10 Pa. The effective leakage area (ELA) was developed by the Lawrence Berkeley Laboratory (LBL) and is used in their infiltration model. The effective leakage area is defined as the area of a rounded edge opening through which the same amount of air will leak as that measured at a pressure difference of 4 Pa (Santamouris et al., 2001; Chan et al., 2005; Frontczak et al., 2012; González-Lezcano et al., 2020; Santamaria et al., 2020).

Figure 1 shows the equipment with which all the measurements were carried out.

During the depressurization process, data are captured using a thermography camera, as shown in Figure 1, thus locating the points where the greatest infiltrations occur in the dwelling, for which a thermal gap between the interior and the exterior is necessary.

2.1 Test description

The following equipment was used to carry out the test:

- Blower door equipment 5102 CP DM32 Wi-Fi.
- FLIR E75 thermal imager.
- Anemometers (air speed 0.3–30 m/s) at −10 to 45°C (used for measuring the wind speed).
- Air quality monitor mod. Vertex HD21ABE17 (used to measure the indoor and outdoor temperature, indoor and outdoor relative humidity, and atmospheric pressure).
- Fantastic Pro software.

In all the tests, the atmospheric conditions were adequate to carry out pressurization and depressurization tests, since the pressure difference between the interior and exterior of the house, as indicated by the ISO/DIS 9972 standard, was less than 3 Pa and the outdoor wind speed was less than 3.6 m/s.

The evaluation of the permeability of the envelope has been carried out according to method B (building envelope test) described in the UNE-EN 13829 standard (AENOR, 2002) for the determination of airtightness in buildings by the method of pressurization by means of a fan, commonly known as the blower door test.

3 Results and discussion

Data collected from 151 measurements in collective dwellings in the Community of Madrid, from different years, are listed in Table 1.

The results obtained from the tests carried out in Madrid show an average n_{50} value of 5.80 renovations per hour. Among the factors observed in the dwellings, as in the United States, year of construction is the main factor (A Chan et al., 2013), which leads to a certain way of building and, therefore, a certain airtightness, giving better airtightness values between the years 1921 and 1950. Although 80% of the dwellings were renovated, they all coincide in a

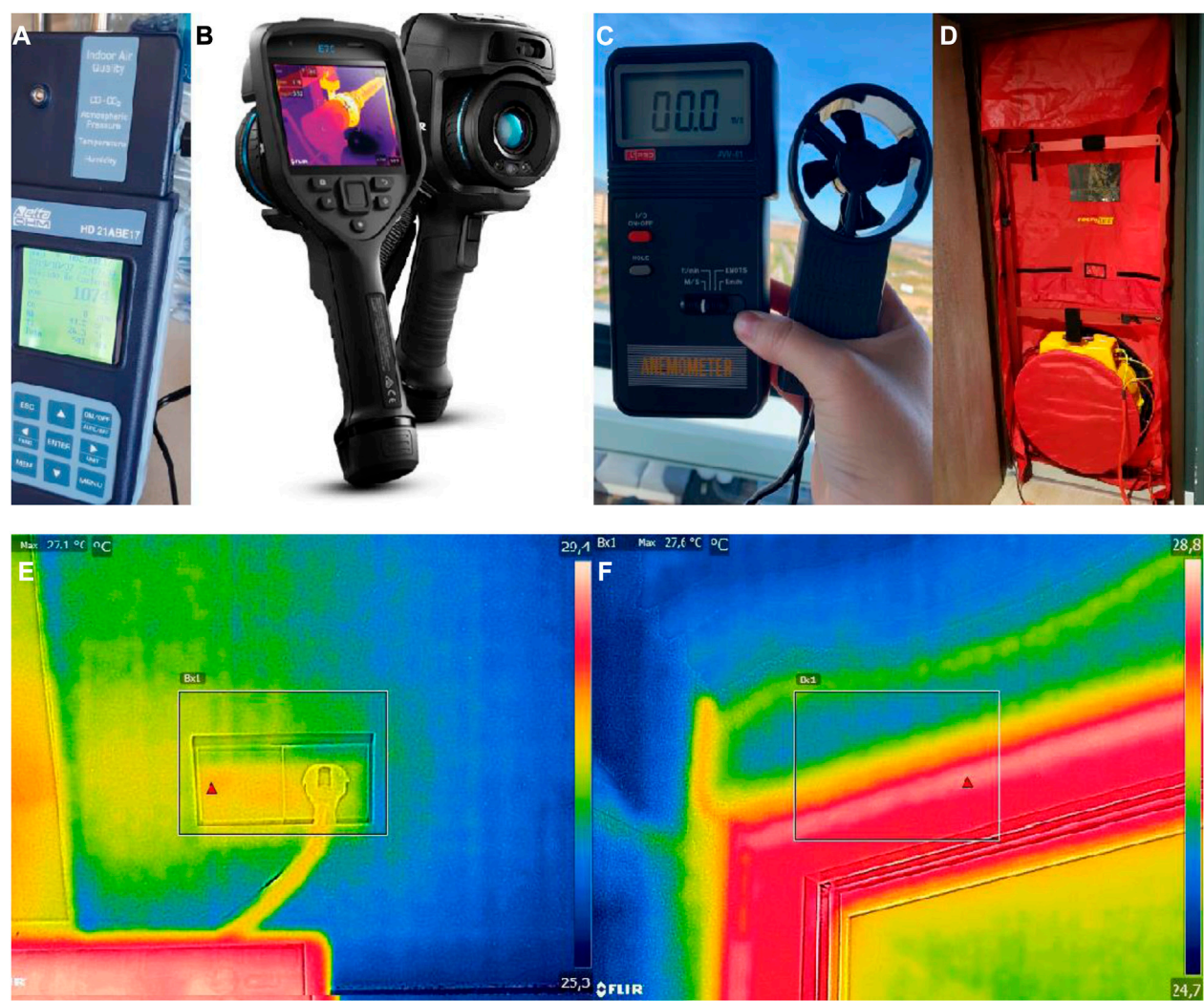


FIGURE 1 (A) Air quality, (B) thermographic camera, (C) anemometer, (D) blower door, (E) air infiltration through sockets, and (F) air infiltration through the carpentry.

TABLE 1 Summarizing the results of airtightness tests. Source: own elaboration.

Construction period	Number of tests	Mean n_{50}	Number of refurbished dwellings	Main cause of infiltration
1900–1920	6	8.80	3	Woodwork and suspended roofs
1921–1940	7	4.42	4	Woodwork
1941–1950	7	2.69	6	Joints and woodwork
1951–1960	12	6.98	9	Suspended roofs and cracks
1961–1970	28	7.16	18	Suspended roofs
				Sockets and woodwork
1971–1980	32	6.40	21	Splayed and sockets
1981–1990	14	5.60	3	Splayed and woodwork
1991–2000	22	7.91	3	Splayed and suspended roofs
2001–2011	20	8.20	4	Sockets and suspended roofs
2012–2020	3	4.20	0	Sockets and suspended roofs

more massive way in their building design, without an air chamber. You cannot invest in increasing insulation if you have unwanted air infiltration, which will not allow you to limit the energy demand (Isaac and van Vuuren, 2009; Friedman and Matheson, 2017; Burgos et al., 2020; Lezcano and Burgos, 2021; Mutschler et al., 2021). Passivhaus is a world reference in efficient housing construction, as one of its principles is to limit the level of infiltration to 0.6 renovations per hour in new buildings and to 1 renovation per hour at 50 Pa in refurbished buildings, while studies are already underway to adapt this standard to hot climates (Sherman, 1987).

In Spain, there are no mandatory regulations regarding the level of airtightness in residential buildings. In the latest update of the Technical Building Code (CTE), it is indicated in its Basic Document on Energy Saving (DB-HE) of 2018 (de la Edificación, 2013) that to calculate the energy demand of buildings, losses due to ventilation and unwanted infiltrations should be considered, but no limit is established (Agee et al., 2021; Gonzalo et al., 2022; González-Lezcano, 2023).

The airtightness of residential buildings is limited, depending on whether it is natural or mechanical ventilation, as the latter will be more demanding in terms of airtightness. It is important to lay the foundations in Spain for these requirements, but always with a link to energy demand, setting the guidelines to achieve these savings and not just demanding a value for renovations.

In addition, the influence of several construction characteristics on permeability results was assessed. General trends have been identified. Nevertheless, no statistically significant results could be obtained, in part due to the reduced sample size for some categories and also because of the difficulty in isolating the variables.

4 Conclusion

The European Union has committed to continuing to reduce greenhouse gas emissions, establishing a sustainable, competitive, and decarbonized energy system by 2050. It is estimated that the building stock is responsible for approximately 36% of all CO₂ emissions and that heating and cooling accounts for almost 50% of the Union's final energy consumption, 80% of which is consumed in buildings (European Commission, 2018). For this reason, it seems essential to establish strategies that support the renovation of national building parks, facilitating their transformation in buildings with almost zero energy consumption.

In this context, one of the factors that have the greatest impact is the presence of uncontrolled airways through an envelope or infiltration. The constant improvement in the transmittance of construction elements has indicated that the entry of outside air has a progressively greater relevance to the total energy consumed by the residential sector, while facilitating the uncontrolled movement of air through the building envelope.

References

A Chan, W. R., Joh, J., and Sherman, M. H. (2013). Analysis of air leakage measurements of US houses. *Energy Build.* 66, 616–625. doi:10.1016/j.enbuild.2013.07.047

This not only implies higher energy consumption but also generates a series of problems that affect the health of the occupants, such as a lack of thermal comfort, entry of pollutants and odours, noise, inadequate operation of ventilation systems, and less protection against fire.

Author contributions

Conceptualization: GS, EL, RG-L, RS, and CI; methodology: GS, EL, RG-L, RS, and CI; validation: GS, EL, RG-L, RS, and CI; formal analysis: GS, EL, RG-L, RS, and CI; investigation: GS, EL, RG-L, RS, and CI; resources: GS and RG-L; data curation: GS, EL, RG-L, RS, and CI; writing—original draft preparation: GS, EL, RG-L, RS, and CI; writing—review and editing: GS, EL, RG-L, RS, and CI; visualization: GS, EL, RG-L, RS, and CI; supervision: RG-L. All authors contributed to the article and approved the submitted version.

Funding

The authors wish to thank the CEU San Pablo University Foundation for the funds dedicated to the GIMIDyL Research Group under Project Ref. G20/6-04 provided by CEU San Pablo University.

Acknowledgments

The authors wish to thank the CEU San Pablo University Foundation for the funds dedicated to the ARIE Research Group by CEU San Pablo University.

Conflict of interest

The authors declare that the research was conducted in the absence of any commercial or financial relationships that could be construed as a potential conflict of interest.

Publisher's note

All claims expressed in this article are solely those of the authors and do not necessarily represent those of their affiliated organizations, or those of the publisher, the editors, and the reviewers. Any product that may be evaluated in this article, or claim that may be made by its manufacturer, is not guaranteed or endorsed by the publisher.

Agee, P., Nikdel, L., and Roberts, S. (2021). A measured energy use, solar production, and building air leakage dataset for a zero energy commercial building. *Sci. Data* 8 (1), 299. doi:10.1038/s41597-021-01082-8

- Almarzouq, A., and Sakhrhieh, A. (2018). Effects of glazing design and infiltration rate on energy consumption and thermal comfort in residential buildings. *Therm. Sci.* 23, 2951–2960. doi:10.2298/TSCI170910073A
- Bhandari, M., Hun, D., Shrestha, S., Pallin, S., and Lapsa, M. (2018). A simplified methodology to estimate energy savings in commercial buildings from improvements in airtightness. *Energies* 11 (12), 3322. doi:10.3390/en11123322
- Bramiana, C. N., Entrop, A. G., and Halman, J. I. M. (2016). Relationships between building characteristics and airtightness of Dutch dwellings. *Energy Procedia* 96, 580–591. Elsevier Ltd. doi:10.1016/j.egypro.2016.09.103
- Burgos, M. J. M., de Toledo, H. S. Á., Lezcano, R. A. G., and de Mera, A. G. (2020). The sedentary process and the evolution of energy consumption in eight native American dwellings: analyzing sustainability in traditional architecture. *Sustain. Switz.* 12 (5), 1–28. doi:10.3390/su12051810
- Cardoso, V. E. M., Pereira, P. F., Ramos, N. M. M., and Almeida, R. M. S. F. (2020). The impacts of air leakage paths and airtightness levels on air change rates. *Buildings* 10 (3), 55. doi:10.3390/buildings10030055
- Chan, W. R., Nazaroff, W. W., Price, P. N., Sohn, M. D., and Gadgil, A. J. (2005). Analyzing a database of residential air leakage in the United States. *Atmos. Environ.* 39 (19), 3445–3455. doi:10.1016/j.atmosenv.2005.01.062
- Darvish, A., Eghbali, S. R., Eghbali, G., and Mahlabani, Y. G. (2020). The effects of building glass facade geometry on wind infiltration and heating and cooling energy consumption. *Int. J. Technol.* 11 (2), 235–247. doi:10.14716/ijtech.v11i2.3201
- de la Edificación, C. T. (2013). *Documento Básico de Ahorro de energía*. CTE, DB-HE.
- European Parliament (2018). *European directive 2018/844 amending directive 2010/31/EU on the energy performance of buildings directive 2012/27*. EU on energy efficiency.
- Fernandez-Antolin, M. M., del Río, J. M., and Gonzalez-Lezcano, R. A. (2021). The use of gamification in higher technical education: perception of university students on innovative teaching materials. *Int. J. Technol. Des. Educ.* 31 (5), 1019–1038. doi:10.1007/s10798-020-09583-0
- Fernandez-Antolin, M. M., del Río, J. M., Costanzo, V., Nocera, F., and Gonzalez-Lezcano, R. A. (2019a). Passive design strategies for residential buildings in different Spanish climate zones. *Sustain. Switz.* 11 (18), 4816. doi:10.3390/su11184816
- Fernandez-Antolin, M. M., Del-Río, J. M., Del Ama Gonzalo, F., and Gonzalez-Lezcano, R. A. (2020). The relationship between the use of building performance simulation tools by recent graduate architects and the deficiencies in architectural education. *Energies* 13 (5), 1134. doi:10.3390/en13051134
- Fernandez-Antolin, M. M., del-Río, J. M., and Gonzalez-Lezcano, R. A. (2019b). Influence of solar reflectance and renewable energies on residential heating and cooling demand in sustainable architecture: A case study in different climate zones in Spain considering their urban contexts. *Sustain. Switz.* 11 (23), 6782. doi:10.3390/su11236782
- Friedman, A., and Matheson, M. (2017). Selecting and installing energy-efficient windows to improve dwelling sustainability. *VITRUVIO - Int. J. Archit. Technol. Sustain.* 2 (2), 2. doi:10.4995/vitruvio-ijats.2017.7687
- Frontczak, M., Schiavon, S., Goins, J., Arens, E., Zhang, H., and Wargocki, P. (2012). Quantitative relationships between occupant satisfaction and satisfaction aspects of indoor environmental quality and building design. *Indoor Air* 22 (2), 119–131. doi:10.1111/j.1600-0668.2011.00745.x
- González-Lezcano, R. A. (2023). Editorial: design of efficient and healthy buildings. *Front. Built Environ.* 9. Frontiers Media S.A. doi:10.3389/fbuil.2023.1210956
- González-Lezcano, R. A., and Hormigos-Jiménez, S. (2016). “Energy saving due to natural ventilation in housing blocks in Madrid,” in IOP Conference Series: Materials Science and Engineering (Institute of Physics Publishing). doi:10.1088/1757-899X/138/1/012002
- González-Lezcano, R. A., López-Fernández, E., Cesteros-García, S., and Sanglier-Contreras, G. (2020). Evaluation of energy-saving strategies according to Spanish regulations. *Int. J. Energy, Environ. Econ.* 26 (3), 197–217.
- Gonzalo, F. D. A., Griffin, M., Laskosky, J., Yost, P., and González-lezcano, R. A. (2022). Assessment of indoor air quality in residential buildings of new england through actual data. *Sustain. Switz.* 14 (2), 739. doi:10.3390/su14020739
- Goubran, S., Qi, D., Saleh, W. F., Wang, L., and Leon, (2017). Comparing methods of modeling air infiltration through building entrances and their impact on building energy simulations. *Energy Build.* 138, 579–590. doi:10.1016/j.enbuild.2016.12.071
- Hamby, D. M. (1994). A review of techniques for parameter sensitivity analysis of environmental models. *Environ. Monit. Assess.* 32 (2), 135–154. doi:10.1007/BF00547132
- Isaac, M., and van Vuuren, D. P. (2009). Modeling global residential sector energy demand for heating and air conditioning in the context of climate change. *Energy Policy* 37 (2), 507–521. doi:10.1016/j.enpol.2008.09.051
- Jokisalo, J., Kurnitski, J., Korpi, M., Kalamees, T., and Vinha, J. (2009). Building leakage, infiltration, and energy performance analyses for Finnish detached houses. *Build. Environ.* 44 (2), 377–387. doi:10.1016/j.buildenv.2008.03.014
- Lee, M. J., Kim, N. I., and Ryou, H. S. (2011). Air tightness measurement with transient methods using sudden expansion from a compressed chamber. *Build. Environ.* 46 (10), 1937–1945. doi:10.1016/j.buildenv.2011.04.001
- Lezcano, R. A. G., and Burgos, M. J. M. (2021). Airflow analysis of the Haida plank house, a breathing envelope. *Energies* 14 (16), 4871. doi:10.3390/en14164871
- Lozinsky, C. H., and Touchie, M. F. (2018). Improving energy model calibration of multi-unit residential buildings through component air infiltration testing. *Build. Environ.* 134, 218–229. doi:10.1016/j.buildenv.2018.02.040
- Mutschler, R., Rüdisüli, M., Heer, P., and Eggimann, S. (2021). Benchmarking cooling and heating energy demands considering climate change, population growth and cooling device uptake. *Appl. Energy* 288, 116636. doi:10.1016/j.apenergy.2021.116636
- Sadineni, S. B., Madala, S., and Boehm, R. F. (2011). Passive building energy savings: A review of building envelope components. *Renew. Sustain. Energy Rev.* 15, 3617–3631. Elsevier Ltd. doi:10.1016/j.rser.2011.07.014
- Santamaria, B. M., Del Ama Gonzalo, F., Pinette, D., Gonzalez-Lezcano, R. A., Aguirregabiria, B. L., and Ramos, J. A. H. (2020). Application and validation of a dynamic energy simulation tool: A case study with water flow glazing envelope. *Energies* 13 (12), 3203. doi:10.3390/en13123203
- Santamouris, M., Papanikolaou, N., Livada, I., Koronakis, I., Georgakis, C., Argiriou, A., et al. (2001). On the impact of urban climate on the energy consumption of buildings. *Sol. Energy* 70 (3), 201–216. doi:10.1016/S0038-092X(00)00095-5
- Sfakianaki, A., Pavlou, K., Santamouris, M., Livada, I., Assimakopoulos, M. N., Mantas, P., et al. (2008). Air tightness measurements of residential houses in Athens, Greece. *Build. Environ.* 43 (4), 398–405. doi:10.1016/j.buildenv.2007.01.006
- Sherman, M. H. (1987). Estimation of infiltration from leakage and climate indicators. *Energy Build.* 10 (1), 81–86. doi:10.1016/0378-7788(87)90008-9
- Sherman, M. (1995). The use of blower door data. *Indoor Air* 5 (3), 215–224. doi:10.1111/j.1600-0668.1995.t01-1-00008.x
- Synnefa, A., Santamouris, M., and Akbari, H. (2007). Estimating the effect of using cool coatings on energy loads and thermal comfort in residential buildings in various climatic conditions. *Energy Build.* 39 (11), 1167–1174. doi:10.1016/j.enbuild.2007.01.004
- Villi, G., Peretti, C., Graci, S., and De Carli, M. (2013). Building leakage analysis and infiltration modelling for an Italian multi-family building. *J. Build. Perform. Simul.* 6 (6), 98–118. doi:10.1080/19401493.2012.699981



OPEN ACCESS

EDITED BY

Hom Bahadur Rijal,
Tokyo City University, Japan

REVIEWED BY

Manoj Kumar Singh,
University of Ljubljana, Slovenia
Samar Thapa,
Ca' Foscari University of Venice, Italy

*CORRESPONDENCE

Roberto Alonso González-Lezcano,
✉ rgonzalezcano@ceu.es

RECEIVED 20 July 2023

ACCEPTED 25 September 2023

PUBLISHED 03 October 2023

CITATION

Maciá-Torregrosa ME, Camacho-Diez J
and González-Lezcano RA (2023),
Strategies for integral rehabilitation and
improvement of the energy efficiency of
Lagos Park building in Madrid.
Front. Built Environ. 9:1264368.
doi: 10.3389/fbuil.2023.1264368

COPYRIGHT

© 2023 Maciá-Torregrosa,
Camacho-Diez and González-Lezcano.
This is an open-access article distributed
under the terms of the [Creative
Commons Attribution License \(CC BY\)](#).
The use, distribution or reproduction in
other forums is permitted, provided the
original author(s) and the copyright
owner(s) are credited and that the original
publication in this journal is cited, in
accordance with accepted academic
practice. No use, distribution or
reproduction is permitted which does not
comply with these terms.

Strategies for integral rehabilitation and improvement of the energy efficiency of Lagos Park building in Madrid

María Eugenia Maciá-Torregrosa, Javier Camacho-Diez and
Roberto Alonso González-Lezcano*

Departamento de Arquitectura y Diseño, Escuela Politécnica Superior, Universidad San Pablo-CEU, CEU
Universities, Madrid, Spain

As a primary goal, Inadequate energy consumption and outdated construction systems are causing financial losses for homeowners. Spain's failure to meet European guidelines on CO₂ emissions highlights the urgent need to address the energy inefficiency of buildings, responsible for 40% of such emissions. This article presents a comprehensive refurbishment project undertaken in the Lagos Park residential building in Madrid. The paper offers a detailed analysis of common building issues related to excessive humidity in the surrounding areas and deficiencies in the energy performance of the building envelope, including facades and roofs. Precise measures for achieving compliance with the Spanish Technical Building Code (CTE), as well as enhancing energy efficiency and functionality, are explained through the renovation of the building envelopes. The study also encompasses improvements made to the domestic hot water supply systems and the air-conditioning system, which contribute to the building's attainment of an optimal energy rating (energy Class A). The extensive renovation undertaken in the complex has transformed Lagos Park homes into "zero energy consumption" residences. The strategies employed, ranging from electrical appliances to the house's structural design, are all geared towards maximizing energy usage efficiency, resulting in significantly reduced monthly electricity bills by 65%–75%.

KEYWORDS

architecture, refurbishment, sustainability, energy evaluation, energy saving

1 Introduction

Existing buildings consume an inordinate amount of energy worldwide. This consumption negatively affects the environment and the economy, so there is a need to improve the energy performance of buildings by retrofitting existing buildings (Mejjiaoui and Alzahrani, 2020). Many cities are striving to develop an urban transformation strategy to move from traditional cities to sustainable cities. Improving the energy efficiency of buildings, especially existing buildings, is key to combating climate change (Gupta and Gregg, 2018).

1.1 Background

On 25 September 2015, world leaders gathered at the historic Sustainable Development Summit adopted the 2030 Agenda containing 17 Sustainable Development Goals (SDGs) that govern the efforts of the countries that are part of the United Nations system in order to achieve a sustainable world by 2030 (Gil, 2018).

Among the goals set out, with specific targets to be achieved in the next 15 years, SDG No. 9 aims to “Build resilient infrastructure, promote inclusive and sustainable industrialization and foster innovation” and more specifically SDG No. 11, which seeks to “Make cities and human settlements inclusive, safe, resilient and sustainable.” In relation to building, these goals pursue technological progress that should underpin efforts to achieve environmental goals, such as increasing resource and energy efficiency, reducing carbon dioxide emissions and ensuring people’s access to safe, adequate, affordable and sustainable housing.

By achieving these two SDGs, the aim is to improve the quality of life of citizens, the prosperity of cities in economic terms, as well as care for the environment.

The European Directive 31/2010 and its 2020 targets have been made effective through the enactment of national laws and regulations. However, they impose complex obligations for existing buildings towards NZEB and do not take into account other real issues (Wells et al., 2018; Hu, 2019; Abrahamsen et al., 2023). It is not only important to achieve a high level of energy efficiency, but also to think about retrofitting actions to mitigate the impact of natural hazards. Nowadays, restoration interventions are conceived that seek a minimum environmental impact in recent buildings. Greenhouse gas emissions are reduced using criteria that are met within a life-cycle analysis, while energy savings are achieved with cost-effective retrofit actions that ensure higher benefits in terms of comfort (Loli and Bertolin, 2018). This issue has been neglected for years, especially in the building sector, but these phenomena are becoming more and more influential and frequent. For this reason, the idea of building resilience is being developed (Wilkinson et al., 2016), which represents the measure of their ability to recover or adapt to an unfavorable situation, an event, or a change in the use of the building (Matthews et al., 2014). The energy consumption inside our buildings comes from the different equipment and facilities in them such as air conditioning, heating, domestic hot water (DHW) generation, the entire lighting system and electrical appliances. Of all of them, heating and air conditioning are the systems that consume the most energy, followed by DHW production. Lighting and appliances take last place. A comfortable interior architecture with some good practices that help us save.

Resilience is a complex challenge at any scale, including that of building systems. In other words, buildings have to be able to survive and maintain their own functionality (Folke et al., 2004) and performance even in an uncertain future. In addition, environmental degradation accelerated by climate change and global warming and by increasing frequency and severity of disturbances. Buildings are largely responsible for global and local climate change (Santamouris, 2016) but, at the same time, they have to resist these phenomena in terms of performance and dynamic reaction.

In fact, facades play an important role in the urban context, as the surface area of facades exceeds that of roofs and sometimes streets by a huge amount of square meters. In addition, each side of a building facade must be appropriate for the environment it faces: interior and exterior (Zhang et al., 2022). Most existing building facades are in need of rehabilitation, but current practices do not require sufficient attention to designing systems that adapt to changing external conditions. Therefore, it is desirable to predict future rehabilitation needs, satisfying the principles of resilient design. In particular, façades have to mitigate the increase or decrease of temperatures in the future, although it is obvious that this function must be supported by the whole building-floor system. The influence of facades requires particular analysis at both the building and pedestrian levels. Moreover, one of the crucial elements defining the energy consumption in the building envelope are the connections between windows and facades that can contribute up to 40% to the total heat loss caused by thermal bridges in the building envelope (Misiopceki et al., 2018). This research aims to expose architectural rehabilitation strategies that favor the reduction of energy consumption of a building by increasing the maximum conditions of thermal comfort through the improvement of the building envelope, always betting on a quality architecture.

1.2 Literature review

One of the alternatives to reduce energy consumption in buildings, recognized and used internationally, is to establish standards for the evaluation and classification of buildings in terms of energy requirements (energy performance) (Fossati et al., 2016). Environmental problems, especially climate change, have become a serious global problem that citizens must solve. In the building sector, the sustainable building concept is being developed to reduce greenhouse gas emissions (Liu et al., 2015). Optimization models for the improvement of energy management are mainly aimed at minimizing the energy consumption of residential buildings during the early design phases (Elbeltagi et al., 2023). In Spanish buildings we can estimate that 55% of the existing housing stock was erected before 1980 (Serrano and Sanchis, 2015), without adequate thermal insulation in facades and roofs since there were no applicable energy efficiency regulations until 1979 (de Gobierno, 1979). Buildings often do not perform at optimal levels and often fail to meet design predictions. These failures affect energy efficiency, indoor environmental quality and occupant satisfaction. Performing energy audits determines and categorizes performance problems that lead to energy inefficiency and inadequate indoor environmental quality (Borgstein et al., 2018). Through various works (Cano-Marín et al., 2014; Cervero Sánchez and Agustín Hernández, 2015) on the rehabilitation of dwellings built during the 1970s, it is possible to observe the analysis of the common pathologies existing at that time and to verify the compliance of different constructive solutions that allow the improvement of the thermal conditions of the buildings. Likewise, it is possible to analyze how some buildings have been rehabilitated (Díaz et al., 2012) through the detailed description of functional aspects, structural safety conditions, degree of thermal insulation, acoustic conditions, fire protection, accessibility and maintenance of these, which elaborate proposals aimed at

reducing the most notable differences. On the other hand, dwellings built between 1980 and 2007, before the approval of the Technical Building Code, have a thermal insulation in their construction systems that is far below what is necessary and essential for adequate thermal comfort.

There are methodologies (Alonso, 2015) for the constructive evaluation of facades in the rehabilitation of social housing. This evaluation aims to assess their impact on the quality of the indoor environment and on the reduction of energy demand for thermal conditioning. Through the analysis of some studies carried out by other authors (Peinado et al., 2012), it is possible to evaluate how ETICS (External Thermal Insulation Composite Systems) on the exterior made with mineral wool improve the acoustic performance with respect to the initial façade and also to systems made with Expanded Polystyrene (EPS) panels. There are other studies (Carbonell, 2016) on comparisons between different façade solutions for the same building. Through them, it is possible to check the percentages of improvement obtained from one solution to another. Some researchers (Negendahl and Nielsen, 2015) point out that energy optimization focuses on certain parameters of the building envelope (building energy consumption, capital cost, daylight distribution and indoor thermal environment). Thanks to comparative dynamic simulations it is possible to see the interaction between the different zones of a building in relation to the energy performance of the building as a whole (Jung et al., 2018).

It is also possible to observe how some studies link the beneficial effects on the health of the population of strategies related to the inclusion of thermal insulation in dwellings (Chapman et al., 2008). The gradual incorporation of improvements in the energy efficiency of a building, taking into account European directives, makes it possible to use the least amount of final energy to satisfy the comfort of the users (Martín-Consu et al., 2014).

Houses lose money thanks to inadequate energy consumption and anachronistic and often ill-advised construction systems. Spain is still far from complying with European guidelines to reduce CO₂ emissions, 40% of which are produced by the energy inefficiency of buildings. Moreover, as indicated in some directives (Directiva, 2010/31/UE, 2010; Directiva, 2012/27/UE, 2012; Directiva, 2018/2002/UE, 2018; Directiva, 2018/844/UE, 2018) and regulations (Reglamento, 2018/1999/UE, 2018), the measures implemented to improve the energy efficiency of buildings should not be limited only to the renovation of the building envelope but should also incorporate passive elements that are part of the techniques aimed at reducing energy needs for heating and cooling and the use of energy for lighting and ventilation. In Spanish residential buildings we can estimate that half of the energy consumption is due to heating and cooling systems (Sendra et al., 2013). Between 25% and 30% of the heating needs are due to heat losses originating from the doors and windows of the home (De La Osa, 2016).

In general, the main hygrothermal problem of the most commonly used facade solutions in the continental climate zone of Spain throughout the century is the interruption of the outer layer of the solid wall and the insulating material at the junction with the horizontal structure or the pillars. There were no movement joints between the structural components and the facades, leading to numerous cracks and fissures in the brick walls (Zaparaín, 2016). Thermal bridges and problems of interstitial condensation and

water seepage appeared in the joints between the brick and mortar and cracks (Monjo, 2005). Another problematic point of façade solutions is roller shutters. Traditionally, the function of solar protection and control had been solved with cord or booklet shutters (Feijó-Muñoz et al., 2019). It is from the 1950s onwards that the use of roller shutters on the inner leaf of the enclosure became generalized, without insulation in most cases. Only in recent decades has this solution been improved with roller shutters integrated into insulated windows (Feijó-Muñoz et al., 2018).

1.3 Research gap

Currently, the European framework on energy efficiency of the building stock (Directiva, 2010/31/UE, 2010) requires a 55% reduction of greenhouse gas emissions and at least 32% from renewable energies by 2030; this should be increased to 38%–40% in accordance with the Climate Target Plan. Considering that up to 40% of CO₂ emissions in Europe come from household energy needs, the transition to clean alternatives such as this will be essential in the fight against global warming. Aerothermal will be one of the keys to the decarbonization of human activity in line with the Paris Agreement (2016) within the framework of the United Nations Framework Convention on Climate Change. All these data necessarily imply that the existing building stock must be rehabilitated and adapted to the new criteria inexorably.

Although there are numerous studies related to the use of geothermal energy in buildings (Ruiz-Larrea, 2010; Sanz et al., 2016; Sekret, 2018), the environmental and economic return problems make us consider another source of clean renewable energy alternative to fossil fuels, such as aerothermal energy (Directiva, 2009/28/CE, 2009), a system that captures energy from the air and stores it to provide domestic hot water, heating and cooling for the home. The integration of renewable energy technologies and building renovation are the two main procedures to improve the energy sustainability of buildings at the neighborhood scale (Le Guen et al., 2018).

Specifically, this article aims to expose the problems detected in the integral rehabilitation of the Lagos Park building and to present the architectural solutions carried out to provide the building with optimum energy efficiency to provide its tenants with the adequate energy comfort required by current regulations.

The work has started with a study of the building from the initial evaluation (inspection and data collection, identification of pathologies, definition of qualities, intervention strategies.), to the Rehabilitation Plan (intervention and improvement proposals, economic estimation, technical reports, rehabilitation project, execution and management of the works.) all of this from an integrated approach that seeks both the energy improvement of the building and its comfort, accessibility, use and safety. In June 2015, the developer iKasa called a restricted ideas competition in order to carry out a comprehensive functional and energy rehabilitation of one of the most relevant developments within its Residential Heritage Division. To this end, it invited some of the most prestigious architectural firms in Madrid to participate in the competition, and the winner was CMA+ Q's proposal under the slogan "Smart living in Nature."

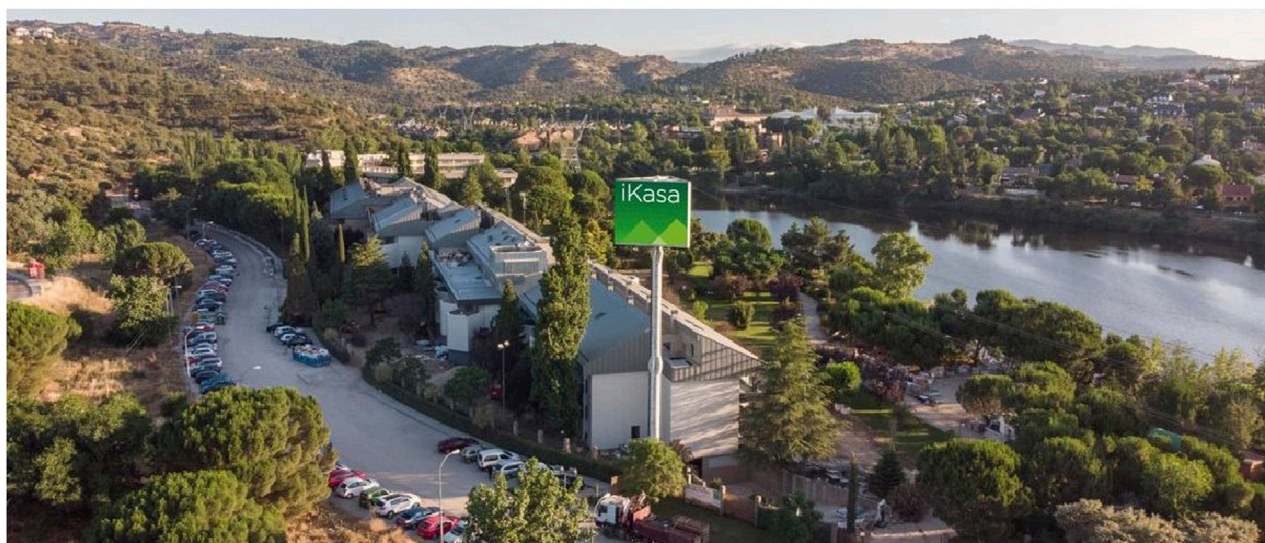


FIGURE 1
Main image and location of the Lagos Park building.

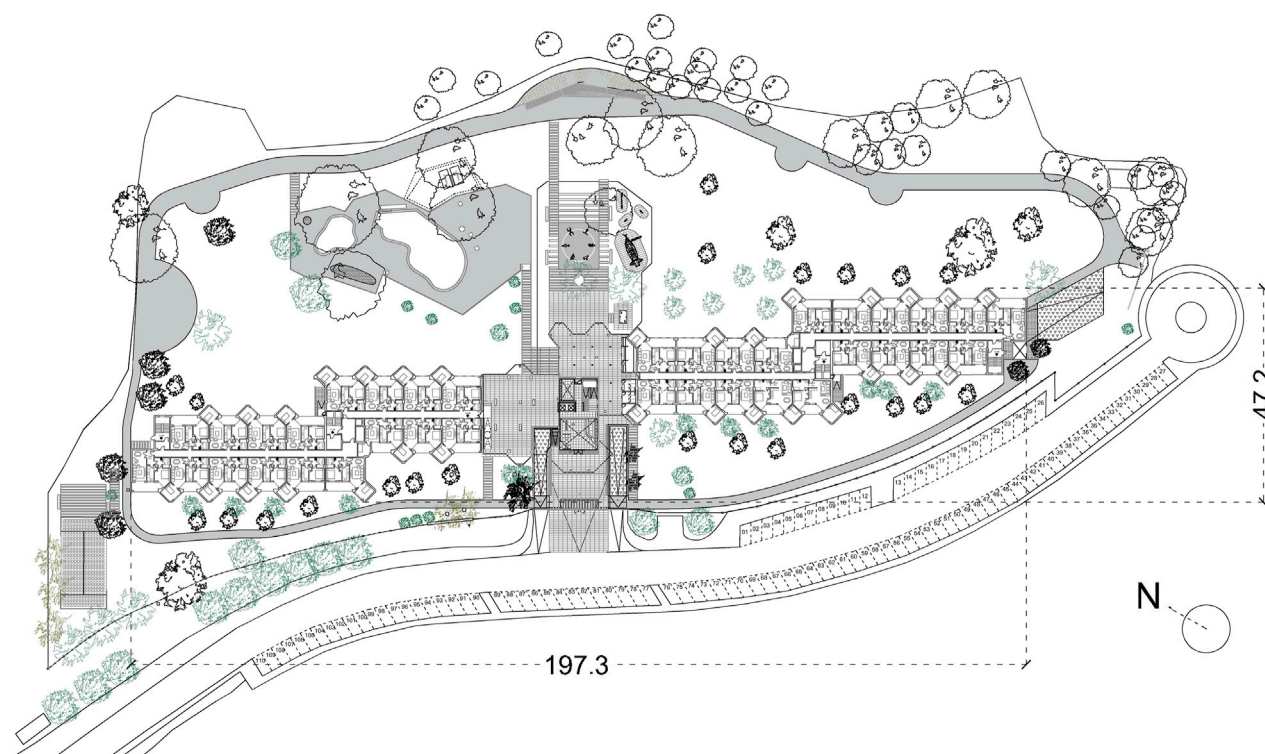


FIGURE 2
Main floor plan, general dimensions and orientation of the Lagos Park building.

1.4 Objectives

The main objective of this article is to expose the construction strategies that have been carried out in the rehabilitation of the Lagos Park building, which was initially formed by 141 apartments to adapt it,

not only to the new regulations in order to turn it into a building of almost zero energy consumption, but also to the architectural, compositional and design criteria that allow to update the interior and exterior appearance of the building, expanding it to 151 housing units. A zero-energy house is a dwelling that does not rely on external

supplies for its proper functioning. This means it has very low energy consumption, and the little energy it needs is generated within the construction itself through renewable energy sources.

The specific objectives to be achieved in the comprehensive renovation of the building are as follows:

- To grant maximum energy efficiency to the building, providing it with an air conditioning system based on aerothermal energy.
- Transform the envelope of the entire facade and roof with a new thermal and acoustic insulation.
- To give a high-level residential character to the complex by providing common leisure, cultural and sports areas with an aesthetic and functional renovation.

2 Materials and methods

2.1 Previous study

The Lagos Park building was built in 1992, its main attraction being its extraordinary location in the middle of the forest park of Granja y Molino de la Hoz, its spectacular garden of 19,649 m² and the tranquility of its location (Figure 1). The Lagos Park building (Figure 2) is a reference in the area and was, at the time of its construction, the most representative building of the iKasa brand. Therefore, one of the objectives of the refurbishment is to adapt the building to the new iKasa image, in terms of commitment to innovation, construction excellence and the enormous importance given to energy efficiency.

2.2 Location

Lagos Park is located in a unique environment, in the municipality of Galapagar, on the banks of the Molino de la Hoz reservoir on the Guadarrama river. Molino de la Hoz is a residential area located in the northwestern end of Las Rozas de Madrid, bordering with Torreldones and Galapagar, in the first foothills of the Guadarrama mountain range, at the foot of the Galapagar pass. This residential area has an important environmental value, since it is located next to the Regional Park of the middle course of the Guadarrama River. In the historical-artistic area, the development is located near the El Gasco dam, which was built in the 18th century as a regulating reservoir for the unfinished Guadarrama canal. Nearby is the Retamar Bridge, which was built in the same century as a work to improve the Camino Real de Castilla.

In Lagos Park (Madrid), the summers are short, warm, dry, and mostly clear and the winters are long, very cold, and partly cloudy. During the course of the year, the temperature generally ranges from 0°C to 33°C and rarely drops below −5°C or rises above 37°C.

2.3 Construction characteristics of the building

The main construction characteristics of the existing building (Table 1) are as follows (Figure 3):

The use of materials and systems, some in disuse, others obsolete, facilitate the existence of very common pathologies

(cracks in walls, detachment of plaster, dirt on facades, thermal bridges in the envelope, water filtration on roofs, capillarity from the subsoil in basements).

2.4 Thermographic analysis

The main challenge was the energy rehabilitation of the existing building complex. For this purpose, an extensive thermographic study was carried out in order to detect all pre-existing pathologies. Thermographic diagnosis is a widely used technique to reveal various types of building pathologies and also to determine an energy diagnosis. The problems detected in the thermographic camera study (Figure 4) are thermal bridges in slab edges and pillars, loss of airtightness and thermal insulation in the building envelope, water seepage in roof areas and air infiltration in many areas of the building.

As mentioned above, the building suffers from innumerable problems which, specifically, can be summarized as follows:

- Lack of insulation in the facade.
- Capillary water seepage.
- Costly and inefficient heating system.
- Condensation in interior walls.
- Lack of use in common areas (possibility of storage rooms).
- Antiquity of the building and apartments (deterioration of materials, aesthetic gap, etc.).

The FLIR E6-XT infrared camera with a 3-inch 320 × 240 color LCD display has been utilized for this study. This tool boasts a thermal resolution of 240 × 180 pixels and exhibits an accuracy of ±2% for hot/cold spot measurements (temperature range extended from −20°C to 550°C). In these images, darker colors, such as blue, indicate colder temperatures (approximately −5°C), while brighter colors, like red, represent warmer temperatures (around +3°C).

3 Results

In order to achieve the overall adaptation of the building to the regulatory standards without losing sight of the architectural quality of the building, the tasks are structured around the following guidelines:

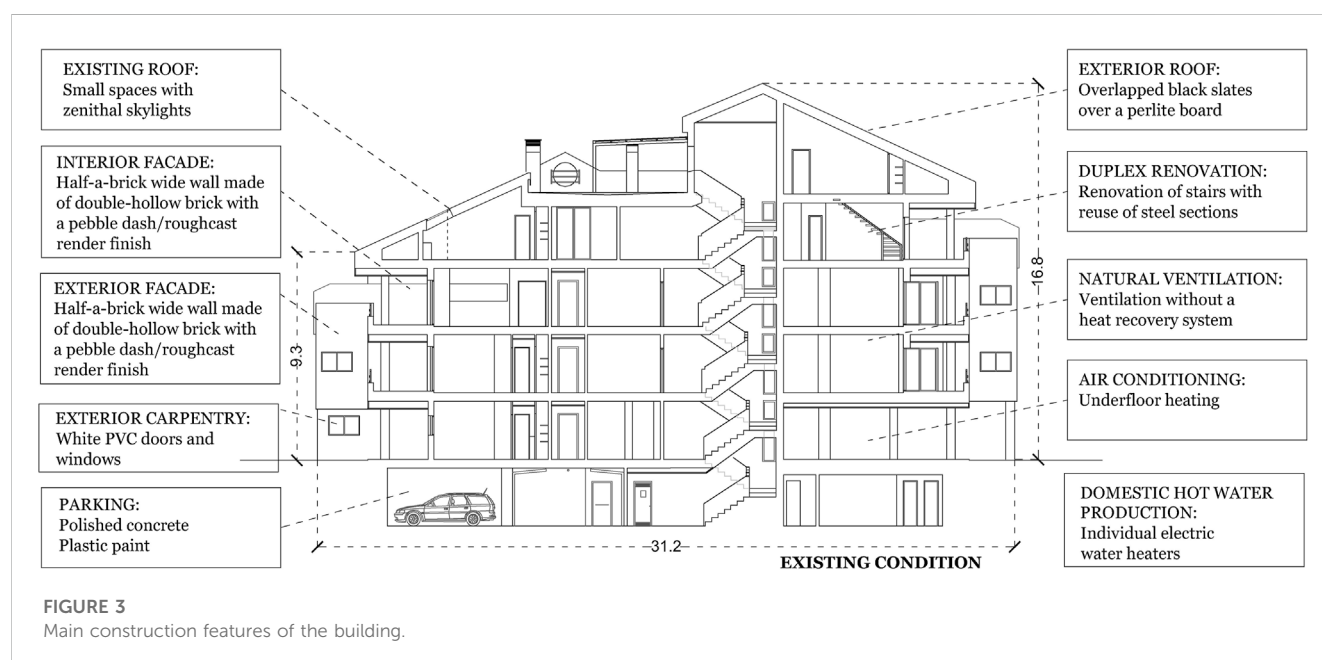
- Adaptation to the Technical Building Code (in relation to Functionality, Safety and Habitability requirements).
- Adoption of various construction strategies to thermally insulate the building's exterior envelope.
- Analysis of the energy efficiency of the rehabilitated building (to check the effect of the action).

3.1 Adaptation to the Spanish technical building code (CTE)

The following is the analysis of the existing regulations, improvement actions and results achieved in each requirement: Functionality, Safety and Habitability.

TABLE 1 Construction characteristics of existing building.

Part of existing building	Constructive system conditions
Gross floor area	14,008 m ² (according to land registry)
Number of floors	Basement + 4 + under roof
Vertical structure	Reinforced concrete
Horizontal structure	Prestressed joist floor slab and ceramic vault
Facade	1/2 foot of double hollow brick, non-ventilated air chamber and double hollow brick partition plastered on the inside. Exterior finish of “garbancillo” type monolayer
Roof	Slate and stoneware tiled terraces
Domestic hot water production	Individual electric water heaters
Heating	Electric underfloor heating



3.1.1 Functionality

In relation to Usability, the existing vertical and horizontal communication elements have not been substantially modified, except for the incorporation of independence vestibules in the protected stairways and two new evacuation exits in the central stairways to comply with the CTE (*Técnico de la Edificación*, 2018).

Regarding Accessibility, existing elements of architectural barriers on the first floor have been corrected, resulting, both the access to the building and its common areas, in a suitable way for the accessibility of people with reduced mobility, according to the provisions of Decree 19/2000 approving the Accessibility Regulations in relation to urban and architectural barriers in development of Law 5/1994 (*Espínola*, 2018). Regarding Access to Audiovisual and Information Telecommunication Services, the existing telecommunication installations are adapted to the current regulations (*Valdivia*, 2007).

With respect to the Facilitation of access to postal services, the first floor of the postal lockers is renewed, and several Smart-Boxes

are provided for the collection of parcels for users of the urbanization.

3.1.2 Safety

In relation to Structural Safety, the main structural elements have not been modified. The only structural reinforcements that have been made are the new roof installation benches, and those corresponding to the variation of the slopes of part of the roofs (630 m²) and the new slabs that replace those demolished in the restaurant area (360 m²).

Regarding fire safety, the existing fire detection installations have been improved and the DB-SI requirements have been adapted. With regard to safety in use, the configuration of the spaces and the fixed and mobile elements installed in the building have been designed in such a way that they can be used for their intended purpose within the limitations of the building's use without posing a risk of accidents to the building's users.

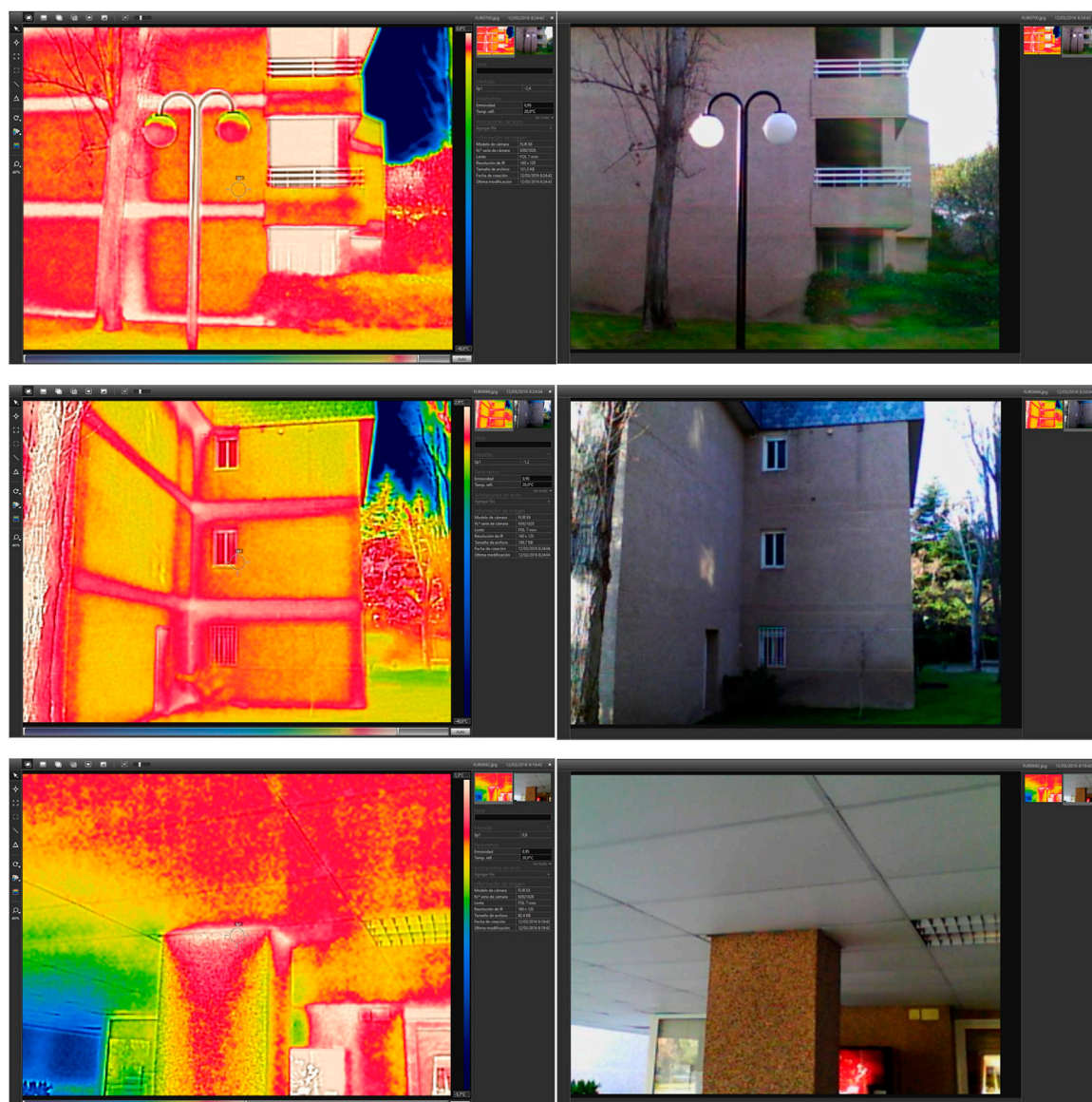


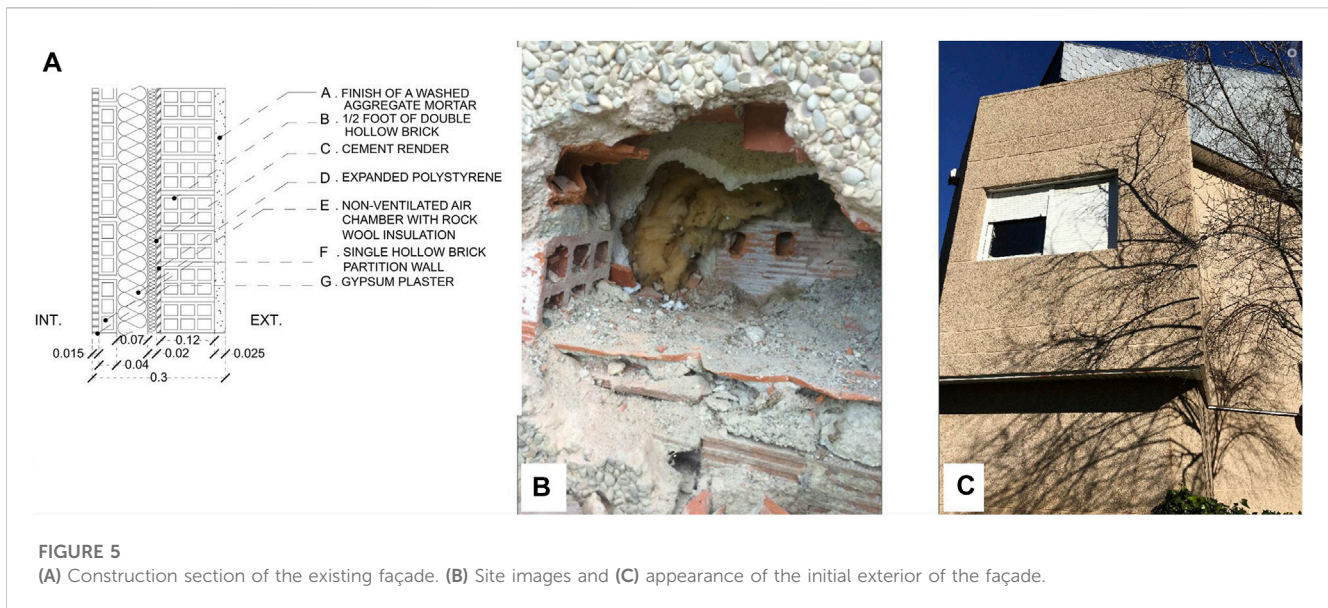
FIGURE 4
Thermographic images of different areas of the existing building.

3.1.3 Habitability

With respect to Hygiene, Health and Environmental Protection, the existing conditions have not been modified. In the specific actions of distribution changes, the requirements of habitability and salubrity have been met. All of the projected building envelopes have been provided with means to prevent the presence of water or inadequate humidity from atmospheric precipitation, from the ground or from condensation, and have been provided with means to prevent its penetration or, if necessary, its evacuation without causing damage.

The apartment building complex and the basement parking lot have been provided with a forced renovation so that their enclosures can be adequately ventilated, eliminating the contaminants that are normally produced during their normal use, so that a sufficient flow of outside air is provided and the extraction and expulsion of the air fouled by contaminants is guaranteed (Técnico de la Edificación, 2017).

- Regarding Noise Protection, an acoustic improvement has been sought in the elements where intervention is carried out (facades and roofs), and in the vertical separating elements between dwellings (Técnico de la Edificación, 2009).
- Regarding Energy Saving and Thermal Insulation, the projected building has an envelope suitable for limiting the energy demand necessary to achieve thermal comfort depending on the climate of the site, the intended use and the summer and winter regime. The inertia and insulation solutions, air permeability and exposure to solar radiation adopted have solved the pre-existing pathologies of surface and interstitial condensation humidity. Special consideration has been given to an improvement in the treatment of thermal bridges through a ventilated facade solution with continuous insulation, in order to limit heat losses or gains



and avoid hygrothermal problems in them (*Técnico de la Edificación, 2012*).

- The projected building has lighting installations that meet the needs of its users and at the same time are energy efficient, with a control system that allows adjusting the lighting to the actual occupancy of the area, as well as a regulation system that optimizes the use of natural light in areas that meet certain conditions (*Técnico de la Edificación, 2012*). In particular, the current incandescent lighting has been replaced by LED type solutions.
- The current underfloor radiant air conditioning has also been replaced by a much more sustainable air-water system with centralized production.

3.2 Construction strategies adopted to resolve deficiencies related to insulation and thermal sealing

From the analysis of the existing deficiencies and pathologies in the building and thanks to the thermographic images of the building, the lack of thermal insulation at the junction of the vertical structure (supports) and the enclosures, at the junction of the horizontal structure (slab edge) and the enclosures, at the junction of the lower floors (landscaped first floor) and the enclosures, under the living spaces over open porches, under the living spaces over the parking basement and in the walkable terraces over the living spaces is detected. In addition, thermal bridges are noted in jambs and lintels of exterior openings.

The following is a description of the existing situations prior to the intervention and the solutions adopted to ensure compliance with the regulations in relation to airtightness and thermal insulation in the building envelope: facades and roofs.

The transmittance values meet the requirements of the Technical Building Code (*Técnico de la Edificación, 2012*) for climate zone D to which Madrid belongs, which is where the project is carried out.

The main constructive characteristics of the building facades are described in *Figure 5A*. The existing constructive system and the initial external façade appearance are shown in *Figures 5B, C*.

A decisive renovation of the perceived representativeness of the Lagos Park development is proposed through the implementation of a new skin (ventilated façade) that will give the current development a modernized and technologically advanced appearance, while allowing the implementation of a new coat of continuous thermal insulation on the façade, thus avoiding the existing thermal bridges (*Figure 6*).

A solution of large-format polished extruded porcelain ceramic tiles (H) is presented, in two tones, white for the emerging facade bodies and anthracite gray for the recessed planes and interior of terraces by including extruded aluminum battens (I) for anchoring the facade. Legends A–G shown in *Figure 5* are valid for *Figure 6*.

A renovation of the exterior carpentry is also proposed, implementing an updated solution using aluminum carpentry with thermal bridge break, in anthracite gray tones and Climalit type thermal and acoustic double glazing. A system of compact pvc blinds with thermal aluminum slats has been chosen.

It is proposed to replace the terrace parapets with a 5 mm + 5 mm laminated safety glass railing solution with colorless butyral and polished edges.

The false terrace ceilings are replaced by a metal ceiling solution of perforated steel trays lacquered in anthracite gray.

A continuous insulation (J) of 1.2 m × 0.6 m × 0.08 m double density rigid rock wool panel is installed, fastened to the facing by means of polypropylene plastic fasteners.

The main construction characteristics of the building's roofs are described in *Figure 7A*. The existing external roof envelope is shown in *Figure 7B*.

The existing roof solution has a very low insulation thickness for the desirable habitability requirements, resulting in real interior temperature conditions, far from comfort conditions, and requiring excessive energy inputs for air conditioning. The waterproofing of the system works adequately thanks to the

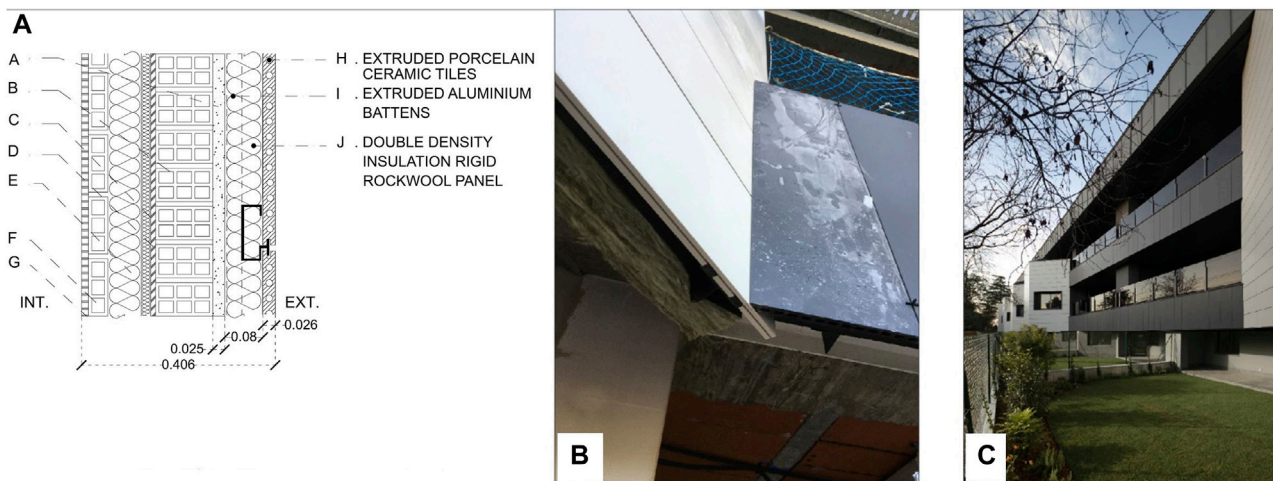


FIGURE 6

(A) Construction section of the rehabilitated façade. Images of (C) the construction site and (B) final exterior appearance of the façade.

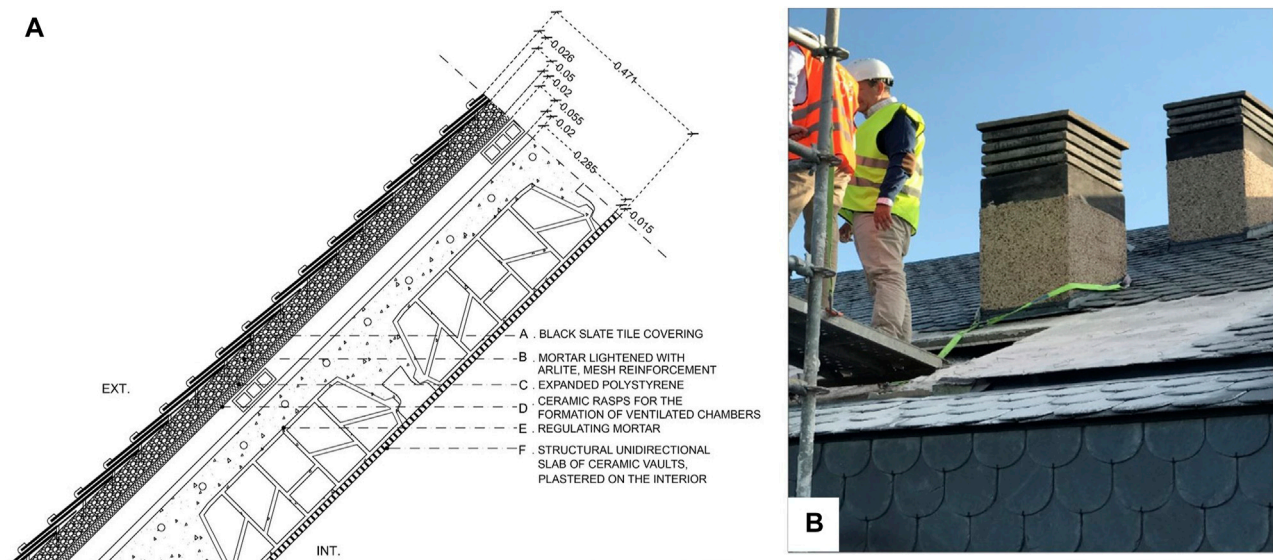


FIGURE 7

(A) Construction section of the existing roof. (B) Site image of the initial exterior appearance of the roof.

high slopes (close to 45%) and only occasional problems have been detected, due to clogging of the hidden gutters, caused by the accumulation of leaves.

The new roof solution (Figure 8) proposes the implementation of a new 8 cm layer of insulation in rigid closed-pore extruded polystyrene panels (J), mechanically fixed to the floating reinforced lightweight mortar slab (H) and coated with a zinc finish (G) in a standing seam over battens and wood decking (I), generating a new ventilated chamber. Legends B–F shown in Figure 7 are valid for Figure 8.

This solution significantly improves the energy saving performance of the envelopes, in addition to generating an aesthetic improvement in accordance with the renovation of the facades.

3.3 Strategies for energy efficiency compliance of the refurbished building

With the aim of obtaining the energy efficiency certificate with an optimal classification, the challenge of making an installation that complies with the current regulations both RITE and CTE and that at the same time is a sustainable and efficient installation is faced. For this purpose, a study of the system has been carried out in order to achieve an installation that complies with the following premises:

- Centralized production of heating, cooling and Domestic Hot Water (DHW).

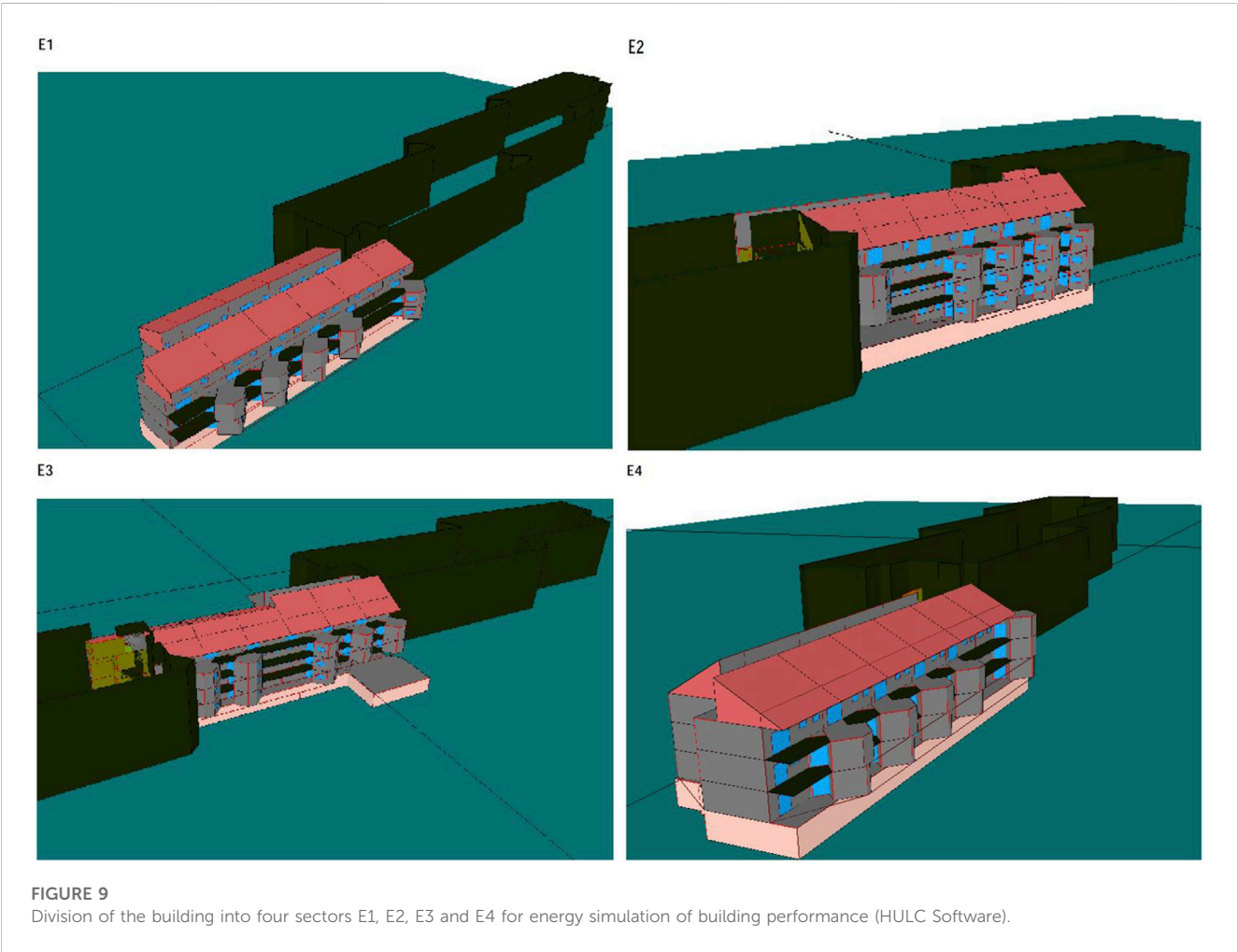
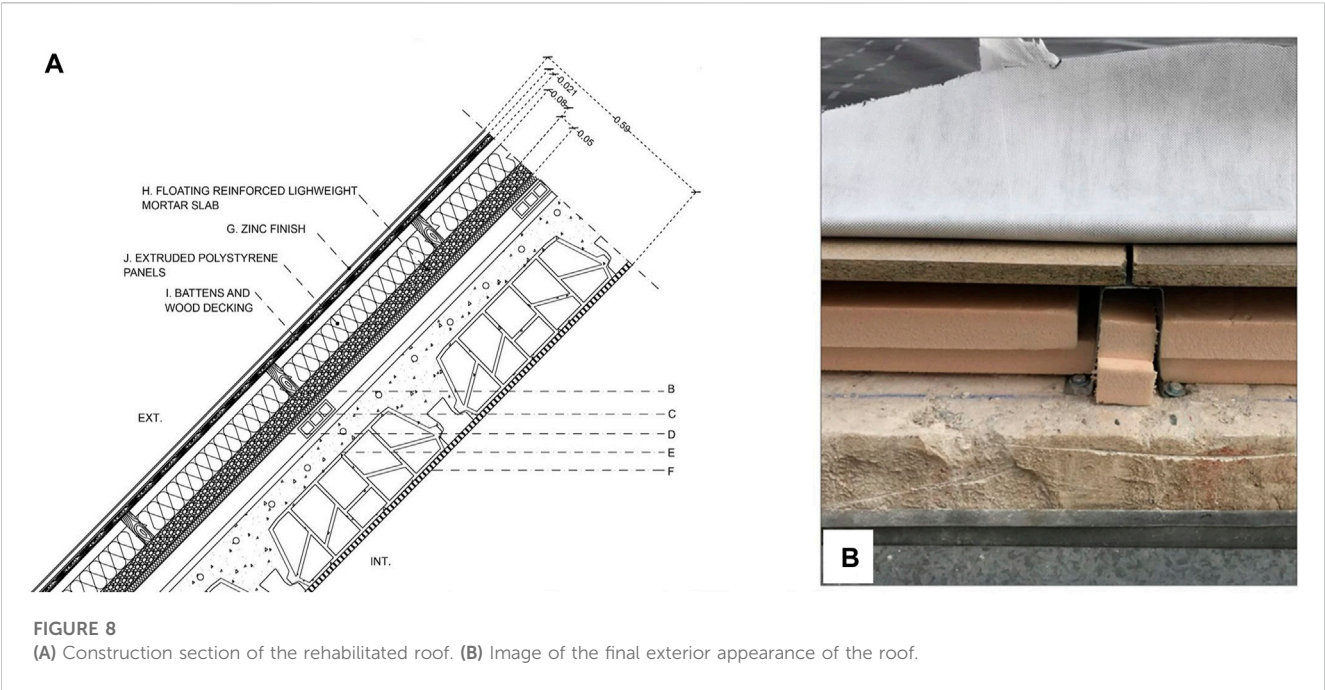


TABLE 2 Percentage and centralized heating production in each module.

Building	Percentage (%)	Heating capacity (kW)
E1	22.0	158.1
E2	27.8	200.1
E3	28.3	203.6
E4	22.0	158.1

- Possibility of detailed regulation of each room and of the whole installation.
- Economy of the energy used.
- Ease of maintenance operations.
- Adequate acoustic levels.
- Protection of the environment.
- Less architectural impact on the building.

Regarding the air conditioning system, the building has a heating and cooling system with two heat pumps of 360 kW nominal power each for production and radiators and fan coils as terminal units. In turn, each dwelling has a heat recovery unit for ventilation.

As the building is divided into four modules (Figure 9) and has centralized heating production, it has been distributed on the basis of the radiator power of each module (Table 2).

The thermal fluid chosen is water and the working conditions are as follows:

- Cooling, air inlet temperature 27°C and air outlet temperature of 19°C with a supply air temperature of 7°C and return air temperature of 12°C.
- Heating, air inlet temperature of 20°C in heating and 50°C supply air and 45°C return air.

From each unit, a network of black steel pipes carries hot or cold water, depending on the time of year, to a buffer tank located in the boiler room in the basement of the building. From there, an air conditioning circuit made of black steel in general and polyethylene pipe that distributes the water to each of the houses in which a fan-coil has been installed in the false ceiling. The pipes in the boiler room, the general pipes that run through the garage floor and those that run through the interior of the skirting boards are properly insulated in accordance with the provisions of the RITE and the overall thermal losses in all the pipes do not exceed 4% of the maximum power transported and are hydraulically balanced.

The efficiency of the production of air conditioning water by these pumps is 3.01 for cooling (EER), and 3.25 for heating (COP).

The Lider-Calener Unified tool does not allow the definition of fan-coils in residential dwellings. Therefore, the cooling and heating system using fan-coils has been modeled using constant performance equipment with the aforementioned parameters.

In compliance with the Technical Building Code, section HE 4 Minimum solar contribution for domestic hot water, the installation must have a system for the production of DHW by means of solar thermal collectors that can be partially or totally replaced by an alternative installation of another renewable energy, for which it is documented that the carbon dioxide emissions and

the consumption of non-renewable primary energy are equal to or lower than those produced by a similar solar thermal installation and its auxiliary support system.

Once the study was carried out, it was found that the DHW needs of the installation, taking into account the occupancy of the building, were approximately 8,000 L per day at 60°C. In order to achieve this heating, a sufficiently large surface area was required for the installation of the solar panels. For this reason, it was finally decided to replace the solar field with a 30 kW CO₂ aerothermal heat pump with a COP of 4.5 and a 100 kW natural gas boiler to heat the domestic hot water return network “radiant air conditioning system” (RACS). In addition, the work of the heat pumps and the volume of the storage tanks was distributed proportionally to the demand (Table 3).

The thermal installation has been equipped with all the necessary automatic control systems to maintain the premises in the design conditions foreseen according to RITE for heating and cooling with a THM-C 3 category control, since it has water variation according to the outside temperature, room temperature control and thermostatic valves in the terminal units to control the environment of each thermal zone, as well as the variation of the water temperature according to the outside conditions, which is carried out in the secondary air-conditioning circuit. The indoor design conditions are established as follows:

- Winter: operating temperature between 21°C and 23°C with relative humidity between 40% and 50%.
- Summer: operating temperature between 23°C and 25°C with relative humidity between 45% and 60%.

Since the thermal installation serves more than one beneficiary, the necessary meters have been installed to distribute the expenses corresponding to each service (heating, cooling and DHW) among the different users, which will be housed in a cabinet on the outside of the house, making it possible to regulate and measure the consumption of each one of them, as well as to interrupt the service. Likewise, the boiler room will have meters for the thermal energy generated for the production of hot/cold, primary and return of sanitary hot water.

In order to comply with the indoor air quality requirements, we have taken into account the provisions of section HS3 “Indoor air quality” of the CTE and we have gone a step further by installing heat recovery equipment. With them, adequate ventilation is achieved with the minimum energy consumption in the dwellings, eliminating the pollutants that are normally produced in the use of the building, considerably improving the indoor air quality, ensuring the necessary supply of outside air and obtaining a recovery of up to 95% of the energy used for air conditioning of the building. It is possible to recover up to 60% of the heat that would be lost in a mechanical ventilation system in which the intake and exhaust air flows are independent, allowing energy savings that can reach over 40% of the consumption of this equipment.

4 Discussion

The following is a summary of the most relevant aspects that have allowed Lagos Park to become a reference within the rental

TABLE 3 Domestic hot water demand, work of heat pumps and volume of storage tanks in each module.

Building	Domestic hot water demand (L/day)	Nominal power (kW)	Volume storage (L)
E1	1.8	12.6	3,362
E2	2.4	16.3	4,350
E3	2.7	18.1	4,822
E4	1.9	13.0	3,465

building typology in the Community of Madrid, thanks to the rehabilitation and functional, aesthetic, regulatory and energy adaptation that allow it to be at the forefront in this type of projects.

One of the characteristics that undoubtedly gives added value to Lagos Park has been the use of quality construction systems such as ventilated facade and ETICS. In this way, a new envelope has been created that has solved the thermal bridges and, at the same time, has provided the building with a new insulation and ventilation chamber. A new exterior skin has been created based on three materials: porcelain tile, ETICS and Zinc. These have been used to solve the ventilated facades, the interiors of terraces and roofs creating the color palette that defines the entire intervention to enhance the geometry of the architectural ensemble (iceberg white, graphite gray and natural zinc).

It is worth mentioning that the houses now have aluminum carpentry with thermal bridge break and double glazing of low emissivity, which causes that the temperature maintenance inside is total (no heat enters in summer and stays inside in winter) and also significantly reduces the acoustic impact.

On the other hand, the old air conditioning system has been replaced in one of the most ambitious interventions of the project by creating a centralization of air conditioning and DHW in order to obtain an A energy rating.

The COVID-19 pandemic has changed the technical and engineering approach to building and facility design. This fact implies that any facility engineering project is really complex. Starting from the current sanitary measures for reopening in the COVID-19 era and the crucial current research on this issue, the feasibility of plant retrofit/retrofit solutions through efficient ventilation and air quality is investigated (Balocco and Leoncini, 2020). For this purpose, each apartment has been equipped with an air conditioning system through centralized heat pump with individual heat recuperators. This means that the hot or cold air generated in each room of the apartment is transmitted through a circuit to come into contact with the outside air. By having this contact in a natural way, this new air enters the house renewed, but with a similar temperature to the air that has left. In this way the air will always be “clean” and this confers an important energy saving to the tenant in the air conditioning of his home.

The HULC tool was used to calculate the hot water demand. The DHW supply for this building has been solved with a system of two air-to-water heat pumps of 30 kW each, centralized, with a COP performance of 4.5 and storage tanks of 16,000 L total volume.

The choice of the ventilation system through an individual heat recovery unit per dwelling with a free-cooling bypass unit with an efficiency of more than 95%, guaranteeing the renewal of air in the dwelling with minimum impact on the ambient temperature of the

dwelling, thus certifying the maximum energy efficiency of the dwelling.

Thanks to the refurbishment carried out and taking into account the energy characteristics of the building, the thermal envelope, its installations, operating conditions and occupancy, it has been possible to obtain an A energy rating for the building by means of the Lider-Calener Unified Tool (HULC) according to the scale of values referred to in Royal Decree 235/2013.

Below, a recreation of the results offered by said Tool is detailed (Table 4). The overall rating of the building is shown after weighting the partial values. To facilitate the calculation, the building has been divided into four blocks based on the different positions they occupy in the building as a whole. Four units are thus formed, which have been named: E1, E2, E3, E4, taken from north to south.

The result of the entire system installed makes the Lagos Park building a model of sustainable and efficient system (Figure 10), since both the energy consumed and the CO₂ emissions to the atmosphere generated by this installation are much lower than any other installation used as a reference, even with the installation of solar thermal panels for the production of DHW, in strict compliance with all the requirements of welfare and hygiene (IT 1.1), the requirement of energy efficiency (IT 1.2) and the requirement of safety (IT 1.3).

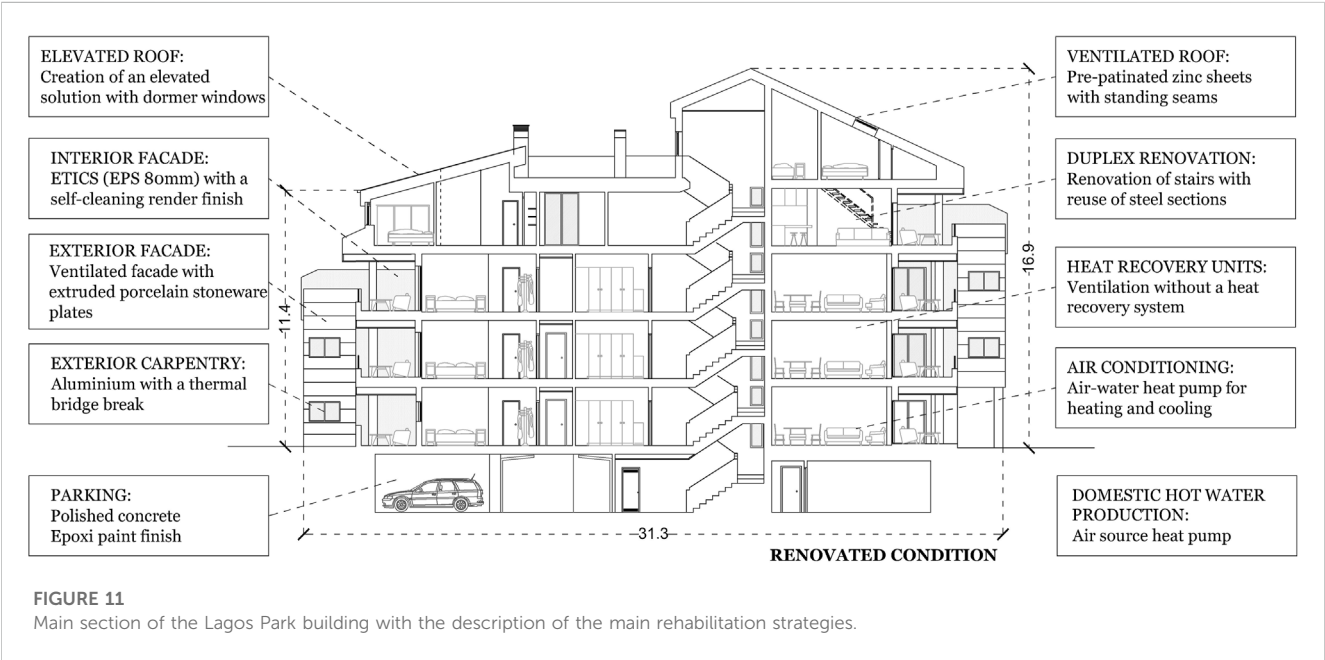
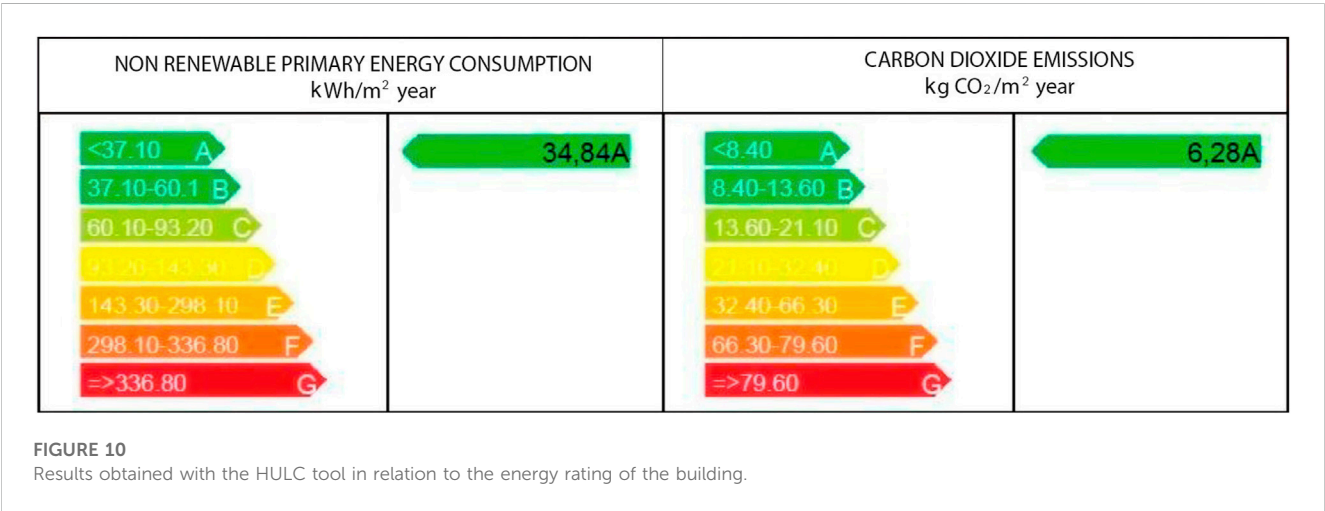
Thanks to the refurbishment carried out and taking into account the energy characteristics of the building, the thermal envelope, its installations, operating conditions and occupancy, it has been possible to obtain an A energy rating for the building. In this way, and given that it is a rental apartment building, the tenants have obtained energy savings of more than 70% as a result of all the strategies implemented. Below (Figure 11) we can see a summary of all the action strategies that have enabled the comprehensive rehabilitation of the existing building, achieving energy, spatial and environmental performance appropriate to the new desired sustainability parameters.

Table 5 shows the results extracted from the Unified Tool program. The projected building complies with all the requirements of the Basic Document HE1 (Limitation of Energy Demand) of the technical building code in terms of energy demand limitations for heating and cooling.

Research (Brandão de Vasconcelos et al., 2016) on the best cost-effective thermal retrofit measures has concluded that i) roof thermal retrofitting produces the largest variation in building primary energy consumption (and floor measures the smallest), ii) the combination of thermal envelope retrofit measures creates synergy effects that lead to better results than individual measures (in relation to overall costs and primary energy consumption), and iii) it is more advantageous to proceed with a package of thermal retrofit measures than to do nothing.

TABLE 4 Non-renewable primary energy consumption and CO₂ emissions per module.

Building	Non-renewable primary energy consumption (kWh/m ² year)	Carbon dioxide emissions (kgCO ₂ /m ² year)
E1	35.8	6.5
E2	34.9	6.3
E3	34.7	6.2
E4	34.0	6.1
Total	34.8	6.3



Retrofitting residential buildings is a commitment by owners. There are economic, technical, social and political barriers, but among them high upfront costs, certainty of payback periods and inexperience are key elements that discourage owners (Pardo-Bosch et al., 2019). In order to involve owners, the following recommendations can be put forward.

- The existence of organizations offering promotion and marketing of retrofitting, comprehensive project with energy retrofitting experts, and the provision of funds and financing schemes. In this regard, the municipality plays an essential role in promoting and organizing activities to inform homeowners about the retrofit process and about

TABLE 5 Annual heating and cooling demand.

Model	Heating (kWh/m ²)		Cooling (kWh/m ²)	
	Building	Compliance	Building	Compliance
E1	18.9	27.8	10.0	15.0
E2	16.1	27.6	10.9	15.0
E3	16.6	27.6	9.7	15.0
E4	18.8	27.8	8.6	15.0
Whole Building	17.4	27.7	9.9	15.0

companies offering integrated energy and financing packages.

- In order to increase the rate of retrofitting residential buildings, the public administration could offer financing. This financing is important as an engagement strategy, especially for low-income owners and residents.
- Cities should emphasize that it is key to include owners in the decision-making processes of building retrofit strategies and interventions.

5 Conclusion

The major refurbishment carried out in the complex, with a comprehensive intervention, has allowed the Lagos Park homes to be practically “homes without consumption.” From the household appliances to the structure of the house, everything is designed to optimize the energy used, which is reflected in electricity bills that reduce the monthly amount by 65%–75%. These data were provided by the building’s residents through individual interviews.

Through this article we have tried to give a global vision of all those constructive aspects that have been relevant at the time of rehabilitating the “LagosPark” building in an integral way.

The rehabilitation of the building has made it a relevant work of the place, responding not only to the regulatory criteria for improving energy efficiency and sustainability in housing, but also responding to architectural strategies that are not usually taken into consideration in projects of similar characteristics.

Actually, in a short-term perspective, the benefit of the rehabilitation of a building’s element condition will not result in any financial savings, which could cover an investment’s costs. However, in long term this will allow one to avoid larger investments, which are necessary, when building’s elements lose their functional purpose (Martinaitis et al., 2004). Such an approach to the twofold benefit of the building’s renovation would stimulate the rehabilitation of a building’s elements and, thereby, result in more considerable savings of the limited energy resources, the increase of the buildings’ value, and a more active construction market. Already previously, other researchers presented an analysis of the trends in the rate of energy improvement per year, due to energy rehabilitations, comparing them with periods of 5 years, using a longitudinal data analysis using variables from the monitoring system (Filippidou et al., 2017).

Both the dwellings and the common areas have been favored by the use of the ventilated facade and ETIC construction systems, as well as the roof construction solution that allows the upper areas of the building not only to obtain a new spatial configuration by gaining height in the roofs, but also to favor a substantial thermal insulation in the upper parts of the building. All the apartments have had their old carpentry systems replaced with aluminium ones with thermal bridge breakage and low emissivity double glazing, which produces invaluable acoustic and thermal benefits.

In addition, each apartment has been equipped with a centralized heat pump air conditioning system with individual heat recuperators, which benefits the sustainability of the whole.

Although the choice of aerothermal energy as a system for obtaining the energy needed by the house is faced with the lack of knowledge of the system or the initial investment required for the provision of equipment, the truth is that there are many advantages and strengths of aerothermal energy:

- Its multifunctionality, since a single unit provides clean energy for the use of domestic hot water, heating and cooling.
- Savings in air conditioning, since, although they require electrical energy for their operation, they can achieve savings of 50% compared to alternatives such as diesel boilers (which were used in the homes before their refurbishment). Compared to natural gas boilers, the cost can be contained by at least a quarter.
- It generates no waste or emissions, making it the best environmentally sustainable alternative.

This study provides integrated passive and active design strategies that quantify the impact of retrofitting energy efficient building components to meet the requirements of residential building regulations. The active strategies integrated with the passive strategies seek the optimization of the demand with the integration of both; so that it can serve as a guideline for decision making on improving energy efficiency for designers and related groups, such as contractors and homeowners.

Based on the strategies established, the aim is to lay the foundations for the calculation of energy efficiency.

The main calculation methods used to determine energy demands are based on simulations and tests on the real model. The savings data provided are relatively reliable and repeatable. However, their variability should be duly completed in future research taking into consideration occupant habits and user/family profiles.

Data availability statement

The original contributions presented in the study are included in the article/Supplementary Material, further inquiries can be directed to the corresponding author.

Author contributions

MM-T: Data curation, Formal Analysis, Supervision, Writing—original draft, Writing—review and editing,

Conceptualization, Funding acquisition, Investigation, Methodology, Project administration, Resources. JC-D: Conceptualization, Data curation, Formal Analysis, Investigation, Methodology, Resources, Supervision, Writing—original draft, Validation, Visualization, Software. RG-L: Data curation, Formal Analysis, Supervision, Validation, Visualization, Writing—original draft, Writing—review and editing.

Funding

The author(s) declare that no financial support was received for the research, authorship, and/or publication of this article.

References

- Abrahamsen, F. E., Ruud, S. G., and Gebremedhin, A. (2023). Assessing efficiency and environmental performance of a nearly zero-energy university building's energy system in Norway. *Buildings* 13, 169. doi:10.3390/buildings13010169
- Alonso, C. (2015). *Rehabilitación energética de fachadas: Propuesta metodológica para la evaluación de soluciones innovadoras, basándose en el diagnóstico de viviendas sociales construidas entre 1940 y 1980* (Madrid, España: E.T.S.I. Agrónomos). Tesis Doctoral.
- Balocco, C., and Leoncini, L. (2020). Energy cost for effective ventilation and air quality for healthy buildings: plant proposals for a historic building school reopening in the covid-19 era. *Sustainability* 12 (20), 8737–8816. doi:10.3390/su12208737
- Borgstein, E. H., Lamberts, R., and Hensen, J. L. M. (2018). Mapping failures in energy and environmental performance of buildings. *Energy Build.* 158, 476–485. doi:10.1016/j.enbuild.2017.10.038
- Brandão de Vasconcelos, A., Pinheiro, M. D., Manso, A., and Cabaço, A. (2016). EPBD cost-optimal methodology: application to the thermal rehabilitation of the building envelope of a portuguese residential reference building. *Energy Build.* 111, 12–25. doi:10.1016/j.enbuild.2015.11.006
- Cano-Marín, R. D., Jaramillo-Morilla, A., Bernal-Serrano, F. J., and Moreno-Rangel, D. (2014). Un estudio de caso: rehabilitación singular de edificios de viviendas en la barriada del parque alcosa, análisis de daños constructivos comunes y propuesta de intervención. *Inf. Construcción* 66 (534), e017. doi:10.3989/ic.12.112
- Carbonell, J. F. (2016). *La rehabilitación como oportunidad de evolución. Estudio y análisis de las estrategias presentadas en el Concurso de la Rehabilitación de la fachada ligera del Colegio de Arquitectos de Cataluña* (Barcelona, España: Universidad Politécnica de Catalunya). Trabajo Fin de Máster.
- Cervero Sánchez, N., and Agustín Hernández, L. (2015). Remodelación, Transformación y Rehabilitación. Tres formas de intervenir en la Vivienda Social del siglo XX. *Inf. Construcción* 67, m026. doi:10.3989/ic.14.049
- Chapman, R., Howden-Chapman, P., Viggers, H., O'Dea, D., and Kennedy, M. (2008). Retrofitting houses with insulation: A cost–benefit analysis of a randomised community trial. *J. Epidemiol. Community Health* 63, 271–277. doi:10.1136/jech.2007.070037
- de Gobierno, P. (1979). Real Decreto 2429/1979, de 6 de julio, por el que se aprueba la norma básica de edificación NBE-CT-79, sobre condiciones térmicas en los edificios. *Bol. Of. del Estado* 253.
- De La Osa, J. (2016). *Edificios saludables, edificios sostenibles. Observatorio de Salud y Medio Ambiente*. Budapest, Hungary: DKV.
- Díaz, C., Cornadó, C., Llorens, I., Pardo, F., and Hormías, E. (2012). Un estudio de caso: la rehabilitación de los edificios de viviendas del barrio de la mina en sant adrià del besòs (barcelona). análisis funcional y de las condiciones de seguridad, habitabilidad y mantenimiento. *Inf. Construcción* 64 (525), 19–34. doi:10.3989/ic.11.005
- Directiva 2009/28/CE (2009). *Parlamento Europeo y del Consejo de 23 de abril de 2009 relativa al fomento del uso de energía procedente de fuentes renovables y por la que se modifican y se derogan las Directivas 2001/77/CE y 2003/30/CE*.
- Directiva 2010/31/UE (2010). *Parlamento Europeo y del Consejo, de 19 de mayo de 2010, relativa a la eficiencia energética de los edificios*. (DO L 153 de 18.6.2010, p. 13).
- Directiva 2012/27/UE (2012). *Parlamento Europeo y del Consejo, de 25 de octubre de 2012, relativa a la eficiencia energética, por la que se modifican las Directivas 2009/125/CE y 2010/30/UE, y por la que se derogan las Directivas 2004/8/CE y 2006/32/CE*. (DO L 315 de 14.11.2012, p. 1).
- Directiva 2018/2002/UE (2018). *Parlamento Europeo y del Consejo de 11 de diciembre de 2018 por la que se modifica la Directiva 2012/27/UE relativa a la eficiencia energética*.
- Directiva 2018/844/UE (2018). *Parlamento Europeo y del Consejo de 30 de mayo de 2018 por la que se modifica la Directiva 2010/31/UE relativa a la eficiencia energética de los edificios y la Directiva 2012/27/UE relativa a la eficiencia energética*.
- Elbeltagi, E., Wefki, H., and Khallaf, R. (2023). Sustainable building optimization model for early-stage design. *Buildings* 13, 74. doi:10.3390/buildings13010074
- Espinola, A. (2018). *Estudio comparativo sobre normativa de accesibilidad de las Comunidades Autónomas españolas*.
- Feijó-Muñoz, J., González-Lezcano, R. A., Poza-Casado, I., Padilla-Marcos, M. Á., and Meiss, A. (2019). Airtightness of residential buildings in the Continental area of Spain. *Build. Environ.* 148, 299–308. doi:10.1016/j.buildenv.2018.11.010
- Feijó-Muñoz, J., Poza-Casado, I., González-Lezcano, R. A., Pardo, C., Echarri, V., Rafael Assiego, R., et al. (2018). Methodology for the study of the envelope airtightness of residential buildings in Spain: A case study. *Energies* 11 (4), 704. doi:10.3390/en11040704
- Filippidou, F., Nieboer, N., and Visscher, H. (2017). Are we moving fast enough? The energy renovation rate of the Dutch non-profit housing using the national energy labelling database. *Energy Policy* 109, 488–498. doi:10.1016/j.enpol.2017.07.025
- Folke, C., Carpenter, S., Walker, B., Scheffer, M., Elmqvist, T., Gunderson, L., et al. (2004). Regime shifts, resilience, and biodiversity in ecosystem management. *Annu. Rev. Ecol. Evol. Syst.* 35, 557–581. doi:10.1146/annurev.ecolsys.35.021103.105711
- Fossati, M., Scalco, V. A., Linczuk, V. C., and Lamberts, R. (2016). Building energy efficiency: an overview of the brazilian residential labeling scheme. *Renew. Sustain. Energy Rev.* 65, 1216–1231. doi:10.1016/j.rser.2016.06.048
- Gil, C. G. (2018). Objetivos de Desarrollo sostenible (ODS): una revisión crítica. *Papeles Relac. ecosociales cambio Glob.* 140, 107–118.
- Gupta, R., and Gregg, M. (2018). Assessing energy use and overheating risk in Net Zero Energy dwellings in UK. *Energy Build.* 158, 897–905. doi:10.1016/j.enbuild.2017.10.061
- Hu, M. (2019). Does zero energy building cost more? – An empirical comparison of the construction costs for zero energy education building in United States. *Sustain. Cities Soc.* 45, 324–334. doi:10.1016/j.scs.2018.11.026
- Jung, N., Paiho, S., Shemeikka, J., Lahdelma, R., and Airaksinen, M. (2018). Energy performance analysis of an office building in three climate zones. *Energy Build.* 158, 1023–1035. doi:10.1016/j.enbuild.2017.10.030
- Le Guen, M., Mosca, L., Perera, A. T. D., Cocolo, S., Mohajeri, N., and Scartezzini, J. L. (2018). Improving the energy sustainability of a Swiss village through building renovation and renewable energy integration. *Energy Build.* 158, 906–923. doi:10.1016/j.enbuild.2017.10.057
- Liu, S., Meng, X., and Tam, C. (2015). Building information modeling-based building design optimization for sustainability. *Energy Build.* 105, 139–153. doi:10.1016/j.enbuild.2015.06.037
- Loli, A., and Bertolin, C. (2018). Towards zero-emission refurbishment of historic buildings: A literature review. *Buildings* 8, 22. doi:10.3390/buildings8020022
- Martín-Consuegra, F., Oteiza, I., Alonso, C., Cuervo-Vilches, T., and Frutos, B. (2014). Análisis y propuesta de mejoras para la eficiencia energética del edificio principal del Instituto C.C. Eduardo Torroja-CSIC. *Inf. Construcción* 66, e043. e043. doi:10.3989/ic.14.125
- Martinaitis, V., Rogoza, A., and Bikmaniene, I. (2004). Criterion to evaluate the “twofold benefit” of the renovation of buildings and their elements. *Energy Build.* 36 (1), 3–8. doi:10.1016/S0378-7788(03)00054-9

Conflict of interest

The authors declare that the research was conducted in the absence of any commercial or financial relationships that could be construed as a potential conflict of interest.

Publisher's note

All claims expressed in this article are solely those of the authors and do not necessarily represent those of their affiliated organizations, or those of the publisher, the editors and the reviewers. Any product that may be evaluated in this article, or claim that may be made by its manufacturer, is not guaranteed or endorsed by the publisher.

- Matthews, E. C., Sattler, M., and Friedland, C. J. (2014). A critical analysis of hazard resilience measures within sustainability assessment frameworks. *Environ. Impact Assess. Rev.* 48, 59–69. doi:10.1016/j.eiar.2014.05.003
- Mejjaoui, S., and Alzahrani, M. (2020). Decision-making model for optimum energy retrofitting strategies in residential buildings. *Sustain. Prod. Consum.* 24, 211–218. doi:10.1016/j.spc.2020.07.008
- Misiiopecki, C., Bouquin, M., Gustavsen, A., and Jelle, B. P. (2018). Thermal modeling and investigation of the most energy-efficient window position. *Energy Build.* 158, 1079–1086. doi:10.1016/j.enbuild.2017.10.021
- Monjo, J. (2005). La evolución de los sistemas constructivos en la edificación. Procedimientos para su industrialización. *Inf. La Construcción* 57, 37–54. doi:10.3989/ic.2005.v57.i499-500.481
- Ngendahl, K., and Nielsen, T. R. (2015). Building energy optimization in the early design stages: A simplified method. *Energy Build.* 105, 88–99. doi:10.1016/j.enbuild.2015.06.087
- Pardo-Bosch, F., Cervera, C., and Ysa, T. (2019). Key aspects of building retrofitting: strategizing sustainable cities. *J. Environ. Manag.* 248, 109247. doi:10.1016/j.jenvman.2019.07.018
- Peinado, F., Rodero, C., Arines, S., and Pérez, M. (2012). Comportamiento acústico de sistemas ETICS de rehabilitación por el exterior de la fachada con lanas minerales (Proyecto BALI). *Rev. Acústica* 43 (3/4), 15–21.
- Reglamento 2018/1999/UE (2018). *Parlamento Europeo y del Consejo de 11 de diciembre de 2018 sobre la gobernanza de la Unión de la Energía y de la Acción por el Clima, y por el que se modifican los Reglamentos (CE) n.º 663/2009 y (CE) n.º 715/2009 del Parlamento Europeo y del Consejo, las Directivas 94/22/CE, 98/70/CE, 2009/31/CE, 2009/73/CE, 2010/31/UE, 2012/27/UE y 2013/30/UE del Parlamento Europeo y del Consejo y las Directivas 2009/119/CE y (UE) 2015/652 del Consejo, y se deroga el Reglamento (UE) 525/2013 del Parlamento Europeo y del Consejo.*
- Ruiz-Larrea, C. (2010). La hora solar. Entre la casa y la ciudad, del Solar Decathlon a Masdar. Hemiciclo Solar, Móstoles. *Arquit. Viva* 130, 52–57.
- Santamouris, M. (2016). Innovating to zero the building sector in Europe: minimising the energy consumption, eradication of the energy poverty and mitigating the local climate change. *Sol. Energy* 128, 61–94. doi:10.1016/j.solener.2016.01.021
- Sanz, D. M., Pacios, A. M., Barrero, I. A., Amorós, A. O., and Mellado, A. S. (2016). Weatherization of 80 houses with geothermal energy through heat pump, Tres cantos Project, Madrid, Spain. *Geothermia* 29 (1), 35–42.
- Sekret, R. (2018). Environmental aspects of energy supply of buildings in Poland. *E3S Web Conf. SOLINA* 49, 00097. doi:10.1051/e3sconf/20184900097
- Sendra, J. J., Domínguez-Amarillo, S., Bustamante, P., and León, A. L. (2013). Intervención 243;233;tica en el sector residencial del sur de España 241;a: retos actuales. *Inf. construcción* 65 (532), 457–464. doi:10.3989/ic.13.074
- Serrano, B., and Sanchis, A. (2015). La Inspección Técnica de Edificios como herramienta de la mejora energética de la edificación existente. *Inf. Construcción* 67, nt003. extra-1. doi:10.3989/ic.14.052
- Técnico de la Edificación, C. (2012). *Documento básico HE: Ahorro de Energía*. Madrid, España: Ministerio de Vivienda.
- Técnico de la Edificación, C. (2009). *Documento básico HR: Protección frente al Ruido*. Madrid, España: Ministerio de Vivienda.
- Técnico de la Edificación, C. (2017). *Documento Básico HS3: Calidad del Aire Interior*. Madrid, España: Ministerio de Vivienda.
- Técnico de la Edificación, C. (2018). *Documento Básico SUA: Seguridad de Utilización y Accesibilidad. DB-SUA/2: Adecuación efectiva de las condiciones de accesibilidad en edificios existentes*. Madrid, España: Ministerio de Vivienda.
- Valdivia, D. Z. (2007). Infraestructura de Servicios públicos y utilización de Dominio público y privado: el caso del servicio público de telecomunicaciones. *Rev. Derecho Adm.* 3, 161–180.
- Wells, L., Rismanchi, B., and Aye, L. A. (2018). A review of net zero energy buildings with reflections on the Australian context. *Energy Build.* 158, 616–628. doi:10.1016/j.enbuild.2017.10.055
- Wilkinson, S., Chang-Richards, A. Y., Sapciay, Z., and Costello, S. B. (2016). Improving construction sector resilience. *Int. J. Disaster Resil. Built Environ.* 7 (2), 173–185. doi:10.1108/IJDRBE-04-2015-0020
- Zaparaín, F. (2016). *El uso moderno del ladrillo en Valladolid: Claves de lectura. Real academia de Bellas artes de la Purísima concepción: 77-94. IX curso patrim. Cult. Conoc. Valladolid. España.*
- Zhang, G., Pan, Y., and Zhang, L. (2022). Deep learning for detecting building façade elements from images considering prior knowledge. *Automation Constr.* 133, 104016. doi:10.1016/j.autcon.2021.104016

Nomenclature

COP	Coefficient Of Performance
CTE	Spanish Technical Building Code
DWH	Domestic Hot Water
EER	Energy Efficiency Ratio
EPS	Expanded Polystyrene
ETICS	External thermal Insulation Composite Systems
HE1	Limitation of Energy Demand document
HULC	Lider-Calener Unified Tool
NZEB	Nearly Zero-Emission Building
RACS	Radiant Air Conditioning System
RITE	Spanish regulation of thermal installations in buildings
SDGs	Sustainable Development Goals
THM-C3	The system ventilates, cools, heats and deshumifies

Frontiers in Built Environment

Innovations in the engineering of sustainable
buildings, cities, and urban spaces

An innovative journal that advances our
knowledge of civil engineering. It focuses on the
development of sustainable methodologies for
the design and management of resilient buildings
and infrastructure.

Discover the latest Research Topics

[See more →](#)

Frontiers

Avenue du Tribunal-Fédéral 34
1005 Lausanne, Switzerland
frontiersin.org

Contact us

+41 (0)21 510 17 00
frontiersin.org/about/contact



Frontiers in Built Environment

